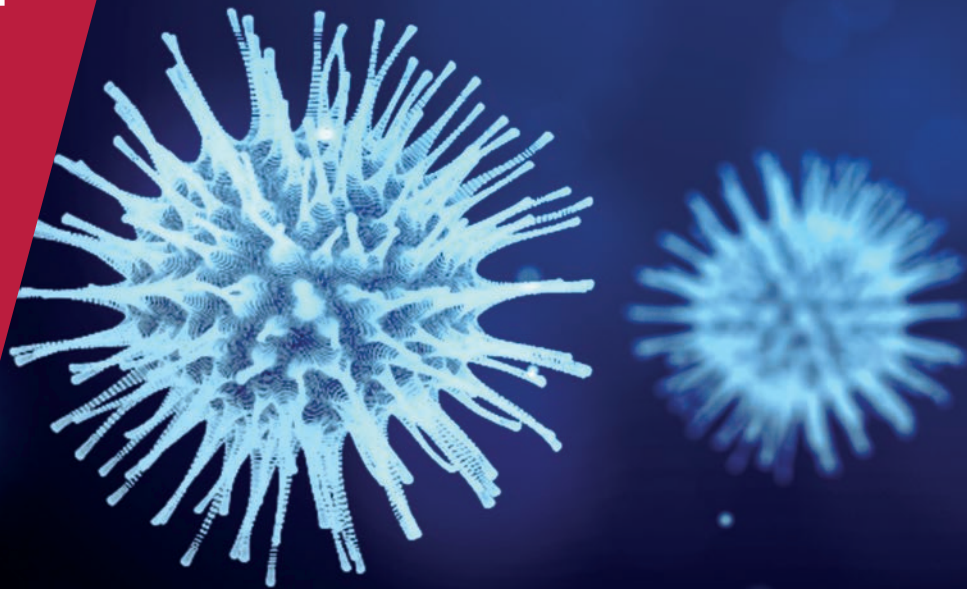


**CENTRE FOR
ECONOMIC
POLICY
RESEARCH**

CEPR PRESS



COVID ECONOMICS
VETTED AND REAL-TIME PAPERS

ISSUE 49
18 SEPTEMBER 2020

GLOBALIZATION AND PANDEMICS

Pol Antràs, Stephen J. Redding and
Esteban Rossi-Hansberg

**IMPACT OF FOX NEWS
ON MOBILITY**

Maxim Ananyev, Michael Poyker
and Yuan Tian

**PRODUCTIVITY OF WORKING
FROM HOME**

Masayuki Morikawa

**GLOBAL CONNECTEDNESS
AND MARKET POWER**

Jay Hyun, Daisoon Kim
and Seung-Ryong Shin

MUTUAL FUND DERIVATIVES

Ron Kaniel and Pingle Wang

ETHNIC DISCRIMINATION

Maria Mavlikeeva

Covid Economics

Vetted and Real-Time Papers

Covid Economics, Vetted and Real-Time Papers, from CEPR, brings together formal investigations on the economic issues emanating from the Covid outbreak, based on explicit theory and/or empirical evidence, to improve the knowledge base.

Founder: Beatrice Weder di Mauro, President of CEPR

Editor: Charles Wyplosz, Graduate Institute Geneva and CEPR

Contact: Submissions should be made at <https://portal.cepr.org/call-papers-covid-economics>. Other queries should be sent to covidecon@cepr.org.

Copyright for the papers appearing in this issue of *Covid Economics: Vetted and Real-Time Papers* is held by the individual authors.

The Centre for Economic Policy Research (CEPR)

The Centre for Economic Policy Research (CEPR) is a network of over 1,500 research economists based mostly in European universities. The Centre's goal is twofold: to promote world-class research, and to get the policy-relevant results into the hands of key decision-makers. CEPR's guiding principle is 'Research excellence with policy relevance'. A registered charity since it was founded in 1983, CEPR is independent of all public and private interest groups. It takes no institutional stand on economic policy matters and its core funding comes from its Institutional Members and sales of publications. Because it draws on such a large network of researchers, its output reflects a broad spectrum of individual viewpoints as well as perspectives drawn from civil society. CEPR research may include views on policy, but the Trustees of the Centre do not give prior review to its publications. The opinions expressed in this report are those of the authors and not those of CEPR.

Chair of the Board

Sir Charlie Bean

Founder and Honorary President

Richard Portes

President

Beatrice Weder di Mauro

Vice Presidents

Maristella Botticini

Ugo Panizza

Philippe Martin

Hélène Rey

Chief Executive Officer

Tessa Ogden

Editorial Board

Beatrice Weder di Mauro, CEPR

Charles Wyplosz, Graduate Institute Geneva and CEPR

Viral V. Acharya, Stern School of Business, NYU and CEPR

Guido Alfani, Bocconi University and CEPR

Franklin Allen, Imperial College Business School and CEPR

Michele Belot, European University Institute and CEPR

David Bloom, Harvard T.H. Chan School of Public Health

Nick Bloom, Stanford University and CEPR

Tito Boeri, Bocconi University and CEPR

Alison Booth, University of Essex and CEPR

Markus K Brunnermeier, Princeton University and CEPR

Michael C Burda, Humboldt Universitaet zu Berlin and CEPR

Aline Bütikofer, Norwegian School of Economics

Luis Cabral, New York University and CEPR

Paola Conconi, ECARES, Universite Libre de Bruxelles and CEPR

Giancarlo Corsetti, University of Cambridge and CEPR

Fiorella De Fiore, Bank for International Settlements and CEPR

Mathias Dewatripont, ECARES, Universite Libre de Bruxelles and CEPR

Jonathan Dingel, University of Chicago Booth School and CEPR

Barry Eichengreen, University of California, Berkeley and CEPR

Simon J Evenett, University of St Gallen and CEPR

Maryam Farboodi, MIT and CEPR

Antonio Fatás, INSEAD Singapore and CEPR

Francesco Giavazzi, Bocconi University and CEPR

Christian Gollier, Toulouse School of Economics and CEPR

Timothy J. Hatton, University of Essex and CEPR

Ethan Ilzetzki, London School of Economics and CEPR

Beata Javorcik, EBRD and CEPR

Simon Johnson, MIT and CEPR

Sebnem Kalemli-Ozcan, University of Maryland and CEPR Rik Frehen

Tom Kompas, University of Melbourne and CEBRA

Miklós Koren, Central European University and CEPR

Anton Korinek, University of Virginia and CEPR

Michael Kuhn, Vienna Institute of Demography

Maarten Lindeboom, Vrije Universiteit Amsterdam

Philippe Martin, Sciences Po and CEPR

Warwick McKibbin, ANU College of Asia and the Pacific

Kevin Hjortshøj O'Rourke, NYU Abu Dhabi and CEPR

Evi Pappa, European University Institute and CEPR

Barbara Petrongolo, Queen Mary University, London, LSE and CEPR

Richard Portes, London Business School and CEPR

Carol Propper, Imperial College London and CEPR

Lucrezia Reichlin, London Business School and CEPR

Ricardo Reis, London School of Economics and CEPR

Hélène Rey, London Business School and CEPR

Dominic Rohner, University of Lausanne and CEPR

Paola Sapienza, Northwestern University and CEPR

Moritz Schularick, University of Bonn and CEPR

Flavio Toxvaerd, University of Cambridge
Christoph Trebesch, Christian-Albrechts-Universitaet zu Kiel and CEPR

Karen-Helene Ulltveit-Moe, University of Oslo and CEPR

Jan C. van Ours, Erasmus University Rotterdam and CEPR

Thierry Verdier, Paris School of Economics and CEPR

Ethics

Covid Economics will feature high quality analyses of economic aspects of the health crisis. However, the pandemic also raises a number of complex ethical issues. Economists tend to think about trade-offs, in this case lives vs. costs, patient selection at a time of scarcity, and more. In the spirit of academic freedom, neither the Editors of *Covid Economics* nor CEPR take a stand on these issues and therefore do not bear any responsibility for views expressed in the articles.

Submission to professional journals

The following journals have indicated that they will accept submissions of papers featured in *Covid Economics* because they are working papers. Most expect revised versions. This list will be updated regularly.

<i>American Economic Review</i>	<i>Journal of Economic Growth</i>
<i>American Economic Review, Applied Economics</i>	<i>Journal of Economic Theory</i>
<i>American Economic Review, Insights</i>	<i>Journal of the European Economic Association*</i>
<i>American Economic Review, Economic Policy</i>	<i>Journal of Finance</i>
<i>American Economic Review, Macroeconomics</i>	<i>Journal of Financial Economics</i>
<i>American Economic Review, Microeconomics</i>	<i>Journal of International Economics</i>
<i>American Journal of Health Economics</i>	<i>Journal of Labor Economics*</i>
<i>Canadian Journal of Economics</i>	<i>Journal of Monetary Economics</i>
<i>Econometrica*</i>	<i>Journal of Public Economics</i>
<i>Economic Journal</i>	<i>Journal of Public Finance and Public Choice</i>
<i>Economics of Disasters and Climate Change</i>	<i>Journal of Political Economy</i>
<i>International Economic Review</i>	<i>Journal of Population Economics</i>
<i>Journal of Development Economics</i>	<i>Quarterly Journal of Economics</i>
<i>Journal of Econometrics*</i>	<i>Review of Corporate Finance Studies*</i>

(*) Must be a significantly revised and extended version of the paper featured in *Covid Economics*.

Covid Economics

Vetted and Real-Time Papers

Issue 49, 18 September 2020

Contents

Globalization and pandemics <i>Pol Antràs, Stephen J. Redding and Esteban Rossi-Hansberg</i>	1
The safest time to fly: Pandemic response in the era of Fox News <i>Maxim Ananyev, Michael Poyker and Yuan Tian</i>	85
Productivity of working from home during the COVID-19 pandemic: Evidence from an employee survey <i>Masayuki Morikawa</i>	123
The role of global connectedness and market power in crises: Firm-level evidence from the COVID-19 pandemic <i>Jay Hyun, Daisoon Kim and Seung-Ryong Shin</i>	148
Unmasking mutual fund derivative use during the COVID-19 crisis <i>Ron Kaniel and Pingle Wang</i>	172
Assessing the ethnic employment gap during the early stages of COVID-19 <i>Maria Mavlikeeva</i>	222

Globalization and pandemics¹

Pol Antràs,² Stephen J. Redding³ and
Esteban Rossi-Hansberg⁴

Date submitted: 14 September 2020; Date accepted: 16 September 2020

We develop a model of human interaction to analyze the relationship between globalization and pandemics. Our framework provides joint microfoundations for the gravity equation for international trade and the Susceptible-Infected-Recovered (SIR) model of disease dynamics. We show that there are cross-country epidemiological externalities, such that whether a global pandemic breaks out depends critically on the disease environment in the country with the highest rates of domestic infection. A deepening of global integration can either increase or decrease the range of parameters for which a pandemic occurs, and can generate multiple waves of infection when a single wave would otherwise occur in the closed economy. If agents do not internalize the threat of infection, larger deaths in a more unhealthy country raise its relative wage, thus generating a form of general equilibrium social distancing. Once agents internalize the threat of infection, the more unhealthy country typically experiences a reduction in its relative wage through individual-level social distancing. Incorporating these individual-level responses is central to generating large reductions in the ratio of trade to output and implies that the pandemic has substantial effects on aggregate welfare, through both deaths and reduced gains from trade.

1 We thank Elena Aguilar, Maxim Alekseev, Gordon Ji, Daniel Ramos, Sean Zhang, and Shuhan Zou for research assistance. We have received valuable comments from participants at the Sardinia Empirical Trade Conference and Purdue University. All errors, opinions and omissions are our own.

2 Harvard University.

3 Princeton University.

4 Princeton University

Copyright: Pol Antràs, Stephen J. Redding and Esteban Rossi-Hansberg

“As to foreign trade, there needs little to be said. The trading nations of Europe were all afraid of us; no port of France, or Holland, or Spain, or Italy would admit our ships or correspond with us.” (*A Journal of the Plague Year*, Daniel Defoe, 1665)

1 Introduction

Throughout human history, globalization and pandemics have been closely intertwined. The Black Death arrived in Europe in October 1347 when twelve ships from the Black Sea docked at the Sicilian port of Messina – the word quarantine originates from the Italian word for a forty-day period of isolation required of ships and their crews during the Black Death pandemic. Much more recently, on January 21, 2020, the first human-to-human infections of COVID-19 in Europe are presumed to have taken place in Starnberg, Germany, when a local car parts supplier (Webasto) organized a training session with a Chinese colleague from its operation in Wuhan, China. These examples are by no means unique; accounts of contagion through international business travel abound. In this paper we study the interplay between human interactions – motivated by an economically integrated world – and the prevalence and severity of pandemics.

We develop a conceptual framework to shed light on a number of central questions about the two-way interaction between trade and pandemics. Does a globalized world make societies more vulnerable to pandemics? To what extent are disease dynamics different in closed and open economies? What are the implications of pandemics for the volume and pattern of international trade? How do these changes in the volume and pattern of international trade in turn influence the spread of the disease? To what extent are there externalities between the health policies of different countries in the open economy equilibrium? Will the threat of future pandemics have a permanent impact on the nature of globalization?

Our conceptual framework combines the canonical model of international trade from economics (the gravity equation) with the seminal model of the spread of infectious diseases from epidemiology (the Susceptible-Infected-Recovered or SIR model). We provide joint microfoundations for these relationships in a single underlying theory in which both international trade and the spread of disease are driven by human interactions. Through jointly modelling these two phenomena, we highlight a number of interrelationships between them. On the one hand, the contact rate among individuals, which is a central parameter in benchmark epidemiology models, is endogenous in our framework, and responds to both economic forces (e.g., the gains from international trade) and to the dynamics of the pandemic (e.g., the perceived health risk associated with international travel). On the other hand, we study how the emergence of a pandemic and the perceived risk of future outbreaks shapes the dynamics of international trade, and the net gains from international trade once the death toll from the pandemic is taken into account.

We consider an economic setting – described in Section 2 – in which agents in each country consume differentiated varieties and choose the measures of these varieties to source from home and abroad. We suppose that sourcing varieties is costly, both in terms of the fixed costs of meeting

with other agents that sell varieties – an activity that involves intranational or international travel – and the variable costs of shipping varieties. Within this environment, the measures of varieties sourced at home and abroad are endogenously determined by trade frictions, country sizes, and the state of a pandemic, thus determining the intensity with which agents meet one another. If a healthy (susceptible) agent meets an infected agent, the probability that the disease is transmitted between them depends on the local epidemiological environment where the meeting takes place. This contagion risk associated with the local epidemiological environment is in turn shaped by local climate, by local social and cultural norms, and also by local health policies. Therefore, since domestic agents meet with other agents at home and abroad, the rate at which they are infected by the disease depends not only on their home health policies but also on those abroad.

To build intuition, we begin in Sections 3 and 4 by assuming that infection does not affect the ability of agents to produce and trade, and that agents are unaware of the threat of the infection, which implies that they do not have an incentive to alter their individual behavior (though, in Section 4, we allow the pandemic to cause deaths). In such a case, we show that human interactions and trade flows are characterized by gravity equations that feature origin characteristics, destination characteristics and measures of bilateral trade frictions. Using these gravity equations, we show that the welfare gains from trade can be written in terms of certain sufficient statistics, namely the domestic trade share, the change in a country's population (i.e., deaths) that can ascribed to trade integration, and model parameters. This is similar to the celebrated Arkolakis et al. (2012) formula for the gains from trade, but how trade shares map into welfare changes now depends on a wider range of model parameters than the conventional elasticity of trade with respect to trade costs. These gravity equations also determine the dynamics of the pandemic, which take a similar form to those of multi-group SIR model, but one in which the intensity of interactions between the different groups is endogenously determined by international trade, and potentially evolves over the course of the disease outbreak due to general-equilibrium effects. We find that these disease dynamics differ systematically between the open-economy case and the closed-economy case. In particular, in the open economy, the condition for a pandemic to be self-sustaining (i.e., $\mathcal{R}_0^{Open} > 1$, where \mathcal{R}_0^{Open} is the global basic reproduction number) depends critically on the epidemiological environment in the country with the highest rates of domestic infection.

We show that globalization and pandemics interact in a number of subtle ways. First, we demonstrate that the dynamics of the disease are significantly impacted by the degree of trade openness. More specifically, we show that a decline in any international trade or mobility friction reduces the rates at which agents from the same country meet one another and increases the rates at which agents from different countries meet one another. If countries are sufficiently symmetric in all respects, a decline in any (symmetric) international trade friction also leads to an overall increase in the total number of human interactions (domestic plus foreign). As a result, whenever countries are sufficiently symmetric, a decline in any (symmetric) international trade friction *increases* the range of parameters for which a global pandemic occurs. More precisely, even if an epidemic would not be self-sustaining in either of the two symmetric countries in the closed economy (because

$\mathcal{R}_0^{Closed} < 1$), it can be self-sustaining in an open economy ($\mathcal{R}_0^{Open} > 1$), because of the enhanced rate of interactions between agents in the open economy.

In contrast, if countries are sufficiently different from one another in terms of some of their primitive epidemiological parameters (i.e., the exogenous component of the infection rate or the recovery rate from the disease), a decline in any international trade friction can have the opposite effect of *decreasing* the range of parameters for which a global pandemic occurs. This situation arises because the condition for the pandemic to be sustaining in the open economy depends critically on the domestic rate of infections in the country with the worst disease environment. As a result, when one country has a much worse disease environment than the other, trade liberalization can reduce the share of that country's interactions that occur in this worse disease environment, thereby taking the global economy below the threshold for a pandemic to be self-sustaining for the world as a whole. Hence, in this case, on top of the negative effect on income, tightening trade or mobility restrictions can worsen the spread of the disease in all countries, including the relatively healthy one.

More generally, when a pandemic occurs in the open economy, we show that its properties are influenced by the disease environments in all countries, and can display significantly richer dynamics than in the standard closed-economy SIR model. For instance, even without lockdowns, multiple waves of infection can occur in the open economy, when there would only be a single wave in each country in the closed economy.

All the results discussed so far hold even in an environment in which the pandemic causes no deaths (or dead individuals are immediately replaced by newborn individuals). When we allow in Section 4 for the pandemic to cause deaths and thus a decline in population, we obtain additional general-equilibrium effects. In this case, for instance, a country with a worse disease environment tends to experience a larger reduction in population and labor supply, which in turn leads to an increase in its relative wage. This wage increase reduces the share of interactions that occur in that country's bad disease environment, and increases the share that occur in better disease environments, which again can take the global economy below the threshold for a pandemic to be self-sustaining. Therefore, the general equilibrium effects of the pandemic on wages and trade patterns induce a form of "general-equilibrium social distancing" from bad disease environments that operates even in the absence purposeful social distancing motivated by health risks.¹

In Section 5, we allow individuals to internalize the threat of infection and optimally adjust their behavior depending on the observed state of the pandemic. As in recent work (see Farboodi et al., 2020), it proves useful to assume that agents are uncertain about their own health status, and simply infer their health risk from the shares of their country's population with different health status (something they can infer from data on pandemic-related deaths). Technically, this turns the problem faced by agents into a dynamic optimal control problem in which the number of varieties that agents source from each country responds directly to the relative severity of the disease in

¹Similar effects would operate if infections reduced the productivity of agents in the labor market, in addition to their effects on mortality.

each country. As in recent closed-economy models of social distancing (such as Farboodi et al., 2020, or Toxvaerd et al., 2020), these behavioral responses reduce human interactions, and thereby tend to flatten the curve of infections. In contrast to these closed-economy setups, these behavioral responses now have international general equilibrium implications. In both countries, agents skew their interactions away from the relatively unhealthy country, which leads to the largest falls in the ratio of trade to income in the relatively healthier country. This redirection of interactions reduces the relative demand for the unhealthy country's goods, which in turn reduces its relative wage, thereby having the opposite effect to the reduction in its relative labor supply from greater death. Depending of the timing of the wave of infections in each country, which country has more infections than the other can change over the course of the pandemic, thereby reversing this pattern of changes in trade openness and relative wages over time. We show that introducing these individual-level responses is central to generating large reductions in the ratio of trade to output and implies that the pandemic has substantial effects on aggregate welfare, through both deaths and reduced gains from trade.

Finally, we consider an extension of our dynamic framework in which there are adjustment costs of establishing the human interactions needed to sustain trade. In the presence of these adjustment costs, households react less aggressively to the pandemic and their reaction is smoother, which leads to a faster and more severe pandemic with a greater total number of deaths, but less pronounced temporary reductions in real income and trade. In deciding to accumulate contacts, households now anticipate the costs incurred in adjusting these contacts during a pandemic, although in practice with symmetric adjustment costs we find that these anticipatory effects are negligible.

Throughout the paper, we use as our core setup an economy with two countries where agents can interact across borders but are subject to trade and migration frictions. Most of our results can be easily extended to contexts with multiple regions or even a continuum of them. We focus on international trade as our main application because of the close relationship between trade and pandemics throughout human history. Nevertheless, these extensions could be used to flexibly study interactions across regions within countries or neighborhoods in a city. Ultimately, the decision of which stores to patronize in a city, and how these decisions affect local disease dynamics, is shaped by many of the same economic trade-offs that we study in an international context in this paper.

Our paper connects with several strands of existing research. Within the international trade literature, we build on the voluminous gravity equation literature, which includes, among many others, the work of Anderson (1979), Anderson and Van Wincoop (2003), Eaton and Kortum (2003), Chaney (2008), Helpman et al. (2008), Arkolakis (2010), Allen and Arkolakis (2014), and Allen et al. (2020). As in the work of Chaney (2008) and Helpman et al. (2008), international trade frictions affect both the extensive and intensive margin of trade, but our model features selection into importing rather than selection into exporting (as in Antràs et al., 2017) and, more importantly, it emphasizes human interactions among buyers and sellers. In that latter respect, we connect with the work on the diffusion of information in networks, which has been applied to a trade context by Chaney (2014). By endogenizing the interplay between globalization and pandemics,

we study the nature and size of trade-induced welfare losses associated with disease transmission, thereby contributing to the very active recent literature on quantifying the gains from international trade (see, for instance, Eaton and Kortum, 2002, Arkolakis et al., 2012, Melitz and Redding, 2014, Costinot and Rodriguez-Clare, 2015, Ossa, 2015).

Although our model is admittedly abstract, we believe that it captures the role of international business travel in greasing the wheels of international trade. With this interpretation, our model connects with an empirical literature that has studied the role of international business travel in facilitating international trade (see Cristea, 2011, Blonigen and Cristea, 2015, and Startz, 2018), and more generally, in fostering economic development (see Hovhannisyan and Keller, 2015, Campante and Yanagizawa-Drott, 2018). Our simple microfounded model of trade through human interaction provides a natural rationalization for a gravity equation in international trade and shows how different types of trade frictions affect the extensive and intensive margins of trade.

Our paper also builds on the literature developing epidemiological models of disease spread, starting with the seminal work of Kermack and McKendrick (1927, 1932). More specifically, our multi-country SIR model shares many features with multigroup models of disease transmission, as in the work, among others, of Hethcote (1978), Hethcote and Thieme (1985), van den Driessche and Watmough (2002), and Magal et al. (2016).² A key difference is that the interaction between groups is endogenously determined by the gravity structure of international trade. The recent COVID-19 pandemic has triggered a remarkable explosion of work by economists studying the spread of the disease (see, for instance, Fernández-Villaverde and Jones, 2020) and exploring the implications of several types of policies (see, for instance, Alvarez et al., 2020, Acemoglu et al., 2020, Atkeson, 2020, or Jones et al., 2020). Within this literature, a few papers have explored the spatial dimension of the COVID-19 pandemic by simulating multi-group SIR models applied to various urban and regional contexts (see, among others, Argente et al., 2020, Bisin and Moro, 2020, Cuñat and Zymek, 2020, Birge et al., 2020, and Fajgelbaum et al., 2020). Our paper also connects with a subset of that literature, exemplified by the work of Alfaro et al. (2020), Farboodi et al. (2020), Fenichel et al. (2011), and Toxvaerd (2020) that has studied how the behavioral response of agents (e.g., social distancing) affects the spread and persistence of pandemics. Whereas most of this research is concerned with COVID-19 and adopts a simulation approach, our main goal is to develop a model of human interaction that jointly provides a microfoundation for a gravity equation and multi-group SIR dynamics, and can be used to analytically characterize the two-way relationship between globalization and pandemics in general.

Our work is also related to a literature in economic history that has emphasized the role of international trade in the transmission of disease. For the case of the Black Death, Christakos et al. (2005), Boerner and Severgnini (2014), Ricci et al. (2017), and Jedwab et al. (2019) argue that trade routes are central to understanding the spread of the plague through medieval Europe. In a review of a broader range of infection diseases, Saker et al. (2002) argue that globalization

²See Hethcote (2000) and Brauer and Castillo-Chavez (2012) for very useful reviews of mathematical modelling in epidemiology, and Ellison (2020) for an economist's overview of SIR models with heterogeneity.

has often played a pivotal role in disease transmission. The recent COVID-19 pandemic has also provided numerous examples of the spread of the virus through business travel.³

The rest of the paper is structured as follows. In Section 2, we present our baseline gravity-style model of international trade with endogenous intranational and international human interactions. In Section 3, we consider a first variant of the dynamics of disease spread in which the rate of contact between agents (though endogenous) is time-invariant during the pandemic. In Section 4, we incorporate labor supply responses to the pandemic, which affect the path of relative wages (and thus the rate of contact of agents within and across countries) during the pandemic. In Section 5, we incorporate individual behavioral responses motivated by agents adjusting their desired number of human interactions in response to their fear of being infected by the disease. We offer some concluding remarks in Section 6.

2 Baseline Economic Model

We begin by developing a stylized model of the global economy in which international trade is sustained by human interactions. Our baseline model is a simple two-country world, in which countries use labor to produce differentiated goods that are exchanged in competitive markets via human interactions. In Section 2.3, we outline how our model can be easily extended to settings featuring (i) multiple countries, (ii) intermediate inputs, and (iii) scale economies and imperfect competition.

2.1 Environment

Consider a world with two locations: East and West, indexed by i or j . We denote by \mathcal{J} the set of countries in the world, so for now $\mathcal{J} = \{East, West\}$. Location $i \in \mathcal{J}$ is inhabited by a continuum of measure L_i of households, and each household is endowed with the ability to produce a differentiated variety using labor as the only input in production. We denote by w_i the wage rate in country i .

Trade is costly. There are iceberg bilateral trade cost $\tau_{ij} = t_{ij} \times (d_{ij})^\delta$, when shipping from j back to i , where $d_{ij} \geq 1$ is the symmetric distance between i and j , and t_{ij} is a man-made additional trade friction imposed by i on imports from country j . We let these man-made trade costs be potentially asymmetric reflecting the fact that one country may impose higher restrictions to trade (e.g., tariffs, or delays in goods clearing customs) than the other country. For simplicity,

³A well-known example in the U.S. is the conference held by biotech company Biogen in Boston, Massachusetts on February 26 and 27, and attended by 175 executive managers, who spread the covid-19 virus to at least six states, the District of Columbia and three European countries, and caused close to 100 infections in Massachusetts alone <http://www.nytimes.com/2020/04/12/us/coronavirus-biogen-boston-superspreader.html>). Another example is Steve Walsh, the so-called British “super spreader,” who is linked to at least 11 new infections of COVID-19, and who caught the disease in Singapore, while he attended a sales conference in late January of 2020 (see https://www.washingtonpost.com/world/europe/british-coronavirus-super-spreader-may-have-infected-at-least-11-people-in-three-countries/2020/02/10/016e9842-4c14-11ea-967b-e074d302c7d4_story.html). The initial spread of COVID-19 to Iran and Nigeria has also been tied to international business travel.

there are no man-made frictions to internal shipments, so $t_{ii} = 1$ and $\tau_{ii} = (d_{ii})^\delta$, where $d_{ii} < d_{ij}$ can be interpreted as the average internal distance in country $i = East, West$.

Each household is formed by two individuals. One of these individuals – the *seller* – is in charge of producing and selling the household-specific differentiated variety from their home, while the other individual – the *buyer* – is in charge of procuring varieties for consumption from other households in each of the two locations. We let all households in country i be equally productive in manufacturing varieties, with one unit of labor delivering Z_i units of goods. Goods markets are competitive and sellers make their goods available at marginal cost. Households have CES preferences over differentiated varieties, with an elasticity of substitution $\sigma > 1$ regardless of the origin of these varieties, and they derive disutility from the buyer spending time away from home. More specifically, a household in country i incurs a utility cost

$$c_{ij}(n_{ij}) = \frac{c}{\phi} \times \mu_{ij} \times (d_{ij})^\rho \times (n_{ij})^\phi, \quad (1)$$

whenever the household's buyer secures n_{ij} varieties from location j , at a distance $d_{ij} \geq 1$ from i . The parameter μ_{ij} captures (possibly asymmetric) travel restrictions imposed by country j 's government on visitors from i . The parameter c governs the cost of travel and we assume it is large enough to ensure an interior solution in which $n_{ij} \leq L_j$ for all i and $j \in \mathcal{J}$. We assume that whenever $n_{ij} < L_j$, the set of varieties procured from j are chosen at random, so if all households from i procure n_{ij} from j , each household's variety in j will be consumed by a fraction n_{ij}/L_j of households from i .⁴

Welfare of households in location i is then given by

$$W_i = \left(\sum_{j \in \mathcal{J}} \int_0^{n_{ij}} q_{ij}(k)^{\frac{\sigma-1}{\sigma}} dk \right)^{\frac{\sigma}{\sigma-1}} - \frac{c}{\phi} \sum_{j \in \mathcal{J}} \mu_{ij} (d_{ij})^\rho \times (n_{ij})^\phi, \quad (2)$$

where $q_{ij}(k)$ is the quantity consumed in location i of the variety produced in location j by household k .

2.2 Equilibrium

Let us first consider consumption choices in a given household for a given n_{ij} . Maximizing (2) subject to the households' budget constraint, we obtain:

$$q_{ij} = \frac{w_i}{(P_i)^{1-\sigma}} \left(\frac{\tau_{ij} w_j}{Z_j} \right)^{-\sigma}, \quad (3)$$

⁴It may seem arbitrary that it is buyers rather than sellers who are assumed to travel. In section 2.3, we offer an interpretation of the model in which trade is in intermediate inputs and the buyer travels in order to procure the parts of components necessary for the household to produce a final consumption good. In section 2.3, we also consider the case in which travel costs are in terms of labor, rather than a utility cost. Finally, in that same section 2.3, we also explore a variant of the model in which it is sellers rather than buyers who travel, as is often implicitly assumed in standard models of firm participation in trade (cf., Melitz, 2003).

where w_i is household income, w_j/Z_j is the common free-on-board price of all varieties produced in location j , τ_{ij} are trade costs when shipping from j to i , and P_i is a price index given by

$$P_i = \left(\sum_{j \in \mathcal{J}} n_{ij} \left(\frac{\tau_{ij} w_j}{Z_j} \right)^{1-\sigma} \right)^{1/(1-\sigma)}. \tag{4}$$

Multiplying equation (3) by $(q_{ij})^{(\sigma-1)/\sigma}$, summing across locations, and rearranging, it is straightforward to show that

$$Q_i = \left(\sum_{j \in \mathcal{J}} n_{ij} (q_{ij})^{(\sigma-1)/\sigma} \right)^{\sigma/(\sigma-1)} = \frac{w_i}{P_i}, \tag{5}$$

so real consumption equals real income.

In order to characterize each household's choice of n_{ij} , we first plug (3) and (4) into (2) to obtain

$$W_i = w_i \left(\sum_{j \in \mathcal{J}} n_{ij} \left(\frac{\tau_{ij} w_j}{Z_j} \right)^{1-\sigma} \right)^{\frac{1}{(\sigma-1)}} - \frac{c}{\phi} \sum_{j \in \mathcal{J}} \mu_{ij} (d_{ij})^\rho \times (n_{ij})^\phi. \tag{6}$$

The first order condition associated with the choice of n_{ij} delivers (after plugging in (5)):

$$n_{ij} = (c(\sigma-1)\mu_{ij})^{-1/(\phi-1)} (d_{ij})^{-\frac{\rho+(\sigma-1)\delta}{\phi-1}} \left(\frac{t_{ij} w_j}{Z_j P_i} \right)^{-\frac{\sigma-1}{\phi-1}} \left(\frac{w_i}{P_i} \right)^{1/(\phi-1)}. \tag{7}$$

Notice that bilateral human interactions follow a ‘gravity-style’ equation that is log-separable in origin and destination terms, and a composite of bilateral trade frictions. Evidently, natural and man-made barriers to trade (d_{ij} , t_{ij}) and to labor mobility (μ_{ij}) will tend to reduce the number of human interactions sought by agents from country i in country j . As we show in Appendix A.1, for the second-order conditions to be met for all values of μ_{ij} , d_{ij} , and t_{ij} , we need to impose $\phi > 1/(\sigma-1)$ and $\sigma > 2$.

Bilateral import flows by country i from country j are in turn given by

$$X_{ij} = n_{ij} p_{ij} q_{ij} L_i = (c(\sigma-1)\mu_{ij})^{-\frac{1}{\phi-1}} (d_{ij})^{-\frac{\rho+\phi(\sigma-1)\delta}{\phi-1}} \left(\frac{t_{ij} w_j}{Z_j P_i} \right)^{-\frac{\phi(\sigma-1)}{\phi-1}} \left(\frac{w_i}{P_i} \right)^{\frac{1}{\phi-1}} w_i L_i. \tag{8}$$

Notice that the trade shares can be written as

$$\pi_{ij} = \frac{X_{ij}}{\sum_{\ell \in \mathcal{J}} X_{i\ell}} = \frac{(w_j/Z_j)^{-\frac{\phi(\sigma-1)}{\phi-1}} \times (\mu_{ij})^{-\frac{1}{\phi-1}} (d_{ij})^{-\frac{\rho+\phi(\sigma-1)\delta}{\phi-1}} (t_{ij})^{-\frac{\phi(\sigma-1)}{\phi-1}}}{\sum_{\ell \in \mathcal{J}} (\mu_{i\ell})^{-\frac{1}{\phi-1}} (d_{i\ell})^{-\frac{\rho+\phi(\sigma-1)\delta}{\phi-1}} (t_{i\ell} w_\ell/Z_\ell)^{-\frac{\phi(\sigma-1)}{\phi-1}}}, \tag{9}$$

and are thus log-separable in an origin-specific term S_j , a destination-specific term Θ_i , and a composite bilateral trade friction term given by:⁵

$$(\Gamma_{ij})^{-\varepsilon} = (\mu_{ij})^{-\frac{1}{\phi-1}} (d_{ij})^{-\frac{\rho+\phi(\sigma-1)\delta}{\phi-1}} (t_{ij})^{-\frac{\phi(\sigma-1)}{\phi-1}}, \tag{10}$$

⁵More specifically, $S_j = (w_j/Z_j)^{-\frac{\phi(\sigma-1)}{\phi-1}}$ and $\Theta_i = \sum_{\ell \in \mathcal{J}} (\mu_{i\ell})^{-\frac{1}{\phi-1}} (d_{i\ell})^{-\frac{\rho+\phi(\sigma-1)\delta}{\phi-1}} (t_{i\ell} w_\ell/Z_\ell)^{-\frac{\phi(\sigma-1)}{\phi-1}}$.

which encompasses mobility frictions (μ_{ij}), transport costs (d_{ij}) and trade frictions (t_{ij}).

Following Head and Mayer (2014), it then follows that bilateral trade flows in (8) also follow a standard gravity equation

$$X_{ij} = \frac{X_i Y_j}{\Phi_i \Omega_j} (\Gamma_{ij})^{-\varepsilon},$$

where X_i is total spending in country i , Y_j is country j 's value of production, and

$$\Phi_i = \sum_{j \in \mathcal{J}} \frac{Y_j}{\Omega_j} (\Gamma_{ij})^{-\varepsilon}; \quad \Omega_j = \sum_{i \in \mathcal{J}} \frac{X_i}{\Phi_i} (\Gamma_{ji})^{-\varepsilon}.$$

Notice that the distance elasticity is affected by the standard substitutability σ , but also by the traveling cost elasticity ρ , and by the convexity ϕ of the traveling costs. It is clear that both $\rho > 0$ and $\phi > 1$ increase the distance elasticity relative to a standard Armington model (in which the distance elasticity would be given by $\delta(\sigma - 1)$). The other man-made bilateral frictions also naturally depress trade flows.⁶

We next solve for the price index and household welfare in each country. Invoking equation (5), plugging (3) and (7), and simplifying delivers

$$P_i = \left(\frac{w_i}{c(\sigma - 1)} \right)^{-\frac{1}{\phi(\sigma-1)-1}} \left(\sum_{j \in \mathcal{J}} (\Gamma_{ij})^{-\varepsilon} (w_j/Z_j)^{-\frac{(\sigma-1)\phi}{\phi-1}} \right)^{-\frac{(\phi-1)}{\phi(\sigma-1)-1}}. \quad (11)$$

Going back to the expression for welfare in (2), and plugging (5), (7) and (11), we then find

$$W_i = \frac{\phi(\sigma - 1) - 1}{\phi(\sigma - 1)} \frac{w_i}{P_i}, \quad (12)$$

which combined with (9) implies that aggregate welfare is given by

$$W_i L_i = \frac{\phi(\sigma - 1) - 1}{\phi(\sigma - 1)} \times (\pi_{ii})^{-\frac{(\phi-1)}{\phi(\sigma-1)-1}} \times \left(\frac{(Z_i)^{\phi(\sigma-1)}}{c(\sigma - 1)} (\Gamma_{ii})^{-\varepsilon(\phi-1)} \right)^{\frac{1}{\phi(\sigma-1)-1}} L_i. \quad (13)$$

This formula is a variant of the Arkolakis et al. (2012) welfare formula indicating that, with estimates of ϕ and σ at hand, one could compute the change in welfare associated with a shift to autarky only with information on the domestic trade share π_{ii} . A key difference relative to their contribution, however, is that the combination of ϕ and σ relevant for welfare cannot easily be backed out from estimation of a ‘trade elasticity’ (see equation (10)). Later, when we allow trade to affect the transmission of disease and this disease to affect mortality, a further difference will be that the effect of trade on aggregate welfare will also depend on its effect on mortality (via changes in L_i).

⁶It is also worth noting that when $\mu_{ij} = \mu_{ji}$ and $t_{ji} = t_{ij}$, this gravity equation is fully symmetric, and

$$\Phi_i = \Omega_i = \sum_j S_j \phi_{ij} = \sum_j (w_j/Z_j)^{-\frac{\phi(\sigma-1)}{\phi-1}} (\mu_{ij})^{-\frac{1}{\phi-1}} (d_{ij})^{-\frac{\rho+\phi(\sigma-1)\delta}{\phi-1}} (t_{ij})^{-\frac{\phi(\sigma-1)}{\phi-1}}.$$

We conclude our description of the equilibrium of our model by discussing the determination of equilibrium wages. For that, it is simplest to just invoke the equality between income and spending in each country, that is $\pi_{ii}w_iL_i + \pi_{ji}w_jL_j = w_iL_i$, which plugging in (9), can be written as

$$\pi_{ii}(w_i, w_j) \times w_iL_i + \pi_{ji}(w_i, w_j) \times w_jL_j = w_iL_i, \tag{14}$$

where $\pi_{ii}(w_i, w_j)$ and $\pi_{ji}(w_i, w_j)$ are given in equation (9). This pair of equations (one for i and one for j) allow us to solve for w_i and w_j as a function of the unique distance d_{ij} , the pair of mobility restriction parameters μ_{ij} and μ_{ji} , the pair of man-made trade barriers t_{ij} and t_{ji} , and the parameters ϕ, σ, δ , and ρ . Setting one of the country's wages as the numéraire, the general equilibrium only requires solving one of these non-linear equations in (14). Once one has solved for this (relative) wage, it is straightforward to solve for trade flows and for the flow of buyers across locations, as well as for the implied welfare levels.

Note that the general-equilibrium condition in (14) is identical to that obtained in standard gravity models, so from the results in Alvarez and Lucas (2007), Allen and Arkolakis (2014), or Allen et al. (2020), we can conclude that:⁷

Proposition 1 *As long as trade frictions Γ_{ij} are bounded, there exists a unique vector of equilibrium wages $\mathbf{w}^* = (w_i, w_j) \in \mathbb{R}_{++}^2$ that solves the system of equations in (14).*

Using the implicit-function theorem, it is also straightforward to see that the relative wage w_j/w_i will be increasing in $L_i, \Gamma_{ii}, \Gamma_{ji}$, and Z_j , while it will be decreasing in $L_j, \Gamma_{jj}, \Gamma_{ij}$, and Z_i .

Given the vector of equilibrium wages $\mathbf{w} = (w_i, w_j)$, we are particularly interested in studying how changes in trade frictions (d_{ij}, t_{ij} , or μ_{ij}) affect the rate of human-to-human interactions at home, abroad and worldwide. Note that, combining equations (3), (8), and (9), we can express

$$n_{ij}(\mathbf{w}) = \left(\frac{t_{ij}(d_{ij})^\delta w_j}{P_i(\mathbf{w})Z_j} \right)^{\sigma-1} \pi_{ij}(\mathbf{w}), \tag{15}$$

where $\pi_{ij}(\mathbf{w})$ is given in (9) and $P_i(\mathbf{w})$ in (11). Studying how $n_{ii}(\mathbf{w})$ and $n_{ij}(\mathbf{w})$ are shaped by the primitive parameters of the model is complicated by the general equilibrium nature of our model, but in Appendix A.2 we are able to show that:

Proposition 2 *A decline in any international trade or mobility friction ($d_{ij}, t_{ij}, t_{ji}, \mu_{ij}, \mu_{ji}$) leads to: (a) a decline in the rates (n_{ii} and n_{jj}) at which individuals will meet individuals in their own country; and (b) an increase in the rates at which individuals will meet individuals from the other country (n_{ij} and n_{ji}).*

In words, despite the fact that changes in trade and mobility frictions obviously impact equilibrium relative wages, the more open are economies to the flow of goods and people across borders,

⁷In Alvarez and Lucas (2007), uniqueness requires some additional (mild) assumptions due to the existence of an intermediate-input sector. Because our model features no intermediate inputs, we just need to assume that trade frictions remain bounded.

the larger will be international interactions and the lower will be domestic interactions.

We can also study the effect of reductions in international trade and mobility frictions on the *overall* measure of varieties consumed by each household, which also corresponds to the number of human interactions experienced by each household's buyer (i.e., $n_{ii} + n_{ij}$). Similarly, we can also study the total number of human interactions carried out by each household's seller (i.e., $n_{ii} + n_{ji}$).⁸ General equilibrium forces complicate this comparative static, but we are able to show that (see Appendix A.3).

Proposition 3 *Suppose that countries are symmetric, in the sense that $L_i = L$, $Z_i = Z$, and $\Gamma_{ij} = \Gamma$ for all i . Then, a decline in any (symmetric) international trade frictions leads to an overall increase in human interactions ($n_{dom} + n_{for}$) experienced by both household buyers and household sellers.*

The assumption of full symmetry is extreme, but the result of course continues to hold true if country asymmetries are small and trade frictions are not too asymmetric across countries. Furthermore, exhaustive numerical simulations suggest that the result continues to hold true for arbitrarily asymmetric declines in trade frictions, as long as countries are symmetric in size ($L_i = L$) and in technology ($Z_i = Z$).

Reverting back to our general equilibrium with arbitrary country asymmetries, we can also derive results for how changes in the labor force in either country affect the per-household measure of interactions at home and abroad. More specifically, from equation (14), it is straightforward to see that the relative wage w_j/w_i is monotonic in the ratio L_i/L_j . Furthermore, working with equations (7) and (11), we can establish (see Appendix A.4 for a proof):

Proposition 4 *A decrease in the relative size of country i 's population leads to a decrease in the rates n_{ii} and n_{ji} at which individuals from all countries will meet individuals in country i , and to an increase in the rates n_{jj} and n_{ij} at which individuals from all countries will meet individuals in the other country j .*

This result will prove useful in Section 4, where we study how general equilibrium forces partly shape the dynamics of an epidemic. For instance, if the epidemic affects labor supply disproportionately in one of the countries, then the implied increase in that country's relative wage will induce a form of general equilibrium social distancing, as it will incentivize home buyers to avoid that country, even without social distancing motivated by health risks.

2.3 Extensions

Our baseline economic model is special among many dimensions, so it is important to discuss the robustness of some of the key insights we take away from our economic model. Because the gravity equation of international trade can be derived under a variety of economic environments and market

⁸Note that despite us modeling a frictionless labor market, the assumed symmetry of all households implies that no household has any incentive to hire anybody to buy or sell goods on its behalf.

structures, it is perhaps not too surprising that many of the key features of our model carry over to alternative environments featuring multiple countries, intermediate input trade, scale economies and imperfect competition. We next briefly describe four extensions of our model, but we leave all mathematical details to the Appendix (see Appendix C).

Some readers might object to the fact that, in our baseline model, production uses labor, while the traveling cost is specified in terms of a utility cost. We make this assumption to identify international travel with specific members of the household, which facilitates a more transparent transition to a model of disease transmission driven by human-to-human interactions. Nevertheless, in terms of the mechanics of our economic model, this assumption is innocuous. More specifically, in the first extension studied in Appendix C, we show that Propositions 1 through 4 continue to hold whenever travel costs in equation (1) are specified in terms of labor rather than being modelled as a utility cost. In fact, this version of the model is isomorphic to our baseline model above, except for a slightly different expression for the equilibrium price index P_i .

The assumption that households travel internationally to procure consumption goods may seem unrealistic. Indeed, international business travel may be better thought as being a valuable input when firms need specialized inputs and seek potential providers of those inputs in various countries. Fortunately, it is straightforward to re-interpret our model along those lines by assuming that the differentiated varieties produced by households are intermediate inputs, which all households combine into a homogeneous final good, which in equilibrium is not traded. The details of this re-interpretation are worked out in the second extension studied in Appendix C.

Returning to our baseline economic model, in Appendix C we next derive our key equilibrium conditions for a world economy with multiple countries. In fact, all the equations above, except for the labor-market clearing condition (14) apply to that multi-country environment once the set of countries \mathcal{J} is re-defined to include multiple countries. The labor-market condition is in turn simply given by $\sum_{j \in \mathcal{J}} \pi_{ij}(\mathbf{w}) w_j L_j = w_i L_i$, where $\pi_{ij}(\mathbf{w})$ is defined in (9). Similarly, the model is also easily adaptable to the case in which there is a continuum of locations $i \in \Omega$, where Ω is a closed and bounded set of a finite-dimensional Euclidean space. The equilibrium conditions are again unaltered, with integrals replacing summation operators throughout.

Finally, in Appendix C we explore a variant of our model in which it is the household's seller rather than the buyer who travels to other locations. We model this via a framework featuring scale economies, monopolistic competition and fixed cost of exporting, as in the literature on selection into exporting emanating from the seminal work of Melitz (2003), except that the seller fixed costs are a function of the measure of buyers reached in a destination market. Again, Propositions 1 through 4 continue to hold in such an environment.

3 A Two-Country SIR Model with Time-Invariant Interactions

So far, we have just characterized a static (steady-state) model of international trade supported by international travel. Now let us consider the case in which the model above describes a standard

“day” in the household. More specifically, in the morning the buyer in each household in i leaves the house and visits n_{ii} sellers in i and n_{ij} sellers in j , procuring goods from each of those households. For simplicity, assume that buyers do not travel together or otherwise meet each other. While the buyer visits other households and procures goods, the seller in each household sells its own goods to visitors to their household. There will be n_{ii} domestic visitors and n_{ji} foreign visitors. In the evening, the two members of the household reunite.

3.1 Preliminaries

With this background in mind, consider now the dynamics of contagion. As in the standard epidemiological model, we divide the population at each point in time into **S**usceptible households, **I**nfectious households, and **R**ecovered households (we will incorporate deaths in the next section). We think of the health status as being a household characteristic, implicitly assuming a perfect rate of transmission within the household (they enjoy a passionate marriage), and also that recovery is experienced contemporaneously by all household members. For simplicity, we ignore the possibility that a vaccine puts an end to an epidemic before herd immunity is achieved.

In this section we seek to study the dynamics of a two-country SIR model in which the pandemic only generates cross-country externalities via contagion (and not via terms of trade effects), and in which households do not exert any pandemic-motivated social distancing. Hence, we assume that the infection has no effect on the ability to work and trade or mortality, and that agents are unaware of the threat of infection and their health status, which implies that they have no incentive to change their individual behavior. Labor supply and aggregate income are constant in each country and over time, because there are no deaths and households have no incentive to social distance. We relax these assumptions in Section 4, where we allow for deaths from the disease, but assume that agents remain unaware of the threat of infection and their health status, and hence continue to have no incentive to change their individual behavior. The result is a model in which the dynamics of the pandemic affect the evolution of the labor supply and aggregate income in each country. In Section 5 we go further and assume that agents understand that if they become infected, they have a positive probability of dying (an event that they, of course, do notice!). The possibility of dying generates behavioral responses to prevent contagion by reducing interactions.

In sum, the goal of this section is to understand how cross-country interactions motivated by economic incentives affect the spread of a pandemic in a world in which these interactions are *time-invariant* during the pandemic. It is important to emphasize, however, that the fixed measure of interactions chosen by each household is still endogenously shaped by the primitive parameters of our model, as described in Section 2. We will be particularly interested in studying the incidence and dynamics of the pandemic for different levels of trade integration, and different values of the primitive epidemiological parameters (the contagion rate conditional on a number of interactions and the recovery rate) in each country.

3.2 The Dynamic System

As argued above, for now, the population, technology and relative wage will all be time-invariant, so we can treat n_{ii} , n_{ij} , n_{ji} and n_{jj} as fixed parameters (though obviously their constant level is shaped by the primitives of the model).

The share of households of each type evolve according to the following laws of motion (we ignore time subscripts for now to keep the notation tidy):

$$\dot{S}_i = -2n_{ii} \times \alpha_i \times S_i \times I_i - n_{ij} \times \alpha_j \times S_i \times I_j - n_{ji} \times \alpha_i \times S_i \times I_j \quad (16)$$

$$\dot{I}_i = 2n_{ii} \times \alpha_i \times S_i \times I_i + n_{ij} \times \alpha_j \times S_i \times I_j + n_{ji} \times \alpha_i \times S_i \times I_j - \gamma_i I_i \quad (17)$$

$$\dot{R}_i = \gamma_i I_i \quad (18)$$

To better understand this system, focus first on how infections grow in equation (17). The first term $2n_{ii} \times \alpha_i \times S_i \times I_i$ in this equation captures newly infected households in country i . Sellers in i receive (in expectation) n_{ii} domestic buyers, while buyers meet up with n_{ii} domestic sellers. The household thus jointly has $2n_{ii}$ domestic contacts. In those encounters, a new infection occurs with probability α_i whenever one of the agents is susceptible (which occurs with probability S_i) and the other agent is infectious (which occurs with probability I_i).⁹ The second term of equation (17) reflects new infections of country i 's households that occur in the foreign country when susceptible buyers from i (of which there are S_i) visit foreign households with infectious sellers. There are n_{ij} of those meetings, leading to an new infection with probability α_j whenever the foreign seller is infectious (which occurs with probability I_j). Finally, the third term in (17) reflects new infections associated with susceptible sellers in country i receiving infectious buyers from abroad (country j). Each susceptible domestic buyer (constituting a share S_i of i 's population) has n_{ji} such meetings, which cause an infection with probability α_i whenever the foreign buyer is infectious (which occurs with probability I_j). The final term in equation (17) simply captures the rate at which infectious individuals recover (γ_i), and note that we assume that this recovery rate only depends on the country in which infected agents reside, regardless of where they got infected.

Once the equation determining the dynamics of new infections is determined, the one determining the change of susceptible agents in (16) is straightforward to understand, as it just reflects a decline in the susceptible population commensurate with new infections. Finally, equation (18) governs the transition from infectious households to recovered households.

In Section B of the Appendix, we provide further details on the numerical simulations of the two-country SIR model that we use in the figures below to illustrate our results, including a justification for the parameter values we use.

⁹In summing the buyer and seller domestic contact rates to obtain a domestic contact rate of $2n_{ii}$ for the household, we use the property of continuous time that there is zero probability that the buyer and seller are simultaneously infected at exactly the same instant.

3.3 The Closed-Economy Case

Our model reduces to a standard SIR model when there is no movement of people across countries, and thus no international trade. In such a case, the system in (16)-(18) reduces to

$$\begin{aligned} \dot{S}_i &= -\beta_i \times S_i \times I_i \\ \dot{I}_i &= \beta_i \times S_i \times I_i - \gamma_i I_i \\ \dot{R}_i &= \gamma_i I_i \end{aligned}$$

where $\beta_i = 2n_{ii}$ is the so-called contact rate. The dynamics of this system have been studied extensively since the pioneering work of Kermack and McKendrick (1927, 1932). Suppose that at some time t_0 , there is an outbreak of a disease which leads to initial infections $I_i(t_0) = \varepsilon > 0$, where ε is small. Because ε is small, $S_i(t_0)$ is very close to 1, and from the second equation, we have the standard result that if the so-called *basic reproduction number* $\mathcal{R}_{0i} = \beta_i/\gamma_i$ is less than one, then, $\dot{I}_i(t) < 0$ for all $t > t_0$, and the infection quickly dies out. In other words, when $\mathcal{R}_{0i} = \beta_i/\gamma_i < 1$ an *epidemic-free* equilibrium is globally stable. If instead $\mathcal{R}_{0i} = \beta_i/\gamma_i > 1$, the number of new infections necessarily rises initially and the share of susceptible households declines until the system reaches a period t^* at which $S_i(t^*) = \gamma_i/\beta_i$, after which infections decline and eventually go to 0. The steady-state values of $S_i(\infty)$ in this *epidemic* equilibrium is determined by the solution to this simple non-linear equation:¹⁰

$$\ln S_i(\infty) = -\frac{\beta_i}{\gamma_i} (1 - S_i(\infty)). \tag{19}$$

This equation admits a unique solution with $1 > S_i(\infty) > 0$.¹¹ Furthermore, because $S_i(\infty) < \gamma_i/\beta_i$ (since $S_i(t^*) = \gamma_i/\beta_i$ at the peak of infections), differentiation of (19) implies that the steady-state share of susceptible households $S_i(\infty)$ is necessarily decreasing in \mathcal{R}_{0i} . In sum, in the closed-economy case, $S_i(\infty) = 1$ as long as $\mathcal{R}_{0i} \leq 1$, but when $\mathcal{R}_{0i} > 1$, the higher is \mathcal{R}_{0i} , the lower is $S_i(\infty)$, and the more people will have been infected by the end of the epidemic.

3.4 The Open-Economy Case

We can now return to the two-country system in (16)-(18). We first explore the conditions under which a pandemic-free equilibrium is stable, and infections quickly die out worldwide, regardless of where the disease originated. For that purpose, it suffices to focus on the laws of motion for

¹⁰To see this, begin by writing

$$\frac{\dot{S}_i}{S_i} = -\beta_i I_i = -\frac{\beta_i}{\gamma_i} \dot{R}_i.$$

Now taking logs and integrating, and imposing $I_i(\infty) = 0$, delivers

$$\ln S_i(\infty) - \ln S_i(t_0) = -\frac{\beta_i}{\gamma_i} (1 - S_i(\infty) - R_i(0)).$$

Finally, imposing $\ln S_i(t_0) \simeq 0$ and $R_i(t_0) \simeq 0$, we obtain equation (19).

¹¹Equation (19) is obviously also satisfied when $S_i(\infty) = 1$, but this equilibrium is not stable when $\mathcal{R}_{0i} > 1$.

(S_i, S_j, I_i, I_j) evaluated at the pandemic-free equilibrium, in which $S_i = S_j \simeq 1$ and $I_i = I_j \simeq 0$. The Jacobian of this system is given by

$$J = \begin{bmatrix} 0 & 0 & -2\alpha_i n_{ii} & -(\alpha_j n_{ij} + \alpha_i n_{ji}) \\ 0 & 0 & -(\alpha_j n_{ij} + \alpha_i n_{ji}) & -2\alpha_j n_{jj} \\ 0 & 0 & 2\alpha_i n_{ii} - \gamma_i & \alpha_j n_{ij} + \alpha_i n_{ji} \\ 0 & 0 & \alpha_j n_{ij} + \alpha_i n_{ji} & 2\alpha_j n_{jj} - \gamma_j \end{bmatrix},$$

and the largest positive eigenvalue of this matrix (see Appendix D) is given by

$$\lambda_{\max} = \frac{1}{2} (2\alpha_i n_{ii} - \gamma_i) + \frac{1}{2} (2\alpha_j n_{jj} - \gamma_j) + \frac{1}{2} \sqrt{4(\alpha_j n_{ij} + \alpha_i n_{ji})^2 + ((2\alpha_i n_{ii} - \gamma_i) - (2\alpha_j n_{jj} - \gamma_j))^2}.$$

Since we are interested in finding necessary conditions for stability of this equilibrium (i.e., $\lambda_{\max} < 0$), and noting that λ_{\max} is increasing in n_{ij} and n_{ji} , we have that

$$\lambda_{\max} \geq \lambda_{\max}|_{n_{ij}=n_{ji}=0} = \max \{2\alpha_i n_{ii} - \gamma_i, 2\alpha_j n_{jj} - \gamma_j\}. \tag{20}$$

As a result, a pandemic-free equilibrium can only be stable whenever $2\alpha_i n_{ii}/\gamma_i \leq 1$ and $2\alpha_j n_{jj}/\gamma_j \leq 1$. In words, if the reproduction number \mathcal{R}_{0i} based only on domestic interactions (but evaluated at the world equilibrium value of n_{ii}) is higher than 1 in *any* country, the pandemic-free equilibrium is necessarily unstable, and the world will experience at least one period of rising infections along the dynamics of the pandemic. This result highlights the externalities that countries exert on other countries when the disease is not under control purely based on the domestic interactions of agents.

It is interesting to note that we achieve the exact same result when studying the global reproduction number \mathcal{R}_0 associated with the world equilibrium dynamics. Remember that \mathcal{R}_0 is defined as the expected number of secondary cases produced by a single (typical) infection starting from a completely susceptible population. Because our model maps directly to multigroup models of disease transmission, we can invoke (and verify) results from that literature to provide an alternative analysis of the stability of the pandemic-free equilibrium in our two-country dynamic system (cf., Hethcote, 1978, Hethcote and Thieme, 1985, van den Driessche and Watmough, 2002, Magal et al. 2016). In particular, it is a well-known fact that the pandemic-free equilibrium is necessarily stable if $\mathcal{R}_0 < 1$. In order to compute \mathcal{R}_0 , we follow the approach in Diekmann et al. (1990), and write the two equations determining the dynamics of infections as

$$\begin{bmatrix} \dot{I}_i \\ \dot{I}_j \end{bmatrix} = \underbrace{\begin{bmatrix} 2\alpha_i n_{ii} S_i & (\alpha_j n_{ij} + \alpha_i n_{ji}) S_i \\ (\alpha_j n_{ij} + \alpha_i n_{ji}) S_j & 2\alpha_j n_{jj} S_j \end{bmatrix}}_F \begin{bmatrix} I_i \\ I_j \end{bmatrix} - \underbrace{\begin{bmatrix} \gamma_i & 0 \\ 0 & \gamma_j \end{bmatrix}}_V \begin{bmatrix} I_i \\ I_j \end{bmatrix}.$$

The next generation matrix FV^{-1} (evaluated at $t = t_0$, and thus $S_i(t_0) = S_j(t_0) \simeq 1$) is given by

$$FV^{-1} = \begin{bmatrix} 2\alpha_i n_{ii} / \gamma_i & (\alpha_j n_{ij} + \alpha_i n_{ji}) / \gamma_j \\ (\alpha_j n_{ij} + \alpha_i n_{ji}) / \gamma_i & 2\alpha_j n_{jj} / \gamma_j \end{bmatrix}.$$

From the results in Diekmann et al. (1990), we thus have that

$$\mathcal{R}_0 = \rho(FV^{-1}),$$

where $\rho(FV^{-1})$ is the spectral radius of the next generation matrix. In our case, this is given by

$$\mathcal{R}_0 = \frac{1}{2} \left(\frac{2\alpha_i n_{ii}}{\gamma_i} + \frac{2\alpha_j n_{jj}}{\gamma_j} \right) + \frac{1}{2} \sqrt{\left(\frac{2\alpha_i n_{ii}}{\gamma_i} - \frac{2\alpha_j n_{jj}}{\gamma_j} \right)^2 + 4 \frac{(\alpha_j n_{ij} + \alpha_i n_{ji})^2}{\gamma_i \gamma_j}}. \quad (21)$$

As in the case of λ_{\max} in equation (20), we have that \mathcal{R}_0 is nondecreasing in n_{ij} and n_{ji} , and thus

$$\mathcal{R}_0 \geq \mathcal{R}_0|_{n_{ij}=n_{ji}=0} = \max \left\{ \frac{2\alpha_i n_{ii}}{\gamma_i}, \frac{2\alpha_j n_{jj}}{\gamma_j} \right\}. \quad (22)$$

This confirms again that the disease can only be contained (that is, the pandemic-free equilibrium is stable) only if both countries' disease reproduction rate based on their domestic interactions is less than one.¹² Therefore, even if a country has a strict disease environment that would prevent an epidemic under autarky, it may be drawn into a world pandemic in the open economy equilibrium, if its trade partner has a lax disease environment, as measured by its open economy domestic reproduction rate.

Having described the existence and stability of a pandemic-free equilibrium, we next turn to a situation in which $\mathcal{R}_0 > 1$ and the resulting contagion dynamics lead to a pandemic. Building on the existing literature on multigroup models of disease transmission, it is well known that whenever the global reproduction rate satisfies $\mathcal{R}_0 > 1$, there exists a unique asymptotically globally stable 'pandemic' equilibrium in which the growth in the share of *worldwide* infected households necessarily increases for a period of time, and then declines to a point at which infections vanish and the share of susceptible households in the population in each country ($S_i(\infty), S_j(\infty)$) takes a value strictly between 0 and 1 (see, for instance, Hethcote, 1978).¹³ Starting from equations (16)-(18), and going through analogous derivations as in the closed-economy case (see Appendix D), we obtain the following system of nonlinear equations pinning down the steady-state values ($S_i(\infty), S_j(\infty)$)

¹² Although the expressions for λ_{\max} and \mathcal{R}_0 appear different, it is straightforward to show that a necessary condition for both $\lambda_{\max} < 0$ and $\mathcal{R}_0 < 1$ is

$$\frac{2\alpha_i n_{ii}}{\gamma_i} + \frac{2\alpha_j n_{jj}}{\gamma_j} - \frac{2\alpha_i n_{ii}}{\gamma_i} \frac{2\alpha_j n_{jj}}{\gamma_j} + \frac{(\alpha_j n_{ij} + \alpha_i n_{ji})^2}{\gamma_i \gamma_j} < 1.$$

If either $2\alpha_i n_{ii} / \gamma_i > 1$ or $2\alpha_j n_{jj} / \gamma_j > 1$, this condition cannot possibly hold.

¹³ Proving global stability of the endemic equilibrium is challenging for some variants of the SIR model, but for the simple one in (16)-(18), featuring permanent immunity and no vital dynamics, global stability of the endemic equilibrium is implied by the results in Hethcote (1978), particularly section 6.

of the share of susceptible households in each country in that pandemic equilibrium:

$$\ln S_i(\infty) = -\frac{2\alpha_i n_{ii}}{\gamma_i} (1 - S_i(\infty)) - \frac{\alpha_j n_{ij} + \alpha_i n_{ji}}{\gamma_j} (1 - S_j(\infty)) \tag{23}$$

$$\ln S_j(\infty) = -\frac{2\alpha_j n_{jj}}{\gamma_j} (1 - S_j(\infty)) - \frac{\alpha_j n_{ij} + \alpha_i n_{ji}}{\gamma_i} (1 - S_i(\infty)). \tag{24}$$

Although we cannot solve this system in closed form, we can easily derive some comparative statics. In particular, total differentiating we find that the steady-state values of S_i and S_j are decreasing in n_{ii} , n_{jj} , n_{ij} , and n_{ji} , and are increasing in γ_i and γ_j (see Appendix D).

We summarize these results in this section with the following proposition (see Appendix D for a proof):

Proposition 5 *Assume that there is trade between the two countries (i.e., $\alpha_j n_{ij} + \alpha_i n_{ji} > 0$), which implies that the next generation matrix FV^{-1} is irreducible. If $\mathcal{R}_0 \leq 1$, the no-pandemic equilibrium is the unique stable equilibrium. If $\mathcal{R}_0 > 1$, the no-pandemic equilibrium is unstable, and there exists a unique stable endemic equilibrium with a steady-state featuring no infections ($I_i(\infty) = I_j(\infty) = 0$) and shares of susceptible agents $S_i(\infty) \in (0, 1)$ and $S_j(\infty) \in (0, 1)$ that satisfy equations (23) and (24).*

In Figure 1, we illustrate these analytical results by holding the infection rate in Country 1 (α_1) constant and varying the infection rate in Country 2 (α_2). The starting point is two identical countries with a common infection rate of $\alpha_1 = \alpha_2 = 0.04$. The rest of the parameter values are described in Appendix B. For this initial common infection rate, the global reproduction number is $\mathcal{R}_0 = 0.75$, and the open economy domestic reproduction rates are $\mathcal{R}_{01} = \mathcal{R}_{02} = 0.46$. Thus, the initial infection quickly dies out and there is no global pandemic. The fraction of recovered agents in the long run, $R_i(\infty)$, which is equal to the cumulative number of infected agents in the absence of deaths, is essentially zero in both countries. The left panel of Figure 1 plots $R_i(\infty)$ as a function of \mathcal{R}_0 as we progressively increase α_2 from 0.04 to 0.10. The value of \mathcal{R}_0 is monotone in α_2 and increases from 0.75 to 1.46. Hence, as the exogenous infection rate of Country 2 increases, the global reproduction rate increases beyond the critical value of 1, and the world experiences a global pandemic. Note how the fraction of the cumulative number of recovered agents rises rapidly once \mathcal{R}_0 increases beyond 1 and both countries go through increasingly severe pandemics. Note also the importance of cross-country contagion in the open economy. Even though nothing is changing in the domestic characteristics of Country 1, it is dramatically affected by the worsening conditions in Country 2. The right panel shows the evolution of the pandemic in Country 1 for different levels of severity of the disease environment in Country 2.¹⁴ The most severe and rapid pandemics are associated with the highest values of α_2 (the lightest curve in the graph). As α_2 declines and \mathcal{R}_0 falls and crosses the value of 1, the evolution of infections flattens and becomes longer, until the pandemic eventually disappears.

¹⁴The color of each curve, correspond to the colors of the points in the left panel.

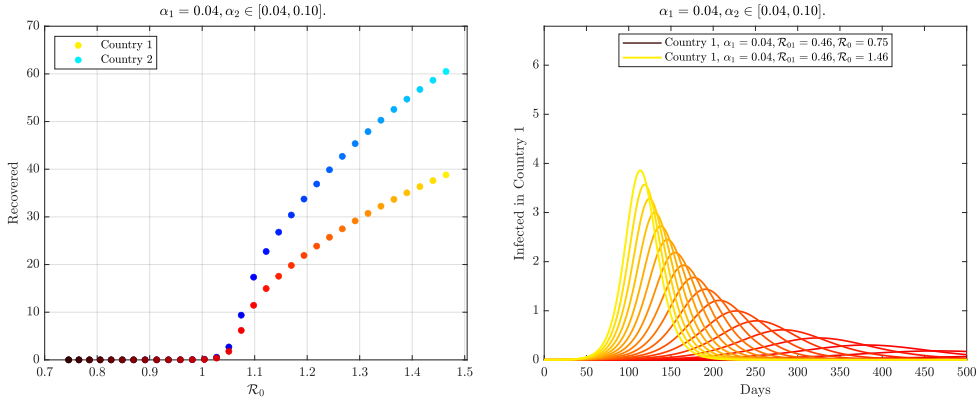


Figure 1: The Impact of Changes in the Exogenous Infection Rate in Country 2, α_2

The value of \mathcal{R}_0 is critical to determine the stability of a pandemic-free equilibrium. However, it is worth emphasizing that it is not critical to determine the existence of a pandemic cycle in *each* country. For values of \mathcal{R}_0 close enough to 1, an individual country can experience a pandemic, even if the world as a whole does not, if the declining number of cases in the other country is sufficiently large. Similarly, even if $\mathcal{R}_0 > 1$, some countries might not experience a pandemic when \mathcal{R}_0 is close enough to 1, even if the world economy as a whole does, since cases might be rising sufficiently fast in the other country. In Figure 1, in fact, cases rise slowly when the economy crosses the $\mathcal{R}_0 = 1$ threshold. At that point, pandemics are small and happen only in the sick country, while the number of cases in the healthy country remain essentially steady. The peak of infections in both countries is a smooth function of the value of α_2 .

3.5 Trade Integration and Global Pandemics

We now turn to the question of how globalization affects the prevalence and severity of a pandemic in both countries. In terms of the stability of a pandemic-free equilibrium, inspection of equations (20) and (22) might lead one to infer that avoiding a pandemic is always more difficult in a globalized world. On the one hand, it is obvious that, for given positive values of n_{ii} and n_{jj} , if the ratio α_i/γ_j is sufficiently high in *any* country in the world, a global pandemic affecting *all* countries cannot be avoided, even though the country with the lower ratio α_i/γ_j might well have avoided it under autarky. On the other hand, it would seem that even when $\alpha_i = \alpha_j$ and $\gamma_i = \gamma_j$, the max operator in (20) and (22) implies that the pandemic-free equilibrium is less likely to be stable in the open economy. It is important to emphasize, however, that n_{ii} and n_{jj} are endogenous objects and will naturally be lower, the lower are trade frictions, as formalized in Proposition 2. Still, it seems intuitive that globalization will typically foster more human interactions, as these are necessary to materialize the gains associated with trade integration, and that this will generally make it easier

for pandemics to occur.

To explore this more formally, let us first consider a fully symmetric world in which all primitives of the model (population size, technology, trade barriers, recovery rates, etc.) are common in both countries, so that we have $n_{ii} = n_{jj} = n_{dom}$, $n_{ij} = n_{ji} = n_{for}$, $\alpha_i = \alpha_j = \alpha$, and $\gamma_i = \gamma_j = \gamma$. In such a case, we have

$$\lambda_{\max} = 2\alpha(n_{dom} + n_{for}) - \gamma; \quad \mathcal{R}_0 = \frac{2\alpha(n_{dom} + n_{for})}{\gamma},$$

and it thus follows immediately from Proposition 3 that a decline in any (symmetric) international trade friction increases \mathcal{R}_0 and thus decreases the range of parameters for which a pandemic-free equilibrium is stable. Furthermore, in this same symmetric case, the steady-state share of susceptible households in the population is identical in both countries and implicitly given by

$$\ln S_i(\infty) = -\frac{2\alpha(n_{dom} + n_{for})}{\gamma} (1 - S_i(\infty)),$$

and thus not only the frequency but also the severity of the pandemic are higher the lower are (symmetric) trade frictions.

We summarize these results as follows:

Proposition 6 *Suppose that countries are symmetric, in the sense that $L_i = L$, $Z_i = Z$, $\Gamma_{ij} = \Gamma$, $\alpha_i = \alpha_j$, and $\gamma_i = \gamma$ for all i . Then, a decline in any (symmetric) international trade friction: (i) increases \mathcal{R}_0 , thus decreasing the range of parameters for which a pandemic-free equilibrium is stable, and (ii) increases the share of each country’s population that becomes infected during the pandemic when $\mathcal{R}_0 > 1$.*

Although we have so far focused on a fully symmetric case, the main results in this Proposition continue to hold true even if countries are not perfectly symmetric. More generally, and as noted in footnote 12, a necessary condition for the pandemic-free equilibrium to be stable is

$$\frac{2\alpha_i n_{ii}}{\gamma_i} + \frac{2\alpha_j n_{jj}}{\gamma_j} - \frac{2\alpha_i n_{ii}}{\gamma_i} \frac{2\alpha_j n_{jj}}{\gamma_j} + \frac{(\alpha_j n_{ij} + \alpha_i n_{ji})^2}{\gamma_i \gamma_j} < 1, \tag{25}$$

and thus what is key for the effects of reductions of trade and mobility barriers on the occurrence of pandemics is whether the left-hand-side of this expression increases or declines with those reductions in barriers.

Figure 2 illustrates part (i) of Proposition 6 for a case in which we introduce an asymmetry in the exogenous infection rate across countries but the parameter condition in (25) is still satisfied. We let $\alpha_1 = 0.04$ and $\alpha_2 = 0.07$ and study the cumulative number of recovered agents when we increase symmetric international trade frictions (t_{ij} , left panel) and mobility frictions (μ_{ij} , right panel). The first point on both graphs, when $t_{12} = t_{21} = \mu_{12} = \mu_{21} = 1$, is one of the cases we studied in Figure 1. The large infection rate in Country 2 generates a pandemic in both countries. Globalization is essential to generate this pandemic. As both graphs illustrate, as we increase

either tariffs or mobility restrictions, global interactions decline, and the total number of recovered agents decreases. Eventually, when the world is sufficiently isolated, the pandemic disappears and the pandemic-free equilibrium becomes stable. In both graphs, the value of \mathcal{R}_0 (plotted in orange and measured in the right axis) declines smoothly with frictions. The vertical line in the figure indicates the value of tariffs or mobility frictions, respectively, corresponding to $\mathcal{R}_0 = 1$.¹⁵ Clearly, both types of barriers generate similar qualitative reductions in $R_i(\infty)$, although for this specific set of parameter values, the migration restrictions needed to eliminate the pandemic are larger than the corresponding trade frictions.

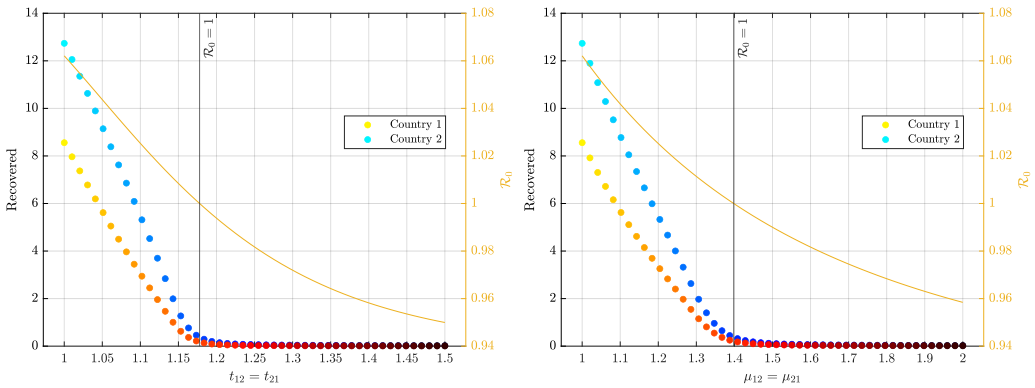


Figure 2: The Impact of Changes in Trade (left) and Mobility (right) Frictions

Figure 3 illustrates part (ii) of Proposition 6 by depicting the evolution of the fraction of agents infected for different levels of trade frictions. It corresponds to the exercise on the left panel of Figure 2 (with $\alpha_2 = 0.07 > 0.04 = \alpha_1$), so the lightest curves represent the evolution of the fraction of infected for the case with free trade ($t_{12} = t_{21} = 1$), and the darkest curves represent the case when $t_{12} = t_{21} = 1.5$. Clearly, as we increase tariffs, the epidemic in both countries becomes less severe and prolonged. The peak of the infection curve declines monotonically, as does the total number of recovered agents. Eventually, although impossible to appreciate in the graph, high tariffs eliminate the pandemic altogether and infections decline monotonically from their initial value.

Although in most cases condition (25) becomes tighter the lower are trade and mobility barriers, it is instructive to explore scenarios in which greater integration may actually *reduce* the risk of a pandemic. Suppose, in particular, that country j is a much lower risk environment, in the sense that α_j is very low – so infections are very rare – and γ_j is very high – so infected households

¹⁵Note that the value of $R_i(\infty)$, does not become zero for either country right at the point where tariffs or mobility frictions lead \mathcal{R}_0 to become greater than one. The reason is that even though one of the countries necessarily avoids a pandemic, it lingers close to its initial value of infections for a long time, which accumulates to a positive cumulative number of recovered agents.

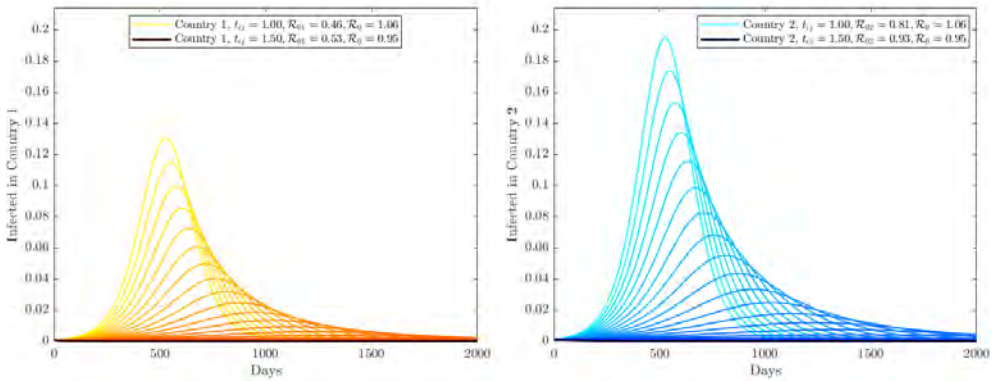


Figure 3: The Impact of Changes in Trade Frictions on the Evolution of Infections

quickly recover in that country. In the limiting case $\alpha_j \rightarrow 0$, condition (25) reduces to

$$\frac{2\alpha_i n_{ii}}{\gamma_i} + \frac{1}{\gamma_j} \frac{(\alpha_i n_{ji})^2}{\gamma_i} < 1.$$

For a high value of γ_j , it is then straightforward to see that the fall in country i 's domestic interactions n_{ii} associated with a reduction in international barriers makes this constraint laxer, even if n_{ji} goes up with that liberalization. In those situations it is perfectly possible for a pandemic-free equilibrium worldwide to only be stable when barriers are low. The intuition for this result is straightforward. In such a scenario, globalization makes it economically appealing for agents from a high-risk country to increase their interactions with agents in a low-risk country, and despite the fact that overall interactions by these agents may increase, the reduction in domestic interactions in their own high-risk environment is sufficient to maintain the disease in check.

More generally, beyond this limiting case, if countries differ enough in their epidemiological parameters, even when $\mathcal{R}_0 > 1$, it may well be the case that a decline in international trade frictions actually ameliorates the pandemic by incentivizing agents in the high-risk country to shift more of their interactions to the low-risk country.

We summarize this result as follows:

Proposition 7 *When the contagion rate α_i and the recovery rate γ_i vary sufficiently across countries, a decline in any international trade friction (i) decreases \mathcal{R}_0 , thus increasing the range of parameters for which a pandemic-free equilibrium is stable, and (ii) when $\mathcal{R}_0 > 1$, it reduces the share of the population in the high-risk (high α_i , low γ_i) country that becomes infected during the pandemic, and it may also reduce the share of the population in the low-risk (low α_i , high γ_i) country that become infected during the pandemic.*

An interesting implication of the last statement of Proposition 7 is that although it would seem intuitive that a healthy country should impose high restrictions to the inflow of individuals from a high-risk country where a disease has just broken out, in some cases such restrictions may in fact contribute to the spread of the disease in the high-risk country, which may then make a global pandemic inevitable unless mobility restrictions are set at prohibitive levels.

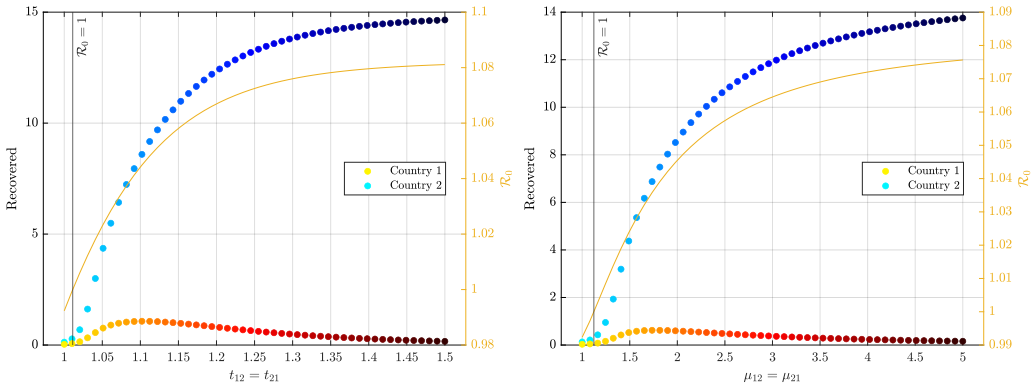


Figure 4: The Impact of Changes in Trade (left) and Mobility (right) Frictions with Large Differences in Infection Rates Across Countries ($\alpha_1 = 0.008$ and $\alpha_2 = 0.052$)

Figure 4 presents examples in which increases in trade and mobility barriers eliminate the possibility of a pandemic-free equilibrium (as predicted by part (i) of Proposition 7). As we argued above, to generate these examples we need large differences in exogenous infection rates. The figure makes the exogenous infection rate in the healthy country, Country 1, extremely small at $\alpha_1 = 0.008$, and sets $\alpha_2 = 0.052$ (a standard value).¹⁶ In both panels, increases in frictions now lead to increases in \mathcal{R}_0 (again depicted in orange and measured in the right axis). Without frictions the pandemic-free equilibrium is stable. Agents in Country 2 interact sufficiently with the healthier Country 1, which helps them avoid the pandemic. As both economies impose more frictions, domestic interactions increase rapidly, while foreign interactions drop. This is bad news for Country 2, since its larger infection rate now leads to a pandemic. Perhaps surprisingly, it is also bad news for Country 1 since, although it interacts less with Country 2, it does so sufficiently to experience a pandemic. Larger frictions, which decrease aggregate income in both countries smoothly, also worsen the pandemic in both countries, at least when frictions are not too large; a clear case for free trade and mobility. Of course, as frictions increase further, eventually they isolate Country 1 sufficiently and so the severity of its local pandemic declines. In autarky, Country 1 avoids the pandemic completely, but at a large cost in the income of both countries. In contrast, higher frictions always worsen the pandemic in Country 2. Contacts with the healthy country are

¹⁶Relative to the baseline parameters the example also lowers c to 0.1 and ϕ to 1.5. These additional changes increase the overall number of domestic and foreign interactions.

always beneficial, since they dilute interactions with locals, which are more risky.

In Figure 5 we illustrate part (ii) of Proposition 7 for the case with high differences in exogenous infection rates across countries that we presented in Figure 4. We focus on three specific exercises: A case with free trade where $t_{12} = t_{21} = 1$, another with intermediate tariffs where $t_{12} = t_{21} = 1.2$, and a third one where countries are in autarky. With free trade, there is no pandemic in either country. As we increase trade frictions, a pandemic develops in both countries, although it is much more severe in Country 2, the country with the higher exogenous infection rate. Still, the pandemic in Country 1 ends up infecting around 1% of the population. Moving to autarky eliminates the pandemic for Country 1, but makes it even more severe, faster, and with a higher peak, in Country 2. Closing borders helps the healthy country eliminate the pandemic only if trade is completely eliminated, and at the cost of a much more severe pandemic in Country 2 and larger income losses for everyone. Although Figure 5 uses countries of identical size and studies the case of changes in symmetric tariffs, we obtain very similar results when countries are asymmetric, or when Country 1, the healthy country, is the only country closing its borders. Similar examples can also be generated when considering mobility rather than trade frictions, as in the right panel of Figure 4. The essential ingredient for declines in international frictions to ameliorate the pandemic, on top of increasing incomes, is for countries to exhibit large asymmetries in epidemiological conditions.

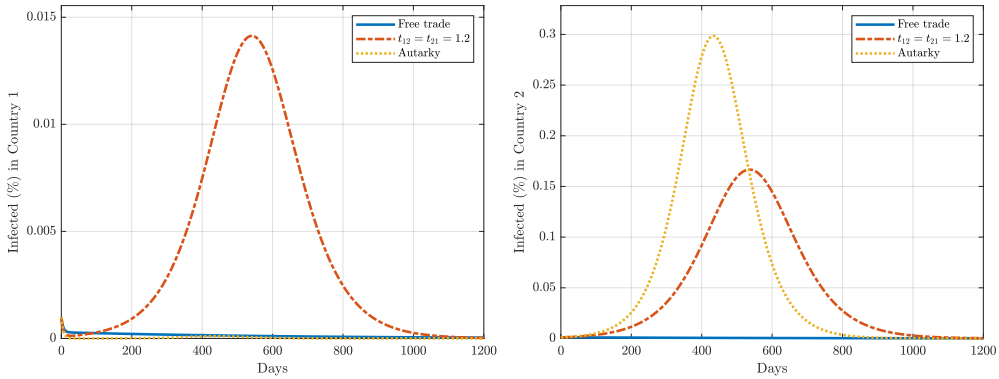


Figure 5: Evolution of Infections under Free Trade, Intermediate Trade Frictions, and Autarky with Large Differences in Infection Rates Across Countries ($\alpha_1 = 0.008$ and $\alpha_2 = 0.052$)

3.6 Transitional Dynamics: A Second Wave

When $\mathcal{R}_0 > 1$ and the world economy converges to the pandemic steady-state equilibrium in equations (23) and (24), convergence to that steady-state may entail significantly richer dynamics than in the closed-economy SIR model. In particular, in the open economy, integrating the dynamics of infections in each country using the initial conditions $S_i(0) = S_j(0) = 1$ and $R_i(0) = R_j(0) = 0$,

we have the following closed-form solutions for infections in each country at each point in time (I_{it} , I_{jt}) as a function of susceptibles in each country ($S_i(t)$, $S_j(t)$):

$$I_i(t) = 1 - S_i(t) + \frac{\log S_i(t) - \frac{\alpha_j n_{ij} + \alpha_i n_{ji}}{2\alpha_j n_{jj}} \log S_j(t)}{\frac{2\alpha_i n_{ii}}{\gamma_i} - \frac{\alpha_j n_{ij} + \alpha_i n_{ji}}{2\alpha_j n_{jj}} \frac{\alpha_i n_{ji} + \alpha_j n_{ij}}{\gamma_i}}, \tag{26}$$

$$I_j(t) = 1 - S_j(t) + \frac{\log S_j(t) - \frac{\alpha_i n_{ji} + \alpha_j n_{ij}}{2\alpha_i n_{ii}} \log S_i(t)}{\frac{2\alpha_j n_{jj}}{\gamma_j} - \frac{\alpha_i n_{ji} + \alpha_j n_{ij}}{2\alpha_i n_{ii}} \frac{\alpha_j n_{ij} + \alpha_i n_{ji}}{\gamma_j}}. \tag{27}$$

In the closed economy, there is necessarily a single wave of infections in the absence of a lockdown or other time-varying health policies. In contrast, in the open economy, it becomes possible for a country to experience multiple waves of infections, even in the absence of lockdowns or other time-varying health policies. From equations (26) and (27), the rate of growth of infections in each country is highest when $S_i(t) = S_j(t) = 1$, and declines as the number of susceptibles in each country falls, but the decline with $S_i(t)$ occurs at a different rate from the decline with $S_j(t)$. It is this difference that creates the possibility of multiple waves. If one country has a wham-bam epidemic that is over very quickly in the closed economy, while the other country has an epidemic that builds slowly in the closed economy, this creates the possibility for the country with the quick epidemic in the closed economy to have multiple peaks of infections in the open economy. The first peak reflects the rapid explosion of infections in that country, which dissipates quickly. The second peak, which is in general smaller, reflects the evolution of the pandemic in its trading partner.

In Figure 6 we provide an example of such a case, in which Country 1 experiences two waves of infections in the open economy, whereas Country 2 experiences a single, more prolonged and severe, wave. Country 1 features a large value of α_1 , but also a large value of γ_1 . Thus, although the infection rate is large, people remain contagious only briefly (perhaps because of a good contact tracing program). The resulting domestic reproduction rate $\mathcal{R}_{01} = 1.08$ and the resulting first peak of the pandemic is relatively small and quick. Since Country 1 is assumed ten times smaller than Country 2, its small initial pandemic has no significant effect on Country 2. There, the infection rate is much smaller, but the disease remains contagious for much longer, leading to a larger $\mathcal{R}_{01} = 1.66$, which also results in a global reproduction number $\mathcal{R}_0 = 1.66$.¹⁷ The result is a more protracted but also much longer singled-peaked pandemic in Country 2. This large pandemic does affect the smaller country through international economic interactions. The large country amounts for many of the interactions of the small country, which leads to the second wave of the pandemic in Country 2. Essential for this example is that countries have very different timings for their own pandemics in autarky, but also that in the open economy the relationship is very asymmetric, with the small country having little effect on the large country but the large country influencing the small country significantly. If the interactions are large enough in both directions, both countries will end up with a synchronized pandemic with only one peak.

¹⁷The parameter values used in the exercise are $\sigma = 4.5$, $L_1 = 2$, $L_2 = 20$, $d_{12} = d_{11}$, $c = 0.12$, $\alpha_1 = 0.69$, $\alpha_2 = 0.09$, $\gamma_1 = 2.1$ and $\gamma_2 = 0.18$. All other values are identical to the baseline case.

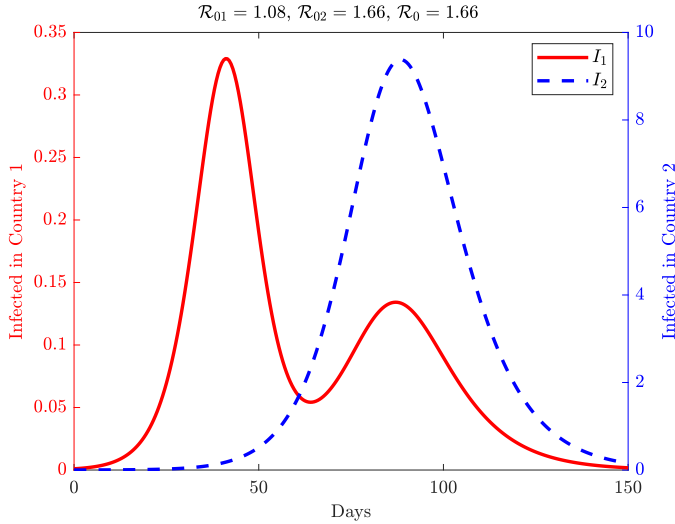


Figure 6: Multiple Waves of Infection in the Open Economy

4 General-Equilibrium Induced Responses

In this section, we allow the infection to affect mortality, but continue to assume that agents are unaware of the threat of infection.¹⁸ There are two main implications of introducing deaths. First, the pandemic will now affect aggregate income (and thus welfare) in both countries, as households that die as a result of the pandemic will forego the net present discounted value of their future lifetime utility, which in our model is proportional to real income. Second, because deaths are not immediately replaced by new inflows into the labor force, the pandemic will affect labor supply and aggregate demand in each country, and this will impact equilibrium relative wages and real income.¹⁹ In Section 5, we further generalize the analysis to allow individuals to internalize the threat of infection and incorporate behavioral responses.

With this new assumption, the shares of households of each type evolve according to the following laws of motion (where we again ignore time subscripts to keep the notation tidy):

$$\dot{S}_i = -2n_{ii}(\mathbf{w}) \times \alpha_i \times S_i \times I_i - [n_{ij}(\mathbf{w}) \times \alpha_j + n_{ji}(\mathbf{w}) \times \alpha_i] \times S_i \times I_j \tag{28}$$

$$\dot{I}_i = 2n_{ii}(\mathbf{w}) \times \alpha_i \times S_i \times I_i + [n_{ij}(\mathbf{w}) \times \alpha_j + n_{ji}(\mathbf{w}) \times \alpha_i] \times S_i \times I_j - (\gamma_i + \eta_i) I_i \tag{29}$$

$$\dot{R}_i = \gamma_i I_i \tag{30}$$

$$\dot{D}_i = \eta_i I_i \tag{31}$$

¹⁸We implicitly assume that if one of the household members dies, the other one does too. So it is not only a passionate marriage, but also a *romantic* one (in the narrow sense of the word).

¹⁹We could easily introduce a set of agents that are symptomatic infected agents who also reduce their labor supply, but that would complicate the analysis and blur the comparison with the results in the previous section.

There are two main differences between this dynamic system and the one above in (16)-(18). First, we now have four types of agents, as some infected agents transition to death rather than recovery. The rate at which infected agents die is given by η_i , and as in the case of the rate of recovery γ_i , it only depends on the country in which infected agents reside, and not on where they got infected. Second, we now need to make explicit the dependence of the contact rates $n_{ii}(\mathbf{w})$, $n_{ij}(\mathbf{w})$ and $n_{ij}(\mathbf{w})$ on the vector of equilibrium wages \mathbf{w} . As the changes in each country's population caused by deaths affect wages, these contact rates are no longer time invariant, and evolve endogenously over the course of the pandemic. In particular, the equilibrium wage vector is determined by the following goods market clearing condition:

$$\sum_{j \in \mathcal{J}} \pi_{ji}(\mathbf{w}) w_j (1 - D_j) L_j = w_i (1 - D_i) L_i,$$

where remember that $\pi_{ij}(\mathbf{w})$ and $n_{ij}(\mathbf{w})$ are given by (9) and (15), respectively.

We now show that this endogeneity of wages introduces a form of general equilibrium social distancing into the model. In particular, if the country with a worse disease environment experiences more deaths, its relative wage will rise. As this country's relative wage increases, its varieties become relatively less attractive to agents in the country with the better disease environment. Therefore, purely from the general equilibrium force of changes in relative labor supplies, agents in the healthy country engage in a form of endogenous social distancing, in which they skew their interactions away from the country with a worse disease environment, as summarized in the following proposition (see Appendix A.8 for a proof):

Proposition 8 *If country j experiences more deaths than country i , the resulting change in relative wages (w_j/w_i) leads country i to reduce its interactions with country j and increase its interactions with itself (general equilibrium social distancing).*

It is worth stressing that even if one of the countries features more favorable primitive health parameters than the other one, which country appears *de facto* more unhealthy can change over the course of the pandemic if the two countries' waves of infection are staggered in time. In the initial stages of the pandemic one country may experience a larger relative reduction in its labor supply (leading to endogenous social distancing in the other country), while in the later stages of the pandemic the other country experiences a larger relative reduction in its labor supply (leading to the opposite pattern of endogenous social distancing).²⁰

Another straightforward implication of explicitly modeling deaths is that they naturally affect aggregate income in both countries. More specifically, whenever changes in trade or mobility barriers affect population, aggregate real income ($w_i L_i / P_i$) and aggregate welfare ($W_i L_i$) are directly impacted by trade-induced changes in population. Because around $\mathcal{R}_0 = 1$ deaths are particularly

²⁰ Although we have established this general equilibrium social distancing mechanism using death as the source of changes in relative labor supplies, if the disease also were to reduce the productivity of workers while they are infected, this additional source of labor supply movements would naturally exacerbate the general equilibrium interactions between countries.

responsive to changes in trade frictions, this effect is not necessarily negligible when evaluating the welfare implications of trade in a world with global pandemics.

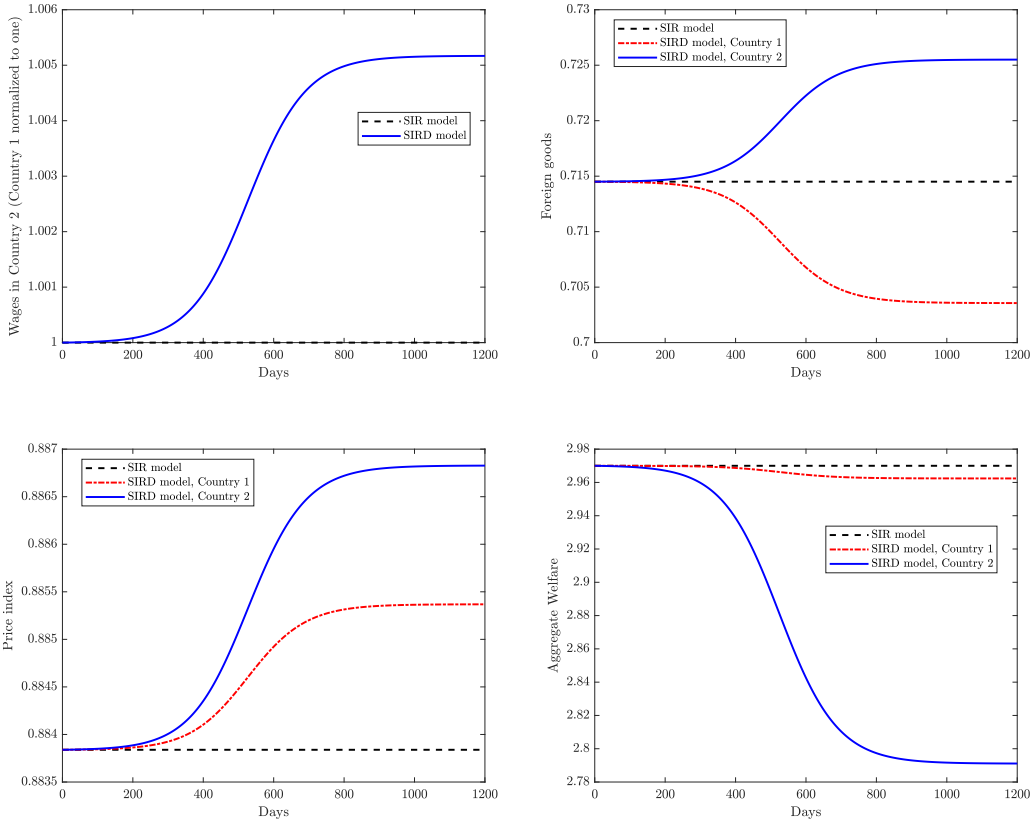


Figure 7: General Equilibrium Induced Social Distancing

We close this section by illustrating the result in Proposition 8 with a numerical example, where we let $\eta_1 / (\eta_1 + \gamma_1) = 0.01$ and $\eta_2 / (\eta_2 + \gamma_2) = 0.50$. Namely, we let the death rate among the infected be 1% in Country 1 and, an admittedly extreme, 50% in Country 2. The large difference in death rates amplifies the general equilibrium effects. The rest of the parameters are set to their baseline, symmetric values, across countries. Figure 7 presents the results. We denote by ‘SIRD model’ the case in which we incorporate deaths. For comparison purposes, we also present results for the case when $\eta_1 = \eta_2 = 0$, which we label the ‘SIR model.’ The larger death rate in Country 2 leads to a relative decrease in its labor supply, which increases relative wages, as illustrated in the top-left panel. Since the countries are otherwise symmetric and we chose the wage of Country 1 as

the numéraire, only the wage of Country 2 increases above one in the case where death rates are positive. The resulting increase in relative wage is small (0.5%) even though about 6% of agents end up dying in Country 2. Labor supply falls, but so does the aggregate demand for goods in that country. The larger wage in Country 2 implies that both countries bias their consumption towards Country 1 varieties. As the top-right panel illustrates, the consumption of foreign varieties increases in Country 2 but falls in Country 1. Of course, we see the opposite effect on domestic varieties although the adjustments are smaller. Ultimately, agents in both countries consume less varieties, which increases the price index in both countries, although by more in Country 2 (see the bottom-left panel). Real income falls in Country 1, both per capita and in aggregate, because of this increase in the price index. In contrast, in Country 2, real income per capita rises, because the wage increases by more than the price index. Nevertheless, aggregate real income falls as result of the reduction in labor supply from deaths (bottom-right panel).

5 Behavioral Responses

Up to this point, we have assumed that agents do not change their behavior during the pandemic, unless changes in relative wages induce them to do so. Implicitly, we were assuming that although households may observe that other households are dying, they do not understand the underlying cause of those deaths and go on with their lives.

In this section, we instead consider the more realistic (but also more complicated) case in which households realize that the deaths they observe are related to the outbreak of a pandemic. Following the approach in Farboodi et al. (2020), we continue to assume, however, that all infected individuals are asymptomatic, in the sense that household behavior is independent of their specific health status, though their actual behavior is shaped by their expectation of the probability with which they are susceptible, infected, or recovered households. How is that expectation formed? A natural assumption is that agents have rational expectations and that their belief of the probability with which they have a specific health status is equal to the share of the population in their country with that particular health status.²¹

We denote the individual beliefs of the probability of being infected, susceptible recovered or dead with lowercase letters, except for their belief of their death rate, which we denote by $k_i(t)$ (instead of $d_i(t)$) to avoid a confusion with the notation we used for distance. The maximization

²¹This may raise the question among some readers as to how households are able to form this belief if, according to our assumptions, nobody observes their own health status. It suffices to assume, however, that agents have common knowledge of all parameters of the model, and form rational expectations of the path of the pandemic. For the latter, it suffices to assume that agents observe pandemic-related deaths at the outbreak of the disease. More specifically, at $t = 0$, notice from equation (31) that (i) I_{i0} can be obtained from $I_{i0} = D_0\eta_i$ since $D_{-1} \simeq 0$; (ii) $R_{i0} \simeq 0$; and (iii) S_{it} is then trivially $S_{i0} = 1 - I_{i0} - R_{i0} - D_{i0}$. With this initial condition, agents can solve for the future path of the pandemic using rational expectations.

problem of the individual, for known $i_i(0)$, $s_i(0)$ and $k_i(0) = 0$, is given by

$$\begin{aligned}
 W_i^s(0) &= \max_{n_{ii}(\cdot), n_{ij}(\cdot)} \int_0^\infty e^{-\xi t} [[Q_i(n_{ii}(t), n_{ij}(t)) - C_i(n_{ii}(t), n_{ij}(t))] (1 - k_i(t))] dt \\
 \text{s.t.} \quad & \dot{s}_i(t) = -s_i(t) \left[(\alpha_i n_{ii}(t) + \alpha_i n_{ii}^*(t)) I_i(t) + (\alpha_j n_{ij}(t) + \alpha_i n_{ji}^*(t)) I_j(t) \right], \\
 & \dot{i}_i(t) = s_i(t) \left[(\alpha_i n_{ii}(t) + \alpha_i n_{ii}^*(t)) I_i(t) + (\alpha_j n_{ij}(t) + \alpha_i n_{ji}^*(t)) I_j(t) \right] \\
 & \quad - (\gamma_i + \eta_i) i_i(t), \\
 & \dot{k}_i(t) = \eta_i i_i(t),
 \end{aligned}$$

where ξ is the rate of time preference, and where from equation (6),

$$Q_i(n_{ii}(t), n_{ij}(t)) = w_i(t) \left(\sum_{j \in \mathcal{J}} n_{ij}(t) \left(\frac{\tau_{ij} w_j(t)}{Z_j} \right)^{1-\sigma} \right)^{\frac{1}{(\sigma-1)}},$$

and

$$C_i(n_{ii}(t), n_{ij}(t)) = \frac{c}{\phi} \sum_{j \in \mathcal{J}} \mu_{ij} (d_{ij})^\rho \times (n_{ij}(t))^\phi.$$

Notice that we denote with an asterisk variables chosen by *other* households that affect the dynamics of infection of a given household.²² In equilibrium, aggregate consistency implies that $i_i(t) = I_i(t)$, $s_i(t) = S_i(t)$, and $k_i(t) = D_i(t)$. Implicitly, we are assuming that agents decide their optimal path of $n_{ii}(\cdot)$ and $n_{ij}(\cdot)$ at period zero and commit to following it. Otherwise, without commitment, at some future period and conditional on being alive, agents would want to reoptimize their choices by solving the problem above but setting $k_i(t) = 0$.²³

The Hamiltonian of the problem faced by each household is given by

$$\begin{aligned}
 & H(s, i, n_{ii}, n_{ij}, \theta^i, \theta^s, \theta^k) \\
 &= [Q_i(n_{ii}(t), n_{ij}(t)) - C_i(n_{ii}(t), n_{ij}(t))] (1 - k_i(t)) e^{-\xi t} \\
 & \quad - \theta_i^s(t) s_i(t) [(\alpha_i n_{ii}(t) + \alpha_i n_{ii}^*(t)) I_i(t) + (\alpha_j n_{ij}(t) + \alpha_i n_{ji}^*(t)) I_j(t)] \\
 & \quad + \theta_i^i(t) [s_i(t) [(\alpha_i n_{ii}(t) + \alpha_i n_{ii}^*(t)) I_i(t) + (\alpha_j n_{ij}(t) + \alpha_i n_{ji}^*(t)) I_j(t)] - (\gamma_i + \eta_i) i_i(t)] \\
 & \quad + \theta_i^k(t) \eta_i i_i(t).
 \end{aligned}$$

Hence, the optimality condition with respect to the choice of n_{ij} is

$$\left[\frac{\partial Q_i(n_{ii}(t), n_{ij}(t))}{\partial n_{ij}(t)} - \frac{\partial C_i(n_{ii}(t), n_{ij}(t))}{\partial n_{ij}(t)} \right] (1 - k_i(t)) e^{-\xi t} = [\theta_i^s(t) - \theta_i^i(t)] s_i(t) \alpha_j I_j(t), \quad (32)$$

²²For instance, though the aggregate domestic rate of contact in i is $2\alpha_i n_{ii}$, a household has no control over how many buyers visit the household's seller, so the household only controls the rate $\alpha_i n_{ii}$ of contacts generated by the household's buyer.

²³The reason for this is that the probability of deaths acts like non-exponential discounting in the value function solved by agents, and it is well-understood that non-exponential discounting creates a wedge between the solution of dynamic problems with and without commitment. Farboodi et al. (2020) bypass this issue by assuming that, instead of foregoing future utility when dying, agents pay a one-time utility cost (or value of life) at the moment they die.

while the optimality conditions associated with the co-state variables are given by:

$$-\dot{\theta}_i^s(t) = -[\theta_i^s(t) - \theta_i^i(t)] [(\alpha_i n_{ii}(t) + \alpha_i n_{ii}^*(t)) I_i(t) + (\alpha_j n_{ij}(t) + \alpha_i n_{ji}^*(t)) I_j(t)], \quad (33)$$

$$-\dot{\theta}_i^i(t) = \eta_i \theta_i^k(t) - (\gamma_i + \eta_i) \theta_i^i(t), \quad (34)$$

$$-\dot{\theta}_i^k(t) = -[Q_i(n_{ii}(t), n_{ij}(t)) - C_i(n_{ii}(t), n_{ij}(t))] e^{-\xi t}. \quad (35)$$

Finally, the transversality conditions are

$$\begin{aligned} \lim_{t \rightarrow \infty} \theta_i^i(t) i_i(t) &= 0, \\ \lim_{t \rightarrow \infty} \theta_i^s(t) s_i(t) &= 0, \\ \lim_{t \rightarrow \infty} \theta_i^k(t) k_i(t) &= 0. \end{aligned}$$

To complete the description of the model, we need to specify the general equilibrium determination of wages. As in the version of our model with deaths in Section 4, we again have that wages are determined by the following goods market clearing condition:

$$\sum_{j \in \mathcal{J}} \pi_{ji}(\mathbf{w}, t) \times w_j(t) \times (1 - D_j(t)) L_j = w_i(t) \times (1 - D_i(t)) \times L_i.$$

Importantly, however, the trade shares $\pi_{ji}(\mathbf{w}, t)$ are now impacted by the fact that the level of interactions $n_{ij}(t)$ are directly affected by the dynamics of the pandemic. Still, computationally, it is straightforward to solve for a dynamic equilibrium in which $\pi_{ij}(\mathbf{w}, t) = X_{ij}(t) / \sum_{\ell \in \mathcal{J}} X_{i\ell}(t)$, and $X_{ij}(t) = n_{ij}(t) p_{ij}(t) q_{ij}(t) (1 - D_i(t)) L_i$. More specifically, the dynamic model can be solved through a backward shooting algorithm (see Appendix E for details).

This is obviously a rather complicated system characterized by several differential equations, and two (static) optimality conditions for the choices of n_{ii} and n_{ij} in each country. Nevertheless, we are able to show analytically that the solution to this problem necessarily involves individual-level social distancing. In the absence of a pandemic, households equate the marginal utility from sourcing varieties from each location to the marginal cost of sourcing those varieties. During a pandemic, households internalize that the interactions involved in sourcing varieties expose them to infection, which leads them to reduce interactions until the marginal utility from those interactions exceeds the marginal cost, as summarized in the following proposition (proven in Appendix A.9).

Proposition 9 *Along the transition path, $\theta_i^s(t) - \theta_i^i(t) \geq 0$ for all t , which implies:*

$$\frac{\partial Q_i(n_{ii}(t), n_{ij}(t))}{\partial n_{ij}(t)} > \frac{\partial C_i(n_{ii}(t), n_{ij}(t))}{\partial n_{ij}(t)}, \quad \text{as long as } I_j(t) > 0.$$

An implication of this result is that the pandemic generically has a larger impact on foreign interactions than on domestic interactions. This implication can be seen by re-arranging the

optimality condition (32) and substituting for the marginal utility and marginal cost for interactions:

$$\frac{1}{n_{ij}} \frac{n_{ij} q_{ij}^{\frac{\sigma-1}{\sigma}}}{\sum_{\ell \in \mathcal{J}} n_{i\ell} q_{i\ell}^{\frac{\sigma-1}{\sigma}}} Q_i = \frac{1}{n_{ij}} c \mu_{ij} d_{ij}^{\rho} n_{ij}^{\phi} + \frac{[\theta_i^s(t) - \theta_i^i(t)] s_i(t) \alpha_j I_j(t)}{(1 - k_i(t)) e^{-\xi t}},$$

where the term on the left-hand side is the marginal utility from interactions; the first term on the right-hand side is the marginal cost of interactions; and the second term on the right-hand side is the wedge capturing the threat of infection. As foreign interactions are generically a smaller share of the consumption index than domestic interactions, the fraction on the left-hand side is generically smaller for foreign interactions ($i \neq j$). Therefore, as a pandemic emerges and the threat of infection becomes positive, a larger reduction in n_{ij} is generically needed for foreign interactions, in order to raise the marginal utility on the left-hand side until it is equal to the marginal cost plus the positive wedge capturing the threat of infections on the right-hand side.

We now illustrate some of these implications of behavioral responses for the case of symmetric countries. We use the baseline parameters with $\alpha_i = 0.1$, $\gamma_i + \eta_i = 0.2$, and $\eta_i / (\eta_i + \gamma_i) = 0.0062$ (a 0.62% death rate among those infected) for all i . We also show a specification with half the death rate of $\eta_i / (\eta_i + \gamma_i) = 0.003$ for all i , as well as the case without behavioral responses from the previous section. As we choose the wage in one country as the numéraire, with symmetric countries, the relative wage is also equal to one and constant over time. In the absence of any behavioral responses, this constant relative wage implies that both the mass of varieties and price index are constant over time, as shown in the Proof of Proposition A.4. In contrast, in the presence of behavioral responses, households reduce the intensity of their interactions in response to the threat of infection, which leads to changes in the mass of varieties and the price index over time.

In the top-left panel of Figure 8, we show the percentage of individuals infected in Country 2 for all three specifications (with symmetry the figure for Country 1 is identical). Households' behavioral response of reducing interactions leads to a "flattening of the curve of the pandemic," such that the pandemic has lower peak and lower cumulative infections, but takes longer to subside. Clearly, the larger the death rate, the stronger the behavioral response and the flatter the resulting curve of infections. The top-right panel in Figure 8 presents the resulting evolution of cumulative deaths in Country 2. Behavioral responses delay and reduce total deaths, with the level (and proportional reduction) larger, the larger the death rate. Naturally, the behavioral response and the associated reductions in the number of deaths come at an economic cost for survivors. As the bottom-left panel shows, the reductions in the number of purchased domestic and foreign varieties increase the price index in each country, which results in a corresponding decline in real income. This increase in the price index, and reduction in real income, is larger the stronger the behavioral response, and hence increases with the death rate. Finally, the bottom-right panel displays the trade over GDP ratio (calculated as imports plus exports over GDP). In the example, trade/GDP falls from about 0.45 to less than 0.25 when the death rate is 0.3%, and to 0.17 when the death rate is 0.62%. Therefore, the flattening of the curve of infections and reduction in the number

of deaths comes at the cost of lower trade and real income. Of course, behavioral responses are ex-ante privately optimal, so it is not surprising that they improve individual welfare.²⁴

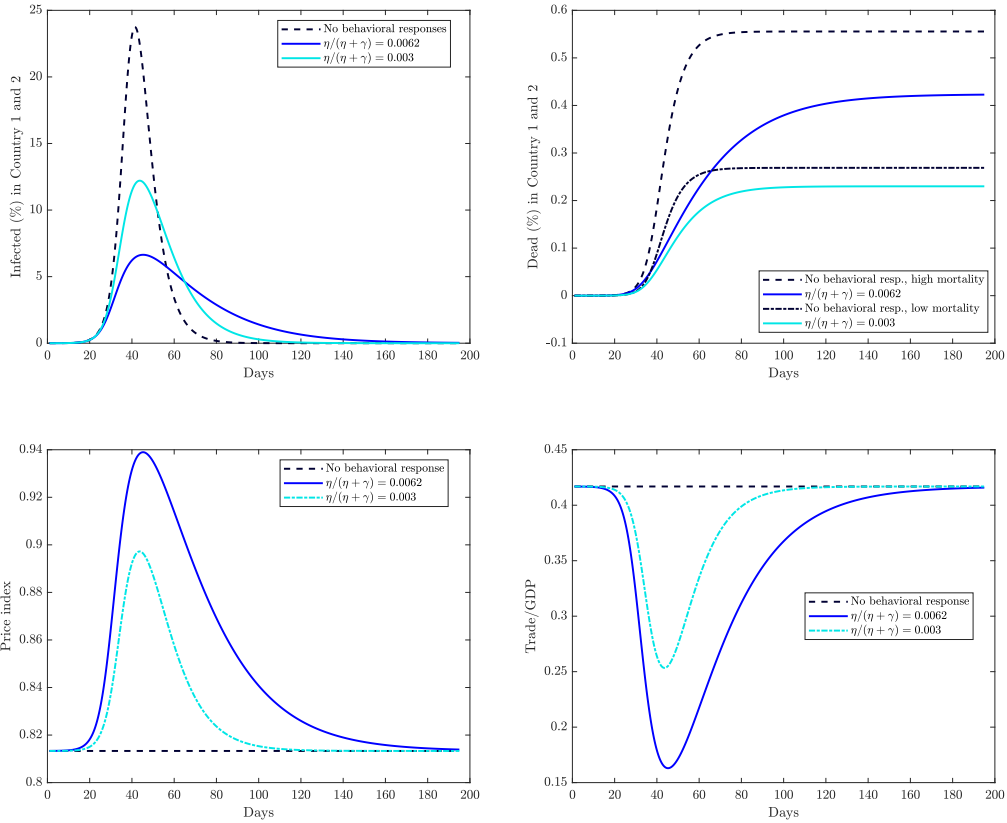


Figure 8: Behavioural Responses with Symmetric Countries for Various Death Rates

The presence of behavioral responses in the model thus leads to endogenous social distancing that has both economic and epidemiological implications. Households keep reducing interactions until the (monotonically decreasing) reproduction number, $\mathcal{R}_0 \times S_i(t)$, falls below 1. Once this reproduction number crosses that threshold, interactions start growing again, as herd immunity reduces the number of infections. An implication is that the magnitude of households' behavioral responses depends crucially on the value of \mathcal{R}_0 . The larger this value, the larger the resulting behavioral response. Furthermore, the model with behavioral responses results in reproduction numbers that linger closer to one as economic activity endogenously recovers, once the worst of the

²⁴It is worth stressing that these responses are not necessarily socially optimal due to the externalities that agents exert on other agents when traveling.

pandemic has passed.

The value of mobility and trade frictions plays an important role in shaping the magnitude and pattern of behavioral responses. First, with symmetric countries, higher mobility and trade frictions imply a reduction in the overall volume of human interactions, which leaves less scope for behavioral responses. Second, higher mobility and trade frictions imply that more of the burden of adjustment falls on domestic rather than foreign transactions. In Figure 9, we show the evolution of the trade/GDP ratios for symmetric countries for two different levels of mobility (left panel) and trade (right panel) frictions and the baseline values of our other parameters. As discussed above, in the symmetric case without behavioral responses, all human contacts $n_{ii}(t)$ and $n_{ij}(t)$ are constant in time, which implies that mobility and trade frictions only reduce the level of the trade/GDP ratios. Once we incorporate behavioral responses, trade/GDP follows the trajectory of the pandemic. The larger value of trade frictions reduces trade openness, which dampens the absolute magnitude of the behavioral response, although trade openness can end up falling to quite low levels. In this example with 10% trade frictions, ($t_{12} = t_{21} = 1.1$), trade essentially falls to zero in the most severe phase of the pandemic. For each level of trade frictions, behavioral responses reduce the total number of deaths, and for the parameter values considered here, higher trade and mobility frictions also reduce the total number of deaths.

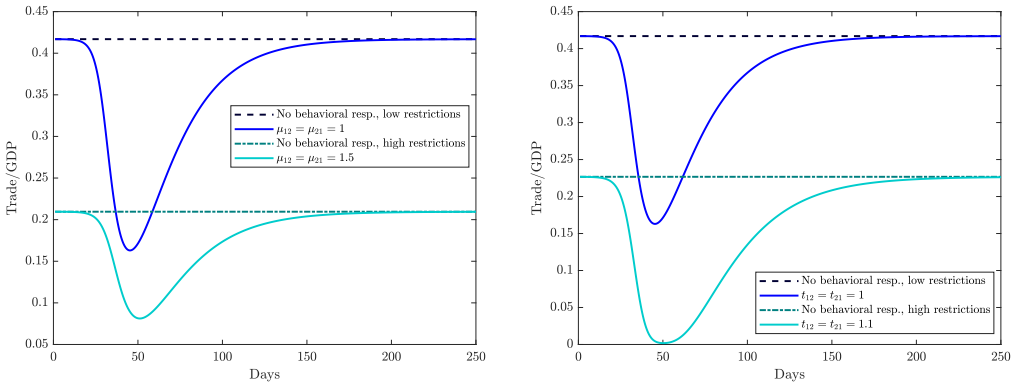


Figure 9: The Effect of Mobility and Trade Frictions on Trade/GDP with Behavioural Responses

We next illustrate some of the implications of our model when countries are asymmetric. We focus on a case in which countries differ in their mortality rate, where remember that we assume that mortality is determined by the country in which a household lives rather than the country in which it was infected. We let Country 1 have a relatively low mortality rate of 0.3% and we leave the mortality rate of Country 2 at the higher baseline value of 0.62%. Figure 10 presents the results. The top-left panel shows the percent of infections in each country. As benchmarks, we also display the average of infections in the two countries, as well as infections in the case of two

symmetric countries with an average mortality rate of 0.46% (the mean of 0.3 and 0.62%). There is a stronger behavioral response in the high-mortality Country 2 because households internalize the greater risk that infection leads to death, which results in a “flatter” curve of infections in this country. The low-mortality Country 1 ends up with about 10% higher total infections, because of its more subdued behavioral response. However, its lower mortality rate implies that it ends up with only about half the total number of deaths. This asymmetric behavioral response implies that Country 1 is a relatively dangerous destination for doing business in the early stages of the pandemic, but a relatively safe destination in the later stages of the pandemic, since it reaches herd immunity faster. Comparing the average response for the world with asymmetric countries to the response in the symmetric case with average mortality rates illustrates the implied aggregate effects from differences across countries in mortality rates. In the asymmetric case, the world’s infection curve is marginally flatter than in a symmetric world with average mortality rates.

The top-right panel in Figure 10 displays Country 1’s relative wage. As a result of the smaller behavioral response in this lower mortality country, there is a greater risk of infection in Country 1 in the early stages of the pandemic, which leads to a decline in demand for this country’s varieties and a fall in its relative wage. Once Country 1’s infection rate falls, demand for its varieties recovers, and hence so does its wage. Eventually, once Country 1’s infection rate falls below that of Country 2, it becomes the relatively safe environment in which to source varieties, and its relative wage rises temporarily above one, before falling back to one as the pandemic ends. Therefore, these behavioral responses in general equilibrium with asymmetric countries lead to demand effects that reduce the relative wage of the country with a relatively higher infection rate. In addition, as shown in the previous section, there is another general equilibrium effect from changes in relative labor supply. A country with a higher death rate experiences a reduction in its relative labor supply, which leads to an increase in its relative wage. The top-right panel of Figure 10 shows the balance of these forces, and demonstrates that relative demand effects generally dominates and overturns the result in Section 4 linking higher death rates to higher relative wages.

As before, the stronger behavioral response in Country 2 as a result of its higher mortality rate comes with greater economic costs. Country 2’s reduction in domestic and foreign purchases raises its price index and reduces its real income. The effect on the price index in Country 1 is more nuanced. Country 1 also reduces domestic and foreign interactions, which tends to increase its price index. However, the decline in its relative wage during the first part of the pandemic reduces the price of domestic varieties. The bottom-left panel in Figure 10 shows how these forces result in a price index with multiple peaks. Overall, the effect of the pandemic on the real income of Country 1 is negative but substantially smaller in magnitude than in Country 2. As shown in the bottom-right panel, the reduction in human interactions from social distancing reduces trade openness dramatically, particularly in Country 2, where behavioral responses are stronger. The asymmetry in mortality rates between the two countries initially leads to a larger reduction in trade openness than in a symmetric world with average mortality rates, in part because the behavioral response of Country 2 is particularly strong in the earlier phases of the pandemic. Later in the pandemic,

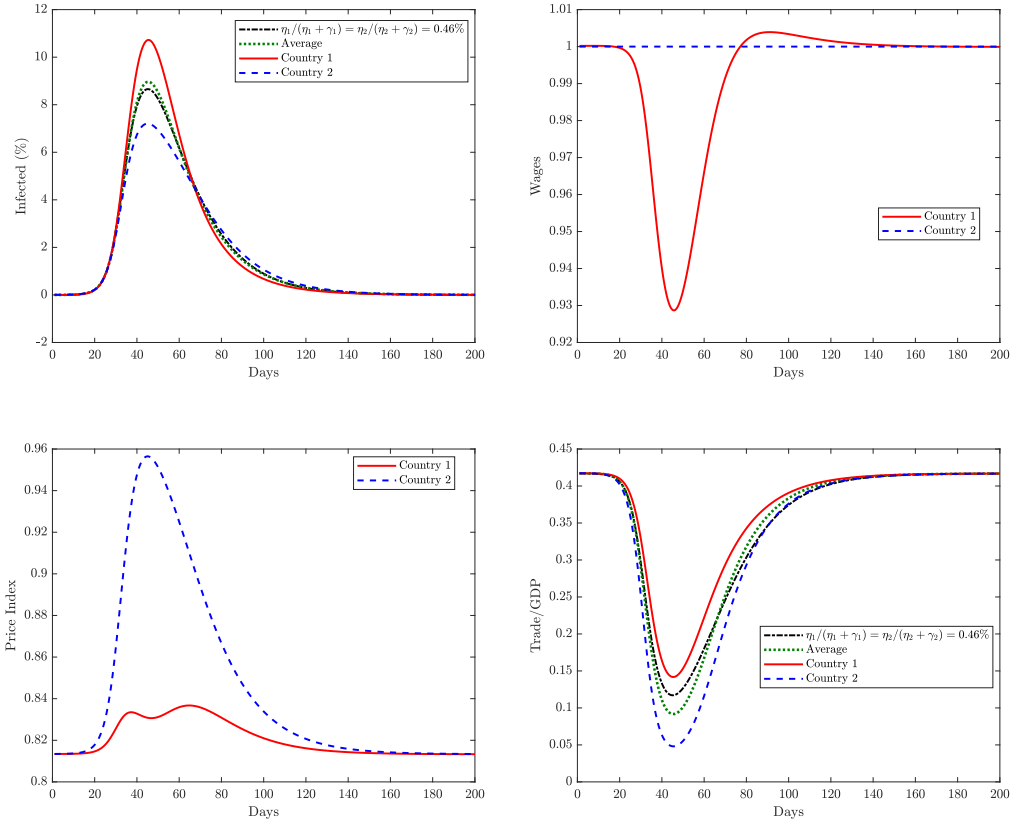


Figure 10: Behavioural Responses with Asymmetric Mortality Rates

the asymmetric case has higher trade openness than in a symmetric world, because the initially subdued behavioral response of Country 1 creates a more pronounced and faster wave of infections.

Adjustment Costs and the Risk of a Pandemic

Despite the potential for significant disruptions in international trade during a pandemic, a clear implication of the first-order condition (32) is that as long as $I_i(t) = I_j(t) = 0$, human interactions are at the same level as in a world without the potential for pandemics. In other words, although we have generated rich dynamics of international trade during a pandemic, as soon as this pandemic is overcome (via herd immunity or the arrival of a vaccine), our model predicts that life immediately goes back to normal. We next explore an extension of our model that explores the robustness of this notion of a rapid V-shape recovery in economic activity and international trade flows after a

global pandemic.

The main novel feature we introduce is adjustment costs associated with changes in the measures of human contacts $n_{ii}(t)$ and $n_{ij}(t)$. More specifically, we assume that whenever a household wants to change the measure of contacts $n_{ij}(t)$, it needs to pay a cost $\psi_1 |\dot{n}_{ij}(t)|^{\psi_2}$, where $\psi_1 > 0$ and $\psi_2 > 1$. An analogous adjustment cost function applies to changes in domestic interactions n_{ii} . Notice that this formulation assumes that the cost of reducing or increasing the number of contacts are symmetric. This leads to the following modified first-order condition for the choice of n_{ij} at any point in time t_0 (an analogous condition holds for n_{ii}):

$$\begin{aligned} \int_{t_0}^{\infty} e^{-\xi t} \left[\frac{\partial Q_i(n_{ii}(t), n_{ij}(t))}{\partial n_{ij}} - \frac{\partial C_i(n_{ii}(t), n_{ij}(t))}{\partial n_{ij}} \right] (1 - k_i(t)) dt \\ = \int_{t_0}^{\infty} e^{-\xi t} [\theta_i^s(t_0) - \theta_i^i(t_0)] s_i(t_0) a_j I_j(t_0) dt + e^{-\xi t_0} \psi_1 \psi_2 |\dot{n}_{ij}(t_0)|^{\psi_2 - 1} (1 - k_i(t_0)). \end{aligned}$$

Since dead individuals do not pay adjustment costs, equation (35) becomes

$$-\dot{\theta}_i^k(t) = - \left[Q_i(n_{ii}(t), n_{ij}(t)) - C_i(n_{ii}(t), n_{ij}(t)) - \psi_1 (|\dot{n}_{ii}(t)|^{\psi_2} + |\dot{n}_{ij}(t)|^{\psi_2}) \right] e^{-\xi t}.$$

The rest of the system is as before with the added feature that the values of $n_{ii}(t)$ and $n_{ij}(t)$ are now state variables, with exogenous initial conditions $n_{ii}(0)$ and $n_{ij}(0)$.²⁵

As the first-order condition makes evident, the choice of $\dot{n}_{ij}(t_0)$ now affects the values of $n_{ii}(t)$ and $n_{ij}(t)$ in the future directly and not only through its impact on the pandemic (and the corresponding co-state variables $\theta_i^s(t_0)$ and $\theta_i^i(t_0)$). This has two important implications. First, adjustment costs imply that agents will react less aggressively to a pandemic and overall their reaction will be smoother. Of course, the counterpart is that their endogenous response will attenuate the flattening of the curve of infections associated with behavioral responses. Second, if households anticipate that the probability of a future pandemic is $\lambda > 0$, the growth in the resurgence of human interactions will be slower than in the world in which the perceived probability of a future pandemic is 0, and the more so the larger is λ . As a result, if due to recency effects, households perceive a particularly high risk of future pandemics in the aftermath of a pandemic, this could slow the recovery of international trade flows after a pandemic occurs.

Figure 11 presents a numerical example of an economy with symmetric countries, behavioral responses, and adjustment costs. The figure uses the baseline parameters from the previous section for symmetric countries, together with $\psi_1 = 1$ and $\psi_2 = 4$ for the adjustment cost parameters. The left-panel shows the evolution of foreign varieties consumed, $n_{ij}(t)$, and compares it with the case with no adjustment costs ($\psi_1 = 0$). Clearly, adjustment costs reduce the magnitude of the behavioral response. Not only do agents take longer to start the adjustment, but the adjustment is substantially smaller. In computing this example we assume that the pandemic never repeats itself. Hence, eventually the number of varieties consumed is the same as in the behavioral case without

²⁵Alternatively we can use terminal conditions. This is what we do in the numerical exercise below where we assume that a pandemic ends, and never happens again, after some large time period T .

adjustment costs. We use this value as the terminal condition and compare the resulting initial $n_{ij}(1)$. Anticipatory effects, agents adjusting in anticipation of a pandemic, imply that the initial value should be smaller than the terminal one. Figure 11 shows no indication that these effects are significant. Although $n_{ij}(1) < n_{ij}(T)$, the effect is negligible and cannot be perceived in the graph. This is the case, even though the effect on the evolution of domestic and foreign contacts is fairly large. This pattern of results is consistent with the view that economies will quickly return to normal after the pandemic, although with the caveat that we have here assumed that adjustment costs are symmetric and that the pandemic does not affect agents' beliefs of the probability of future pandemics. The right panel of Figure 11 presents the corresponding evolution of infections with and without adjustment costs. As discussed above, the milder and delayed behavioral response in the case with adjustment costs leads to a faster increase in the number of infections. It also leads to a corresponding faster decline, since herd immunity starts reducing the number of infections earlier. The result is a faster, but more severe, pandemic with more overall deaths, but less pronounced temporary reductions in real income and trade.

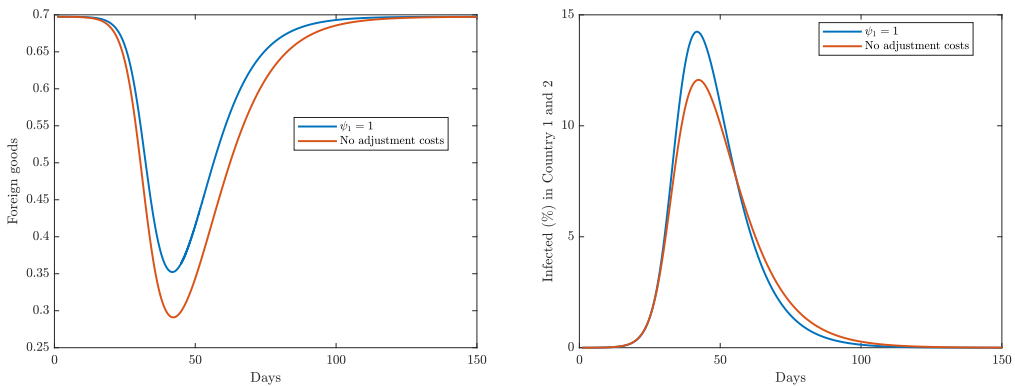


Figure 11: Behavioural Responses with Adjustment Costs

6 Conclusions

Although globalization brings aggregate economic gains, it is often argued that it also makes societies more vulnerable to disease contagion. In this paper, we develop a model of human interaction to analyze the relationship between globalization and pandemics. We jointly microfound both the canonical model of international trade from economics (the gravity equation) with the seminal model pandemics from epidemiology (the Susceptible-Infected-Recovered (SIR) model) using a theory of human interaction. Through jointly modelling these two phenomena, we highlight a number of interactions between them. On the one hand, the contact rate among individuals, which

is a central parameter in benchmark epidemiology models, is endogenous in our framework, and responds to both economic forces (e.g., the gains from international trade) and to the dynamics of the pandemic (e.g., the perceived health risk associated with international travel). On the other hand, we study how the emergence of a pandemic and the perceived risk of future outbreaks shapes the dynamics of international trade, and the net gains from international trade once the death toll from the pandemic is taken into account.

We begin by considering the case in which the disease does not affect the ability of agents to produce and trade, and agents are unaware of the threat of infection, which implies that they do not have an incentive to alter their individual behavior. Even in this case, globalization influences the dynamics of the disease, because it changes patterns of human interaction. We show that there are cross-country epidemiological externalities, such that whether a pandemic occurs in the open economy depends critically on the disease environment in the country with the highest rate of domestic infection. If countries are symmetric, a decline in any (symmetric) international trade friction also leads to an overall increase in the total number of human interactions (domestic plus foreign), which *increases* the range of parameters where a pandemic occurs. In this case, even if an epidemic would not be self-sustaining in a country in the closed economy, it can be self-sustaining in an open economy. In contrast, if countries are sufficiently different from one another in terms of their primitive epidemiological parameters (e.g., as a result of different health policies), a decline in any international trade friction can have the opposite effect of *decreasing* the range of parameters where a pandemic occurs. In this case where one country has a much worse disease environment than the other, trade liberalization can reduce the share of that country's interactions that occur in this bad disease environment, thereby taking the global economy below the threshold for a pandemic to be self-sustaining. In the presence of differences in the timing of infections, multiple waves of infection can occur in the open economy, when there would be a single wave in the closed economy.

We next allow the infection to cause deaths (or reduce productivity in the labor market), but assume that agents remain unaware of the threat of infection, and hence continue to have no incentive to alter their individual behavior. In this case, a country with a worse disease environment experiences a larger reduction in labor supply, which in turn leads to an increase in its relative wage. This wage increase reduces the share of interactions that occur in that country's bad disease environment and increases the share that occur in better disease environments, which again can take the global economy below the threshold for a pandemic to be self-sustaining. Therefore, the general equilibrium effects of the pandemic on wages and trade patterns induce a form of "general equilibrium social distancing" from bad disease environments that operates even in the absence of purposeful social distancing motivated by health risks.

We then allow individuals to become aware of the threat of infections and optimally adjust their behavior depending on the observed state of the pandemic. In this case, agents are not willing to interact as much with the unhealthy country thereby decreasing its relative wage. Overall, we find that behavioral responses lead to amplified reductions in international trade and income, but

save lives. Adding adjustment costs of establishing the human interactions needed to sustain trade delays and diminishes these behavioral responses.

Although we have argued that our results are robust to alternative specifications of our model of international trade, our theoretical framework is still missing a number of realistic features. For example, in future work it would be interesting to explore the implications of allowing for cross-sectoral heterogeneity in the importance of face-to-face interactions for sustaining international trade. Similarly, and although we have studied the effects of various parameters that are at least partly shaped by government policies, it would be fruitful to more thoroughly study optimal policy in our framework. We leave these extensions for future work.

References

- Acemoglu, Daron, Victor Chernozhukov, Iván Werning, Michael D. Whinston (2020), “Optimal Targeted Lockdowns in a Multi-Group SIR Model, NBER Working Paper No. 27102.
- Alfaro, Laura, Ester Faia, Nora Lamersdorf, and Farzad Saidi (2020), “Social Interactions in Pandemics: Fear, Altruism, and Reciprocity,” NBER Working Paper No. 27134.
- Allen, Treb, and Costas Arkolakis (2014), “Trade and the Topography of the Spatial Economy,” *Quarterly Journal of Economics* 129, no. 3: 1085-1140.
- Allen, Treb, Costas Arkolakis, and Yuta Takahashi (2020), “Universal Gravity,” *Journal of Political Economy* 128, no. 2: pp. 393-433.
- Alvarez, Fernando, David Argente, and Francesco Lippi (2020), “A Simple Planning Problem for COVID-19 Lockdown,” *Covid Economics* 14, 1-32.
<https://cepr.org/file/9054/download?token=oJYTY87E>
- Alvarez, Fernando, and Robert E. Lucas Jr. (2007), “General Equilibrium Analysis of the Eaton-Kortum model of International Trade,” *Journal of Monetary Economics* 54, no. 6 (2007): 1726-1768.
- Anderson, James E. (1979), “A Theoretical Foundation for the Gravity Equation,” *American Economic Review*, 69(1), pp.106-116.
- Anderson, James E. and Eric Van Wincoop (2003), “Gravity with Gravitas: A Solution to the Border Puzzle,” *American Economic Review*, 93(1), pp.170-192.
- Antràs, Pol, Teresa C. Fort and Felix Tintelnot (2017) “The Margins of Global Sourcing: Theory and Evidence from US Firms,” *American Economic Review*, 107(9), 2514-64.
- Argente, David O., Chang-Tai Hsieh, and Munseob Lee (2020), “The Cost of Privacy: Welfare Effect of the Disclosure of COVID-19 Cases,” NBER Working Paper No.27220.
- Arkolakis, Costas (2010), “Market Penetration Costs and the New Consumers Margin in International Trade,” *Journal of Political Economy* 118, no. 6, pp: 1151-1199.
- Arkolakis, Costas, Arnaud Costinot, and Andrés Rodríguez-Clare (2012), “New trade models, same old gains?” *American Economic Review* 102.1: 94-130.
- Atkeson, Andrew (2020), “What Will Be the Economic Impact of COVID-19 in the US? Rough Estimates of Disease Scenarios,” NBER Working Paper No. 26867.
- Birge, John R., Ozan Candogan, and Yiding Feng (2020), “Controlling Epidemic Spread: Reducing Economic Losses with Targeted Closures,” Becker-Friedman Institute Working Paper No. 2020-57.
- Bisin, Alberto, and Andrea Moro (2020), “Learning Epidemiology by Doing: The Empirical Implications of a Spatial SIR Model with Behavioral Responses,” mimeo New York University.

- Blonigen, Bruce A. and Anca D. Cristea (2015), "Air Service and Urban Growth: Evidence from a Quasi-Natural Policy Experiment," *Journal of Urban Economics* 86, 128–146.
- Boerner, Lars and Battista Severgnini (2014) "Epidemic Trade," *Economic History Working Papers*, 212, London School of Economics.
- Brauer, Fred, and Carlos Castillo-Chavez (2012), *Mathematical Models in Population Biology and Epidemiology*, Vol. 2. New York: Springer, 2012.
- Campante, Filipe, and David Yanagizawa-Drott (2018), "Long-Range Growth: Economic Development in the Global Network of Air Links," *Quarterly Journal of Economics* 133, no. 3 (2018): 1395-1458.
- Chaney, Thomas (2008), "Distorted Gravity: the Intensive and Extensive Margins of International Trade," *American Economic Review* 98, no. 4: 1707-21.
- Chaney, Thomas (2014), "The Network Structure of International Trade," *American Economic Review* 104, no. 11: 3600-3634.
- Christakos, George, Ricardo A. Olea, Marc L. Serre, Hwa-Lung Yu and Lin-Lin Wang (2005) *Interdisciplinary Public Health Reasoning and Epidemic Modelling: The Case of Black Death*, Amsterdam: Springer.
- Costinot, Arnaud, and Andrés Rodríguez-Clare (2015), "Trade Theory with Numbers: Quantifying the Consequences of Globalization" in *Handbook of International Economics*, vol. 4: pp. 197-261.
- Cristea, Anca D. (2011), "Buyer-Seller Relationships in International Trade: Evidence from U.S. States' Exports and Business-Class Travel," *Journal of International Economics* 84, no. 2: 207-220.
- Cuñat, Alejandro, and Robert Zymek (2020), "The (Structural) Gravity of Epidemics" *Covid Economics* 17, 153-173. <https://cepr.org/file/9084/download?token=j5lblrHs>
- Diekmann, O., J.A.P. Heesterbeek, J.A.J. Metz (1990), "On the Definition and the Computation of the Basic Reproduction Ratio R_0 in Models for Infectious Diseases in Heterogeneous Populations," *Journal of Mathematical Biology* 28, 365-382.
- Ellison, Glenn (2020), "Implications of Heterogeneous SIR Models for Analyses of COVID-19," NBER Working Paper No. 27373.
- Eaton, Jonathan and Samuel Kortum, (2002), "Technology, Geography, and Trade," *Econometrica*, 70:5, 1741-1779.
- Fajgelbaum, Pablo D., Amit Khandelwal, Wookun Kim, Cristiano Mantovani, and Edouard Schaal (2020), "Optimal Lockdown in a Commuting Network," mimeo UCLA.

- Farboodi, Maryam, Gregor Jarosch, and Robert Shimer (2020), "Internal and External Effects of Social Distancing in a Pandemic," *Covid Economics* 9, 22-58.
<https://cepr.org/file/9043/download?token=MZ89DuPo>
- Fenichel, Eli P., Carlos Castillo-Chavez, M. Graziano Ceddia, Gerardo Chowell, Paula A. Gonzalez Parra, Graham J. Hickling, Garth Holloway et al. (2011), "Adaptive Human Behavior in Epidemiological Models," *Proceedings of the National Academy of Sciences* 108, no. 15: 6306-6311.
- Fernández-Villaverde, Jesús and Chad Jones (2020), "Estimating and Simulating a SIRD Model of COVID-19 for Many Countries, States, and Cities," NBER Working Paper No. 27128.
- Giannone, Elisa, Nuno Paixao, and Xinle Pang (2020), "Pandemic in an Inter-regional Model: Optimal Lockdown Policies," mimeo Penn State University.
- Head, Keith, and Philippe Mayer (2014), "Gravity Equations: Workhorse, Toolkit, and Cookbook," Ch. 3 in *Handbook of International Economics*, Gopinath, Gita, Elhanan Helpman and Kenneth Rogoff (Eds), Vol. 4.
- Helpman, Elhanan, Marc Melitz, and Yona Rubinstein (2008), "Estimating Trade Flows: Trading Partners and Trading Volumes," *Quarterly Journal of Economics* 123, no. 2: 441-487.
- Hethcote, Herbert W. (1978), "An Immunization Model for a Heterogeneous Population," *Theoretical Population Biology* 14, no. 3: 338-349.
- Hethcote, Herbert W (2000), "The Mathematics of Infectious Diseases," *SIAM Review*, 42(4), pp.599-653.
- Hethcote, H.W. and Thieme, H.R., (1985), "Stability of the Endemic Equilibrium in Epidemic Models with Subpopulations," *Mathematical Biosciences*, 75(2), pp. 205-227.
- Hovhannisyanyan, Nune and Wolfgang Keller (2015), "International Business Travel: An Engine of Innovation?," *Journal of Economic Growth*, 20:75-104.
- Kermack, William Ogilvy and A. G. McKendrick, (1927), "A Contribution to the Mathematical Theory of Epidemics, Part I," *Proceedings of the Royal Society of London. Series A*, 115 (772), pp. 700-721.
- Kermack, William Ogilvy and A. G. McKendrick, (1932), "Contributions to the Mathematical Theory of Epidemics. II – The Problem of Endemicity," *Proceedings of the Royal Society of London. Series A*, 138 (834), pp. 55-83.
- Jedwab, Remi, Noel D. Johnson and Mark Koyama (2019) "Pandemics, Places, and Populations: Evidence from the Black Death," George Washington University, mimeograph.
- Jones, Callum J, Thomas Philippon, and Venky Venkateswaran (2020), "Optimal Mitigation Policies in a Pandemic: Social Distancing and Working from Home," NBER Working Paper 26984.

- Magal, Pierre, Seydi Ousmane, and Glenn Webb (2016) “Final Size of an Epidemic for a Two-group SIR Model,” *Society for Industrial and Applied Mathematics*, 76(5), 2042-2059.
- Melitz, Marc J. (2003), “The Impact of Trade on Intra-Industry Reallocations and Aggregate Industry Productivity,” *Econometrica* 71, no. 6 (2003): 1695-1725.
- Melitz, Marc J., and Stephen J Redding (2014), “Missing Gains from Trade?” *American Economic Review* 104 (5): pp. 317-21.
- Ossa, Ralph (2015), “Why Trade Matters After All,” *Journal of International Economics* 97(2): pp. 266-277.
- Ricci P. H. Yue, Harry F. Lee and Connor Y. H. Wu (2017) “Trade Routes and Plague Transmission in Pre-industrial Europe,” *Nature*, Scientific Reports, 7, 12973, 1-10.
- Saker, Lance, Kelley Lee, Barbara Cannito, Anna Gilmore and Diarmid Campbell-Lendrum (2004) “Globalization and Infectious Diseases: A Review of the Linkages,” *Special Topics in Social, Economic and Behavioural (SEB) Research*, Geneva: World Health Organization.
- Startz, Meredith (2018), “The Value of Face-To-Face: Search and Contracting Problems in Nigerian Trade,” mimeo Stanford University.
- Toxvaerd, Flavio (2020), “Equilibrium Social Distancing,” *Covid Economics* 15, 110-133.
<https://cepr.org/file/9064/download?token=j-TM2EbY>
- Van den Driessche, Pauline, and James Watmough (2002), “Reproduction Numbers and Sub-Threshold Endemic Equilibria for Compartmental Models of Disease Transmission,” *Mathematical Biosciences* 180, no. 1-2, pp. 29-48.

A Theoretical Appendix

A.1 Second-Order Conditions for Choice of n_{ij}

From equation (6), we obtain, for all $j \in \mathcal{J}$,

$$\begin{aligned} \frac{\partial W(i)}{\partial n_{ij}} &= \frac{w_i}{(\sigma-1)} \left(\sum_{j \in \mathcal{J}} n_{ij} \left(\frac{\tau_{ij} w_j}{Z_j} \right)^{1-\sigma} \right)^{\frac{1}{(\sigma-1)}-1} \left(\frac{\tau_{ij} w_j}{Z_j} \right)^{1-\sigma} - c\mu_{ij} (d_{ij})^\rho (n_{ij})^{\phi-1} ; \\ \frac{\partial W(i)}{\partial (n_{ij})^2} &= \frac{w_i}{(\sigma-1)} \frac{(2-\sigma)}{(\sigma-1)} \left(\sum_{j \in \mathcal{J}} n_{ij} \left(\frac{\tau_{ij} w_j}{Z_j} \right)^{1-\sigma} \right)^{\frac{1}{(\sigma-1)}-2} \left(\frac{\tau_{ij} w_j}{Z_j} \right)^{1-\sigma} \left(\frac{\tau_{ij} w_j}{Z_j} \right)^{1-\sigma} \\ &\quad - (\phi-1) c\mu_{ij} (d_{ij})^\rho \times (n_{ij})^{\phi-2} \\ &= \left(\frac{2-\sigma}{\sigma-1} \right) \left(\sum_{j \in \mathcal{J}} n_{ij} \left(\frac{\tau_{ij} w_j}{Z_j} \right)^{1-\sigma} \right)^{-1} \left(\frac{\tau_{ij} w_j}{Z_j} \right)^{1-\sigma} c\mu_{ij} (d_{ij})^\rho \times (n_{ij})^{\phi-1} \\ &\quad - (\phi-1) c\mu_{ij} (d_{ij})^\rho \times (n_{ij})^{\phi-2} \\ &= c\mu_{ij} (d_{ij})^\rho \times (n_{ij})^{\phi-2} \left[\left(\frac{1}{(\sigma-1)} - 1 \right) \left(\frac{n_{ij} \frac{\tau_{ij} w_j}{Z_j}}{\sum_{j \in \mathcal{J}} n_{ij} \left(\frac{\tau_{ij} w_j}{Z_j} \right)^{1-\sigma}} \right)^{1-\sigma} - (\phi-1) \right] ; \\ \frac{\partial^2 W(i)}{\partial n_{ij} \partial n_{ii}} &= \frac{w_i}{(\sigma-1)} \frac{(2-\sigma)}{(\sigma-1)} \left(\sum_{j \in \mathcal{J}} n_{ij} \left(\frac{\tau_{ij} w_j}{Z_j} \right)^{1-\sigma} \right)^{\frac{1}{(\sigma-1)}-2} \left(\frac{\tau_{ij} w_j}{Z_j} \right)^{1-\sigma} \left(\frac{\tau_{ii} w_i}{Z_i} \right)^{1-\sigma} . \end{aligned}$$

Notice that $\frac{\partial W(i)}{\partial (n_{ij})^2} < 0$ if only if:

$$\left(\frac{2-\sigma}{\sigma-1} \right) \left(\frac{n_{ij} \frac{\tau_{ij} w_j}{Z_j}}{\sum_{j \in \mathcal{J}} n_{ij} \left(\frac{\tau_{ij} w_j}{Z_j} \right)^{1-\sigma}} \right)^{1-\sigma} < (\phi-1) ,$$

so this condition could be violated for large enough τ_{ij} , unless $\sigma > 2$, in which case the condition is surely satisfied as long as $\phi(\sigma-1) > 1$.

Next note that

$$\left(\frac{\partial^2 W(i)}{\partial n_{ij} \partial n_{ii}} \right)^2 = \left(\frac{w_i}{\sigma-1} \frac{2-\sigma}{\sigma-1} \left(\sum_{j \in \mathcal{J}} n_{ij} \left(\frac{\tau_{ij} w_j}{Z_j} \right)^{1-\sigma} \right)^{\frac{1}{(\sigma-1)}-2} \left(\frac{\tau_{ij} w_j}{Z_j} \right)^{1-\sigma} \left(\frac{\tau_{ii} w_i}{Z_i} \right)^{1-\sigma} \right)^2 = \Xi^2$$

and

$$\begin{aligned} \frac{\partial W(i)}{\partial (n_{ii})^2} \frac{\partial W(i)}{\partial (n_{ij})^2} &= \left(\frac{1}{(\sigma-1)^{\frac{2-\sigma}{\sigma-1}}} w_i \left(\sum_{j \in \mathcal{J}} n_{ij} \left(\frac{\tau_{ij} w_j}{Z_j} \right)^{1-\sigma} \right)^{\frac{1}{(\sigma-1)^{-2}}} \left(\frac{\tau_{ii} w_i}{Z_i} \right)^{1-\sigma} \left(\frac{\tau_{ij} w_j}{Z_j} \right)^{1-\sigma} \right) \\ &\quad - (\phi - 1) c \mu_{ii} (d_{ii})^\rho \times (n_{ii})^{\phi-2} \\ &\times \left(\frac{1}{(\sigma-1)^{\frac{2-\sigma}{\sigma-1}}} w_i \left(\sum_{j \in \mathcal{J}} n_{ij} \left(\frac{\tau_{ij} w_j}{Z_j} \right)^{1-\sigma} \right)^{\frac{1}{(\sigma-1)^{-2}}} \left(\frac{\tau_{ij} w_j}{Z_j} \right)^{1-\sigma} \left(\frac{\tau_{ij} w_j}{Z_j} \right)^{1-\sigma} \right) \\ &\quad - (\phi - 1) c \mu_{ij} (d_{ij})^\rho \times (n_{ij})^{\phi-2} \\ &= \Xi^2 - \varkappa_{ij}^i - \varkappa_{ij}^j + \varpi_{ij}, \end{aligned}$$

where $\varkappa_{ij}^i < 0$ and $\varkappa_{ij}^j < 0$, and $\varpi_{ij} > 0$, whenever $\sigma > 2$ and $\phi > 1$.

In sum, when $\sigma > 2$ and $\phi(\sigma - 1) > 0$, we have

$$\frac{\partial W(i)}{\partial (n_{ii})^2} \frac{\partial W(i)}{\partial (n_{ij})^2} > \left(\frac{\partial^2 W(i)}{\partial n_{ij} \partial n_{ii}} \right)^2,$$

and the second-order conditions are met.

A.2 Proof of Proposition 2

Proof of part a):

From equation (7), we can write

$$n_{ii}(\mathbf{w}) = (c(\sigma - 1) \mu_{ii})^{-1/(\phi-1)} (d_{ii})^{-\frac{\rho+(\sigma-1)\delta}{\phi-1}} \left(\frac{t_{ii}}{Z_i} \right)^{-\frac{\sigma-1}{(\phi-1)}} \left(\frac{w_i}{P_i} \right)^{-\frac{\sigma-2}{\phi-1}},$$

but remember from (13) that

$$\frac{w_i}{P_i} = (\pi_{ii})^{-\frac{(\phi-1)}{\phi(\sigma-1)-1}} \times \left(\frac{(Z_i)^{\phi(\sigma-1)}}{c(\sigma-1)} (\Gamma_{ii})^{-\varepsilon(\phi-1)} \right)^{\frac{1}{\phi(\sigma-1)-1}}.$$

This implies that, in order to study the effect of international trade frictions on $n_{ii}(\mathbf{w})$, it suffices to study their effect on π_{ii} , with the dependence of n_{ii} on π_{ii} being monotonically positive. Now from

$$\pi_{ii} = \frac{(w_i/Z_i)^{-\frac{\phi(\sigma-1)}{\phi-1}} \times (\Gamma_{ii})^{-\varepsilon}}{\sum_{\ell \in \mathcal{J}} (w_\ell/Z_\ell)^{-\frac{\phi(\sigma-1)}{\phi-1}} \times (\Gamma_{i\ell})^{-\varepsilon}},$$

it is clear that the impact effect of a lower $\Gamma_{i\ell}$ is to decrease π_{ii} and thus to decrease n_{ii} . To take into account general-equilibrium forces, we can write equation (14) as

$$\frac{(Z_i)^{\frac{\phi(\sigma-1)}{\phi-1}} (\Gamma_{ii})^{-\varepsilon}}{(Z_i)^{\frac{\phi(\sigma-1)}{\phi-1}} (\Gamma_{ii})^{-\varepsilon} + (Z_j/\omega)^{\frac{\phi(\sigma-1)}{\phi-1}} (\Gamma_{ij})^{-\varepsilon}} L_i + \frac{(Z_i)^{\frac{\phi(\sigma-1)}{\phi-1}} (\Gamma_{ji})^{-\varepsilon}}{(Z_j/\omega)^{\frac{\phi(\sigma-1)}{\phi-1}} (\Gamma_{jj})^{-\varepsilon} + (Z_i)^{\frac{\phi(\sigma-1)}{\phi-1}} (\Gamma_{ji})^{-\varepsilon}} \omega L_j = L_i, \tag{A.1}$$

where $\omega \equiv w_j/w_i$ is the relative wage in country j . From this equation, it is easy to see that if Γ_{ij} falls, ω cannot possibly decrease. If it did, both terms in the left-hand-side of (A.1) would fall. But if ω goes up, then π_{ii} goes up *by more* than as implied by the direct fall in Γ_{ij} . Similarly, if Γ_{ji} falls, π_{ij} falls on impact, so ω needs to increase to re-equilibrate the labor market, and again π_{ii} must decline.

Because the results above hold for Γ_{ij} and Γ_{ji} , they must hold for any of the constituents of those composite parameters.

Proof of part b):

Note from equations (2), (5), and (12) that

$$\frac{c}{\phi} \sum_{j \in \mathcal{J}} \mu_{ij} (d_{ij})^\rho \times (n_{ij})^\phi = \frac{1}{\phi(\sigma-1)} \frac{w_i}{P_i}.$$

In part a) of the proof, we have established that when any international trade friction decreases, π_{ii} goes down, and from (13), w_i/P_i goes up. Thus, $\mu_{ii} (d_{ii})^\rho \times (n_{ii})^\phi + \mu_{ij} (d_{ij})^\rho \times (n_{ij})^\phi$ goes up when any international trade friction decreases. But because n_{ii} goes down and μ_{ij} and d_{ij} (weakly) go down, it must be the case that n_{ij} increases.

A.3 Proof of Proposition 3

We begin by considering the case with general country asymmetries. Consider the sum

$$\mu_{ii} (d_{ii})^\rho \times (n_{ii})^\phi + \mu_{ij} (d_{ij})^\rho \times (n_{ij})^\phi.$$

Differentiating:

$$\phi \left[\mu_{ii} (d_{ii})^\rho \times (n_{ii})^{\phi-1} \underbrace{dn_{ii}}_{<0} + \mu_{ij} (d_{ij})^\rho \times (n_{ij})^{\phi-1} dn_{ij} \right] + \underbrace{d(\mu_{ij} (d_{ij})^\rho)}_{\leq 0} \times (n_{ij})^\phi > 0. \tag{A.2}$$

Clearly, we must have

$$\mu_{ii} (d_{ii})^\rho \times (n_{ii})^{\phi-1} dn_{ii} + \mu_{ij} (d_{ij})^\rho \times (n_{ij})^{\phi-1} dn_{ij} > 0.$$

So if

$$\mu_{ii} (d_{ii})^\rho (n_{ii})^{\phi-1} > \mu_{ij} (d_{ij})^\rho \times (n_{ij})^{\phi-1},$$

we must have

$$dn_{ij} > -dn_{ii},$$

which would prove the Proposition.

Now, from the FOC for the choice of n 's, that is equation (7),

$$\begin{aligned} \mu_{ii} (d_{ii})^\rho (n_{ii})^{\phi-1} &= \left(\frac{w_i}{P_i}\right)^{1/(\phi-1)} \frac{(P_i)^{\frac{\sigma-1}{\phi-1}}}{(\sigma-1)c} \times \left(\frac{(d_{ii})^\delta t_{ii} w_i}{Z_i}\right)^{-\frac{\sigma-1}{\phi-1}} \\ \mu_{ij} (d_{ij})^\rho (n_{ij})^{\phi-1} &= \left(\frac{w_i}{P_i}\right)^{1/(\phi-1)} \frac{(P_i)^{\frac{\sigma-1}{\phi-1}}}{(\sigma-1)c} \times \left(\frac{(d_{ij})^\delta t_{ij} w_j}{Z_j}\right)^{-\frac{\sigma-1}{\phi-1}}, \end{aligned}$$

so a sufficient condition for the result is

$$\frac{(d_{ii})^\delta t_{ii} w_i}{Z_i} < \frac{(d_{ij})^\delta t_{ij} w_j}{Z_j}.$$

This amounts to prices for domestic varieties being lower than prices for foreign varieties. This makes sense, in such a case, desired quantities of domestic varieties will be higher, and the marginal benefit of getting more of them will be higher.

Note finally that with full symmetry, we must have $w_i = w_j$ and $Z_j = Z_i$, and the condition above trivially holds since $t_{ij} > t_{ii}$ and $d_{ij} > d_{ii}$.

A.4 Proof of Proposition 4

Note from equation (11), that we can write

$$\begin{aligned} \frac{w_i}{P_i} &= \text{const} \times \left(\left(\frac{1}{Z_i}\right)^{-\frac{\phi(\sigma-1)}{\phi-1}} (\Gamma_{ii})^{-\varepsilon} + \left(\frac{\omega}{Z_j}\right)^{-\frac{\phi(\sigma-1)}{\phi-1}} (\Gamma_{ij})^{-\varepsilon} \right)^{\frac{(\phi-1)}{\phi(\sigma-1)-1}} \\ \frac{w_j}{P_i} &= \text{const} \times \omega \left(\left(\frac{1}{Z_i}\right)^{-\frac{\phi(\sigma-1)}{\phi-1}} (\Gamma_{ii})^{-\varepsilon} + \left(\frac{\omega}{Z_j}\right)^{-\frac{\phi(\sigma-1)}{\phi-1}} (\Gamma_{ij})^{-\varepsilon} \right)^{\frac{(\phi-1)}{\phi(\sigma-1)-1}} \end{aligned}$$

where $\omega = w_j/w_i$. Plugging in (7), we have

$$n_{ii} = \text{const} \times \left(\frac{w_i}{P_i}\right)^{-\frac{\sigma-2}{\phi-1}} \times \left(\left(\frac{1}{Z_i}\right)^{-\frac{\phi(\sigma-1)}{\phi-1}} (\Gamma_{ii})^{-\varepsilon} + \left(\frac{\omega}{Z_j}\right)^{-\frac{\phi(\sigma-1)}{\phi-1}} (\Gamma_{ij})^{-\varepsilon} \right)^{-\frac{\sigma-2}{\phi(\sigma-1)-1}},$$

and thus n_{ii} increases in ω . Next, note

$$\begin{aligned} n_{ij} &= \text{const} \times \left(\frac{w_j}{P_i}\right)^{-\frac{\sigma-1}{\phi-1}} \left(\frac{w_i}{P_i}\right)^{1/(\phi-1)} \\ &= \text{const} \times \omega^{-\frac{\sigma-1}{\phi-1}} \left(\left(\frac{1}{Z_i}\right)^{-\frac{\phi(\sigma-1)}{\phi-1}} (\Gamma_{ii})^{-\varepsilon} + \left(\frac{\omega}{Z_j}\right)^{-\frac{\phi(\sigma-1)}{\phi-1}} (\Gamma_{ij})^{-\varepsilon} \right)^{-\frac{\sigma-2}{\phi(\sigma-1)-1}} \end{aligned}$$

The effect of ω may look ambiguous, but in fact we have that n_{ij} decreases if ω goes up. To see this, note that

$$\frac{\partial \omega^{-a} (b + c\omega^{-d})^{-g}}{\partial \omega} = -\frac{(a - dg)c + ab\omega^d}{\left(\frac{1}{\omega^d} (c + b\omega^d)\right)^g \omega^a \omega (c + b\omega^d)},$$

which is negative if $a - dg > 0$. But here we have

$$a - dg = \frac{\sigma - 1}{(\phi - 1)} - \frac{\phi(\sigma - 1)}{\phi - 1} \frac{\sigma - 2}{\phi(\sigma - 1) - 1} = \frac{\sigma - 1}{\phi(\sigma - 1) - 1} > 0.$$

In sum, n_{ij} decreases in ω . Because an increase in L_i/L_j increases in ω (from straightforward use of the implicit function theorem to (14)), the Proposition follows.

Notice also that

$$\begin{aligned} n_{ji} &= \text{const} \times \left(\frac{w_i}{P_j}\right)^{-\frac{\sigma-1}{\phi-1}} \left(\frac{w_j}{P_j}\right)^{1/(\phi-1)} \\ &= \text{const} \times \omega^{\frac{\sigma-1}{\phi-1}} \left(\left(\frac{\omega}{Z_j}\right)^{-\frac{\phi(\sigma-1)}{\phi-1}} (\Gamma_{jj})^{-\varepsilon} + \left(\frac{1}{Z_i}\right)^{-\frac{\phi(\sigma-1)}{\phi-1}} (\Gamma_{ji})^{-\varepsilon} \right)^{-\frac{\sigma-2}{\phi(\sigma-1)-1}}, \end{aligned}$$

and by an analogous argument above, we have that n_{ji} increases in ω , and thus an increase in population in i leads to an increase n_{ji} (while also decreasing n_{jj}).

A.5 Proof of Proposition 5

See main text and Online Appendix D. Here we just discuss the derivation of the system of equations in (23)-(24), and derive the comparative statics mentioned in the main text.

We begin with the law of motion for susceptible agents in each country in equation (16):

$$\begin{aligned} \dot{S}_i &= -2\alpha_i n_{ii} \times S_i \times I_i - \alpha_j n_{ij} \times S_i \times I_j - \alpha_i n_{ji} \times S_i \times I_j \\ \dot{S}_j &= -2\alpha_j n_{jj} \times S_j \times I_j - \alpha_j n_{ij} \times S_j \times I_i - \alpha_i n_{ji} \times S_j \times I_i \end{aligned}$$

Dividing by the own share of susceptibles, and plugging the expression for \dot{R}_i and \dot{R}_j in (18), we

obtain

$$\begin{aligned} \frac{\dot{S}_i}{S_i} &= -\frac{2\alpha_i n_{ii}}{\gamma_i} \dot{R}_i - \frac{\alpha_j n_{ij} + \alpha_i n_{ji}}{\gamma_j} \dot{R}_j \\ \frac{\dot{S}_j}{S_j} &= -\frac{2\alpha_j n_{jj}}{\gamma_j} \dot{R}_j - \frac{\alpha_j n_{ij} + \alpha_i n_{ji}}{\gamma_i} \dot{R}_i. \end{aligned}$$

Turning the growth rate in the left-hand-side to a log-difference, and integrating we get

$$\begin{aligned} \ln S_i(t) - \ln S_i(0) &= -\frac{2\alpha_i n_{ii}}{\gamma_i} (R_i(t) - R_i(0)) - \frac{\alpha_j n_{ij} + \alpha_i n_{ji}}{\gamma_j} (R_j(t) - R_j(0)) \\ \ln S_j(t) - \ln S_j(0) &= -\frac{2\alpha_j n_{jj}}{\gamma_j} (R_j(t) - R_j(0)) - \frac{\alpha_j n_{ij} + \alpha_i n_{ji}}{\gamma_i} (R_i(t) - R_i(0)) \end{aligned}$$

Finally, noting $S_i(0) \simeq 1$ and $R_i(0) \simeq 1$, and $R_i(\infty) = 1 - S_i(\infty)$ (since $I_i(\infty) = 0$), we obtain the system in (23)-(24), that is:

$$\begin{aligned} \ln S_i(\infty) &= -\frac{2\alpha_i n_{ii}}{\gamma_i} (1 - S_i(\infty)) - \frac{\alpha_j n_{ij} + \alpha_i n_{ji}}{\gamma_j} (1 - S_j(\infty)) \\ \ln S_j(\infty) &= -\frac{2\alpha_j n_{jj}}{\gamma_j} (1 - S_j(\infty)) - \frac{\alpha_j n_{ij} + \alpha_i n_{ji}}{\gamma_i} (1 - S_i(\infty)) \end{aligned}$$

Although we cannot solve the system in closed-form, we can derive some comparative statics. In particular, total differentiating we find

$$\begin{aligned} &\frac{1}{S_i(\infty)} dS_i(\infty) - \frac{2\alpha_i n_{ii}}{\gamma_i} dS_i(\infty) + (1 - S_i(\infty)) d\left(\frac{2\alpha_i n_{ii}}{\gamma_i}\right) \\ &= \left(\frac{\alpha_j n_{ij} + \alpha_i n_{ji}}{\gamma_j}\right) dS_j(\infty) - d\left(\frac{\alpha_j n_{ij} + \alpha_i n_{ji}}{\gamma_j}\right) (1 - S_j(\infty)) \\ &\frac{1}{S_j(\infty)} dS_j(\infty) - \frac{2\alpha_j n_{jj}}{\gamma_j} dS_j(\infty) + (1 - S_j(\infty)) d\left(\frac{2\alpha_j n_{jj}}{\gamma_j}\right) \\ &= \left(\frac{\alpha_j n_{ij} + \alpha_i n_{ji}}{\gamma_i}\right) dS_i(\infty) - d\left(\frac{\alpha_j n_{ij} + \alpha_i n_{ji}}{\gamma_i}\right) (1 - S_i(\infty)) \end{aligned}$$

Solving

$$\begin{aligned} dS_i(\infty) &= -\frac{\left[\frac{\alpha_j n_{ij} + \alpha_i n_{ji}}{\gamma_j} \left(d\left(\frac{\alpha_j n_{ij} + \alpha_i n_{ji}}{\gamma_j}\right) + (1 - S_j(\infty)) d\left(\frac{2\alpha_j n_{jj}}{\gamma_j}\right) \right) \right. \\ &\quad \left. + \left(\frac{1}{S_j(\infty)} - \frac{2\alpha_j n_{jj}}{\gamma_j}\right) \left(d\left(\frac{\alpha_j n_{ij} + \alpha_i n_{ji}}{\gamma_j}\right) (1 - S_j(\infty)) + (1 - S_i(\infty)) d\left(\frac{2\alpha_i n_{ii}}{\gamma_i}\right) \right) \right]}{\left(\frac{1}{S_i(\infty)} - \frac{2\alpha_i n_{ii}}{\gamma_i}\right) \left(\frac{1}{S_j(\infty)} - \frac{2\alpha_j n_{jj}}{\gamma_j}\right) - \frac{(\alpha_j n_{ij} + \alpha_i n_{ji})^2}{\gamma_i \gamma_j}} \\ dS_j(\infty) &= -\frac{\left[\frac{\alpha_j n_{ij} + \alpha_i n_{ji}}{\gamma_i} \left(d\left(\frac{\alpha_j n_{ij} + \alpha_i n_{ji}}{\gamma_i}\right) + (1 - S_i(\infty)) d\left(\frac{2\alpha_i n_{ii}}{\gamma_i}\right) \right) \right. \\ &\quad \left. + \left(\frac{1}{S_i(\infty)} - \frac{2\alpha_i n_{ii}}{\gamma_i}\right) \left(d\left(\frac{\alpha_j n_{ij} + \alpha_i n_{ji}}{\gamma_i}\right) (1 - S_i(\infty)) + (1 - S_j(\infty)) d\left(\frac{2\alpha_j n_{jj}}{\gamma_j}\right) \right) \right]}{\left(\frac{1}{S_j(\infty)} - \frac{2\alpha_j n_{jj}}{\gamma_j}\right) \left(\frac{1}{S_i(\infty)} - \frac{2\alpha_i n_{ii}}{\gamma_i}\right) - \frac{(\alpha_j n_{ij} + \alpha_i n_{ji})^2}{\gamma_i \gamma_j}} \end{aligned}$$

Next, note that because new infections eventually go to zero, there have to be (at least) two peaks of infection (t_i^* and t_j^*) defined by $\dot{I}_i(t_i^*) = \dot{I}_j(t_j^*) = 0$. Whenever there are more than two peaks in one country, should set t_i^* and t_j^* to the latest periods for which $\dot{I}_i(t_i^*) = \dot{I}_j(t_j^*) = 0$.

Now we have two cases to consider:

- **Case 1:** $t_i^* \geq t_j^*$. Then $\dot{I}_i(t_i^*) = 0 > \dot{I}_j(t_j^*)$ and

$$\begin{aligned} \frac{2\alpha_i n_{ii}}{\gamma_i} S_i(t_i^*) + \frac{\alpha_j n_{ij} + \alpha_i n_{ji}}{\gamma_i} S_i(t_i^*) \times \frac{I_j(t_j^*)}{I_i(t_i^*)} &= 1 \\ \frac{2\alpha_j n_{jj}}{\gamma_j} S_j(t_j^*) + \frac{\alpha_j n_{ij} + \alpha_i n_{ji}}{\gamma_j} S_j(t_j^*) \times \frac{I_i(t_i^*)}{I_j(t_j^*)} &\leq 1 \end{aligned}$$

and thus

$$\left(\frac{1}{S_i(t_i^*)} - \frac{2\alpha_i n_{ii}}{\gamma_i} \right) \left(\frac{1}{S_j(t_j^*)} - \frac{2\alpha_j n_{jj}}{\gamma_j} \right) \geq \frac{(\alpha_j n_{ij} + \alpha_i n_{ji})^2}{\gamma_i \gamma_j} \times \frac{I_j(t_j^*)}{I_i(t_i^*)} \times \frac{I_i(t_i^*)}{I_j(t_j^*)} = \frac{(\alpha_j n_{ij} + \alpha_i n_{ji})^2}{\gamma_i \gamma_j}$$

But at $S_i(t_i^*) > S_i(\infty)$ and $S_j(t_j^*) > S_i(\infty)$, so we must have $\frac{2\alpha_i n_{ii}}{\gamma_i} S_i(\infty) \leq 1$ and $\frac{2\alpha_j n_{jj}}{\gamma_j} S_j(\infty) \leq 1$, as well as

$$\left(\frac{1}{S_i(\infty)} - \frac{2\alpha_i n_{ii}}{\gamma_i} \right) \left(\frac{1}{S_j(\infty)} - \frac{2\alpha_j n_{jj}}{\gamma_j} \right) \geq \frac{(\alpha_j n_{ij} + \alpha_i n_{ji})^2}{\gamma_i \gamma_j}.$$

- **Case 2:** $t_j^* \geq t_i^*$. Then $\dot{I}_j(t_j^*) = 0 > \dot{I}_i(t_i^*)$ and

$$\begin{aligned} \frac{2\alpha_i n_{ii}}{\gamma_i} S_i(t_j^*) + \frac{\alpha_j n_{ij} + \alpha_i n_{ji}}{\gamma_i} S_i(t_j^*) \times \frac{I_j(t_j^*)}{I_i(t_j^*)} &\leq 1 \\ \frac{2\alpha_j n_{jj}}{\gamma_j} S_j(t_j^*) + \frac{\alpha_j n_{ij} + \alpha_i n_{ji}}{\gamma_j} S_j(t_j^*) \times \frac{I_i(t_j^*)}{I_j(t_j^*)} &= 1 \end{aligned}$$

and thus

$$\left(\frac{1}{S_i(t_j^*)} - \frac{2\alpha_i n_{ii}}{\gamma_i} \right) \left(\frac{1}{S_j(t_j^*)} - \frac{2\alpha_j n_{jj}}{\gamma_j} \right) \geq \frac{(\alpha_j n_{ij} + \alpha_i n_{ji})^2}{\gamma_i \gamma_j} \times \frac{I_j(t_j^*)}{I_i(t_j^*)} \times \frac{I_i(t_j^*)}{I_j(t_j^*)} = \frac{(\alpha_j n_{ij} + \alpha_i n_{ji})^2}{\gamma_i \gamma_j}$$

But $S_i(t_j^*) > S_i(\infty)$ and $S_j(t_j^*) > S_i(\infty)$, so we must again have $\frac{2\alpha_i n_{ii}}{\gamma_i} S_i(\infty) \leq 1$ and $\frac{2\alpha_j n_{jj}}{\gamma_j} S_j(\infty) \leq 1$, as well as

$$\left(\frac{1}{S_i(\infty)} - \frac{2\alpha_i n_{ii}}{\gamma_i} \right) \left(\frac{1}{S_j(\infty)} - \frac{2\alpha_j n_{jj}}{\gamma_j} \right) \geq \frac{(\alpha_j n_{ij} + \alpha_i n_{ji})^2}{\gamma_i \gamma_j}$$

Going back to the system, this means that an increase in any n or a decrease in any γ will decrease the steady-state values for $S_i(\infty)$ and $S_j(\infty)$, and thus increase infections everywhere.

A.6 Proof of Proposition 6

See main text. In particular, the result is an immediate corollary of Proposition 3.

A.7 Proof of Proposition 7

See main text.

A.8 Proof of Proposition 8

The goods market clearing condition with deaths defines the following implicit function:

$$\Lambda_i = \left[\begin{aligned} & \frac{(Z_i)^{\frac{\phi(\sigma-1)}{\phi-1}} (\Gamma_{ii})^{-\varepsilon}}{(Z_i)^{\frac{\phi(\sigma-1)}{\phi-1}} (\Gamma_{ii})^{-\varepsilon} + (Z_j/\omega)^{\frac{\phi(\sigma-1)}{\phi-1}} (\Gamma_{ij})^{-\varepsilon}} (1 - D_i) L_i \\ & + \frac{(Z_i)^{\frac{\phi(\sigma-1)}{\phi-1}} (\Gamma_{ji})^{-\varepsilon}}{(Z_j/\omega)^{\frac{\phi(\sigma-1)}{\phi-1}} (\Gamma_{jj})^{-\varepsilon} + (Z_i)^{\frac{\phi(\sigma-1)}{\phi-1}} (\Gamma_{ji})^{-\varepsilon}} \omega (1 - D_j) L_j - (1 - D_i) L_i \end{aligned} \right] = 0.$$

Taking partial derivatives of this implicit function, we have:

$$\frac{\partial \Lambda_i}{\partial D_i} > 0, \quad \frac{\partial \Lambda_i}{\partial D_j} < 0, \quad \frac{\partial \Lambda_i}{\partial \omega} > 0.$$

Therefore, from the implicit function theorem, we have the following comparative statics of the relative wage with respect to deaths in the two countries:

$$\frac{d\omega}{dD_i} = -\frac{\partial \Lambda_i / \partial D_i}{\partial \Lambda_i / \partial \omega} < 0, \quad \frac{d\omega}{dD_j} = -\frac{\partial \Lambda_i / \partial D_j}{\partial \Lambda_i / \partial \omega} > 0. \tag{A.3}$$

We now combine these results above with the comparative statics of bilateral interactions with respect to the relative wage (ω) from Proposition 4. In particular, from the proof of that proposition, we have the following results:

$$\frac{dn_{ii}}{d\omega} > 0, \quad \frac{dn_{ij}}{d\omega} < 0. \tag{A.4}$$

Combining these two sets of relationships (A.3) and (A.4), we have the following results stated in the proposition:

$$\begin{aligned} \frac{dn_{ii}}{dD_i} &= \frac{dn_{ii}}{d\omega} \underbrace{\frac{d\omega}{dD_i}}_{>0} < 0, & \frac{dn_{ii}}{dD_j} &= \frac{dn_{ii}}{d\omega} \underbrace{\frac{d\omega}{dD_j}}_{>0} > 0. \\ \frac{dn_{ij}}{dD_i} &= \frac{dn_{ij}}{d\omega} \underbrace{\frac{d\omega}{dD_i}}_{<0} > 0, & \frac{dn_{ij}}{dD_j} &= \frac{dn_{ij}}{d\omega} \underbrace{\frac{d\omega}{dD_j}}_{<0} < 0. \end{aligned}$$

A.9 Proof of Proposition 9

Because $Q_i(n_{ii}(t), n_{ij}(t)) \geq C_i(n_{ii}(t), n_{ij}(t))$, from equation (35), we must have $\dot{\theta}_i^k(t) \geq 0$ at all t . This in turn implies that we must have $\theta_i^k(t) \leq 0$ at all t for the transversality condition to be met (i.e., convergence to 0 from below).

We next show that $\dot{\theta}_i^i(t) \geq 0$ and $\theta_i^i(t) \leq 0$ for all t . First note that we must have

$$\eta_i \theta_i^k(t) < (\gamma_i + \eta_i) \theta_i^i(t)$$

and thus (from equation (34)) $\dot{\theta}_i^i(t) > 0$ for all t . To see this, note that if instead we had

$$\eta_i \theta_i^k(t_0) > (\gamma_i + \eta_i) \theta_i^i(t_0),$$

at any time t_0 , then $\dot{\theta}_i^i(t_0) < 0 < \dot{\theta}_i^k(t_0)$ so this inequality would continue to hold for all $t_0 > t$. But then we would have $\dot{\theta}_i^i(t) < 0$ for all $t > t_0$, and for $\theta_i^i(t)$ to meet its transversality condition, we would need to have $\theta_i^i(t) > 0$ at all $t > t_0$. But if $\theta_i^i(t) > 0$ and $\theta_i^k(t) \leq 0$ for $t > t_0$, it is clear from equation (34) that $\dot{\theta}_i^i(t) > 0$ for $t > t_0$, which is a contradiction. In sum, $\dot{\theta}_i^i(t) > 0$ for all t . But then for $\theta_i^i(t)$ to meet its transversality condition (from below), we need $\theta_i^i(t) \leq 0$ for all t .

Finally, to show that $\theta_i^s(t) > \theta_i^i(t)$ for all t , suppose that $\theta_i^s(t_0) < \theta_i^i(t_0)$ for some t_0 . From equation (33), this would imply $\dot{\theta}_i^s(t_0) < 0$. But because $\dot{\theta}_i^i(t) > 0$ for all t , we would continue to have $\theta_i^s(t) < \theta_i^i(t)$ for all $t > t_0$, and thus $\dot{\theta}_i^s(t) < 0$ for all $t > t_0$. This would imply that, for $t > t_0$, $\theta_i^s(t)$ would converge to its steady-state value of 0 from above, i.e., $\theta_i^s(t) > 0$ for $t > t_0$. But because $\theta_i^i(t) \leq 0$ for all t , from equation (33), we would have $\dot{\theta}_i^s(t) > 0$ for $t > t_0$, which is a contradiction. In sum, we must have $\theta_i^s(t) > \theta_i^i(t)$ for all t .

B Simulation Appendix

In this section of the Appendix, we discuss our choice of parameter values. A description of the computational algorithms used is presented in Appendix E. The simulation presented in the main text are supposed to be illustrative rather than a detailed calibration for a specific circumstance. Nevertheless, the baseline calibration adopts the central values of the epidemiology parameters in Fernández-Villaverde and Jones (2020). For example, in Figure 1 we set the value of the exogenous component of the infection rate in the healthy country, $\alpha_1 = 0.04$, and we vary the value for the sick country between $\alpha_2 \in [0.04, 0.1]$. Using the equilibrium values of interactions, this leads to a value of $2n_{ii}\alpha_i + n_{ij}\alpha_j + n_{ji}\alpha_i$ (the actual infection rate in Country i if $I_i = I_j$) in the range $[0.15, 0.20]$ in Country 1 and $[0.15, 0.33]$ in Country 2, well in the range of values estimated in Fernández-Villaverde and Jones (2020). We also set $\gamma_i = 0.2$, which implies an infectious period of 5 days.

The economic model also involves a number of parameters. We set the elasticity of substitution $\sigma = 5$, a central value in the trade literature (Costinot and Rodríguez-Clare, 2015), and normalize productivity $Z_i = 1$ for all i . We also set Country size $L_i = 3$ when countries are symmetric. We choose values so that the choice of trading partners n_{ij} is never constrained. We choose a baseline

value for the elasticity of the cost of consuming more varieties in a region of $\phi = 2$. Hence, the second order conditions discussed in the text are satisfied since $\phi > 1/(\sigma - 1)$. Note that we also require $\phi > 1$. We eliminate all man-made frictions in the baseline, so $t_{ij} = \mu_{ij} = 1$ for all i, j , and let $d_{ij} = 1.1$ for $i \neq j$ and 1 otherwise. We set to one the elasticity of trade costs with respect to distance, so $\delta = 1$. Finally we set the level of the cost of creating contacts, $c = 0.15$, which guarantees that equilibrium contacts are always in an interior solution. Of course, in the main text we show a number of exercises in which we change these parameter values, and in particular introduce trade and mobility frictions. Whenever we vary from the parameter values mentioned above we state that in the discussion of the relevant graph.

Globalization and Pandemics

Pol Antràs, Stephen J. Redding, and Esteban Rossi-Hansberg

Online Appendix (Not for Publication)

C Extensions of Economic Model

In this Appendix, we flesh out some of the details of the four extensions of our framework mentioned in Section 2.3 of the main text.

C.1 Traveling Costs in Terms of Labor

If traveling costs are specified in terms of labor (rather than utility), welfare at the household level depends only on consumption

$$W_i = \left(\sum_{j \in \mathcal{J}} \int_0^{n_{ij}} q_{ij}(k) \frac{\sigma-1}{\sigma} dk \right)^{\frac{\sigma}{\sigma-1}},$$

and the implied demand (for a given n_{ii} and n_{ij}) is given by

$$q_{ij}(k) = \left(\frac{p_{ij}}{P_i} \right)^{-\sigma} \frac{\mathcal{I}_i}{P_i},$$

where \mathcal{I}_i is household income, which is given by

$$\mathcal{I}_i = w_i \left(1 - \frac{c}{\phi} \sum_{j \in \mathcal{J}} \mu_{ij} d_{ij}^{\rho} n_{ij}^{\phi} \right),$$

since the household now needs to hire labor to be able to secure final-good differentiated varieties, and where

$$P_i = \left(\sum_{j \in \mathcal{J}} n_{ij} p_{ij}^{1-\sigma} \right)^{\frac{1}{1-\sigma}}.$$

Welfare can therefore be rewritten as

$$W_i = \frac{\mathcal{I}_i}{P_i} = w_i \left(1 - \frac{c}{\phi} \sum_{j \in \mathcal{J}} \mu_{ij} d_{ij}^{\rho} n_{ij}^{\phi} \right) \left(\sum_{j \in \mathcal{J}} n_{ij} p_{ij}^{1-\sigma} \right)^{\frac{1}{\sigma-1}}$$

The first-order condition for the choice of n_{ij} delivers:

$$n_{ij} = (c(\sigma - 1))^{-\frac{1}{\phi-1}} \left(\frac{\mathcal{I}_i}{w_i} \right)^{\frac{1}{\phi-1}} \left(\frac{t_{ij} w_j}{Z_j P_i} \right)^{-\frac{\sigma-1}{\phi-1}} \mu_{ij}^{-\frac{1}{\phi-1}} d_{ij}^{-\frac{\rho+\delta(\sigma-1)}{\phi-1}}$$

Bilateral import flows by country i from country j are given by

$$X_{ij} = n_{ij} p_{ij} q_{ij} L_i = (c(\sigma - 1))^{-\frac{1}{\phi-1}} \left(\frac{\mathcal{I}_i}{w_i} \right)^{\frac{1}{\phi-1}} \left(\frac{t_{ij} w_j}{Z_j P_i} \right)^{-\frac{\phi(\sigma-1)}{\phi-1}} \mu_{ij}^{-\frac{1}{\phi-1}} d_{ij}^{-\frac{\rho+\phi\delta(\sigma-1)}{\phi-1}} \mathcal{I}_i L_i,$$

and the trade share can be written as

$$\pi_{ij} = \frac{X_{ij}}{\sum_{l \in \mathcal{J}} X_{il}} = \frac{\left(\frac{w_j}{Z_j}\right)^{-\frac{\phi(\sigma-1)}{\phi-1}} \times \mu_{ij}^{-\frac{1}{\phi-1}} d_{ij}^{-\frac{\rho+\phi\delta(\sigma-1)}{\phi-1}} t_{ij}^{-\frac{\phi(\sigma-1)}{\phi-1}}}{\sum_{l \in \mathcal{J}} \left(\frac{w_l}{Z_l}\right)^{-\frac{\phi(\sigma-1)}{\phi-1}} \times \mu_{il}^{-\frac{1}{\phi-1}} d_{il}^{-\frac{\rho+\phi\delta(\sigma-1)}{\phi-1}} t_{il}^{-\frac{\phi(\sigma-1)}{\phi-1}}} = \frac{S_j}{\Phi_i} \times \Gamma_{ij}^{-\varepsilon},$$

where

$$\Gamma_{ij}^{-\varepsilon} = \mu_{ij}^{-\frac{1}{\phi-1}} d_{ij}^{-\frac{\rho+\phi\delta(\sigma-1)}{\phi-1}} t_{ij}^{-\frac{\phi(\sigma-1)}{\phi-1}},$$

which is identical to equation (9) applying to our baseline model with traveling costs in terms of labor.

The price index is in turn given by

$$P_i = (c(\sigma - 1))^{\frac{1}{\phi(\sigma-1)}} \left(\frac{\mathcal{I}_i}{w_i}\right)^{-\frac{1}{\phi(\sigma-1)}} \left(\sum_{j \in \mathcal{J}} \left(\frac{w_j}{Z_j}\right)^{-\frac{\phi(\sigma-1)}{\phi-1}} \Gamma_{ij}^{-\varepsilon}\right)^{-\frac{\phi-1}{\phi(\sigma-1)}},$$

and using this expression together for the one for π_{ij} , one can verify that we can write

$$n_{ij} = \left(\frac{t_{ij} d_{ij}^\delta w_j}{Z_j P_i}\right)^{\sigma-1} \pi_{ij},$$

just as in equation (15) of the main text.

Plugging this expression back into the budget constraint yields

$$\mathcal{I}_i = \frac{\phi(\sigma - 1)}{\phi(\sigma - 1) + 1} w_i,$$

and a resulting price index equal to

$$P_i = \left(\frac{c\phi}{\phi(\sigma - 1) + 1}\right)^{\frac{1}{\phi(\sigma-1)}} \left(\sum_{j \in \mathcal{J}} \left(\frac{w_j}{Z_j}\right)^{-\frac{\phi(\sigma-1)}{\phi-1}} \Gamma_{ij}^{-\varepsilon}\right)^{-\frac{\phi-1}{\phi(\sigma-1)}},$$

which is only slightly different than expression (11) in the main text,

The labor-market conditions are given by

$$\pi_{ii} \mathcal{I}_i L_i + \pi_{ji} \mathcal{I}_j L_j = \mathcal{I}_i L_i$$

or, equivalently,

$$\pi_{ii} w_i L_i + \pi_{ji} w_j L_j = w_i L_i,$$

just as in the main text, and remember that the expressions for π_{ii} and π_{ji} are also left unchanged.

We next turn to verifying that Propositions 1 through 4 in the main text continue to hold whenever travel costs in equation (1) are specified in terms of labor rather than being modelled as

a utility cost.

Proposition 1’: *As long as trade frictions (Γ_{ij}) are bounded, there exists a unique vector of equilibrium wages $w^* = (w_i, w_j) \in R_{++}^2$ that solves the system of equations above.*

Proof. By results in standard gravity models in Alvarez and Lucas (2007), Allen and Arkolakis (2014), and Allen et al. (2020). ■

Proposition 2’: *A decline in any international trade or mobility friction $(d_{ij}, t_{ij}, t_{ji}, \mu_{ij}, \mu_{ji})$ leads to: (a) a decline in the rates $(n_{ii}$ and $n_{jj})$ at which individuals will meet individuals in their own country; and (b) an increase in the rates at which individuals will meet individuals from the other country $(n_{ij}$ and $n_{ji})$.*

Proof. (a) Given that $\mathcal{I}_i = \frac{\phi(\sigma-1)}{\phi(\sigma-1)+1}w_i$,

$$n_{ii} = (c(\sigma - 1))^{-\frac{1}{\phi-1}} \left(\frac{\mathcal{I}_i}{w_i}\right)^{\frac{1}{\phi-1}} \left(\frac{t_{ii}w_i}{Z_iP_i}\right)^{-\frac{\sigma-1}{\phi-1}} \mu_{ii}^{-\frac{1}{\phi-1}} d_{ii}^{-\frac{\rho+\delta(\sigma-1)}{\phi-1}} = const \times \left(\frac{P_i}{w_i}\right)^{\frac{\sigma-1}{\phi-1}}$$

Then

$$\frac{P_i}{w_i} = \left(\frac{c\phi}{\phi(\sigma - 1) + 1}\right)^{\frac{1}{\phi(\sigma-1)}} \left(Z_i^{\frac{\phi(\sigma-1)}{\phi-1}} \Gamma_{ii}^{-\varepsilon} + \left(\frac{Z_j}{\omega}\right)^{\frac{\phi(\sigma-1)}{\phi-1}} \Gamma_{ij}^{-\varepsilon} \right)^{-\frac{\phi-1}{\phi(\sigma-1)}},$$

where $\omega = w_j/w_i$ is the relative wage in country j .

Note that the labor constraint can be rewritten as

$$\frac{Z_i^{\frac{\phi(\sigma-1)}{\phi-1}} \Gamma_{ii}^{-\varepsilon}}{Z_i^{\frac{\phi(\sigma-1)}{\phi-1}} \Gamma_{ii}^{-\varepsilon} + \left(\frac{Z_j}{\omega}\right)^{\frac{\phi(\sigma-1)}{\phi-1}} \Gamma_{ij}^{-\varepsilon}} L_i + \frac{Z_i^{\frac{\phi(\sigma-1)}{\phi-1}} \Gamma_{ji}^{-\varepsilon}}{Z_i^{\frac{\phi(\sigma-1)}{\phi-1}} \Gamma_{ji}^{-\varepsilon} + \left(\frac{Z_j}{\omega}\right)^{\frac{\phi(\sigma-1)}{\phi-1}} \Gamma_{jj}^{-\varepsilon}} \omega L_j = L_i$$

Consider a case when Γ_{ij} decreases, while other Γ_{kl} remain constant. That means that the first term in the sum goes down, while the second term is constant. For the equality to hold, ω should increase. After re-equilibration, the second term in the sum increased, which means that the first term decreased. This means that P_i/w_i decreased, and n_{ii} as well.

Consider now a case when Γ_{ji} decreases, while other Γ_{kl} remain constant. The second term increases, so ω needs to go down to equilibrate the model. That means that the first term decreases, and P_i/w_i and n_{ii} decrease by extension.

Therefore, whenever one decreases any international friction $(d_{ij}, t_{ij}, t_{ji}, \mu_{ij}, \mu_{ji})$, Γ_{ij} or Γ_{ji} goes down, and, hence, n_{ii} and n_{jj} go down.

(b) Note that

$$\frac{\mathcal{I}_i}{w_i} = 1 - \frac{c}{\phi} \sum_{j \in \mathcal{J}} \mu_{ij} d_{ij}^\rho n_{ij}^\phi$$

Since $\mathcal{I}_i = \frac{\phi(\sigma-1)}{\phi(\sigma-1)+1}w_i$, the left-hand side is constant. Since n_{ii} and n_{jj} decrease, n_{ij} and n_{ji} must increase. ■

Proposition 3’: *Suppose that countries are symmetric, in the sense that $L_i = L$, $Z_i = Z$, and $\Gamma_{ij} = \Gamma$ for all i . Then a decline in any (symmetric) international trade frictions leads to an overall increase in human interactions ($n_{dom} + n_{for}$) experienced by both household buyers and household sellers.*

Proof. We begin by considering the case with general country asymmetries. Consider the sum

$$\mu_{ii}d_{ii}^\rho n_{ii}^\phi + \mu_{ij}d_{ij}^\rho n_{ij}^\phi = \frac{1}{\phi(\sigma - 1) + 1}$$

Differentiating yields

$$\phi\mu_{ii}d_{ii}^\rho n_{ii}^{\phi-1} dn_{ii} + \phi\mu_{ij}d_{ij}^\rho n_{ij}^{\phi-1} dn_{ij} + \underbrace{\phi n_{ij}^\phi d(\mu_{ij}d_{ij}^\rho)}_{\leq 0} = 0$$

Hence,

$$\phi\mu_{ii}d_{ii}^\rho n_{ii}^{\phi-1} dn_{ii} + \phi\mu_{ij}d_{ij}^\rho n_{ij}^{\phi-1} dn_{ij} \geq 0,$$

and if $\mu_{ii}d_{ii}^\rho n_{ii}^{\phi-1} > \mu_{ij}d_{ij}^\rho n_{ij}^{\phi-1}$, then $dn_{ij} > -dn_{ii}$.

From the FOC for the choice of n_{ii} and n_{ij} ,

$$\mu_{ii}d_{ii}^\rho n_{ii}^{\phi-1} = \frac{1}{c(\sigma - 1)} \frac{\mathcal{I}_i}{w_i} \left(\frac{p_{ii}}{P_i}\right)^{1-\sigma}$$

$$\mu_{ij}d_{ij}^\rho n_{ij}^{\phi-1} = \frac{1}{c(\sigma - 1)} \frac{\mathcal{I}_i}{w_i} \left(\frac{p_{ij}}{P_i}\right)^{1-\sigma}$$

Therefore, $\mu_{ii}d_{ii}^\rho n_{ii}^{\phi-1} > \mu_{ij}d_{ij}^\rho n_{ij}^{\phi-1}$ is satisfied if and only if $p_{ii} < p_{ij}$.

When countries are symmetric, this holds trivially because of international trade costs $t_{ij} > t_{ii}$ and $d_{ij} > d_{ii}$. Hence, $dn_{ij} > -dn_{ii}$, and $n_{dom} + n_{for}$ increases. ■

Proposition 4’: *An increase in the relative size of country i ’s population leads to an increase in the rate n_{ii} at which individuals from i will meet individuals in their own country, and to a decrease in the rate n_{ij} at which individuals will meet individuals abroad.*

Proof. Consider again

$$\frac{Z_i^{\frac{\phi(\sigma-1)}{\phi-1}} \Gamma_{ii}^{-\varepsilon}}{Z_i^{\frac{\phi(\sigma-1)}{\phi-1}} \Gamma_{ii}^{-\varepsilon} + \left(\frac{Z_j}{\omega}\right)^{\frac{\phi(\sigma-1)}{\phi-1}} \Gamma_{ij}^{-\varepsilon}} L_i + \frac{Z_i^{\frac{\phi(\sigma-1)}{\phi-1}} \Gamma_{ji}^{-\varepsilon}}{Z_i^{\frac{\phi(\sigma-1)}{\phi-1}} \Gamma_{ji}^{-\varepsilon} + \left(\frac{Z_j}{\omega}\right)^{\frac{\phi(\sigma-1)}{\phi-1}} \Gamma_{jj}^{-\varepsilon}} \omega L_j = L_i$$

An increase in L_i makes the left-hand side smaller than the right-hand side. Therefore, ω grows to

re-equilibrate. Then

$$\frac{P_i}{w_i} = \left(\frac{c\phi}{\phi(\sigma-1)+1} \right)^{\frac{1}{\phi(\sigma-1)}} \left(Z_i^{\frac{\phi(\sigma-1)}{\phi-1}} \Gamma_{ii}^{-\varepsilon} + \left(\frac{Z_j}{\omega} \right)^{\frac{\phi(\sigma-1)}{\phi-1}} \Gamma_{ij}^{-\varepsilon} \right)^{-\frac{\phi-1}{\phi(\sigma-1)}},$$

increases, and $n_{ii} = \text{const} \times \left(\frac{P_i}{w_i} \right)^{\frac{\sigma-1}{\phi-1}}$ increases with it.

Since

$$\mu_{ii} d_{ii}^\rho n_{ii}^\phi + \mu_{ij} d_{ij}^\rho n_{ij}^\phi = \frac{1}{\phi(\sigma-1)+1},$$

n_{ij} decreases.

Therefore, following a growth in population L_i , n_{ii} increases while n_{ij} decreases. ■

C.2 International Sourcing of Inputs

The assumption that households travel internationally to procure final goods may seem unrealistic. Perhaps international travel is better thought as being a valuable input when firms need specialized inputs and seek potential providers of those inputs in various countries. It is straightforward to re-interpret our model along those lines. In particular, suppose now that all households in country i produce a homogeneous final good but also produce differentiated intermediate input varieties. The household's final good is produced combining a bundle of the intermediate inputs produced by other households. Technology for producing the final good is given by

$$Q_i = \left(\sum_{j \in \mathcal{J}} \int_0^{n_{ij}^I} q_{ij}^I(k)^{\frac{\sigma-1}{\sigma}} dk \right)^{\frac{\sigma}{\sigma-1}}$$

and this final good is not traded (this is without loss of generality if households are homogeneous in each country and trade costs for final goods are large enough). Household welfare is linear in consumption of the final good and is reduced by the disutility cost of a household's member having to travel to secure intermediate inputs. In particular, we have

$$W_i = \left(\sum_{j \in \mathcal{J}} \int_0^{n_{ij}^I} q_{ij}^I(k)^{\frac{\sigma-1}{\sigma}} dk \right)^{\frac{\sigma}{\sigma-1}} - \frac{c}{\phi} \sum_{j \in \mathcal{J}} \mu_{ij} (d_{ij})^\rho \times (n_{ij}^I)^\phi.$$

Under this model is isomorphic to the one above, except that trade will be in intermediate inputs rather than in final goods.

C.3 Multi-Country Model

We next consider a version of our model with a world economy featuring multiple countries. It should be clear that all our equilibrium conditions, except for the labor-market clearing condition (14) apply to that multi-country environment once the set of countries \mathcal{J} is redefined to include

multiple countries. The labor-market condition is in turn simply given by

$$\sum_{j \in \mathcal{J}} \pi_{ij}(\mathbf{w}) w_j L_j = w_i L_i,$$

where $\pi_{ij}(\mathbf{w})$ is defined in (9) for an arbitrary set of countries \mathcal{J} . Similarly, the model is also easily adaptable to the case in which there is a continuum of locations $i \in \Omega$, where Ω is a closed and bounded set of a finite dimensional Euclidean space. The equilibrium conditions are again unaltered, with integrals replacing summation operators throughout.

From the results in Alvarez and Lucas (2007), Allen and Arkolakis (2014), and Allen et al. (2020), it is clear that Proposition 1 in the main text on existence and uniqueness will continue to hold. In the presence of arbitrary asymmetries across countries, it is hard however to derive crisp comparative static results of the type in Propositions 2 and 4. Nevertheless, our result in Proposition 3 regarding the positive effect of declines of trade and mobility barriers on the overall level of human interactions between symmetric countries is easily generalizable to the case of many countries (details available upon request - future versions of the paper will include an Online Appendix with the details).

C.4 Traveling Salesman Model

Finally, we explore a variant of our model in which it is the household’s seller rather than the buyer who travels to other locations. We model this via a framework featuring scale economies, monopolistic competition and fixed cost of exporting, as in the literature on selection into exporting emanating from the seminal work of Melitz (2003), except that the fixed costs of selling are defined at the buyer level rather than at the country level, as in the work of Arkolakis (2010).

On the consumption side, households maximize their utility, given by

$$W_i = \left(\sum_{j \in \mathcal{J}} \int_0^{\eta_{ij}} q_{ij}(k)^{\frac{\sigma-1}{\sigma}} dk \right)^{\frac{\sigma}{\sigma-1}},$$

where η_{ij} is the measure of varieties available to them, subject to the household budget constraint. This yields

$$q_{ij}(k) = \left(\frac{p_{ij}}{P_i} \right)^{-\sigma} \frac{\mathcal{I}_i}{P_i},$$

where \mathcal{I}_i is household income and the price index is

$$P_i = \left(\sum_{j \in \mathcal{J}} \eta_{ij} p_{ij}^{1-\sigma} \right)^{\frac{1}{1-\sigma}}.$$

Household sellers in country j produce N_j varieties and make them available to n_{ij} consumers. Both N_j and n_{ij} are endogenous and pinned down as part of the equilibrium. Note that because there are L_i and L_j households in i and j , respectively, the measure of varieties available from j to consumers in i is given by $\eta_{ij} = n_{ij} N_j L_j / L_i$ (where implicitly we assume that which $n_{ij} < L_j$

consumers in j get access to a seller's varieties is chosen at random).

The level of output and price of each variety, as well as the measure of consumers n_{ij} sellers reach out to follows from profit maximization:

$$\max_{n_{ij}, p_{ij}} n_{ij} \left(p_{ij} - \frac{\tau_{ij} w_j}{Z_j} \right) q_{ij} - w_j \frac{c}{\phi} \mu_{ij} d_{ij}^\rho n_{ij}^\phi,$$

where again n_{ij} is the number of customers served, and where the remaining parameters are analogous to those in our baseline model.

Sellers naturally charge a constant markup over marginal cost,

$$p_{ij} = \frac{\sigma}{\sigma - 1} \frac{\tau_{ij} w_j}{Z_j},$$

so the choice of n_{ij} boils down to

$$\max_{n_{ij}} \frac{n_{ij}}{\sigma} p_{ij} q_{ij} - w_j \frac{c}{\phi} \mu_{ij} d_{ij}^\rho n_{ij}^\phi.$$

The first-order condition of this problem yields

$$\frac{p_{ij} q_{ij}}{\sigma} = w_j c \mu_{ij} d_{ij}^\rho n_{ij}^{\phi-1} \Rightarrow n_{ij} = \left(\frac{p_{ij} q_{ij}}{c \sigma \mu_{ij} d_{ij}^\rho w_j} \right)^{\frac{1}{\phi-1}}$$

Developing a new variety costs $w_i f$. Hence, by free entry, $\sum_k \Pi_{ki} = w_i f$, and the zero-profit condition also entails $\mathcal{I}_i = w_i$. As a result, we can express n_{ij} as

$$n_{ij} = (c\sigma)^{-\frac{1}{\phi-1}} \mu_{ij}^{-\frac{1}{\phi-1}} d_{ij}^{-\frac{\rho+(\sigma-1)\delta}{\phi-1}} \left(\frac{\sigma}{\sigma-1} \frac{\tau_{ij} w_j}{P_i Z_j} \right)^{-\frac{\sigma-1}{\phi-1}} \left(\frac{w_i}{w_j} \right)^{\frac{1}{\phi-1}}.$$

With this expression at hand, we can compute the import volume of country i from country j :

$$\begin{aligned} X_{ij} &= \eta_{ij} p_{ij} q_{ij} L_i = n_{ij} p_{ij} q_{ij} N_j L_j \\ &= w_j c \sigma \mu_{ij} d_{ij}^\rho n_{ij}^\phi N_j L_j \\ &= (c\sigma)^{-\frac{1}{\phi-1}} \mu_{ij}^{-\frac{1}{\phi-1}} d_{ij}^{-\frac{\rho+(\sigma-1)\delta}{\phi-1}} \left(\frac{\sigma}{\sigma-1} \frac{\tau_{ij} w_j}{P_i Z_j} \right)^{-\frac{\phi(\sigma-1)}{\phi-1}} \left(\frac{w_i}{w_j} \right)^{\frac{1}{\phi-1}} w_i N_j L_j \\ &= (c\sigma)^{-\frac{1}{\phi-1}} \Gamma_{ij}^{-\varepsilon} \left(\frac{\sigma}{\sigma-1} \frac{w_j}{P_i Z_j} \right)^{-\frac{\phi(\sigma-1)}{\phi-1}} \left(\frac{w_i}{w_j} \right)^{\frac{1}{\phi-1}} w_i N_j L_j \end{aligned}$$

Hence, the share of country j in country i 's import is

$$\pi_{ij} = \frac{\Gamma_{ij}^{-\varepsilon} \left(\frac{w_j}{Z_j} \right)^{-\frac{\phi(\sigma-1)}{\phi-1}} w_j^{-\frac{1}{\phi-1}} N_j L_j}{\sum_k \Gamma_{ik}^{-\varepsilon} \left(\frac{w_k}{Z_k} \right)^{-\frac{\phi(\sigma-1)}{\phi-1}} w_k^{-\frac{1}{\phi-1}} N_k L_k}.$$

Solving for price index yields

$$\begin{aligned}
 w_i L_i &= \sum_j X_{ij} \\
 w_i L_i &= \sum_j (c\sigma)^{-\frac{1}{\phi-1}} \Gamma_{ij}^{-\varepsilon} \left(\frac{\sigma}{\sigma-1} \frac{w_j}{P_i Z_j} \right)^{-\frac{\phi(\sigma-1)}{\phi-1}} \left(\frac{w_i}{w_j} \right)^{\frac{1}{\phi-1}} w_i N_j L_j \\
 P_i &= \frac{\sigma}{\sigma-1} (c\sigma)^{\frac{1}{\phi(\sigma-1)}} L_i^{\frac{\phi-1}{\phi(\sigma-1)}} \left(\sum_j \Gamma_{ij}^{-\varepsilon} \left(\frac{w_j}{Z_j} \right)^{-\frac{\phi(\sigma-1)}{\phi-1}} \left(\frac{w_i}{w_j} \right)^{\frac{1}{\phi-1}} N_j L_j \right)^{-\frac{\phi-1}{\phi(\sigma-1)}}.
 \end{aligned}$$

We can next study the choice of the number of varieties N_j produced by sellers. Profits of sellers are given by

$$\Pi_{ij} = \frac{\phi-1}{\phi} \frac{n_{ij} p_{ij} q_{ij}}{\sigma} = \frac{\phi-1}{\phi} \frac{X_{ij}}{\sigma N_j L_j},$$

so the zero-profit condition implies

$$\sum_k \Pi_{ki} = w_i f \Rightarrow \frac{\phi-1}{\phi} \frac{1}{\sigma N_i L_i} \sum_k X_{ki} = w_i f.$$

Since $\sum_k X_{ki} = w_i L_i$,

$$\frac{\phi-1}{\phi} \frac{w_i L_i}{\sigma N_i L_i} = w_i f \Rightarrow N_i = \frac{\phi-1}{\phi \sigma f}$$

Hence, the number of varieties is constant and independent of many of the parameters of the model.

We finally turn to the general equilibrium of the model, which is associated with the condition:

$$\pi_{ii} w_i L_i + \pi_{ji} w_j L_j = w_i L_i$$

Plugging in the expressions for trade shares yields

$$\frac{\Gamma_{ii}^{-\varepsilon} \left(\frac{w_i}{Z_i} \right)^{-\frac{\phi(\sigma-1)}{\phi-1}} w_i^{-\frac{1}{\phi-1}} L_i}{\sum_k \left(\Gamma_{ik}^{-\varepsilon} \frac{w_k}{Z_k} \right)^{-\frac{\phi(\sigma-1)}{\phi-1}} w_k^{-\frac{1}{\phi-1}} L_k} w_i L_i + \frac{L_i \left(\frac{w_i}{Z_i} \right)^{-\frac{\phi(\sigma-1)}{\phi-1}} w_i^{-\frac{1}{\phi-1}} \Gamma_{ji}^{-\varepsilon}}{\sum_k L_k \left(\frac{w_k}{Z_k} \right)^{-\frac{\phi(\sigma-1)}{\phi-1}} w_k^{-\frac{1}{\phi-1}} \Gamma_{jk}^{-\varepsilon}} w_j L_j = w_i L_i.$$

We are now ready to state and proof results analogous to those in Propositions 1 and 4 in the main text.

Proposition 1”: As long as trade frictions (Γ_{ij}) are bounded, there exists a unique vector of equilibrium wages $\mathbf{w}^* = (w_i, w_j) \in \mathbb{R}_{++}^2$ that solves the system of equations above.

Proof. This follows again from results in standard gravity models in Alvarez and Lucas (2007), Allen and Arkolakis (2014), and Allen et al. (2020), and the fact that if there exists a unique wage vector, the remaining equilibrium variables in this single-sector economy are uniquely determined.

■

Proposition 2”: A decline in any international trade or mobility friction ($d_{ij}, t_{ij}, t_{ji}, \mu_{ij}, \mu_{ji}$) leads to: (a) a decline in the rates (n_{ii} and n_{jj}) at which individuals will meet individuals in their own country; and (b) an increase in the rates at which individuals will meet individuals from the other country (n_{ij} and n_{ji}).

Proof. (a) First, note that

$$n_{ii} = \xi \mu_{ii}^{-\frac{1}{\phi-1}} d_{ii}^{-\frac{\rho+(\sigma-1)\delta}{\phi-1}} \left(\frac{t_{ii} w_i}{P_i Z_i} \right)^{-\frac{\sigma-1}{\phi-1}} = const \times \left(\frac{P_i}{w_i} \right)^{\frac{\sigma-1}{\phi-1}}$$

Then

$$\frac{P_i}{w_i} = const \times L_i^{\frac{\phi-1}{\phi(\sigma-1)}} \left(L_i \Gamma_{ii}^{-\varepsilon} Z_i^{\frac{\phi(\sigma-1)}{\phi-1}} + L_j \Gamma_{ij}^{-\varepsilon} \left(\frac{Z_j}{\omega} \right)^{\frac{\phi(\sigma-1)}{\phi-1}} \omega^{-\frac{1}{\phi-1}} \right)^{-\frac{\phi-1}{\phi(\sigma-1)}}$$

where $\omega = w_j/w_i$ is the relative wage in country j .

Note that the equilibrium equations can be rewritten as

$$\frac{L_i Z_i^{\frac{\phi(\sigma-1)}{\phi-1}} \Gamma_{ii}^{-\varepsilon}}{L_i Z_i^{\frac{\phi(\sigma-1)}{\phi-1}} \Gamma_{ii}^{-\varepsilon} + L_j \left(\frac{Z_j}{\omega} \right)^{\frac{\phi(\sigma-1)}{\phi-1}} \omega^{-\frac{1}{\phi-1}} \Gamma_{ij}^{-\varepsilon}} L_i \tag{C.1}$$

$$+ \frac{L_i Z_i^{\frac{\phi(\sigma-1)}{\phi-1}} \Gamma_{ji}^{-\varepsilon}}{L_i Z_i^{\frac{\phi(\sigma-1)}{\phi-1}} \Gamma_{ji}^{-\varepsilon} + L_j \left(\frac{Z_j}{\omega} \right)^{\frac{\phi(\sigma-1)}{\phi-1}} \omega^{-\frac{1}{\phi-1}} \Gamma_{jj}^{-\varepsilon}} \omega L_j = L_i \tag{C.2}$$

Consider a case when Γ_{ij} decreases, while other Γ_{kl} remain constant. That means that the first term in the sum goes down, while the second term is constant. For the equality to hold, ω should increase. After re-equilibration, the second term in the sum increased, which means that the first term decreased. This means that P_i/w_i decreased, and n_{ii} as well.

Consider now a case when Γ_{ji} decreases, while other Γ_{kl} remain constant. The second term increases, so ω needs to go down to equilibrate the model. That means that the first term decreases, and P_i/w_i and n_{ii} decrease by extension.

Therefore, whenever one decreases any international friction ($d_{ij}, t_{ij}, t_{ji}, \mu_{ij}, \mu_{ji}$), Γ_{ij} or Γ_{ji} goes down, and, hence, n_{ii} and n_{jj} go down.

(b) Note that $\Pi_{ii} + \Pi_{ji} = w_i f$. That can be rewritten as

$$\frac{\phi-1}{\phi} \frac{n_{ii} p_{ii} q_{ii}}{w_i \sigma} + \frac{\phi-1}{\phi} \frac{n_{ji} p_{ji} q_{ji}}{w_i \sigma} = f$$

Using the FOC for n_{ij} , that yields

$$\frac{\phi-1}{\phi} c \mu_{ii}^\rho d_{ii}^\phi n_{ii}^\phi + \frac{\phi-1}{\phi} c \mu_{ji}^\rho d_{ji}^\rho n_{ji}^\phi = f$$

Since n_{ii} and n_{jj} decrease and frictions do not increase, n_{ij} and n_{ji} have to increase. ■

Proposition 3’: Suppose that countries are symmetric, in the sense that $L_i = L$, $Z_i = Z$, and $\Gamma_{ij} = \Gamma$ for all i . Then a decline in any (symmetric) international trade frictions leads to an overall increase in human interactions ($n_{dom} + n_{for}$) experienced by both household buyers and household sellers.

Proof. We begin by considering the case with general country asymmetries. Consider the sum

$$\mu_{ii}d_{ii}^\rho n_{ii}^\phi + \mu_{ji}d_{ji}^\rho n_{ji}^\phi = const$$

Differentiating yields

$$\phi\mu_{ii}d_{ii}^\rho n_{ii}^{\phi-1} dn_{ii} + \phi\mu_{ji}d_{ji}^\rho n_{ji}^{\phi-1} dn_{ji} + \underbrace{n_{ji}^\phi d\left(\frac{\mu_{ji}d_{ji}^\rho}{\omega}\right)}_{\leq 0} = 0$$

Hence,

$$\mu_{ii}d_{ii}^\rho n_{ii}^{\phi-1} dn_{ii} + \mu_{ji}d_{ji}^\rho n_{ji}^{\phi-1} dn_{ji} \geq 0,$$

and if $\mu_{ii}d_{ii}^\rho n_{ii}^{\phi-1} > \mu_{ji}d_{ji}^\rho n_{ji}^{\phi-1}$, then $dn_{ji} > -dn_{ii}$.

From the FOC for the choice of n_{ii} and n_{ji} ,

$$\mu_{ii}d_{ii}^\rho n_{ii}^{\phi-1} = const \times \frac{p_{ii}q_{ii}}{w_i} = const \times \left(\frac{p_{ii}}{P_i}\right)^{1-\sigma}$$

$$\mu_{ji}d_{ji}^\rho n_{ji}^{\phi-1} = const \times \frac{p_{ji}q_{ji}}{w_i} = const \times \left(\frac{p_{ji}}{P_j}\right)^{1-\sigma} \left(\frac{w_j}{w_i}\right)$$

Since the countries are symmetric, $P_i = P_j$ and $w_i = w_j$, so the inequality is satisfied if and only if $p_{ii} < p_{ji}$.

When countries are symmetric, this holds trivially because of international trade costs $t_{ji} > t_{ii}$ and $d_{ji} > d_{ii}$. Hence, $dn_{ji} > -dn_{ii}$, and $n_{dom} + n_{for}$ increases. ■

Proposition 4’: An increase in the relative size of country i ’s population leads to an increase in the rate n_{ii} at which individuals from i will meet individuals in their own country, and to a decrease in the rate n_{ji} at which individuals will meet individuals abroad.

Proof. Consider again

$$\frac{L_i Z_i^{\frac{\phi(\sigma-1)}{\phi-1}} \Gamma_{ii}^{-\varepsilon}}{L_i Z_i^{\frac{\phi(\sigma-1)}{\phi-1}} \Gamma_{ii}^{-\varepsilon} + L_j \left(\frac{Z_j}{\omega}\right)^{\frac{\phi(\sigma-1)}{\phi-1}} \omega^{-\frac{1}{\phi-1}} \Gamma_{ij}^{-\varepsilon}} L_i \tag{C.3}$$

$$+ \frac{L_i Z_i^{\frac{\phi(\sigma-1)}{\phi-1}} \Gamma_{ji}^{-\varepsilon}}{L_i Z_i^{\frac{\phi(\sigma-1)}{\phi-1}} \Gamma_{ji}^{-\varepsilon} + L_j \left(\frac{Z_j}{\omega}\right)^{\frac{\phi(\sigma-1)}{\phi-1}} \omega^{-\frac{1}{\phi-1}} \Gamma_{jj}^{-\varepsilon}} \omega L_j = L_i \tag{C.4}$$

An increase in L_i makes the left-hand side smaller than the right-hand side. Therefore, ω grows to re-equilibrate. Then

$$\frac{P_i}{w_i} = const \times L_i^{\frac{\phi-1}{\phi(\sigma-1)}} \left(L_i \Gamma_{ii}^{-\varepsilon} Z_i^{\frac{\phi(\sigma-1)}{\phi-1}} + L_j \Gamma_{ij}^{-\varepsilon} \left(\frac{Z_j}{\omega} \right)^{\frac{\phi(\sigma-1)}{\phi-1}} \omega^{-\frac{1}{\phi-1}} \right)^{-\frac{\phi-1}{\phi(\sigma-1)}}$$

increases, and $n_{ii} = const \times \left(\frac{P_i}{w_i} \right)^{\frac{\sigma-1}{\phi}}$ increases with it.

Since

$$\frac{\phi-1}{\phi} c \mu_{ii} d_{ii}^{\rho} n_{ii}^{\phi} + \frac{\phi-1}{\phi} c \mu_{ji} d_{ji}^{\rho} n_{ji}^{\phi} = f,$$

n_{ji} decreases.

Therefore, following a growth in population L_i , n_{ii} increases while n_{ji} decreases. ■

D Proof of Proposition 5

Proposition 5: *Assume that there is trade between the two countries (i.e., $\alpha_j n_{ij} + \alpha_i n_{ji} > 0$), which implies that the next generation matrix FV^{-1} is irreducible. If $\mathcal{R}_0 \leq 1$, the no-pandemic equilibrium is the unique stable equilibrium. If $\mathcal{R}_0 > 1$, the no-pandemic equilibrium is unstable, and there exists a unique stable endemic equilibrium.*

Proof. The proof of existence and uniqueness, depending on whether $\mathcal{R}_0 \leq 1$ or $\mathcal{R}_0 > 1$, follows standard arguments for a two-group SIR model, as in Magal et al. (2016). We proceed in the following steps. (A) The system of dynamic equations for susceptibles, infected and recovered is given by:

$$\dot{S}_i(t) = -2\alpha_i n_{ii} S_i(t) I_i(t) - \alpha_j n_{ij} S_i(t) I_j(t) - \alpha_i n_{ji} S_i(t) I_j(t), \tag{D.1}$$

$$\dot{S}_j(t) = -2\alpha_j n_{jj} S_j(t) I_j(t) - \alpha_i n_{ji} S_j(t) I_i(t) - \alpha_j n_{ij} S_j(t) I_i(t), \tag{D.2}$$

$$\dot{I}_i(t) = 2\alpha_i n_{ii} S_i(t) I_i(t) + \alpha_j n_{ij} S_i(t) I_j(t) + \alpha_i n_{ji} S_i(t) I_j(t) - \gamma_i I_i(t), \tag{D.3}$$

$$\dot{I}_j(t) = 2\alpha_j n_{jj} S_j(t) I_j(t) + \alpha_i n_{ji} S_j(t) I_i(t) + \alpha_j n_{ij} S_j(t) I_i(t) - \gamma_j I_j(t), \tag{D.4}$$

$$\dot{R}_i(t) = \gamma_i I_i(t), \tag{D.5}$$

$$\dot{R}_j(t) = \gamma_j I_j(t). \tag{D.6}$$

Note that we can re-write the dynamic equations for infections (D.3) and (D.4) as:

$$\begin{bmatrix} \dot{I}_i(t) \\ \dot{I}_j(t) \end{bmatrix} = \left\{ \begin{bmatrix} \frac{2\alpha_i n_{ii}}{\gamma_i} S_i(t) & \frac{\alpha_j n_{ij} + \alpha_i n_{ji}}{\gamma_j} S_i(t) \\ \frac{\alpha_j n_{ij} + \alpha_i n_{ji}}{\gamma_i} S_j(t) & \frac{2\alpha_j n_{jj}}{\gamma_j} S_j(t) \end{bmatrix} - \begin{bmatrix} 1 & 0 \\ 0 & 1 \end{bmatrix} \right\} \begin{bmatrix} \gamma_i I_i(t) \\ \gamma_j I_j(t) \end{bmatrix}. \tag{D.7}$$

The properties of this dynamic system depend crucially on the properties of the matrix B :

$$B \equiv \begin{bmatrix} \frac{2\alpha_i n_{ii}}{\gamma_i} S_i(t) & \frac{\alpha_j n_{ij} + \alpha_i n_{ji}}{\gamma_j} S_i(t) \\ \frac{\alpha_j n_{ij} + \alpha_i n_{ji}}{\gamma_i} S_j(t) & \frac{2\alpha_j n_{jj}}{\gamma_j} S_j(t) \end{bmatrix}.$$

We assume that there is trade between the two countries:

$$\frac{\alpha_j n_{ij} + \alpha_i n_{ji}}{\gamma_i} > 0, \quad \frac{\alpha_j n_{ij} + \alpha_i n_{ji}}{\gamma_j} > 0,$$

which implies that the matrix B is irreducible for all strictly positive susceptibles $S_i(t), S_j(t) > 0$.

(B) Re-writing equations (D.1) and (D.2) in proportional changes, and using equations (D.5) and (D.6), we have:

$$\begin{aligned} \frac{\dot{S}_i(t)}{S_i(t)} &= -\frac{2\alpha_i n_{ii}}{\gamma_i} \dot{R}_i(t) - \frac{\alpha_j n_{ij} + \alpha_i n_{ji}}{\gamma_j} \dot{R}_j(t), \\ \frac{\dot{S}_j(t)}{S_j(t)} &= -\frac{2\alpha_j n_{jj}}{\gamma_j} \dot{R}_j(t) - \frac{\alpha_i n_{ji} + \alpha_j n_{ij}}{\gamma_i} \dot{R}_i(t). \end{aligned}$$

Integrating from 0 to t , we have:

$$\begin{aligned} \log S_i(t) - \log S_i(0) &= -\frac{2\alpha_i n_{ii}}{\gamma_i} (R_i(t) - R_i(0)) - \frac{\alpha_j n_{ij} + \alpha_i n_{ji}}{\gamma_j} (R_j(t) - R_j(0)), \\ \log S_j(t) - \ln S_j(0) &= -\frac{2\alpha_j n_{jj}}{\gamma_j} (R_j(t) - R_j(0)) - \frac{\alpha_i n_{ji} + \alpha_j n_{ij}}{\gamma_i} (R_i(t) - R_i(0)). \end{aligned}$$

Using the accounting identities, $S_i(t) + I_i(t) + R_i(t) = 1$ and $S_j(t) + I_j(t) + R_j(t) = 1$, we obtain:

$$\begin{aligned} \log S_i(t) - \log S_i(0) &= \frac{2\alpha_i n_{ii}}{\gamma_i} [(S_i(t) + I_i(t)) - (S_i(0) + I_i(0))] + \frac{\alpha_j n_{ij} + \alpha_i n_{ji}}{\gamma_j} [(S_j(t) + I_j(t)) - (S_j(0) + I_j(0))], \\ \log S_j(t) - \ln S_j(0) &= \frac{2\alpha_j n_{jj}}{\gamma_j} [(S_j(t) + I_j(t)) - (S_j(0) + I_j(0))] + \frac{\alpha_i n_{ji} + \alpha_j n_{ij}}{\gamma_i} [(S_i(t) + I_i(t)) - (S_i(0) + I_i(0))]. \end{aligned}$$

In steady-state as $t \rightarrow \infty$, we have $I_i(\infty) = I_j(\infty) = 0$, and hence:

$$S_i(\infty) = S_i(0) \exp \left[\frac{2\alpha_i n_{ii}}{\gamma_i} [S_i(\infty) - V_i] + \frac{\alpha_j n_{ij} + \alpha_i n_{ji}}{\gamma_j} [S_j(\infty) - V_j] \right], \quad (D.8)$$

$$S_j(\infty) = S_j(0) \exp \left[\frac{2\alpha_j n_{jj}}{\gamma_j} [S_j(\infty) - V_j] + \frac{\alpha_i n_{ji} + \alpha_j n_{ij}}{\gamma_i} [S_i(\infty) - V_i] \right], \quad (D.9)$$

where $V_i \equiv S_i(0) + I_i(0)$ and $V_j(0) \equiv S_j(0) + I_j(0)$. We now define the following notation:

$$X \leq Y \quad \Leftrightarrow \quad X_k \leq Y_k \text{ for all } k \in \{i, j\},$$

$$X < Y \quad \Leftrightarrow \quad X \leq Y \text{ and } X_k < Y_k \text{ for some } k \in \{i, j\},$$

$$X \ll Y \quad \Leftrightarrow \quad X_k < Y_k \text{ for all } k \in \{i, j\},$$

and represent the system (D.8)-(D.9) as the following map:

$$X = T(X),$$

$$\begin{pmatrix} x_i \\ x_j \end{pmatrix} = T \begin{pmatrix} x_i \\ x_j \end{pmatrix} = \begin{pmatrix} T_i(x_i, x_j) \\ T_j(x_i, x_j) \end{pmatrix},$$

with

$$T_i(x_i, x_j) = S_i(0) \exp \left[\frac{2\alpha_i n_{ii}}{\gamma_i} [x_i - V_i] + \frac{\alpha_j n_{ij} + \alpha_i n_{ji}}{\gamma_j} [x_j - V_j] \right],$$

$$T_j(x_i, x_j) = S_j(0) \exp \left[\frac{\alpha_i n_{ji} + \alpha_j n_{ij}}{\gamma_i} [x_i - V_i] + \frac{2\alpha_j n_{jj}}{\gamma_j} [x_j - V_j] \right].$$

(C) Using this notation, we begin by establishing that all the fixed points of T in $[0, S(0)]$ are contained in the smaller interval $[S^-, S^+]$. To establish this result, note that T is monotone in increasing, which implies that:

$$X \leq Y \Rightarrow T(X) \leq T(Y).$$

Using our assumption of positive trade, $\frac{\alpha_i n_{ji} + \alpha_j n_{ij}}{\gamma_i} > 0$ and $\frac{\alpha_j n_{ij} + \alpha_i n_{ji}}{\gamma_j} > 0$, this implies:

$$X \ll Y \Rightarrow T(X) \ll T(Y).$$

For $S(0) \gg 0$, and using the definitions of V_i and V_j above, this implies:

$$0 \ll T(0) < T(S(0)) < S(0).$$

Therefore, by induction arguments, we have the following result for each $n \geq 1$:

$$0 \ll T(0) \ll \dots \ll T^n(0) \ll T^{n+1}(0) \leq T^{n+1}(S(0)) < \dots < T^n(S(0)) < S(0).$$

By taking the limit as n does to $+\infty$, we obtain:

$$0 \ll \lim_{n \rightarrow +\infty} T^n(0) =: S^- \leq S^+ := \lim_{n \rightarrow +\infty} T^n(S(0)) < S(0).$$

Then, by continuity of T , we have:

$$T(S^-) = S^- \quad \text{and} \quad T(S^+) = S^+.$$

(D) We next establish that if $S^- < S^+$ then $S^- \ll S^+$. This property follows from our assumption that the matrix B above is irreducible. Assume, for example, that $S_i^- < S_i^+$. Then, since $\frac{\alpha_i n_{ji} + \alpha_j n_{ij}}{\gamma_i} > 0$, we have:

$$S_j^- = T_j(S_i^-, S_j^-) \leq T_j(S_i^-, S_j^+) < T_j(S_i^+, S_j^+) = S_j^+.$$

Hence,

$$S_i^- < S_i^+ \Rightarrow S_j^- < S_j^+.$$

By the same argument, $\frac{\alpha_j n_{ij} + \alpha_i n_{ji}}{\gamma_j} > 0$ implies,

$$S_j^- < S_j^+ \Rightarrow S_i^- < S_i^+.$$

(E) We now establish the following result for $\lambda > 1$ and $X \gg 0$:

$$T(\lambda X + S^-) - T(S^-) \gg \lambda [T(X + S^-) - T(S^-)].$$

Note that we can write the left-hand side of this inequality as follows:

$$T(\lambda X + S^-) - T(S^-) = \int_0^1 DT(l\lambda X + S^-)(\lambda X) dl = \lambda \int_0^1 DT(l\lambda X + S^-) X dl,$$

where the differential of T is given by:

$$DT(X) = \begin{pmatrix} \frac{2\alpha_i n_{ii}}{\gamma_i} T_i(x_i, x_j) & \frac{\alpha_j n_{ij} + \alpha_i n_{ji}}{\gamma_j} T_i(x_i, x_j) \\ \frac{\alpha_i n_{ji} + \alpha_j n_{ij}}{\gamma_i} T_j(x_i, x_j) & \frac{2\alpha_j n_{jj}}{\gamma_j} T_j(x_i, x_j) \end{pmatrix}. \tag{D.10}$$

Since $\lambda > 1$ and $X \gg 0$, we have:

$$DT(l\lambda X + S^-) X \gg DT(lX + S^-) X \quad \forall l \in [0, 1].$$

It follows that:

$$\begin{aligned} T(\lambda X + S^-) - T(S^-) &\gg \lambda \int_0^1 DT(lX + S^-) X dl, \\ &= \lambda [T(X + S^-) - T(S^-)], \end{aligned}$$

which establishes the result.

(F) We now show that the map T has at most two equilibria such that either:

- (i) $S^- = S^+$ and T has only one equilibrium in $[0, S(0)]$;
- (ii) $S^- \ll S^+$ and the only equilibria of T in $[0, S(0)]$ are S^- and S^+ .

We prove this result by contradiction. Assume that $S^- \neq S^+$. Then $S^- < S^+$, which implies $S^- \ll S^+$. Now suppose that there exists $\bar{X} \in [S^-, S^+]$ a fixed point T such that:

$$S^- \neq \bar{X} \quad \text{and} \quad \bar{X} \neq S^+.$$

Then, by using the same arguments as in (D) above, we have:

$$S^- \ll \bar{X} \ll S^+.$$

Now define:

$$\gamma := \sup \{ \lambda \geq 1 : \lambda (\bar{X} - S^-) + S^- \leq S^+ \}. \tag{D.11}$$

Since $\bar{X} \ll S^+$ this implies that

$$\gamma > 1.$$

We have

$$\gamma (\bar{X} - S^-) + S^- \leq S^+,$$

and, by applying T to both sides of this inequality, we obtain:

$$T (\gamma (\bar{X} - S^-) + S^-) \leq S^+.$$

Now, using **(E)**, we have:

$$\begin{aligned} T (\gamma (\bar{X} - S^-) + S^-) - T (S^-) &\gg \gamma [T ((\bar{X} - S^-) + S^-) - T (S^-)], \\ &= \gamma [T (\bar{X}) - T (S^-)], \\ &= \gamma [\bar{X} - S^-]. \end{aligned}$$

Therefore we have shown that:

$$S^+ \geq T (\gamma (\bar{X} - S^-) + S^-) \gg \gamma [\bar{X} - S^-],$$

which contradicts the definition of gamma as the supremum of the set in equation **(D.11)**, since $S^- \geq 0$. Therefore we cannot have another fixed point $\bar{X} \in [S^-, S^+]$.

(G) Now consider the case where:

$$S^- \ll S^+.$$

In this case of two equilibria, the differential of T can be written as:

$$DT (S^\pm) = B (S^\pm) = \begin{pmatrix} \frac{2\alpha_i n_{ii}}{\gamma_i} S_i^\pm & \frac{\alpha_j n_{ij} + \alpha_i n_{ji}}{\gamma_j} S_i^\pm \\ \frac{\alpha_i n_{ji} + \alpha_j n_{ij}}{\gamma_i} S_j^\pm & \frac{2\alpha_j n_{jj}}{\gamma_j} S_j^\pm \end{pmatrix}.$$

(H) We now establish the following property of the spectral radius of the matrices $DT (S^-)$ and $DT (S^+)$:

$$\rho (DT (S^-)) < 1 < \rho (DT (S^+)).$$

To prove this result, note that:

$$\begin{aligned} S^+ - S^- &= T (S^+) - T (S^-), \\ &= T ((S^+ - S^-) + S^-) - T (S^-), \\ &= \int_0^1 DT (l (S^+ - S^-) + S^-) (S^+ - S^-) dl. \end{aligned}$$

Since $S^+ - S^- \gg 0$, we also have:

$$\begin{aligned} DT(S^+)(S^+ - S^-) &\gg \int_0^1 DT(l(S^+ - S^-) + S^-)(S^+ - S^-) dl, \\ &\gg DT(S^-)(S^+ - S^-). \end{aligned}$$

Combining these two results, we obtain:

$$DT(S^+)(S^+ - S^-) \gg (S^+ - S^-) \gg DT(S^-)(S^+ - S^-). \tag{D.12}$$

which can be equivalently written as:

$$[DT(S^+) - I](S^+ - S^-) > 0,$$

$$[DT(S^+) - \xi^+ I](S^+ - S^-) = 0, \quad \xi^+ > 1,$$

and

$$[DT(S^-) - I](S^+ - S^-) < 0,$$

$$[DT(S^-) - \xi^- I](S^+ - S^-) = 0, \quad \xi^- < 1,$$

where I is the identity matrix. Noting that the matrices $DT(S^+)$ and $DT(S^-)$ are non-negative and irreducible, the Perron-Frobenius theorem implies:

$$\xi^- = \rho(DT(S^-)) < 1 < \rho(DT(S^+)) = \xi^+.$$

(I) We now solve explicitly for the spectral radius of the matrices $DT(S^\pm)$. We find the eigenvalues of the matrix $DT(S^\pm)$ by solving the characteristic equation:

$$|DT(S^\pm) - \xi^\pm I| = \left| \begin{bmatrix} \frac{2\alpha_i n_{ii}}{\gamma_i} S_i^\pm & \frac{\alpha_j n_{ij} + \alpha_i n_{ji}}{\gamma_j} S_j^\pm \\ \frac{\alpha_j n_{ij} + \alpha_i n_{ji}}{\gamma_j} S_j^\pm & \frac{2\alpha_j n_{jj}}{\gamma_j} S_j^\pm \end{bmatrix} - \begin{bmatrix} \xi^\pm & 0 \\ 0 & \xi^\pm \end{bmatrix} \right| = 0.$$

The characteristic polynomial is:

$$(\xi^\pm)^2 - \left(\frac{2\alpha_i n_{ii}}{\gamma_i} S_i^\pm + \frac{2\alpha_j n_{jj}}{\gamma_j} S_j^\pm \right) \xi^\pm + \left(\frac{2\alpha_i n_{ii}}{\gamma_i} \frac{2\alpha_j n_{jj}}{\gamma_j} S_i^\pm S_j^\pm - \frac{(\alpha_j n_{ij} + \alpha_i n_{ji})^2}{\gamma_i \gamma_j} S_i^\pm S_j^\pm \right) = 0.$$

The spectral radius is the largest eigenvalue:

$$\rho(DT(S^\pm)) = \frac{1}{2} \left(\frac{2\alpha_i n_{ii}}{\gamma_i} S_i^\pm + \frac{2\alpha_j n_{jj}}{\gamma_j} S_j^\pm \right) + \frac{1}{2} \sqrt{\left(\frac{2\alpha_i n_{ii}}{\gamma_i} S_i^\pm - \frac{2\alpha_j n_{jj}}{\gamma_j} S_j^\pm \right)^2 + 4 \frac{(\alpha_j n_{ij} + \alpha_i n_{ji})^2}{\gamma_i \gamma_j} S_i^\pm S_j^\pm}.$$

(J) We now use the results in **(H)** and **(I)** to examine the local stability of the two steady-state

equilibria. From the dynamics of infections in equation (D.7), we have:

$$\begin{bmatrix} I_i^\pm \\ I_j^\pm \end{bmatrix} = \left\{ \begin{bmatrix} \frac{2\alpha_i n_{ii}}{\gamma_i} S_i^\pm & \frac{\alpha_j n_{ij} + \alpha_i n_{ji}}{\gamma_j} S_j^\pm \\ \frac{\alpha_j n_{ij} + \alpha_i n_{ji}}{\gamma_i} S_i^\pm & \frac{2\alpha_j n_{jj}}{\gamma_j} S_j^\pm \end{bmatrix} - \begin{bmatrix} 1 & 0 \\ 0 & 1 \end{bmatrix} \right\} \begin{bmatrix} I_i^\pm \\ I_j^\pm \end{bmatrix}. \tag{D.13}$$

Therefore the spectral radius of the matrix $DT(S^\pm)$ corresponds to the global \mathcal{R}_0 that determines the local stability of the two steady-state equilibria. As we have shown that $\rho(DT(S^+)) > 1$, the steady-state S^+ is locally unstable. As we have shown that $\rho(DT(S^-)) < 1$, the steady-state S^- is locally stable.

■

E Computational Appendix

In this Appendix we describe the algorithms we use to do the numerical simulations in each section of the paper.

E.1 A Two-Country SIR Model with Time-Invariant Interactions

Solution Algorithm

1. Compute the value of n_{ii} , n_{ij} , n_{ij} , and n_{jj} as the outcome of the equilibrium that solves

$$n_{ij} = (c(\sigma - 1)\mu_{ij})^{-1/(\phi-1)} (d_{ij})^{-\frac{\rho+(\sigma-1)\delta}{\phi-1}} \left(\frac{t_{ij}w_j}{Z_j P_i} \right)^{-\frac{\sigma-1}{\phi-1}} \left(\frac{w_i}{P_i} \right)^{1/(\phi-1)}$$

$$\pi_{ii}w_iL_i + \pi_{ji}w_jL_j = w_iL_i,$$

where π_{ij} is given by

$$\pi_{ij} = \frac{X_{ij}}{\sum_{\ell \in \mathcal{J}} X_{i\ell}} = \frac{(w_j/Z_j)^{-\frac{\phi(\sigma-1)}{\phi-1}} \times (\mu_{ij})^{-\frac{1}{\phi-1}} (d_{ij})^{-\frac{\rho+\phi(\sigma-1)\delta}{\phi-1}} (t_{ij})^{-\frac{\phi(\sigma-1)}{\phi-1}}}{\sum_{\ell \in \mathcal{J}} (\mu_{i\ell})^{-\frac{1}{\phi-1}} (d_{i\ell})^{-\frac{\rho+\phi(\sigma-1)\delta}{\phi-1}} (t_{i\ell}w_\ell/Z_\ell)^{-\frac{\phi(\sigma-1)}{\phi-1}}},$$

corresponding to equation (9) in the paper. Call them \bar{n}_{ii} , \bar{n}_{ij} , \bar{n}_{ij} , and \bar{n}_{jj} . Provided population, technology, and relative wages are time invariant, these quantities will be fixed.

2. Set $I_i(0) = 0.1 \times 10^{-4}$, $S_i(0) = 1 - I_i(0)$, and $R_i(0) = 0$ for all i . For each $t \in [1, T]$ solve the following system of equations:

$$\begin{bmatrix} S_i(t+1) \\ I_i(t+1) \\ R_i(t+1) \\ S_j(t+1) \\ I_j(t+1) \\ R_j(t+1) \end{bmatrix} = \begin{bmatrix} -\Omega_i & \Omega_i & 0 & 0 & 0 & 0 \\ 0 & -\gamma_i & \gamma_i & 0 & 0 & 0 \\ 0 & 0 & 0 & 0 & 0 & 0 \\ 0 & 0 & 0 & -\Omega_j & \Omega_j & 0 \\ 0 & 0 & 0 & 0 & -\gamma_j & \gamma_j \\ 0 & 0 & 0 & 0 & 0 & 0 \end{bmatrix} \times (1/step) \times \begin{bmatrix} S_i(t) \\ I_i(t) \\ R_i(t) \\ S_j(t) \\ I_j(t) \\ R_j(t) \end{bmatrix} + \begin{bmatrix} S_i(t) \\ I_i(t) \\ R_i(t) \\ S_j(t) \\ I_j(t) \\ R_j(t) \end{bmatrix}$$

where

$$\Omega_i = \alpha_i \times 2\bar{n}_{ii} \times I_i(t) + \alpha_j \times \bar{n}_{ij} \times I_j(t) + \alpha_i \times \bar{n}_{ji} \times I_j(t).$$

This system corresponds to equations (16) – (18) in the paper. The variable *step* marks the number of steps taken within each time period, in this section we use *step* = 2.

Associated Figures

This section in the paper uses three sets of parameters. Figures 1, 2, and 3 present a general specification in which international trade favors the onset of a pandemic, with standard parameters as listed in Table E.1 for Figure 1 and Table E.2 for Figures 2 and 3. Figures 4 and 5 look at an example in which free trade prevents the onset of a pandemic, using parameters listed in Table E.3. Figure 6 presents the possibility of second waves of infection, using parameters listed in Table E.4.

If no other mention is made, trade frictions are set at baseline values $\mu_{ij} = \mu_{ji} = 1$, $t_{ij} = t_{ji} = 1$, $d_{ij} = d_{ij} = 1.1$. Some of these figures study changes in trade frictions moving one of these parameters. All other parameters are kept at baseline value.

Table E.1: Baseline parameters - Figure 1 in draft.

Parameter	Value
σ	5
ϕ	2
Z_1, Z_2	1
L_1, L_2	3, 3
$d_{12} = d_{21}$	1.1
$\mu_{12} = \mu_{21}, t_{12} = t_{21}$	1
δ	1
ρ	1
c	0.15
α_1	0.04
α_2	{0.04, 0.10}
γ_1, γ_2	0.20, 0.20
η_1, η_2	0.0, 0.0

In order to obtain the result described for the second set of parameters, $\phi = 1.5$ is crucial. The only other difference with respect to the general scenario is a decrease of c to 0.1. This is not necessary: the qualitative result also holds for $c = 0.15$ but it was originally changed so that n_{ii} would be approximately the same in both cases.

There are more parameters that will generate a second wave of infections. The ones presented here were picked to obtain *reasonable* values for R^{0i} and R^0 . What is essential for this feature to occur is that both countries have different timings for their own pandemics in autarky. One (small) country has very fast contagion rates (α) and very short recovery periods (high γ), while in the other (big) country the disease must progress much slower so that when the cycle starts it will drag the first country with it once again. The difference in size is there so that when the small country goes through its first cycle, the big country will remain mostly unaffected.

Table E.2: Baseline parameters - Figures 2, 3 in draft.

Parameter	Value
σ	5
ϕ	2
Z_1, Z_2	1
L_1, L_2	3, 3
$d_{12} = d_{21}$	1.1
$\mu_{12} = \mu_{21}, t_{12} = t_{21}$	1
δ	1
ρ	1
c	0.15
α_1, α_2	0.04, 0.07
γ_1, γ_2	0.20, 0.20
η_1, η_2	0.0, 0.0

Table E.3: "Better trade" parameters - Figures 4, 5 in draft.

Parameter	Value
σ	5
ϕ	1.5
Z_1, Z_2	1
L_1, L_2	3, 3
$d_{12} = d_{21}$	1.1
$\mu_{12} = \mu_{21}, t_{12} = t_{21}$	1
δ	1
ρ	1
c	0.10
α_1, α_2	0.04, 0.07
γ_1, γ_2	0.20, 0.20
η_1, η_2	0.0, 0.0

E.2 General-Equilibrium Induced Responses

Solution Algorithm

1. Compute the value of $n_{ii}(0), n_{ij}(0), n_{ij}(0)$, and $n_{jj}(0)$ as the outcome of the equilibrium that solves

$$n_{ij} = (c(\sigma - 1)\mu_{ij})^{-1/(\phi-1)} (d_{ij})^{-\frac{\rho+(\sigma-1)\delta}{\phi-1}} \left(\frac{t_{ij}w_j}{Z_j P_i}\right)^{-\frac{\sigma-1}{\phi-1}} \left(\frac{w_i}{P_i}\right)^{1/(\phi-1)}$$

$$\pi_{ii}w_iL_i(1 - D_i(t)) + \pi_{ji}w_jL_j(1 - D_j(t)) = w_iL_i(1 - D_i(t)),$$

where π_{ij} is once again given by

$$\pi_{ij} = \frac{X_{ij}}{\sum_{\ell \in \mathcal{J}} X_{i\ell}} = \frac{(w_j/Z_j)^{-\frac{\phi(\sigma-1)}{\phi-1}} \times (\mu_{ij})^{-\frac{1}{\phi-1}} (d_{ij})^{-\frac{\rho+\phi(\sigma-1)\delta}{\phi-1}} (t_{ij})^{-\frac{\phi(\sigma-1)}{\phi-1}}}{\sum_{\ell \in \mathcal{J}} (\mu_{i\ell})^{-\frac{1}{\phi-1}} (d_{i\ell})^{-\frac{\rho+\phi(\sigma-1)\delta}{\phi-1}} (t_{i\ell}w_\ell/Z_\ell)^{-\frac{\phi(\sigma-1)}{\phi-1}}},$$

Table E.4: Second-wave parameters - Figure 6 in draft

Parameter	Value
σ	4.5
ϕ	2
Z_1, Z_2	1
L_1, L_2	2, 20
$d_{12} = d_{21}$	1
δ	1
ρ	1
c	0.12
α_1, α_2	0.69, 0.09
β_1, β_2	2.29, 0.30
γ_1, γ_2	2.1, 0.18

corresponding to equation (9) in the paper. These values are no longer fixed and will evolve as the pandemic progresses.

2. Set $I_i(0) = 0.1 \times 10^{-4}$, $S_i(0) = 1 - I_i(0)$, and $R_i(0) = 0$ for all i . For each $t \in [1, T]$:

(a) Solve the following system of equations:

$$\begin{bmatrix} S_i(t+1) \\ I_i(t+1) \\ R_i(t+1) \\ D_i(t+1) \\ S_j(t+1) \\ I_j(t+1) \\ R_j(t+1) \\ D_j(t+1) \end{bmatrix} = \begin{bmatrix} -\Omega_i & \Omega_i & 0 & 0 & 0 & 0 & 0 & 0 \\ 0 & -\kappa_i & \gamma_i & \eta_i & 0 & 0 & 0 & 0 \\ 0 & 0 & 0 & 0 & 0 & 0 & 0 & 0 \\ 0 & 0 & 0 & 0 & -\Omega_j & \Omega_j & 0 & 0 \\ 0 & 0 & 0 & 0 & 0 & -\kappa_j & \gamma_j & \eta_j \\ 0 & 0 & 0 & 0 & 0 & 0 & 0 & 0 \end{bmatrix} \times (1/step) \times \begin{bmatrix} S_i(t) \\ I_i(t) \\ R_i(t) \\ D_i(t) \\ S_j(t) \\ I_j(t) \\ R_j(t) \\ D_j(t) \end{bmatrix} + \begin{bmatrix} S_i(t) \\ I_i(t) \\ R_i(t) \\ D_i(t) \\ S_j(t) \\ I_j(t) \\ R_j(t) \\ D_j(t) \end{bmatrix}$$

where $\kappa_i = \gamma_i + \eta_i$ and

$$\Omega_i = \alpha_i \times 2n_{ii}(t) \times I_i(t) + \alpha_j \times n_{ij}(t) \times I_j(t) + \alpha_i \times n_{ji}(t) \times I_j(t).$$

This system corresponds to equations (28) – (31) in the paper. The variable *step* marks the number of steps taken within each time period, in this section we use $step = 2$.

(b) Update $n_{ij}(t+1)$ and $w_i(t+1)$ as the values that solve:

$$n_{ij}(t+1) = (c(\sigma - 1)\mu_{ij})^{-1/(\phi-1)} (d_{ij})^{-\frac{\rho+(\sigma-1)\delta}{\phi-1}} \left(\frac{t_{ij}w_j(t+1)}{Z_jP_i} \right)^{-\frac{\sigma-1}{(\phi-1)}} \left(\frac{w_i(t+1)}{P_i} \right)^{1/(\phi-1)}$$

$$\pi_{ii}w_i(t+1)L_i(1 - D_i(t+1)) + \pi_{ji}w_j(t+1)L_j(1 - D_j(t+1)) = w_i(t+1)L_i(1 - D_i(t+1)).$$

Associated Figures

This section in the paper is associated with Figure 7, which uses the parameters described in Table E.5. These correspond to the first set of parameters in the previous section (associated to Figures 1, 2, and 3). The duration of the disease remains the same, as the exit rate from the infected stage ($\gamma_i + \eta_i$) is unchanged, but now both countries experience deaths, with one of them having a much higher death rate than the other (η_i marks the entry into the dead stage, so $\eta_i/(\gamma_i + \eta_i)$ marks how many of those that were infected will end up dying).

Table E.5: Section 4 parameters - Figure 7.

Parameter	Value
σ	5
ϕ	2
Z_1, Z_2	1
L_1, L_2	3, 3
$d_{12} = d_{21}$	1.1
$\mu_{12} = \mu_{21}, t_{12} = t_{21}$	1
δ	1
ρ	1
c	0.15
α_1, α_2	0.04, 0.07
$(\gamma_i + \eta_i)$	0.20
$\eta_i/(\gamma_i + \eta_i)$	0.01, 0.50

E.3 Behavioral Responses - Symmetric Case

Solution Algorithm

1. Choose $T(\infty) = 500,000$ (some large number), and $T = 10,000$. Guess $D(\infty) = \mathcal{D}_i$.
2. Compute the value of $n_{ii}(\infty)$, $n_{ij}(\infty)$, $n_{ij}(\infty)$, and $n_{jj}(\infty)$ as the outcome of the equilibrium that solves

$$n_{ij} = (c(\sigma - 1)\mu_{ij})^{-1/(\phi-1)} (d_{ij})^{-\frac{\rho+(\sigma-1)\delta}{\phi-1}} \left(\frac{t_{ij}w_j}{Z_jP_i}\right)^{-\frac{\sigma-1}{\phi-1}} \left(\frac{w_i}{P_i}\right)^{1/(\phi-1)}$$

$$\pi_{ii}w_iL_i(1 - \mathcal{D}_i) + \pi_{ji}w_jL_j(1 - \mathcal{D}_j) = w_iL_i(1 - \mathcal{D}_i),$$

where π_{ij} is given by

$$\pi_{ij} = \frac{X_{ij}}{\sum_{\ell \in \mathcal{J}} X_{i\ell}} = \frac{(w_j/Z_j)^{-\frac{\phi(\sigma-1)}{\phi-1}} \times (\mu_{ij})^{-\frac{1}{\phi-1}} (d_{ij})^{-\frac{\rho+\phi(\sigma-1)\delta}{\phi-1}} (t_{ij})^{-\frac{\phi(\sigma-1)}{\phi-1}}}{\sum_{\ell \in \mathcal{J}} (\mu_{i\ell})^{-\frac{1}{\phi-1}} (d_{i\ell})^{-\frac{\rho+\phi(\sigma-1)\delta}{\phi-1}} (t_{i\ell}w_\ell/Z_\ell)^{-\frac{\phi(\sigma-1)}{\phi-1}}}$$

corresponding to equation (9) in the paper.

3. Transversality conditions are satisfied if

$$\begin{aligned} \lim_{t \rightarrow \infty} \theta_i^k(t) &= 0 \\ \lim_{t \rightarrow \infty} \theta_i^i(t) &= 0 \\ \lim_{t \rightarrow \infty} \theta_i^s(t) &= 0 \end{aligned}$$

Set $\theta_i^k(\infty) = \theta_i^i(\infty) = \theta_i^s(\infty) = 0$ and let the economy run without infections between T and $T(\infty)$, that is, for each time period $t \in [T, T(\infty)]$ update the Lagrange multipliers as

$$\begin{aligned} \theta_i^k(t) &= \theta_i^k(t+1) - [Q_i(n_{ii}(\infty), n_{ij}(\infty)) - C_i(n_{ii}(\infty), n_{ij}(\infty))] e^{-\xi t} \Delta t \\ \theta_i^i(t) &= \frac{1}{1 + (\gamma_i + \eta_i) \Delta t} [\eta_i \theta_i^k(t) \Delta t + \theta_i^i(t+1)] \end{aligned}$$

where Δt is the step size (one over how many times you update within each day). Keep $\theta^k(T)$ and $\theta^i(T)$ as the terminal values of the Lagrange multipliers.

4. Set $I_i(T) = 10^{-6}$, $\theta_i^s(T) = 0$ and $S_i(T) = 1 - I_i(T) - \mathcal{D}_i/(\eta_i/(\gamma_i + \eta_i))$. Recompute $n_{i.}(T)$ as the values that solve

$$\left[\frac{\partial Q_i(n_{ii}(T), n_{ij}(T))}{\partial n_{ij}} - \frac{\partial C_i(n_{ii}(T), n_{ij}(T))}{\partial n_{ij}} \right] (1 - \mathcal{D}_i) e^{-\xi T} = [\theta_i^s(T) - \theta_i^i(T)] S_i(T) \alpha_j I_j(T),$$

corresponding to equation (32) in the paper. Given perfect symmetry between countries, we will have $w_i = 1$ for all i .

5. For each $t \in [T, 0]$ solve the following system of equations, where all values evaluated at $t+1$ are known, to obtain values at t :

$$\begin{aligned} \theta_i^s(t+1) - \theta_i^s(t) &= [\theta_i^s(t) - \theta_i^i(t)] [2\alpha_i n_{ii}(t) I_i(t) + (\alpha_j n_{ij}(t) + \alpha_i n_{ji}(t)) I_j(t)] \Delta t \\ \theta_i^s(t+1) - \theta_i^i(t) &= (\gamma_i + \eta_i) \theta_i^i(t) \Delta t - \eta_i \theta_i^k(t) \Delta t \\ \theta_i^k(t+1) - \theta_i^k(t) &= [Q_i(n_{ii}(t), n_{ij}(t)) - C_i(n_{ii}(t), n_{ij}(t))] e^{-\xi t} \Delta t \\ I_i(t+1) - I_i(t) &= S_i(t) [2\alpha_i n_{ii}(t) I_i(t) + (\alpha_j n_{ij}(t) + \alpha_i n_{ji}(t)) I_j(t)] \Delta t - (\gamma_i + \eta_i) I_i(t) \Delta t \\ S_i(t+1) - S_i(t) &= -S_i(t) [2\alpha_i n_{ii}(t) I_i(t) + (\alpha_j n_{ij}(t) + \alpha_i n_{ji}(t)) I_j(t)] \Delta t \\ D_i(t+1) - D_i(t) &= \eta_i I_i(t) \Delta t \end{aligned}$$

and where $n_{i.}(t)$ is again obtained as the value that solves:

$$\left[\frac{\partial Q_i(n_{ii}(t), n_{ij}(t))}{\partial n_{ij}} - \frac{\partial C_i(n_{ii}(t), n_{ij}(t))}{\partial n_{ij}} \right] (1 - D_i(t)) e^{-\xi t} = [\theta_i^s(t) - \theta_i^i(t)] S_i(t) \alpha_j I_j(t).$$

These correspond to equations (32)-(35) in the paper plus the equations determining the

evolution of the epidemiological variables, once we have imposed equilibrium conditions.

6. Repeat for all periods until $I(t)$ reaches the desired initial condition, that is, $I(t) = 10^{-5}$. If at this t we have $|D(t)| < 10^{-5}$ stop. Otherwise, adjust guess \mathcal{D}_i .

Associated Figures

This section in the paper is associated with Figures 8 and 9, which uses the parameters described in Table E.6.

Table E.6: Behavioral response parameters - Figures 8, 9 in draft.

Parameter	Value
σ	5
ϕ	1.5
Z_1, Z_2	1
L_1, L_2	3, 3
$d_{12} = d_{21}$	1.1
$\mu_{12} = \mu_{21}, t_{12} = t_{21}$	1
δ	1
ρ	1
c	0.10
α_1, α_2	0.1, 0.1
$\gamma_i + \eta_i$	0.20, 0.20
$\eta_i / (\gamma_i + \eta_i)$	0.0062, 0.0062
Δt	1/5
ξ	0.05 / (365 \times Δt)

The initial guess used in the code Figure 8 is $\mathcal{D}_i = 0.0022$, and the initial guess for Figure 9 is $\mathcal{D}_i = 0.004$.

E.4 Behavioral Responses - Asymmetric Case

Solution Algorithm

1. Choose $T(\infty) = 500,000$ (some large number), and $T = 10,000$. Guess $D_1(\infty) = \mathcal{D}_1$. Fix $I_1(T) = 10^{-7}$.
2. Generate a grid for $D_2(\infty) = \mathcal{D}_2$ wide enough to contain the solution (use solution without behavioral responses as an upper bound for this guess). For each of the points in this grid
 - (a) Compute the value of $n_{ii}(\infty), n_{ij}(\infty), n_{ij}(\infty)$, and $n_{jj}(\infty)$ as the outcome of the equilibrium that solves

$$n_{ij} = (c(\sigma - 1)\mu_{ij})^{-1/(\phi-1)} (d_{ij})^{-\frac{\rho+(\sigma-1)\delta}{\phi-1}} \left(\frac{t_{ij}w_j}{Z_j P_i}\right)^{-\frac{\sigma-1}{\phi-1}} \left(\frac{w_i}{P_i}\right)^{1/(\phi-1)}$$

$$\pi_{ii}w_iL_i(1 - \mathcal{D}_i) + \pi_{ji}w_jL_j(1 - \mathcal{D}_j) = w_iL_i(1 - \mathcal{D}_i),$$

where π_{ij} is once again given by

$$\pi_{ij} = \frac{X_{ij}}{\sum_{\ell \in \mathcal{J}} X_{i\ell}} = \frac{(w_j/Z_j)^{-\frac{\phi(\sigma-1)}{\phi-1}} \times (\mu_{ij})^{-\frac{1}{\phi-1}} (d_{ij})^{-\frac{\rho+\phi(\sigma-1)\delta}{\phi-1}} (t_{ij})^{-\frac{\phi(\sigma-1)}{\phi-1}}}{\sum_{\ell \in \mathcal{J}} (\mu_{i\ell})^{-\frac{1}{\phi-1}} (d_{i\ell})^{-\frac{\rho+\phi(\sigma-1)\delta}{\phi-1}} (t_{i\ell}w_\ell/Z_\ell)^{-\frac{\phi(\sigma-1)}{\phi-1}}}$$

corresponding to equation (9) in the paper.

(b) Transversality conditions are satisfied if

$$\begin{aligned} \lim_{t \rightarrow \infty} \theta_i^k(t) &= 0 \\ \lim_{t \rightarrow \infty} \theta_i^i(t) &= 0 \\ \lim_{t \rightarrow \infty} \theta_i^s(t) &= 0 \end{aligned}$$

Set $\theta_i^k(\infty) = \theta_i^i(\infty) = \theta_i^s(\infty) = 0$ and let the economy run without infections between T and $T(\infty)$, that is, for each time period $t \in [T, T(\infty)]$ update the multipliers as

$$\begin{aligned} \theta_i^k(t) &= \theta_i^k(t+1) - [Q_i(n_{ii}(\infty), n_{ij}(\infty)) - C_i(n_{ii}(\infty), n_{ij}(\infty))] e^{-\xi t} \Delta t \\ \theta_i^i(t) &= \frac{1}{1 + (\gamma_i + \eta_i)\Delta t} [\eta_i \theta_i^k(t) \Delta t + \theta_i^i(t+1)] \end{aligned}$$

where Δt is the step size (one over how many times you update within each day). Keep $\theta^k(T)$ and $\theta^i(T)$ as the terminal values of the Lagrange multipliers.

(c) Guess a value for $I_2(T)$. Set $\theta_i^s(T) = 0$ and $S_i(T) = 1 - I_i(T) - \mathcal{D}_i/(\eta_i/(\gamma_i + \eta_i))$. Recompute $n_i(T)$ as the values that solve

$$\left[\frac{\partial Q_i(n_{ii}(T), n_{ij}(T))}{\partial n_{ij}} - \frac{\partial C_i(n_{ii}(T), n_{ij}(T))}{\partial n_{ij}} \right] (1 - \mathcal{D}_i) e^{-\xi T} = [\theta_i^s(T) - \theta_i^i(T)] S_i(T) \alpha_j I_j(T),$$

corresponding to equation (32) in the paper. Given perfect symmetry between countries, we will have $w_i = 1$ for all i .

i. Given a value for $I_2(T)$, for each $t \in [T, 0]$ solve the following system of equations, where all values evaluated at $t + 1$ are known, to obtain values at t :

$$\begin{aligned} \theta_i^s(t+1) - \theta_i^s(t) &= [\theta_i^s(t) - \theta_i^i(t)] [2\alpha_i n_{ii}(t) I_i(t) + (\alpha_j n_{ij}(t) + \alpha_i n_{ji}(t)) I_j(t)] \Delta t \\ \theta_i^i(t+1) - \theta_i^i(t) &= (\gamma_i + \eta_i) \theta_i^i(t) \Delta t - \eta_i \theta_i^k(t) \Delta t \\ \theta_i^k(t+1) - \theta_i^k(t) &= [Q_i(n_{ii}(t), n_{ij}(t)) - C_i(n_{ii}(t), n_{ij}(t))] e^{-\xi t} \Delta t \\ I_i(t+1) - I_i(t) &= S_i(t) [2\alpha_i n_{ii}(t) I_i(t) + (\alpha_j n_{ij}(t) + \alpha_i n_{ji}(t)) I_j(t)] \Delta t - (\gamma_i + \eta_i) I_i(t) \Delta t \\ S_i(t+1) - S_i(t) &= -S_i(t) [2\alpha_i n_{ii}(t) I_i(t) + (\alpha_j n_{ij}(t) + \alpha_i n_{ji}(t)) I_j(t)] \Delta t \\ D_i(t+1) - D_i(t) &= \eta_i I_i(t) \Delta t \end{aligned}$$

and where $n_i(t)$ is again obtained as the value that solves:

$$\left[\frac{\partial Q_i(n_{ii}(t), n_{ij}(t))}{\partial n_{ij}} - \frac{\partial C_i(n_{ii}(t), n_{ij}(t))}{\partial n_{ij}} \right] (1 - D_i(t)) e^{-\xi t} = [\theta_i^s(t) - \theta_i^i(t)] S_i(t) \alpha_j I_j(t).$$

These correspond to equations (32)-(35) in the paper plus the equations determining the evolution of the epidemiological variables, once we have imposed equilibrium conditions.

- ii. Given a particular grid, two adjacent guesses of \mathcal{D}_2 may lead to diverging paths for I_i . If this is the case, pick the two guesses that split the paths between those diverging upwards and downwards and re-draw a finer grid for \mathcal{D}_2 within these bounds.
- iii. Repeat for all periods until $I_i(t)$ reaches the desired initial condition, that is, $I(t) = 10^{-5}$ and $I_i(t) < I_i(t+1)$ in a flat line (meaning it does not diverge to plus or minus infinity). If at this t we have $D_1(t) = D_2(t)$ go back to outside layer of the loop. Otherwise, adjust guess $I_2(T)$.

3. If at this t we have $|D_i(t)| < 10^{-5}$ stop. Otherwise, adjust guess \mathcal{D}_1 .

Associated Figures

This section in the paper is associated with Figure 10, which uses the parameters described in Table E.7.

Table E.7: Behavioral response parameters - Figure 10 in draft.

Parameter	Value
σ	5
ϕ	1.5
Z_1, Z_2	1
L_1, L_2	3, 3
$d_{12} = d_{21}$	1.1
$\mu_{12} = \mu_{21}, t_{12} = t_{21}$	1
δ	1
ρ	1
c	0.10
α_1, α_2	0.1, 0.1
$\gamma_i + \eta_i$	0.20, 0.20
$\eta_i / (\gamma_i + \eta_i)$	0.003, 0.0062
Δt	1/3
ξ	0.05 / (365 × Δt)

Notes about the Algorithm

This algorithm is not closed, as it still requires a mechanism that will automatically define which are the bounds for \mathcal{D}_2 in step 2(c)ii.

E.5 Adjustment Costs and the Risk of a Pandemic

Solution Algorithm

1. Choose $T(\infty) = 500,000$ (some large number), and $T = 10,000$. Guess $D(\infty) = \mathcal{D}_i$.
2. Compute the value of $n_{ii}(\infty)$, $n_{ij}(\infty)$, $n_{ij}(\infty)$, and $n_{jj}(\infty)$ as the outcome of the equilibrium that solves

$$n_{ij} = (c(\sigma - 1)\mu_{ij})^{-1/(\phi-1)} (d_{ij})^{-\frac{\rho+(\sigma-1)\delta}{\phi-1}} \left(\frac{t_{ij}w_j}{Z_jP_i}\right)^{-\frac{\sigma-1}{\phi-1}} \left(\frac{w_i}{P_i}\right)^{1/(\phi-1)}$$

$$\pi_{ii}w_iL_i(1 - \mathcal{D}_i) + \pi_{ji}w_jL_j(1 - \mathcal{D}_j) = w_iL_i(1 - \mathcal{D}_i),$$

where π_{ij} is once again given by

$$\pi_{ij} = \frac{X_{ij}}{\sum_{\ell \in \mathcal{J}} X_{i\ell}} = \frac{(w_j/Z_j)^{-\frac{\phi(\sigma-1)}{\phi-1}} \times (\mu_{ij})^{-\frac{1}{\phi-1}} (d_{ij})^{-\frac{\rho+\phi(\sigma-1)\delta}{\phi-1}} (t_{ij})^{-\frac{\phi(\sigma-1)}{\phi-1}}}{\sum_{\ell \in \mathcal{J}} (\mu_{i\ell})^{-\frac{1}{\phi-1}} (d_{i\ell})^{-\frac{\rho+\phi(\sigma-1)\delta}{\phi-1}} (t_{i\ell}w_\ell/Z_\ell)^{-\frac{\phi(\sigma-1)}{\phi-1}}}$$

corresponding to equation (9) in the paper.

3. Transversality conditions are satisfied if

$$\lim_{t \rightarrow \infty} \theta_i^k(t) = 0$$

$$\lim_{t \rightarrow \infty} \theta_i^i(t) = 0$$

$$\lim_{t \rightarrow \infty} \theta_i^s(t) = 0$$

Set $\theta_i^k(\infty) = \theta_i^i(\infty) = 0$ and let the economy run without infections between T and $T(\infty)$, that is, for each time period $t \in [T, T(\infty)]$ update the multipliers as

$$\theta_i^k(t) = \theta_i^k(t+1) - [Q_i(n_{ii}(\infty), n_{ij}(\infty)) - C_i(n_{ii}(\infty), n_{ij}(\infty))] e^{-\xi t} \Delta t$$

$$\theta_i^i(t) = \frac{1}{1 + (\gamma_i + \eta_i)\Delta t} [\eta_i \theta_i^k(t) \Delta t + \theta_i^i(t+1)]$$

where Δt is the step size (one over how many times you update within each day). Keep $\theta^k(T)$ and $\theta^i(T)$ as the terminal values of the Lagrange multipliers.

4. Set $I_i(T) = 10^{-7}$, $\theta_i^s(T) = 0$ and $S_i(T) = 1 - I_i(T) - \mathcal{D}_i/(\eta_i/(\gamma_i + \eta_i))$. Recompute $n_i(T)$ as the values that solve

$$\left[\frac{\partial Q_i(n_{ii}(T), n_{ij}(T))}{\partial n_{ij}} - \frac{\partial C_i(n_{ii}(T), n_{ij}(T))}{\partial n_{ij}} \right] (1 - \mathcal{D}_i) e^{-\xi T} = [\theta_i^s(T) - \theta_i^i(T)] S_i(T) \alpha_j I_j(T),$$

corresponding to equation (32) in the paper. Given perfect symmetry between countries, we will have $w_i = 1$ for all i .

5. For each $\tau - 1 \in [T, 0]$ solve the following system of equations, where all values evaluated at τ are known and we have imposed perfect symmetry between countries, to obtain values at t :

$$\begin{aligned} \theta^s(\tau) - \theta^s(\tau - 1) &= [\theta^s(\tau) - \theta^i(\tau)][2\alpha n_i(\tau)I(\tau) + 2\alpha n_j(\tau)I(\tau)]\Delta\tau \\ \theta^s(\tau) - \theta^s(\tau - 1) &= (\gamma + \eta)\theta^i(\tau)\Delta\tau - \eta\theta^k(\tau)\Delta\tau \\ \theta^k(\tau) - \theta^k(\tau - 1) &= \left[Q(n_j(\tau), n_j(\tau)) - C(n_i(\tau), n_j(\tau)) - \psi_1(|g_{ii}(t)|^{\psi_2} + |g_{ij}(t)|^{\psi_2}) \right] e^{-\xi\tau}\Delta\tau \\ I(\tau) - I(\tau - 1) &= S(\tau)[2\alpha n_i(\tau)I(\tau) + 2\alpha n_j(\tau)I(\tau)]\Delta\tau - (\gamma + \eta)I(\tau)\Delta\tau \\ S(\tau) - S(\tau - 1) &= -S(\tau)[2\alpha n_i(\tau)I(\tau) + 2\alpha n_j(\tau)I(\tau)]\Delta\tau \\ D(\tau) - D(\tau - 1) &= \eta I(\tau)\Delta\tau \end{aligned}$$

and where $n_i(\tau)$ is obtained as $n_i(\tau + 1) - g_i(\tau) \times \Delta t$ for the value of $g_i(\tau)$ that solves:

$$\begin{aligned} & e^{-\xi\tau} \left[\frac{\partial Q_i}{\partial n_{ij}}(n_{ij}(\tau)) - \frac{\partial C_i}{\partial n_{ij}}(n_{ij}(\tau)) \right] \times (1 - D(\tau)) \\ & + \sum_{t=\tau+1}^{\infty} e^{-\xi t} \left[\frac{\partial Q_i}{\partial n_{ij}}(n_{ij}(t)) - \frac{\partial C_i}{\partial n_{ij}}(n_{ij}(t)) \right] \times (1 - D(t)) \\ & - (\theta^s(\tau) - \theta^i(\tau)) \times S(\tau) \times \alpha \times I(\tau) - \sum_{t=\tau+1}^{\infty} (\theta^s(t) - \theta^i(t)) \times S(t) \times \alpha \times I(t) \\ & - \psi_1 \psi_2 \left| \frac{n_{ij}(\tau + 1) - n_{ij}(\tau)}{\Delta\tau} \right|^{\psi_2 - 1} \times (1 - D(\tau)) e^{-\xi\tau} \\ & = 0. \end{aligned}$$

Note that, in contrast to the other cases above, we compute changes as happening between τ and $\tau - 1$, rather $\tau + 1$ and τ . This makes the system easier to solve backwards, although the difference in solutions is negligible for small enough step size.

6. Repeat for all periods until $I(\tau)$ reaches the desired initial condition, that is, $I(\tau) = 10^{-5}$. If at this τ we have $D(\tau) = 0$ stop. Otherwise, adjust guess \mathcal{D}_i .

Associated Figures

This section in the paper is associated with Figure 11, which uses the parameters described in Table E.8.

Table E.8: Behavioral response parameters - Figure 10 in draft.

Parameter	Value
σ	5
ϕ	1.5
Z_1, Z_2	1
L_1, L_2	3, 3
$d_{12} = d_{21}$	1.1
$\mu_{12} = \mu_{21}, t_{12} = t_{21}$	1
δ	1
ρ	1
c	0.10
α_1, α_2	0.1, 0.1
$\gamma_i + \eta_i$	0.20, 0.20
$\eta_i / (\gamma_i + \eta_i)$	0.0062, 0.0062
ξ	$0.05 / (365 \times \Delta t)$
ψ_1	1
ψ_2	4
Δt	1/10

The safest time to fly: Pandemic response in the era of Fox News¹

Maxim Ananyev,² Michael Poyker³ and Yuan Tian⁴

Date submitted: 13 September 2020; Date accepted: 17 September 2020

We document a causal effect of conservative Fox News Channel in the United States on physical distancing during COVID-19 pandemic. We measure county-level mobility covering all U.S. states and District of Columbia produced by GPS pings to 15-17 million smartphones and zip-code-level mobility using Facebook location data. Then, using the historical position of Fox News Channel in the cable lineup as the source of exogenous variation, we show that increased exposure to Fox News led to a smaller reduction in distance traveled and smaller increase in the probability to stay home after the national emergency declaration in the United States. Our results show that slanted media can have a harmful effect on containment efforts during a pandemic by affecting people's behaviour.

1 This paper was first submitted for review on May 16, 2020. After completing the paper, we were made aware of a working paper by Simonov et al. (2020) (posted on SSRN on May 14, 2020) that uses the same idea of identifying variation and a different dataset for measuring mobility outcomes. Our results were produced independently. We thank UNACAST for generously sharing mobility data and Facebook's Data for Good initiative for sharing Facebook users' mobility data. We are grateful to Elliott Ash, Sergei Guriev, Vasily Korovkin, Natalia Lamberova, and Alexey Makarin for their thoughtful comments. Poyker is grateful for financial support from the Institute for New Economic Thinking. All errors are ours

2 University of Melbourne.

3 Columbia University.

4 Carnegie Mellon University.

Copyright: Maxim Ananyev, Michael Poyker and Yuan Tian

1 Introduction

Media play many important roles in people's lives by transmitting information and shaping beliefs.¹ Such beliefs include trust in government, trust in science, and perception of threat, which can have behavioural implications in many contexts including public health. In such high-stakes cases as pandemics, the influence on how people comply with policies that promote safe behaviors and limit spread of a contagious disease are especially important.

In this paper, we investigate the causal impact of slanted news media on public behaviour during the COVID-19 crisis. COVID-19 is a contagious disease of respiratory system that caused a pandemic in the early 2020. One of the measures deemed necessary to limit the spread of the disease is physical distancing (limiting travel and person-to-person interactions), because the virus spreads through droplets of infected persons (Hatchett, Mecher and Lipsitch, 2007; Anderson et al., 2020; Hsiang et al., 2020). Fox News Channel (hereafter, FNC), the leading cable channel in the United States, has a well-documented conservative bias in its programming (Martin and Yurukoglu 2017). During the initial days of the COVID-19 pandemic, FNC's commentators concentrated on delivering three messages: (i) emphasizing potential culpability of China and Chinese government in the pandemic; (ii) downplaying potential dangers of the virus and suggesting untested medical procedures; (iii) alleging that Democrats use the pandemic to undermine President Trump before the election. These messages could potentially affect people's evaluation of the risk and thus their willingness to self-isolate during the crisis.

Using an exogenous variation in the exposure to Fox News Channel, we document a statistically significant and economically sizable effect of FNC on physical distancing. Following Martin and Yurukoglu (2017), we exploit the exogeneity of the historical position of FNC in cable lineup. This variable has been shown to be (i) unrelated to the socio-demographic and political condition prior to the introduction of FNC, and (ii) strongly predictive of actual FNC viewership once the channel is introduced. Our effects can come from three channels. First, FNC viewership directly feeds people with the three aforementioned messages. Second, the build-up of the conservative ideology can make people less willing to adopt drastic changes in their behavior and living habits. Third, conservative population may be more susceptible to FNC's messages.

We use internet-based location data to measure social distancing behaviour. It is gen-

¹Scholars have shown that slanted media have an impact on voting and political preferences (DellaVigna and Kaplan, 2007; Enikolopov, Petrova and Zhuravskaya, 2011; Adena et al., 2015), collective actions (Zernike, 2010), political polarization (Prior, 2007; Martin and Yurukoglu, 2017), investment decisions (Friebel and Heinz, 2014), political polarization (Martin and Yurukoglu, 2017), judicial decisions (Ash and Poyker, 2019), city budgets (Galletta and Ash, 2019), and candidate entry (Arceneaux et al., 2020).

erally hard to directly observe people's actions. In our case, however, we measure the county-level changes in distance traveled using location data of 15-17 million smartphones provided by UNACAST, and zip-code-level measures of mobility using GPS pings of smartphones of Facebook users.

In our main specification, we regress the change in physical-distancing measures on FNC exposure — the standardized position of FNC in a cable lineup. Our hypothesis is that after the declaration of national emergency on March 13, people are likely to adopt social distancing practices; less so for regions more exposed to FNC. Although states enacted different orders in terms of shelter-in-place practices and business operations at different times, the declaration of national emergency is a salient landmark in governments' campaign against COVID-19 at the national level. We interact time-invariant FNC lineup position with a dummy for post- and pre-national emergency dates. Consistent with our hypothesis, we find that before the national emergency, the mobility was similar in the pre-COVID period in areas with different FNC positions. After national emergency was announced, a one-standard-deviation increase in FNC exposure led to a 0.5-percentage-point larger decline in the county-level average of distance traveled relative to pre-COVID period and 0.1-percentage-point larger decrease in the probability of staying at home.

We conduct various robustness checks. Our results are not driven by a particular set of states and are not explained by alternative explanations, most notably that high-FNC exposed locations are less likely to have employment composition favourable for work-from-home, or be in more rural locations. Controlling for CNN and MSNBC does not affect the FNC estimates, indicating that our effects are not through crowding out of alternative media. Our result are robust to using county-level and zip-code-level Facebook data for 14 states. We also provide an event-study specification that allows us to control for the time path of the effect and estimate weekly coefficients for weeks before and after the national emergency. We find that the effect of Fox News is constant in the weeks after the national emergency was pronounced and did not diminish in the four weeks of the post-emergency period. Finally, we replicate our results using state-specific shelter-in-place orders. While our results hold for periods after the orders were enacted, we find that people started to self-isolate even before that. Thus, overall we think that national emergency was the most salient starting point of social-distancing.

We interpret our result as the combination of the direct information channel and the indirect effect through the interaction with built-up conservatism. We control for Republican vote shares in the 2016 election, and it does not affect the magnitude and significant of the estimate of FNC exposure effect.

To put the magnitude of our results in context, the biggest decrease in distance traveled

per person after March 13 happened in District of Columbia (59 percent), and the smallest one — in Nevada (13 percent). According to the estimates of [Martin and Yurukoglu \(2017\)](#), moving FNC from channel 10 to channel 40 (approximately, two standard deviations) is associated with a 5-minutes reduction per week per person in time spent watching FNC. According to our results, when FNC is moved 30 positions higher in the cable lineup, it decreases social-distancing by one percentage point. This effect can explain 2% and 8% of the total reduction in population movement in DC and Nevada, respectively. As for the probability of staying at home, among the 14 states (plus DC) where we have zip-code-level data, the 30-positions change in FNC increases of the probability of staying at home by 0.2 percentage point. This explains 2% and 33% of the increase in probability of staying at home in DC and West Virginia, respectively, which had the biggest and smallest changes.

We also provide evidence that these differences were consequential for mortality. Specifically, we find that a one-standard-deviation increase in FNC lineup position decreased the number of COVID-related deaths by 2.2 percent by the end of March. This result is consistent with [Bursztyn et al. \(2020\)](#).

Our paper contributes to several strands of literature. First is the literature on the impact of media. Several pieces of work have documented the impact of media on voting outcomes ([DellaVigna and Kaplan, 2007](#); [Enikolopov, Petrova and Zhuravskaya, 2011](#)), conflict ([Yanagizawa-Drott, 2014](#)), popularity of extreme parties ([Adena et al., 2015](#)), among others. Following [Martin and Yurukoglu \(2017\)](#), we add to the literature by showing how biased media can have public health consequences, a usually non-political outcome, through changing people's behavior. We demonstrate that in addition to shaping people's mindsets in the long run, the information conveyed by the biased media on the interpretation of scientific advice and policies can be costly to the society, especially when collective action is needed in the time of public health crises.

Second, we contribute to the literature on using granular real-time individual-level data to study people's behavior. Researchers have used cell phone location data to measure commuting and economic activities ([Kreindler and Miyauchi, 2019](#)) and segregation ([Athey et al., 2019](#)), cellphones' call data to investigate the impact of social networks on mobility ([Büchel et al., 2019](#); [Blumenstock, Chi and Tan, 2019](#)), information transmission about social distancing practices ([Tian, Caballero and Kovak, 2020](#)), and job referrals ([Barwick et al., 2019](#)), and Facebook friendship data to measure social connectedness ([Bailey et al., 2018](#)) and study its impact on disease transmission in the case of COVID-19 ([Kuchler, Russel and Stroebel, 2020](#)). This type of data is especially useful in our context, since we can directly observe people's behavior in terms of complying with the social distanc-

ing policy and track the real-time changes. In addition to documenting the changes in mobility before and after the declaration of national emergency and the geographically distribution of mobility, we investigate the potential determinants of such geographically variation and highlight the importance of media.

Finally, our paper adds to the rapidly growing literature on the COVID-19 pandemic, especially on determinants of physical distancing and transmission. [Wright et al. \(2020\)](#) shows that shelter-in-place ordinances were effective in reducing mobility and that compliance was correlated with both economic conditions and political opinions. Similarly, [Allcott et al. \(2020\)](#) shows a gap in a physical distancing between places with more Republicans and places with more Democrats and suggests that partisan messaging was one of the mechanisms. We share the features of these two papers by using cellphone location data to measure mobility; however by using a plausibly exogenous variation in exposure to FNC, we causally identify the effect of media on social distancing practices. We emphasize that not only the pre-existing political views but also the flow of information through (politicized) media can shape people's view. [Bursztyn et al. \(2020\)](#) identifies the effect of watching the most popular FNC show, Hannity, on mortality. We instead focus on behavior responses. By using much finer geographically variation (county-level and zip-code-level instead of relatively large Designated Market Area level), the timing of the declaration of national emergency, and direct measures of behavior responses, we show how exactly FNC viewership can affect efforts in combat with the infectious diseases.

A contemporaneous paper by [Simonov et al. \(2020\)](#) uses the same identifying variation and the SafeGraph data for social-distancing measures (we use UNACAST and Facebook data instead). There are several notable differences between our approach and that of [Simonov et al. \(2020\)](#). First, we use the earliest available data on the FNC position (from 2005), while [Simonov et al. \(2020\)](#) use the data from 2015. This difference is important because cable networks are well aware of the influence that channel position has on the viewership and lobby providers to put their channels "lower on the dial" ([Snider and Hall, 1998](#)). This is especially true for FNC: as early as 2007 the movement of the channel from position 46 to position 44 in one of the Time Warner Cable markets was seen as a major win that merited inclusion in a self-congratulatory announcement by FNC.² Thus, FNC position in the later years is more likely to be endogenous to the lobbying efforts of FNC leadership. Second, the effect of FNC exposure on social-distancing can be potentially explained by the two types of channels: conservatism and COVID-19 messaging. The conservatism can influence social-distancing directly by making people skeptical of

²BusinessWire. "FOX Business Network to Launch on Channel 43 on Time Warner Cable. FOX News Channel Moves to Channel 44", September 5, 2007. URL: www.businesswire.com/news/home/20070905006114/en/FOX-Business-Network-Launch-Channel-43-Time.

governmental interventions and academic experts. Because we use the historical position of FNC, we are able to control for the built-up conservatism (by including controls for the 2016 election results), thus isolating the effect of COVID-19 messaging and shedding light on the mechanisms. These differences from [Simonov et al. \(2020\)](#) are consequential.³ While our results are the same in terms of significance and the sign of the effect, the magnitude of our estimates is smaller, while still being economically and epidemiologically important.

This paper proceeds as follows. Section 2 introduces background information about the development of COVID-19 in the United States, policies on social distancing, and its coverage by Fox News. Section 3 describes our data. Section 4 introduces our empirical specification, identifying assumptions, and results. Section 5 concludes.

2 Background: COVID-19 and Fox News Channel

2.1 COVID-19 and Social-Distancing

COVID-19 is a disease of the respiratory system caused by a new coronavirus (SARS-CoV-2). The first case was reported on December 31 in Wuhan, China, and the first death from the new virus was reported in China on January 7. The virus then rapidly spread to other countries (the first case outside China was reported on January 13, 2020). The WHO declared a pandemic on March 11, 2020.⁴ The first confirmed case in the U.S. happened on January 21, 2020. As of April 28, 2020, the Center for Disease Control and Prevention (hereafter, CDC) reported 981,246 total cases in the U.S. and 55,258 deaths related to the illness.⁵ Due to its means of transmission, the CDC advised that “limiting face-to-face contact with others” was “the best way to reduce the spread of coronavirus disease.”⁶

³There are other notable differences in specification choices (we use a specification with date fixed effects) and they use 2SLS specification with time-invariant FNC viewership as the treatment variable.

⁴WHO COVID-19 Timeline. URL: [who.int/news-room/detail/27-04-2020-who-timeline---covid-19](https://www.who.int/news-room/detail/27-04-2020-who-timeline---covid-19).

⁵CDC. URL: [cdc.gov/coronavirus/2019-ncov/cases-updates/cases-in-us.html](https://www.cdc.gov/coronavirus/2019-ncov/cases-updates/cases-in-us.html) (accessed on 28/04/2020).

⁶CDC. URL: [cdc.gov/coronavirus/2019-ncov/prevent-getting-sick/social-distancing.html](https://www.cdc.gov/coronavirus/2019-ncov/prevent-getting-sick/social-distancing.html) (accessed on 28/04/2020).

2.2 Messages of the Fox News Channel

FNC is the leading cable channel in the U.S. with an estimated 3.5 million prime-time viewers.⁷ During the initial days of the COVID-19 spread, FNC engaged in three major discussions on the topic: China's culpability, COVID-19's insubstantiality, and Democrats' partisan interests.

First, when President Trump used the term "Chinese coronavirus," some of his critics suggested that this term would fuel prejudice against Chinese nationals in the U.S. and Chinese-Americans. Some of the FNC hosts spent a significant amount of time rebutting this claim. For example, Sean Hannity said on March 12, 2020:

Over there at fake news CNN, you have fake news Jimmy Acosta, well, he's most worried about the president's terminology, thinking the president's speech was racist because he said the fire started in China.⁸

Another issue was on the credibility of Chinese data. On February, 18, Laura Ingraham, the host of "Ingraham Angle" (the third most-watched FNC show), said:

All right and speaking of China, as the coronavirus spreads, the flow of reliable information from China is basically trickling to a stop, if it ever existed at all. Now why is that? And what exactly are they hiding from us?⁹

FNC personalities also discussed a specific hypothesis about the origin of the virus, suggesting that it might come from Wuhan Institute of Virology. In particular, Tucker Carlson, the host of "Tucker Carlson Tonight" (the second most-watched FNC show), said on March 12, 2020:

In fact, the outbreak may have begun not in a public meat market, but in a poorly run Chinese laboratory. Now, that's not our theory. Anyone who raises that theory on American television is attacked as a conspiracy monger.¹⁰

Second, many of the FNC hosts either were dismissive towards the potential dangers of the virus or ignored it completely. On March 13 (two days after the WHO had declared a pandemic), "Fox & Friends" host Ainsley Earhardt told the viewers that it was

⁷Foxnews.com: "Fox News reaches highest viewership...", URL: <https://www.foxnews.com/media/highest-viewership-network-history-msnbc-cnn-2020>.

⁸Fox News Network Fox Hannity 9:00 pm EST March 12, 2020 Thursday. Source: Nexis Uni database.

⁹Fox News Network Ingraham Angle 10:00 pm EST February 18, 2020 Tuesday. Source: Nexis Uni database.

¹⁰Fox News Network Tucker Carlson Tonight 8:00 pm EST March 12, 2020 Thursday. Source: transcripts of Tucker Carlson Tonight from Nexi Uni database.

“the safest time to fly” because “the terminals are dead.” Another FNC personality, Jeanine Pirro, the host of “Justice with Judge Jeanine,” on March 7 said: “All the talk about coronavirus being much more deadly [than seasonal flu] does not reflect reality.”¹¹ In addition, some shows spread misinformation of diagnostics and preventive methods. For example, Correspondent Geraldo Rivera suggested a simple (but lacking any scientific merit) diagnostic procedure:

If you can't hold your breath for 10 seconds. Everyone should do that. Hold your breath for 10 seconds. If you can hold your breath for 10 seconds then you don't have this disease.¹²

Third, a large amount of air time was devoted to accusation of the Democratic party's “politicizing” the virus and using it opportunistically to harm the reputation of President Trump. On March 9, Fox host Sean Hannity, suggested that opponents of the president were “scaring the living hell out of people.”¹³ Laura Ingraham, the host of “Ingraham Angle,” said on February 25:

After their politically disastrous impeachment and the fierce intraparty fighting ... Democrats needed to change the subject and fast. So, like the Coronavirus itself, Democrats and friends moved to quickly infect the political discussion with viral recriminations.¹⁴

After the declaration of national emergency by President Trump on March 13, 2020, the messaging of FNC shifted towards more emphasis on the importance of distancing and other preventive measures, but not entirely.¹⁵ In addition, the initial period of partisan messaging could have influenced the attitudes of FNC viewers in a way that later shifts could not completely revert due to the confirmation bias (Nickerson, 1998).

The coronavirus coverage by FNC was different from that by other major cable channels. The most popular host of MSNBC (the second most-watched cable channel in the U.S.), Rachel Maddow covered the spread of the virus, both internationally and in the

¹¹Not everyone at Fox was dismissive of the dangers of COVID-19. For example, Tucker Carlson warned his viewers several times during the early days of the disease and even seemed to criticize his FNC colleagues (though he also spent significant time critically discussing state-level lockdown policies). See, for example, Fox News Network Tucker Carlson Tonight 8:00 pm EST from February 27, 28, and March 11. Source: Nexis Uni database.

¹²Mediaite.com, “Fox & Friends...” URL: www.mediaite.com/tv/fox-friends-churns-out-insane-misinformation-on-coronavirus/.

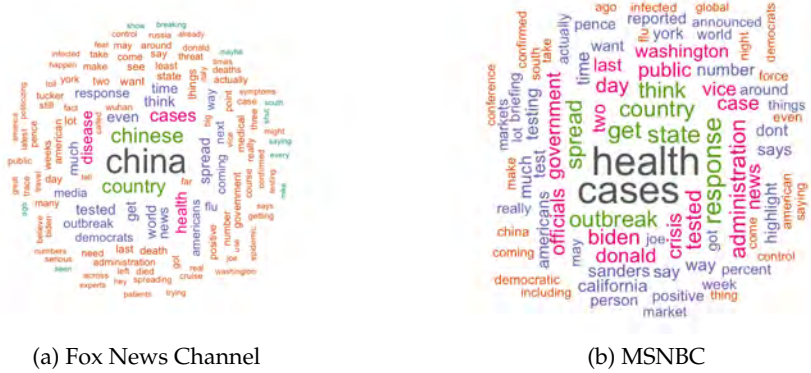
¹³Fox News Network Fox Hannity 9:00 pm EST March 9, 2020 Monday, Source: Nexis Uni database.

¹⁴Fox News Network Ingraham Angle 10:00 pm EST, Source: Nexis Uni Database.

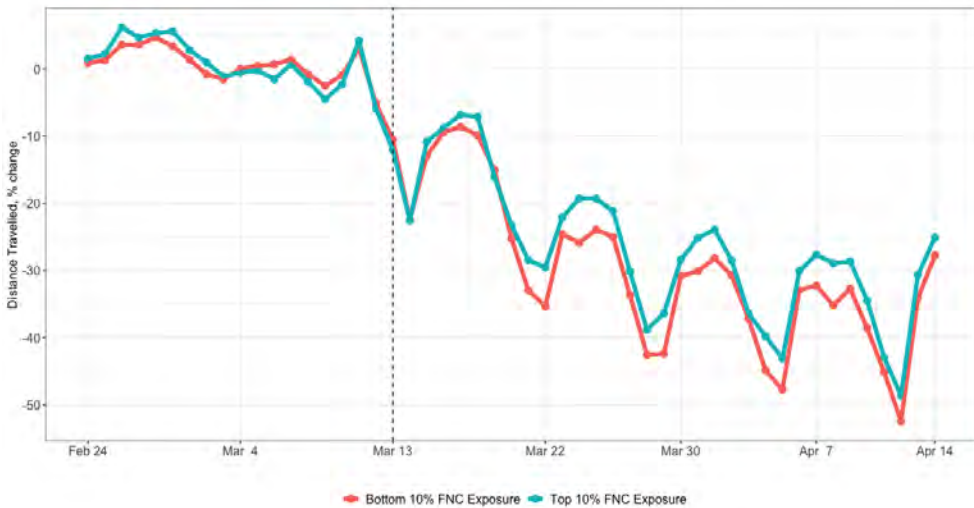
¹⁵Washington Post: “How Fox News has shifted its coronavirus rhetoric,” www.youtube.com/watch?v=ifKbWdf51bA).

Figure 1: Fox News Messaging and Social Distancing

Panel A: Word Clouds of COVID-19 Coverage for Fox News and MSNBC



Panel B: Fox News and Social Distancing



Note: (a) Panel A shows word clouds of COVID-19 coverage from three most-watched FNC shows (Hannity, Tucker Carlson Tonight, and Ingraham Angle) on the left and MSNBC on the right. Transcripts are from February 1, 2020, to March 12, 2020, downloaded via LexisNexis. To build the word clouds, we select only paragraphs containing the word "coronavirus" and remove common English stop-words as well three most common words in both FNC and MSNBC ("president," "Trump," and "people"). We also remove non-informative about the tone of the coverage words like "united," "states," "white," and "house." We built word clouds with remaining words. (b) Panel B shows the changes in daily distance travelled. The red line show changes in counties in bottom 10% of the FOX News exposure (i.e., higher FOX News Channel number, channel positions 64-to-95). The blue line show changes in counties in top 10% of the FOX News exposure (i.e., lower FOX News Channel number, channel positions 1-to-24). Vertical dashed line represents announcement of national state of emergency on March 13th.

Covid Economics 49, 18 September 2020: 85-122

U.S., and criticized the Republican administration for lack of testing capacity and other issues.¹⁶ CNN (the third most-watched cable channel) largely focused on reporting facts, with occasional criticism of some of Trump's epidemiological claims.¹⁷

To illustrate some of the distinct features of FNC coronavirus coverage, Panel A of Figure 1 plots the word-cloud of paragraphs including the word "coronavirus" constructed from LexisNexis transcripts of top-3 FNC shows ("Hannity," "Tucker Carlson Tonight," and "Ingraham Angle") as well as a similar word cloud of MSNBC transcripts from February 1 to March 12. For both networks, we excluded the three most common terms: "President," "Trump," and "people." We see that the most common words in MSNBC coverage were "health" and "cases," while for the top FNC commentators, two most common words were "China" and "Chinese."

2.3 The Effect of Fox News Channel on the Compliance with Social-Distancing

As a preview of our main result, we present a visual evidence on how exposure to FNC affected the compliance with social-distancing. Panel B of Figure 1 plots changes in daily distance traveled for the top 10 percentile of U.S. counties in terms of channel position of FNC (blue line) and that of the bottom 10 percentile (red line).¹⁸ There are three observations from the graph. First, before national emergency (vertical dashed line), both types of counties did not change the patterns of mobility compared to the pre-COVID period. Second, after March 13, both groups reduced mobility. Third, afterwards, counties with lower channel positions (red) experienced a larger decline in the daily distance traveled than those in with the higher channel position, highlighting the role of FNC exposure.

3 Data and Measurement: Fox News Exposure and Social Distancing

3.1 Exogenous Variation in Fox News Exposure

We first construct the measure of exposure to FNC. FNC viewership is correlated with political preferences, which can potentially bias our estimate of the effect of FNC viewership on social distancing. For example, since many of the FNC hosts are conservative,

¹⁶See [msnbc.com/transcripts/rachel-maddow-show/2020-03-09](https://www.msnbc.com/transcripts/rachel-maddow-show/2020-03-09).

¹⁷See <https://edition.cnn.com/2020/04/13/world/cnn-coronavirus-coverage/index.html>.

¹⁸We describe construction of the main variables in the next Section.

its viewers might be inherently more likely to view government measures with suspicion, which might reduce their compliance. Also, given the well-documented urban/rural ideological divide in the U.S., it is likely the people from rural counties watch FNC more and are more limited in how much travel they can avoid.

Instead of using actual viewership, we use an exogenous variation in exposure to FNC: the position of FNC in the cable lineup. FNC was launched in 1996 and quickly expanded its geographic coverage through bilateral negotiations with local cable providers. As a result of those negotiations, those providers started offering FNC as a part of their packages, usually replacing one of their channels with the goal to minimize the change in the existing lineup and not to disrupt the experience of the viewers. This process created quasi-experimental variation in FNC exposure. When FNC has a larger number in the cable lineup position, people are less likely to watch it because it takes more efforts to move to this channel. See detailed discussions in [Martin and Yurukoglu \(2017\)](#).¹⁹

We obtain zip-code-level average historical (2005) position of FNC by Nielsen from [Ash and Poyker \(2019\)](#). FNC became increasingly conservative afterwards and started to lobby lower channel positions as early as in 2007. County-level measures of exposure are aggregates of zip-code-level ones using population weights. FNC channel position varies from 1 in cable lineup to 95, and its standard deviation is about 15 channels.²⁰ [Martin and Yurukoglu \(2017\)](#) demonstrate that FNC channel position is not predicted by the 1996 Republican voting share or electoral contributions and is not explained predicted voting outcomes and viewership using the 2010 demographics. Here, we provide an array of balance tests in [Appendix Table 1](#), where we also regress 2010 demographic and socio-economic variables on FNC position in cable lineup in 2005. All estimates are not statistically different from zero. On the other hand, FNC exposure is correlated with the Republican vote share in 2012 and 2016, suggesting that the channel positions in 2005 affect conservatism in later years.

3.2 Smartphones Data on People's Mobility

The county-level estimates of reductions in mobility come from the New York-based technology company UNACAST, inc ([Unacast, 2020](#)). Using the GPS locations, an identifier (smartphone) is assigned to a county with the largest total duration of stay. There are 15-17 million identifiers for each day in the dataset, from February 24, 2020 to April 14,

¹⁹The first-stage relationship between channel lineup and FNC viewership on the zip-code level is in Table 2 of [Martin and Yurukoglu \(2017\)](#). County-level relationship can be seen in Appendix Figure 1 of [Ash and Poyker \(2019\)](#).

²⁰[Appendix Figure 1](#) shows the distribution of the FNC channel positions on the county-level.

2020, and the total distance traveled per device is then averaged at the county level. To take into account the baseline differences in mobility across regions, each weekday is assigned a baseline distance traveled, using the same weekday during the four weeks before March 8, 2020 (a date that is coded as the start of COVID-19 outbreak in the U.S.). Then, the reduction in distance traveled in a day is measured as the percent reduction between the current date and the baseline weekday. [Appendix Figure 2](#) plots the raw variation in average changes in daily distance traveled (post-March 13, 2020).

The zip-code-level mobility measure is constructed using data from Facebook's Data for Good.²¹ In contrast to the UNACAST dataset, the Facebook data starts on March 10, 2020 and covers only 327 counties on the east coast and west coast of the United States, located in District of Columbia and 14 states.²² There are about 4.8 million devices per day. With information from people using Facebook on their mobile phones with Location History enabled, a person's movement between two time windows is measured as tile-to-tile movements, where a time-window is a 8-hour period and a tile is a 10km by 10km ground square.²³ After assigning tiles to zip codes/counties, we construct two measures using these movement vectors: (i) the probability of staying in the same tile, which we call "staying at home," and (ii) total distance traveled.²⁴ Since there are three time windows per day, we take the mean of the three observations. Pre-COVID period is defined as the 45 days prior to March 10, 2020, and both measures are constructed for this baseline period. Although the baseline data is constant at each tile-to-tile vector, mobility measures at different dates can still have different baseline values since a vector is only recorded if more than 10 users made the move. In addition to the mobility information, we also construct the total Facebook population at the zip code and at the county level.

3.3 Other Factors Affecting Mobility

There are several factors other than media viewership that could potentially affect the extent of social distancing practices. Importantly, some jobs can be more easily switched to the online mode than others. Thus, depending on the industry where people work, a region's compliance with social distancing policy can vary. We computed county-level shares of employment in workable-at-home industries using data from [Dingel and Neiman](#)

²¹<https://dataforgood.fb.com/docs/covid19/>.

²²The 14 states include Arizona, California, Delaware, Idaho, Maryland, Montana, Nevada, New Jersey, Oregon, Pennsylvania, Utah, Virginia, Washington, and West Virginia. Some of these states are only partially in the data. E.g., we only have east of Pennsylvania, from Harrisburg to the border with New Jersey.

²³For details, see <https://docs.microsoft.com/en-us/bingmaps/articles/bing-maps-tile-system>.

²⁴Note that distance traveled is zero if a person stays at the same tile.

(2020). Other county-level measures include voting outcomes in the Presidential elections of 2012 and 2016 and socio-economic and demographics variables in 2010. The details of the data sources and summary of statistics can be found in [Appendix Table 1](#).

4 Empirical Specification and Results

4.1 Empirical Specification

The objective of the empirical exercise is to identify the effect of exposure to FNC on social distancing after the National Emergency was announced on March 13th. The pre-March 13th observations are used to test pre-trends. Our main specification is the following county-date panel regression:

$$SD_{i(s)t} = \beta_1 FNC P_{i(s)} \times \text{Before}_t + \beta_2 FNC P_{i(s)} \times \text{After}_t + X_{i(s)} \Gamma + \mu_s + \lambda_t + \epsilon_{i(s)t}, \quad (1)$$

where $SD_{i(s)t}$ is a measure of social-distancing in a county i located in state s on date t , $FNC P_{i(s)}$ is the 2005 FNC position in channel lineup, and Before_t (After_t) is a dummy equal to one for dates before (after) the national emergency. $FNC P_{i(s)}$ is normalized to have a mean of zero and a standard deviation of one, and a larger $FNC P_{i(s)}$ is associated with a smaller exposure to Fox News. We control for state (μ_s) and date (λ_t) fixed effects. Vector $X_{i(s)}$ includes a set of county-level demographic and economic controls such as population density and poverty rate. Standard errors are clustered at the state level.²⁵

The coefficient of interest β_2 captures the effect of FNC on social distancing after national emergency was announced. We expect it to be negative: counties with larger FNC lineup positions have a larger decrease in the daily distance traveled relative to their pre-COVID baseline. β_1 represents the effect of FNC on social distancing before national emergency was announced, and we expect it to be zero, indicating that counties with difference FNC exposure did not exhibit differential social distancing behaviors in the pre-period.²⁶ Since our FNC lineup is measured in 2005, which is earlier than our study period (2020), we are eventually studying the heterogeneous effect of built-up FNC exposure on people's behavioral choices, given that there is a national policy advocate.

²⁵Results hold if we cluster by county or double-cluster by state and date or county and date. Clustering by state yield the most conservative standard errors.

²⁶Note that the dummy for Before and After sum up to one, and our specification is equivalent to including the FNC levels and the interaction of FNC with the After dummy. We present the results using our current specification to show the absence of pre-trends more straightforwardly.

In addition to the demographic and economic controls mentioned earlier, we take into account the potential confounding effect of the industrial composition on the relationship between FNC exposure and social distancing behaviors. Regions with more FNC exposure may have a particular employment mix, and as shown in [Dingel and Neiman \(2020\)](#), industries and occupations differ in their workability-at-home. We control for it directly in our regressions.

FNC exposure can affect the degree of conservatism, which can directly affect the social distancing behavior if conservative population has different preferences or different constraint, and indirectly, through the interpretation of the COVID-related messages conveyed by FNC. These effects are on top of direct information feeds by FNC that may affect all of its audience, irrespective of their ideology. To separate (1) conservatism, (2) information, and (3) the interaction of the two, we also experiment with directly controlling for the county-level Republican vote shares in the 2012 and 2016 presidential elections and the 2016 turnout rate, which act as proxies for built-up conservatism. In this case, the remaining effect of FNC on social distancing should be either through the information feed or through the interaction of information and conservatism.^{27,28}

One might be concerned that similar as the FNC exposure, other county-level characteristics also affect the social distancing behaviors differentially *before* and *after* the declaration of national emergency. If the FNC exposure is correlated with these characteristics, omitting this differential impact may bias our estimate of the FNC coefficient. To address this concern, we also consider a specification where we add the interaction of the controls $X_{i(s)}$ with the After dummy.

Although we include a wide variety of county characteristics, there might be unobserved variables that are correlated with FNC exposure and affect the social distancing outcome. Thus, we also present a specification where instead of the state fixed effects, we use county fixed effects. Here, both the FNC interaction with the Before dummy and the levels of county characteristics $X_{i(s)}$ will be absorbed by the fixed effects.

²⁷These political economy outcomes are measured after 2005. Thus, they can be affected by the FNC exposure set in 2005. We use these variables to highlight the mechanism, and we find that adding these controls does not affect the coefficient estimate of the FNC exposure, pointing towards the importance of COVID-related direct information transmission.

²⁸In principle, it could be the case that the conservatism ideology can also have an impact on economic outcomes, which affect social distancing behaviors. However, we don't find direct evidence supporting this hypothesis. As shown in [Appendix Table 1](#), the 2005 FNC positions are not correlated with the 2010 demographic and socio-economic conditions.

4.2 Main Results

Table 1 shows the effect of FNC exposure on social distancing using various specifications. In Panel A Column I, we estimate Equation 1 with only state and date fixed effects. The estimand $\hat{\beta}_1$ is statistically insignificant, indicating that counties did not have differential patterns in social distancing before national emergency. The point estimate of interest $\hat{\beta}_2$ is negative and significant. It indicates that a one-standard-deviation increase in FNC lineup led to a 0.6-percentage-point larger decline in average distance traveled in a county.

In Columns II–V, we sequentially add controls for demographic and socio-economic variables. As documented in various other studies, higher education levels and higher incomes at the individual and region levels are positively associated with practicing of social distancing (Brzezinski et al., 2020; Fan, Orhun and Turjeman, 2020; Mongey, Pilosoph and Weinberg, 2020; Wright et al., 2020, among others). We control for unemployment rate, urban dummies, economic-dependence county indicator, poverty rate, median income, population, share of population with high-school education, county's land area, share of nonwhite population, and net domestic migration rate. Column VI further adds the employment share in workable-at-home jobs.²⁹ The coefficient estimate for the FNC effect remains almost identical compared to Column I.

As FNC can affect the general level of conservatism of the local population, it can potentially affect people's response towards recommendations for social distancing. Column VII adds controls for the turnout in 2016 and Republican vote share in the 2012 and 2016 elections. We find that controlling for these conservatism proxies does not affect the coefficient estimate of FNC exposure. It suggests that our results are not driven by the accumulated FNC effect but by its immediate reaction to COVID-19, and possible by the interaction of the two.

We also want to test if the FNC effect come from crowding out viewership of other media. If people watch less FNC and at the same time watch more of other channels such as CNN and MSNBC, our coefficient estimates may reflect the positive effect of other media instead of the negative effect of FNC. Panel B replicates Panel A but adds controls for the channel positions of CNN and MSNBC. Neither of them appears to be significant and the coefficient for the FNC position lineup remains unchanged.

We show the robustness of our results using alternative specifications in Panel C and Panel D. Panel C adds the interaction terms of the controls with the After dummy to take

²⁹In addition, we show that shares of workable-at-home jobs do not correlate with the FNC channel position (see Appendix Table 1). We show robustness to alternative measures of workable-from-home employment in Appendix Table 2.

Table 1: Effects of Fox News Channel Position on Reductions in Mobility

	I	II	III	IV	V	VI	VII
Dependent variable: Difference in daily distance traveled							
<i>Panel A: baseline</i>							
Fox News channel position	0.002	0.003	0.003	0.003	0.003	0.003	0.003
x Before National Emergency	(0.0019)	(0.0018)	(0.0019)	(0.0021)	(0.0021)	(0.0021)	(0.0021)
Fox News channel position	-0.006**	-0.005**	-0.005**	-0.005**	-0.005**	-0.005**	-0.005**
x After National Emergency	(0.0027)	(0.0025)	(0.0024)	(0.0023)	(0.0023)	(0.0024)	(0.0023)
R-squared	0.669	0.678	0.681	0.688	0.688	0.689	0.692
Observations	119,876	119,876	119,876	119,876	119,876	119,876	119,876
<i>Panel B: ~ with other channels</i>							
Fox News channel position	0.002	0.002	0.002	0.002	0.002	0.002	0.002
x Before National Emergency	(0.0020)	(0.0019)	(0.0019)	(0.0022)	(0.0022)	(0.0022)	(0.0021)
Fox News channel position	-0.005*	-0.005*	-0.005**	-0.005*	-0.005*	-0.005**	-0.005**
x After National Emergency	(0.0028)	(0.0026)	(0.0024)	(0.0023)	(0.0023)	(0.0024)	(0.0023)
CNN channel position	-0.003	-0.003	-0.002	-0.002	-0.002	-0.002	-0.001
	(0.0019)	(0.0017)	(0.0016)	(0.0017)	(0.0017)	(0.0017)	(0.0017)
MSNBC channel position	-0.001	-0.000	0.000	0.001	0.001	0.001	0.001
	(0.0018)	(0.0016)	(0.0015)	(0.0014)	(0.0014)	(0.0014)	(0.0013)
R-squared	0.687	0.696	0.699	0.706	0.706	0.707	0.710
Observations	104,400	104,400	104,400	104,400	104,400	104,400	104,400
<i>Panel C: ~ w post-national-emergency controls</i>							
Fox News channel position	0.002	0.002	0.002	0.002	0.002	0.002	0.002
x Before National Emergency	(0.0019)	(0.0016)	(0.0016)	(0.0015)	(0.0015)	(0.0015)	(0.0015)
Fox News channel position	-0.006**	-0.005**	-0.005**	-0.004*	-0.004*	-0.004*	-0.004*
x After National Emergency	(0.0027)	(0.0024)	(0.0023)	(0.0023)	(0.0023)	(0.0023)	(0.0023)
R-squared	0.669	0.683	0.685	0.696	0.697	0.698	0.706
Observations	119,876	119,876	119,876	119,876	119,876	119,876	119,876
<i>Panel D: ~ w county FEs & post-national-emergency controls</i>							
Fox News channel position	-	-	-	-	-	-	-
x Before National Emergency							
Fox News channel position	-0.008**	-0.008**	-0.008**	-0.007**	-0.006**	-0.006**	-0.007**
x After National Emergency	(0.0033)	(0.0030)	(0.0030)	(0.0027)	(0.0026)	(0.0026)	(0.0027)
FEs: County	✓	✓	✓	✓	✓	✓	✓
R-squared	0.756	0.763	0.763	0.770	0.770	0.771	0.774
Observations	119,876	119,876	119,876	119,876	119,876	119,876	119,876
FEs: State	✓	✓	✓	✓	✓	✓	✓
FEs: Date	✓	✓	✓	✓	✓	✓	✓
Economic controls		✓	✓	✓	✓	✓	✓
Urban			✓	✓	✓	✓	✓
Population controls				✓	✓	✓	✓
Share nonwhite & migrant					✓	✓	✓
Workable-from-home emp.						✓	✓
Repub. vote share controls							✓

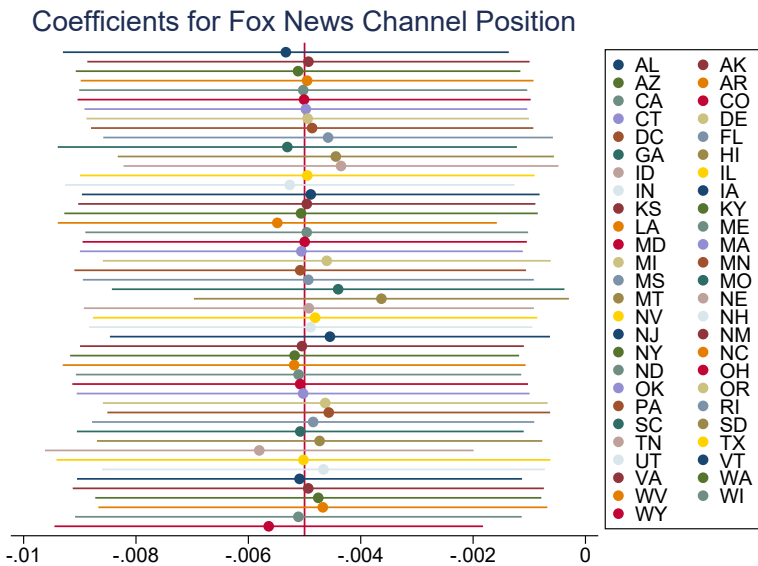
Note: (a) The explanatory variable in all Panels is normalized to mean zero and standard deviation of one. (b) The dependent variable is the difference in daily distance traveled. (c) All regressions include state and date fixed effects. Economic controls include unemployment rate, economic-dependence county indicator, poverty rate, and median income. Urban controls include eight dummies for urban-rural continuum. Population controls include population, share of population with high-school education, and county's land area. Share nonwhite and migration controls include share of nonwhite population and net domestic migration rate. Workable-from-home employment control includes employment share in workable-from-home industries (according to [Dingel and Neiman 2020](#)). Republican vote share controls include Republican vote share in 2012 and 2016 presidential elections, and 2016 turnout rate. (d) In parentheses we report standard errors clustered on state level. *** p<0.01, ** p<0.05, * p<0.1

Covid Economics 49, 18 September 2020: 85-122

into account differential effects of socio-economic and political characteristics on social distancing. Panel D uses county fixed effects instead of state fixed effects to account for additional unobserved factors. The results are very similar to Panel A.

We also check if our results are driven by some specific regions. We find that urban and rural areas did not respond differentially to the FNC exposure (Columns VI–VII of Appendix Table 2). In addition, it was not driven by some particular state (Figure 2).

Figure 2: Results are Not Driven by a Particular State



Note: This figure reports on the point-estimate and 90th-percent confidence band that results when re-estimating the specification in Column VII of Panel A of Table 1, dropping one state at a time. The (red) vertical line is the baseline point estimate. The results are sorted top-to-bottom in alphabetical order, i.e., omit AL, then AK, then AZ, etc. Dropping Montana increases the coefficient the most. Dropping Tennessee decreases the point-estimate the most.

An alternative way to define the start of people’s awareness of the policy recommendation of social distancing is using states’ shelter-in-place orders rather than the national emergency. Suppose that states where voters had been more exposed to FNC also voted for the government that was later in issuing stay-at-home order. In addition, people follow these state-level shelter-in-place orders. Then our effect can be explained by people with more exposure to FNC decreasing their movement less because of the lagged timing of shelter-in-place policies. We find similar results of FNC using the shelter-in-place order

timings, suggesting that people are paying attention to both federal and state recommendations and that the state order timings are not endogenous with respect to FNC channel positions (Appendix Table 3).

4.3 Event Study Evidence

In the previous Section, we show results for non-dynamic specifications, where there is only one coefficient estimate for the FNC exposure for all dates after national emergency was announced. Alternatively, we allow separate point-estimates for weeks from February 24th to April 14th as follows:

$$SD_{i(s)t(w)} = \underbrace{\sum_{l=-4}^{-1} \gamma_l \cdot FNCP_{i(s)} \cdot D(w=l)}_{\text{pre-event period}} + \underbrace{\sum_{l=0}^4 \gamma_l \cdot FNCP_{i(s)} \cdot D(w=l)}_{\text{post-event period}} + X_{i(s)}\Gamma + \lambda_{t(w)} + \mu_s + \varepsilon_{i(s)t(w)}, \tag{2}$$

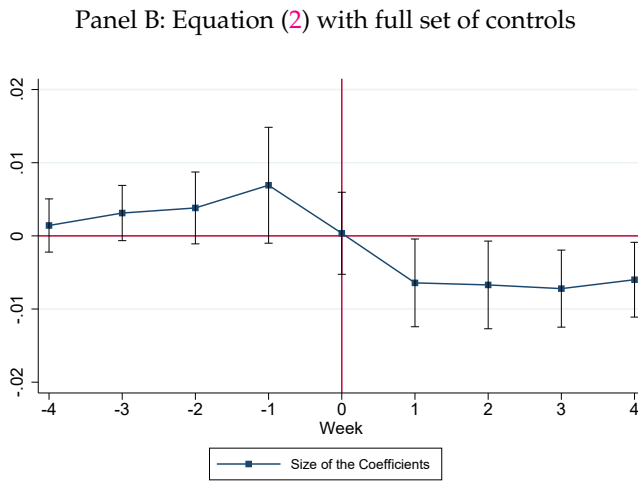
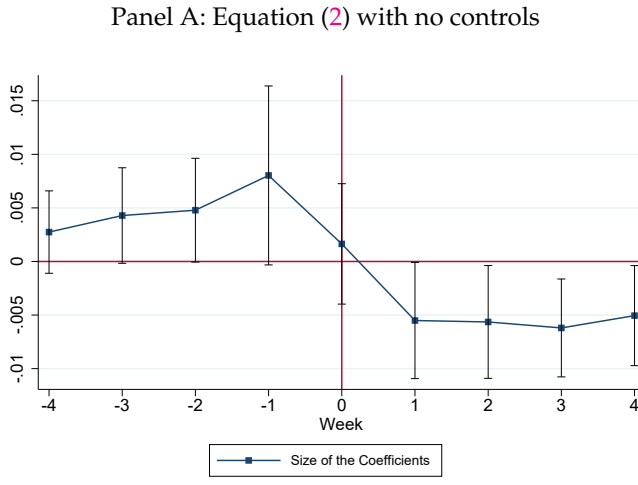
where $SD_{i(s)t(w)}$ is social-distancing outcome of county i in state s at date t in week w . Week $w = 0$ is the week of March 13 to March 20. Week indices run from -4 to 4 and represent the position of weeks relative to Week $w = 0$. $D(w = l)$ is a dummy equal to one if week $w = l$. Here, $\lambda_{t(w)}$ are date fixed effects and μ_s are state fixed effects. Coefficients γ_l with $l \geq 0$ capture the FNC exposure effect in the post national emergency period, and the ones with $l < 0$ capture pre-trends.

Figure 3 plots the resulting coefficients of Equation (2) for the specification without controls (Panel A) and with the full set of controls (Panel B). The first noteworthy feature is that neither specification exhibits pre-trends. There is an increase in the coefficient for the week prior to March 13th; however, the point estimate is insignificant. We fail to reject the joint F-test that the pre-event γ_l s are zero. This suggests that the exact timing of the national emergency is not related to trends in social distancing in more-FNC-exposed counties and that social distancing behaviour did not start to change before the national emergency was announced.³⁰

The second noteworthy feature is that while we do not observe any effect at the week zero (γ_0), four point estimates for four weeks after March 13th have almost the same magnitude as the point estimate of $\hat{\beta}_2$ from the baseline specification in Table 1. Thus the effect is constant across all weeks and our baseline specification (1) captures the full time path of the effect. Results also hold if we add county fixed effects (Appendix Figure 4, which is

³⁰These specifications correspond to Column I and Column VIII of Table 1. Point estimates for Figure 3 are reported in Appendix Table 4.

Figure 3: Event Study Analysis: No Changes in Distanced Traveled Before Week 0 and Large Reductions Afterwards



Note: This Figure graphs the results of estimating equation (2) for specification (in Panel A of Table 1) without controls and with the full set of controls. The former is corresponding to the specification in Column I of Table 1. The latter is corresponding to the specification in Column VII of Table 1. Point estimates are reported in Appendix Table 4. P-values for the joint significance of the pre-trend's coefficients are equal to 0.4034 for Panel A and 0.4480 for Panel B. Following best practice, we bin the end-points, so that the fourth to the fifth week before and after March 13th each share a coefficient (Borusyak and Jaravel 2016; Schmidheiny and Siegloch 2019). This figure reports 90th-percent confidence bands.

Covid Economics 49, 18 September 2020: 85-122

a similar specification to one in Panel D of Table 1), using week $t = -1$ as the baseline.

We also replicate similar event-study graphs for the shelter-at-home orders (see Appendix Figure 3). Here, each state had its own relative time as Week 0 started at the date when the state issued the order. While we see negative effects of the FNC channel position in the post period, there are evident (while insignificant) downward pre-trends. This suggests that people might have started to decrease their mobility after the national emergency was announced but before their state officially ordered them to stay home.

4.4 Zip-Code-Level Results

Thanks to Facebook's "Data for Good" project, we are able to investigate effect of slant media on zip-code-level data for the subsample of 14 states and DC. Since the channel positions are initially on the zip-code level, we decrease potential measurement error.

We first confirm that county-level social distancing measures using Facebook data are highly correlated with measures using UNACAST data. Appendix Figure 5 shows the residual plots of the regression of UNACAST's changes in distance traveled on Facebook's distance traveled (Panel A) and Facebook's probability of staying at home (Panel B). In both graphs, the measures are strongly correlated. We also show that our baseline results in Table 1 hold if we use county-level Facebook measures (Appendix Table 5).

Because Facebook's data start on March 10th, we can't estimate pre-trends as we did in the baseline specification. In addition, instead of the changes in mobility, we observe the levels of mobility in the Facebook data. Thus, we control for the pre-COVID mobility more flexibly using the following equation:

$$M_{j(s)t} = \beta FNC P_{j(s)} + \phi M_{j(s)t-45} + X_{j(s)}\Gamma + \mu_s + \lambda_t + \epsilon_{j(s)t}, \quad (3)$$

where $M_{j(s)t}$ is the mobility measure of zip code j in state s and date t and $M_{j(s)t-45}$ is the corresponding mobility measure in the 45 days before March 10. $FNC P_{j(s)}$ is the FNC lineup position in zip-code j in state s . We again control for state and time fixed effects. Vector $X_{j(s)}$ now contains zip-code-level controls, including the number of Facebook Bing tiles covered, number of Facebook users, population, population density, number of housing units, and land area.

Here, we use two measures of mobility: (i) probability of staying at home (Panel A of Table 2) and (ii) daily distance traveled (Panel B). In Panel A Column I, we only control for baseline probability of staying at home, number of tiles, Facebook's population, and date fixed effects. FNC lineup position has positive effects on staying home: one standard deviation increase in channel position results in a 0.1-percentage-point larger probability

of staying at home. Columns II and III add controls for Facebook’s measure of population density and state fixed effects. Column IV allows for state-and-date fixed effects. Finally, Columns V–VII add controls for population, number of housing units, and land area. The coefficient of interest remains unchanged and highly significant throughout all columns.

Table 2: Zip-Code-Level Evidence: More Fox News Exposure, Longer Distance Traveled, and Smaller Probability of Staying at Home

	I	II	III	IV	V	VI	VII
<i>Panel A:</i>							
	Dependent variable: Probability staying at home						
Fox News channel position	0.001*** (0.0003)	0.001*** (0.0003)	0.001*** (0.0003)	0.001*** (0.0003)	0.001*** (0.0003)	0.001*** (0.0003)	0.001*** (0.0003)
R-squared	0.909	0.914	0.915	0.924	0.924	0.924	0.925
Observations	85,511	83,004	83,004	83,004	83,004	83,004	83,004
<i>Panel B:</i>							
	Dependent variable: Distance traveled						
Fox News channel position	-0.005 (0.0032)	-0.005* (0.0031)	-0.008** (0.0037)	-0.007* (0.0037)	-0.007* (0.0038)	-0.008** (0.0038)	-0.008** (0.0037)
R-squared	0.921	0.924	0.926	0.943	0.943	0.943	0.944
Observations	84,818	82,311	82,311	82,311	82,311	82,311	82,311
Pre-COVID baseline Y	✓	✓	✓	✓	✓	✓	✓
# tiles & Facebook population	✓	✓	✓	✓	✓	✓	✓
FEs: Date	✓	✓	✓				
Population density		✓	✓	✓	✓	✓	✓
FEs: State			✓				
FEs: Date x state				✓	✓	✓	✓
Population					✓	✓	✓
Housing units						✓	✓
Land area							✓

Note: (a) The explanatory variable in both Panels is normalized to mean zero and standard deviation of one. All regressions include date fixed effects, the number of tiles used to construct the dependent variable at date t , number of counties’ Facebook users, and the baseline (pre-COVID) dependent variable constructed using corresponding tiles for date t . (c) In parentheses we report standard errors clustered on zip-code level. *** $p < 0.01$, ** $p < 0.05$, * $p < 0.1$

Panel B reports results for the distance traveled. We, also find results consistent with our findings on the county-level: a one-standard-deviation increase in channel lineup explains 2.5 percent of differences in distance traveled between crisis and baseline measures. Overall, we find consistent evidence that FNC negatively affected social distancing responses both at the county and at the zip-code level.

5 Conclusion

During an outbreak of a contagious disease, public behavior is extremely important, since every policy and each piece of advice from experts can only make a difference if they are followed, and followed by a substantial amount of people. The messages conveyed by

media can either help or hinder these practices. In this paper, we estimate the effect of exposure to one popular media source (FNC) — that spread controversial partisan opinions and some unscientific medical advice during the early days of the COVID-19 pandemic — on mobility reduction and social distancing.

Using county-level mobility data from smartphone locations and the historical position of Fox News Channel in the cable lineup, we show that increased exposure to Fox News led to a smaller reduction in distance traveled and smaller increase in the probability to stay home after the national emergency declaration in the United States. We find that the results are not driven by the conservatism itself, measures as the Republican vote share, but come from the COVID-19-related information conveyed by FNC and its potential interaction with the built-up conservative ideology. We also document that locations more exposed to FNC experienced larger mortality rates from COVID-19 (Appendix Table 6), consistent with Bursztyn et al. (2020). This suggests that the FNC exposure can have important public health consequences through behavioral responses.

Our findings are especially important in the era of increasing affective polarization (Rogowski and Sutherland 2016 and Boxell, Gentzkow and Shapiro 2020). As Iyengar et al. (2019) write:

Ordinary Americans increasingly dislike and distrust those from the other party. Democrats and Republicans both say that the other party's members are hypocritical, selfish, and closed-minded, and they are unwilling to socialize across party lines.

In this highly-charged environment, any criticism of current Republican administration from their Democratic opponents is often perceived as not being done in good faith regardless of its merits, triggering a defensive reaction from conservative media. None other than FNC host Tucker Carlson explained, on March 10, 2020, the logic of some of conservative politicians and media personalities:

Maybe they're just not paying attention, or maybe they believe they're serving some higher cause by shading reality. ... Best not to say anything that might help the other side.³¹

This alleged desire *not to say anything that might help the other side* may impact politics, economic growth, and lives, which are all highly interconnected as we have witnessed in the current COVID-19 pandemic and expect to see in its aftermath.

³¹Foxnews.com: "Tucker Carlson: The Coronavirus Will Get Worse..." URL: [foxnews.com/opinion/tucker-carlson-the-coronavirus-will-get-worse-our-leaders-need-to-stop-lying-about-that](https://www.foxnews.com/opinion/tucker-carlson-the-coronavirus-will-get-worse-our-leaders-need-to-stop-lying-about-that).

References

- Adena, Maja, Ruben Enikolopov, Maria Petrova, Veronica Santarosa, and Ekaterina Zhuravskaya.** 2015. "Radio and the Rise of the Nazis in Prewar Germany." *The Quarterly Journal of Economics*, 130(4): 1885–1939.
- Allcott, Hunt, Levi Boxell, Jacob Conway, Matthew Gentzkow, Michael Thaler, and David Y Yang.** 2020. "Polarization and public health: Partisan differences in social distancing during the Coronavirus pandemic." w26946.
- Anderson, Roy M, Hans Heesterbeek, Don Klinkenberg, and T Déirdre Hollingsworth.** 2020. "How will country-based mitigation measures influence the course of the COVID-19 epidemic?" *The Lancet*, 395(10228): 931–934.
- Arceneaux, Kevin, Johanna Dunaway, Martin Johnson, and Ryan J Vander Wielen.** 2020. "Strategic Candidate Entry and Congressional Elections in the Era of Fox News." *American Journal of Political Science*, 64(2): 398–415.
- Ash, Elliott, and Michael Poyker.** 2019. "Conservative News Media and Criminal Justice: Evidence from Exposure to Fox News Channel." *Columbia Business School Research Paper*.
- Athey, Susan, Billy Ferguson, Matthew Gentzkow, and Tobias Schmidt.** 2019. "Experienced Segregation." Technical Report, Stanford University Working Paper.
- Bailey, Michael, Rachel Cao, Theresa Kuchler, Johannes Stroebel, and Arlene Wong.** 2018. "Social Connectedness: Measurement, Determinants, and Effects." *Journal of Economic Perspectives*, 32(3): 259–80.
- Barwick, Panle Jia, Yanyan Liu, Eleonora Patacchini, and Qi Wu.** 2019. "Information, Mobile Communication, and Referral Effects." National Bureau of Economic Research Working Paper 25873.
- Blumenstock, Joshua Evan, Guanghua Chi, and Xu Tan.** 2019. "Migration and the value of social networks."
- Borusyak, Kirill, and Xavier Jaravel.** 2016. "Revisiting Event Study Designs." Working Paper.
- Boxell, Levi, Matthew Gentzkow, and Jesse M Shapiro.** 2020. "Cross-country trends in affective polarization." National Bureau of Economic Research.
- Brzezinski, Adam, Guido Deiana, Valentin Kecht, and David Van Dijcke.** 2020. "The COVID-19 Pandemic: Government vs. Community Action Across the United States." *Covid Economics* 7, 115–156.
- Büchel, Konstantin, Diego Puga, Elisabet Viladecans-Marsal, and Maximilian von Ehrlich.** 2019. "Calling from the outside: The role of networks in residential mobility."
- Burbidge, John B, Lonnie Magee, and A Leslie Robb.** 1988. "Alternative transformations to handle extreme values of the dependent variable." *Journal of the American Statistical Association*, 83(401): 123–127.
- Bursztyjn, Leonardo, Aakaash Rao, Christopher Roth, and David Yanagizawa-Drott.** 2020. "Misinformation during a pandemic." 2020-44.
- Card, David, and Stefano DellaVigna.** 2017. "What do editors maximize? Evidence from four leading economics journals." National Bureau of Economic Research.
- DellaVigna, Stefano, and Ethan Kaplan.** 2007. "The Fox News effect: Media bias and voting." *The Quarterly Journal of Economics*, 122(3): 1187–1234.
- Dingel, Jonathan I, and Brent Neiman.** 2020. "How many jobs can be done at home?" *Covid Economics* 1, 16–24.
- Enikolopov, Ruben, Maria Petrova, and Ekaterina Zhuravskaya.** 2011. "Media and political persuasion: Evidence from Russia." *American Economic Review*, 101(7): 3253–85.

- Fan, Ying, A Yeşim Orhun, and Dana Turjeman.** 2020. "Heterogeneous Actions, Beliefs, Constraints and Risk Tolerance During the COVID-19 Pandemic." National Bureau of Economic Research.
- Friebel, Guido, and Matthias Heinz.** 2014. "Media slant against foreign owners: Downsizing." *Journal of Public Economics*, 120: 97–106.
- Galletta, Sergio, and Elliott Ash.** 2019. "How Cable News Reshaped Local Government." Available at SSRN 3370908.
- Hatchett, Richard J, Carter E Mecher, and Marc Lipsitch.** 2007. "Public health interventions and epidemic intensity during the 1918 influenza pandemic." *Proceedings of the National Academy of Sciences*, 104(18): 7582–7587.
- Hsiang, Solomon, Daniel Allen, Sebastien Annan-Phan, Kendon Bell, Ian Bolliger, Trinetta Chong, Hannah Druckenmiller, Andrew Hultgren, Luna Yue Huang, Emma Krasovich, et al.** 2020. "The effect of large-scale anti-contagion policies on the coronavirus (covid-19) pandemic." *medRxiv*.
- Iyengar, Shanto, Yphtach Lelkes, Matthew Levendusky, Neil Malhotra, and Sean J Westwood.** 2019. "The origins and consequences of affective polarization in the United States." *Annual Review of Political Science*, 22: 129–146.
- Kreindler, Gabriel E, and Yuhei Miyauchi.** 2019. "Measuring commuting and economic activity inside cities with cell phone records."
- Kuchler, Theresa, Dominic Russel, and Johannes Stroebel.** 2020. "The Geographic Spread of COVID-19 Correlates with Structure of Social Networks as Measured by Facebook." National Bureau of Economic Research Working Paper 26990.
- Martin, Gregory J, and Ali Yurukoglu.** 2017. "Bias in cable news: Persuasion and polarization." *American Economic Review*, 107(9): 2565–99.
- Mongey, Simon, Laura Pilossoph, and Alex Weinberg.** 2020. "Which workers bear the burden of social distancing policies?" *Covid Economics* 12, 69–86.
- Nickerson, Raymond S.** 1998. "Confirmation bias: A ubiquitous phenomenon in many guises." *Review of general psychology*, 2(2): 175–220.
- Prior, Markus.** 2007. *Post-broadcast democracy: How media choice increases inequality in political involvement and polarizes elections.* Cambridge University Press.
- Raifman, J, K Nocka, D Jones, J Bor, S Lipson, J Jay, and P Chan.** 2020. "COVID-19 US state policy database." Available at: www.tinyurl.com/statepolicies.
- Rogowski, Jon C, and Joseph L Sutherland.** 2016. "How ideology fuels affective polarization." *Political Behavior*, 38(2): 485–508.
- Schmidheiny, Kurt, and Sebastian Siegloch.** 2019. "On Event Study Designs and Distributed-Lag Models: Equivalence, Generalization and Practical Implications." CEPR Discussion Papers 13477.
- Simonov, Andrey, Szymon K Sacher, Jean-Pierre H Dubé, and Shirsho Biswas.** 2020. "The persuasive effect of fox news: non-compliance with social distancing during the covid-19 pandemic." National Bureau of Economic Research.
- Snider, JH, and Scott Hall.** 1998. "New Media and Democratic Accountability: The Growth of Government Access TV."
- Tian, Yuan, Maria Esther Caballero, and Brian K. Kovak.** 2020. "Social Learning along International Migrant Networks."
- Unacast.** 2020. "Unacast Social Distancing Dataset." <https://www.unacast.com/data-for-good>. Version from 18 April 2020.

- Wright, Austin L, Konstantin Sonin, Jesse Driscoll, and Jarnickae Wilson.** 2020. "Poverty and Economic Dislocation Reduce Compliance with COVID-19 Shelter-in-Place Protocols." 2020-40.
- Yanagizawa-Drott, David.** 2014. "Propaganda and conflict: Evidence from the Rwandan genocide." *The Quarterly Journal of Economics*, 129(4): 1947–1994.
- Zernike, Kate.** 2010. *Boiling mad: Inside tea party America*. MacMillan.

Online Appendix

to

“The Safest Time to Fly:

Pandemic Response in the Era of Fox News”

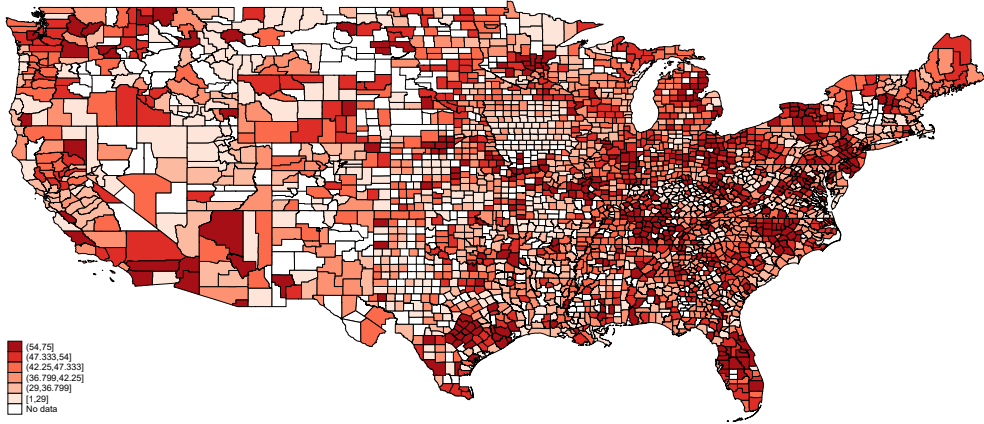
Online Appendix A Additional Results

Table Appendix Table 1: Balance Tests

	I	II	III
	Coefficient	St.er.	P-value
<u>Socio-Demographic Controls:</u>			
Population	0.244	(0.1461)	[0.1010]
Poverty	-0.013	(0.0094)	[0.1888]
Urban/rural	0.030	(0.0184)	[0.1138]
Share nonwhite	0.155	(0.3849)	[0.6896]
Dom. migration	0.356	(0.3198)	[0.2713]
No high school	0.046	(0.1386)	[0.7389]
Median income	0.011	(0.0067)	[0.1005]
Workable-at-home jobs, share	0.007	(0.0078)	[0.3944]
Workable-at-home jobs, share (wage weights)	0.008	(0.0098)	[0.4132]
Workable-at-home jobs alt., share	0.006	(0.0068)	[0.4137]
Workable-at-home jobs alt., share (wage weights)	0.007	(0.0089)	[0.4540]
<u>Republican Vote Shares:</u>			
Presidential election Republican vote share, 2016	-0.684**	(0.3185)	[0.0368]
Presidential election Republican vote share, 2012	-0.787*	(0.4185)	[0.0662]
<u>Pre-COVID Social Distancing:</u>			
Differences in daily distance traveled	0.001	(0.0647)	[0.9820]

Note: (a) Column I contains coefficient of the bivariate regression of Fox News channel position on various outcomes. All regressions include state fixed effects. (b) Column II reports standard errors clustered on state level. (c) Column III reports p-values. None of the regressions are significant at any conventional level. (d) Data on workable-at-home jobs is from [Dingel and Neiman \(2020\)](#). County-level voting data is from https://github.com/tonmcg/County_Level_Election_Results_12-16. Socio-economic data (except for “nonwhite” variable) is from <https://www.ers.usda.gov/data-products/county-level-data-sets/county-level-data-sets-download-data/>. The share of nonwhite population is from <http://library.duke.edu/data/collections/popest>.

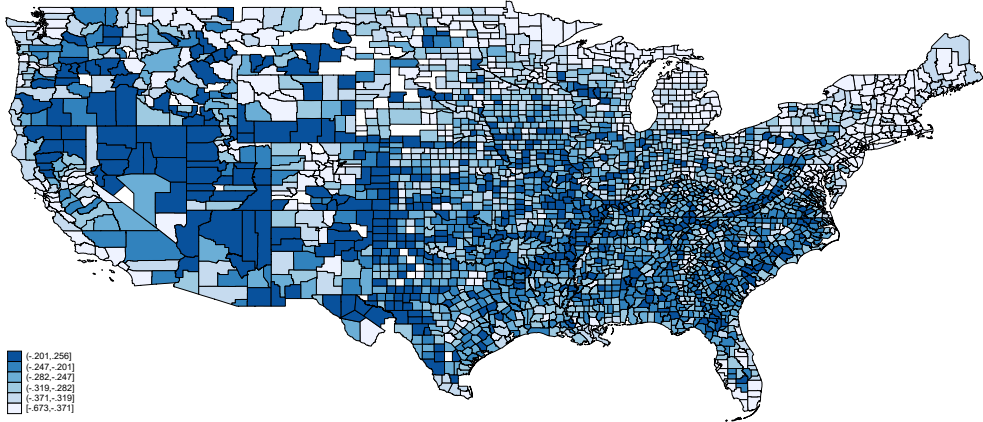
Figure Appendix Figure 1: Map of FOX News Channel Positions



Note: This map shows spatial distribution for the FOX News channel position in 2005. Source: zip-code data is from [Martin and Yurukoglu \(2017\)](#). Aggregated on the county-level using zip-code-level population weights.

Covid Economics 49, 18 September 2020: 85-122

Figure Appendix Figure 2: Map of Changes in Daily Distance Traveled (UNACAST)



Note: This map shows spatial distribution for the differences in the average distance (in percentages) traveled based on UNACAST data. Averaged on post-national emergency sample (March 13th, 2020 — April 14th, 2020).

Table Appendix Table 2: Robustness for the Core Results in Table 1

	I	II	III	IV	V	VI
	Dependent variable: Difference in daily distance traveled					
	Workable-at-home jobs, share	Workable-at-home jobs, share (alt. classification)	Workable-at-home jobs, share (alt. classification)	Workable-at-home jobs, share (alt. classification)	Urban interaction	State x Urban FEs
		w wage weights	w wage weights	w wage weights		
Fox News channel position	0.003	0.003	0.003	0.003	0.003	0.004
x Before National Emergency	(0.0021)	(0.0021)	(0.0021)	(0.0021)	(0.0021)	(0.0021)
Fox News channel position	-0.005**	-0.005**	-0.005**	-0.005**	-0.007*	-0.005*
x After National Emergency	(0.0023)	(0.0023)	(0.0023)	(0.0023)	(0.0038)	(0.0024)
Fox News channel position					0.004	
x Urban					(0.0050)	
Workable-at-home jobs, share	0.003	0.002	0.003	0.002		
	(0.0125)	(0.0099)	(0.0144)	(0.0110)		
FEs: State x urban						✓
R-squared	0.692	0.692	0.692	0.692	0.692	0.692
Observations	119,876	119,876	119,876	119,876	119,876	119,876

Note: (a) This Table uses the baseline specification in Column VII of Panel A of Table 1. (b) Data on shares of workable-at-home jobs in Columns II–V is from [Dingel and Neiman \(2020\)](#). (c) In parentheses we report standard errors clustered on state level. *** $p < 0.01$, ** $p < 0.05$, * $p < 0.1$.

Columns II–IV contain baseline results using alternative measures of workable-from-home industries from [Dingel and Neiman \(2020\)](#). Our results hold.

If FNC position is correlated with rural/urban status of the area, our results could also be explained by difference in mobility patterns between difference types areas. For example, even for their essential needs, people in rural areas often need to travel further thus limiting the potential reduction in mobility that could be sustainable during the pandemic. While we add population controls and urban dummies in Table 1 and show that they are not correlated with the FNC channel position, in [Appendix Table 2](#) we provide additional checks. In Column V of [Appendix Table 2](#), we add interaction of FNC channel position with an urban dummy.³² The result appears to be insignificant while the main coefficient remains negative and significant. In Column VI, we allow each state to have separate intercepts for rural and urban counties; i.e., we use state-urban fixed effects instead of state and rural fixed effects. However, our estimate holds. The results are nearly identical if we use specifications from the other panels of Table 1.

³²Here we split urban-rural continuum variable into a dummy equal zero if it has value of 1,2,3, or 4 and equal to one if it has value of 5, 6, 7, or 8.

Table Appendix Table 3: Robustness with Day of the Shelter-in-Place Order for Table 1

	I	II	III	IV	V	VI	VII
Dependent variable: Difference in daily distance traveled							
<i>Panel A: baseline w shelter-in-place orders</i>							
Fox News channel position	0.002	0.002	0.002	0.002	0.002	0.002	0.003
x Before National Emergency	(0.0022)	(0.0021)	(0.0021)	(0.0023)	(0.0023)	(0.0023)	(0.0023)
Fox News channel position	-0.008*	-0.009**	-0.009**	-0.008*	-0.008*	-0.008*	-0.008*
x After National Emergency	(0.0043)	(0.0042)	(0.0041)	(0.0041)	(0.0041)	(0.0042)	(0.0042)
R-squared	0.699	0.712	0.714	0.722	0.722	0.723	0.726
Observations	87,722	87,722	87,722	87,722	87,722	87,722	87,722
<i>Panel B: ~ with other channels</i>							
Fox News channel position	-0.000	0.001	0.001	0.001	0.001	0.001	0.002
x Before National Emergency	(0.0025)	(0.0022)	(0.0022)	(0.0024)	(0.0024)	(0.0025)	(0.0024)
Fox News channel position	-0.008*	-0.008*	-0.008*	-0.008*	-0.008*	-0.008*	-0.008*
x After National Emergency	(0.0045)	(0.0044)	(0.0043)	(0.0043)	(0.0043)	(0.0044)	(0.0044)
CNN channel position	-0.003	-0.003	-0.002	-0.002	-0.002	-0.002	-0.001
	(0.0023)	(0.0019)	(0.0019)	(0.0020)	(0.0020)	(0.0019)	(0.0019)
MSNBC channel position	-0.002	-0.001	-0.001	0.000	0.000	0.000	0.001
	(0.0022)	(0.0020)	(0.0019)	(0.0016)	(0.0016)	(0.0016)	(0.0014)
R-squared	0.716	0.725	0.727	0.736	0.736	0.737	0.740
Observations	80,592	80,592	80,592	80,592	80,592	80,592	80,592
<i>Panel C: ~ w post-national-emergency controls</i>							
Fox News channel position	0.002	0.002	0.002	0.002	0.002	0.002	0.002
x Before National Emergency	(0.0022)	(0.0020)	(0.0020)	(0.0019)	(0.0018)	(0.0019)	(0.0018)
Fox News channel position	-0.008*	-0.007*	-0.007*	-0.007*	-0.007**	-0.007**	-0.007**
x After National Emergency	(0.0043)	(0.0041)	(0.0040)	(0.0037)	(0.0033)	(0.0033)	(0.0032)
R-squared	0.699	0.714	0.716	0.729	0.731	0.733	0.738
Observations	87,722	87,722	87,722	87,722	87,722	87,722	87,722
<i>Panel D: ~ w county FEs & post-national-emergency controls</i>							
Fox News channel position	-	-	-	-	-	-	-
x Before National Emergency	-	-	-	-	-	-	-
Fox News channel position	-0.009*	-0.008*	-0.008*	-0.007*	-0.007**	-0.007**	-0.007**
x After National Emergency	(0.0052)	(0.0044)	(0.0044)	(0.0042)	(0.0035)	(0.0035)	(0.0034)
FEs: County	✓	✓	✓	✓	✓	✓	✓
R-squared	0.780	0.791	0.791	0.793	0.795	0.795	0.796
Observations	87,722	87,722	87,722	87,722	87,722	87,722	87,722
FEs: State	✓	✓	✓	✓	✓	✓	✓
FEs: Date	✓	✓	✓	✓	✓	✓	✓
Economic controls		✓	✓	✓	✓	✓	✓
Urban			✓	✓	✓	✓	✓
Population controls				✓	✓	✓	✓
Share nonwhite & migrant					✓	✓	✓
Workable-from-home emp.						✓	✓
Repub. vote share controls							✓

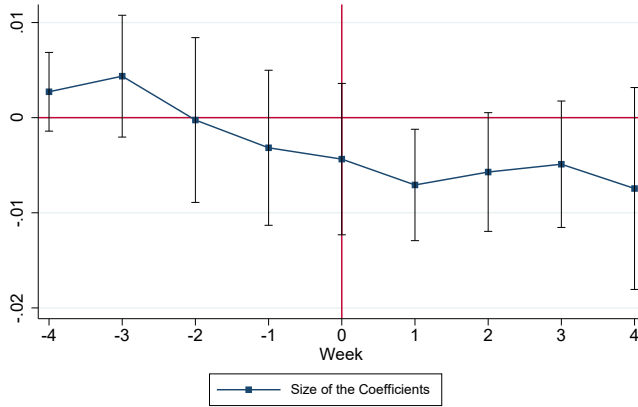
Note: (a) The explanatory variable in all Panels is normalized to mean zero and standard deviation of one. (b) The dependent variable is the difference in daily distance traveled. (c) All regressions include state and date fixed effects. Economic controls include unemployment rate, economic-dependence county indicator, poverty rate, and median income. Urban controls include eight dummies for urban-rural continuum. Population controls include population, share of population with high-school education, and county's land area. Share nonwhite and migration controls include share of nonwhite population and net domestic migration rate. Workable-from-home employment control includes employment share in workable-from-home industries (according to [Dingel and Neiman 2020](#)). Republican vote share controls include Republican vote share in 2012 and 2016 presidential elections, and 2016 turnout rate. (d) We exclude 11 states (Arkansas, Connecticut, Iowa, Kentucky, Nebraska, North Dakota, Oklahoma, South Dakota, Texas, Utah, and Wyoming) that had never issued shelter-in-place orders. (e) In parentheses we report standard errors clustered on state level. *** p<0.01, ** p<0.05, * p<0.1

The first order was issued in California on March 19th, 2020. The last order was issued by South Carolina on April 7th. Eleven states (Arkansas, Connecticut, Iowa, Kentucky, Nebraska, North Dakota, Oklahoma, South Dakota, Texas, Utah, and Wyoming) never issued shelter-in-place orders. We exclude them in [Appendix Table 3](#). All shelter-in-place order dates were collected by [Raifman et al. \(2020\)](#).

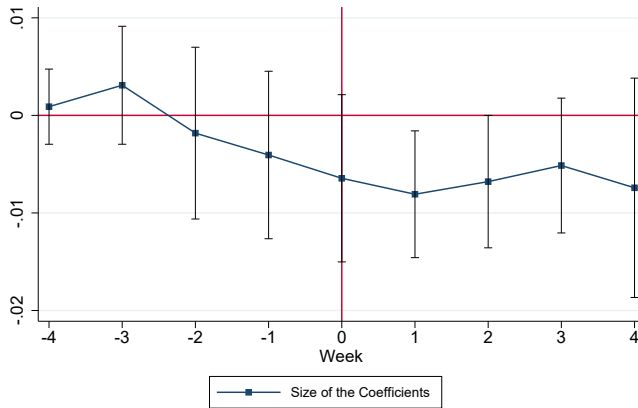
In [Appendix Table 3](#), we replicate [Table 1](#) but instead of the national emergency use the state-specific date of the “shelter-in-place” order. Here variables Before_{st} and After_{st} are state-specific, and, e.g., After_{st} is a dummy equal to one for dates after state s imposed shelter-in-place order at date t . Across all Panels and specifications the coefficient of interest appears to be negative and significant. Nevertheless, we consider this specification not preferable, because people started to decrease their traveled distances even before shelter-in-place orders in their states after the national emergency was issued. We discuss it in greater detail in [Section 4.3](#).

Figure Appendix Figure 3: Event Study Analysis with the day of State’s Shelter-in-Place Order

Panel A: Equation (2) with no controls



Panel B: Equation (2) with full set of controls



Note: This Figure graphs the results of estimating equation (2) for specification (in Panel A of Table 1) without controls and with the full set of controls. The former is corresponding to the specification in Column I of Table 1. The latter is corresponding to the specification in Column VII of Table 1. Point estimates are reported in Appendix Table 4. P-values for the joint significance of the pre-trend’s coefficients are equal to 0.6366 for Panel A and 0.6837 for Panel B. This figure reports 90th-percent confidence bands.

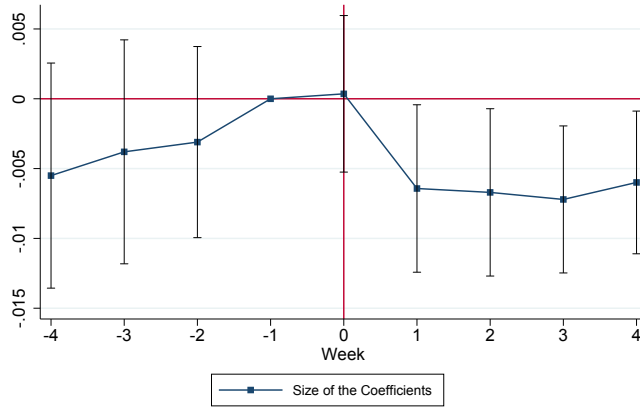
Table Appendix Table 4: Event-Study Coefficients for Figure 3

Event	Dependent variable: Difference in daily distance traveled			
	I	II	III	IV
	National emergency (March 13, 2020)		Shelter-in-place order (state-specific)	
Fox News channel position x				
4 weeks before	0.001 (0.0022)	0.003 (0.0023)	0.001 (0.0023)	0.003 (0.0025)
3 weeks before	0.003 (0.0023)	0.004 (0.0027)	0.003 (0.0036)	0.004 (0.0038)
2 weeks before	0.004 (0.0029)	0.005 (0.0029)	-0.002 (0.0052)	-0.000 (0.0051)
1 week before	0.007 (0.0047)	0.008 (0.0050)	-0.004 (0.0051)	-0.003 (0.0048)
week of national emergency/ or state's shelter-in-place order	0.000 (0.0033)	0.002 (0.0034)	-0.006 (0.0051)	-0.004 (0.0047)
1 week after	-0.006* (0.0036)	-0.006* (0.0032)	-0.008** (0.0039)	-0.007** (0.0035)
2 weeks after	-0.007* (0.0036)	-0.006* (0.0031)	-0.007* (0.0040)	-0.006 (0.0037)
3 weeks after	-0.007** (0.0031)	-0.006** (0.0027)	-0.005 (0.0041)	-0.005 (0.0039)
4 weeks after	-0.006* (0.0030)	-0.005* (0.0028)	-0.007 (0.0067)	-0.007 (0.0063)
Joint F-test for pre-trend coef., p-value	[0.4034]	[0.4480]	[0.6366]	[0.6837]
R-squared	0.691	0.714	0.698	0.732
Observations	119,876	119,876	87,722	87,722
FEs: State	✓	✓	✓	✓
FEs: Date	✓	✓	✓	✓
Economic controls		✓		✓
Urban		✓		✓
Population controls		✓		✓
Share nonwhite & migrant		✓		✓
Workable-from-home emp.		✓		✓
Repub. vote share controls		✓		✓

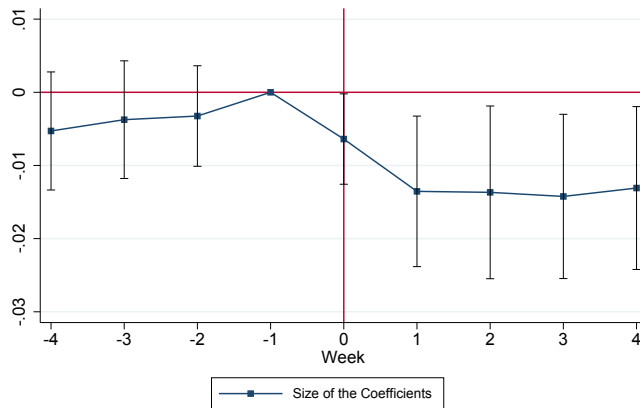
Note: (a) This Table estimates event-study specification 2. Columns I and II report results for the no controls specification. Columns III and IV report results for the specification with the full set of controls. We use the same (most demanding) set of controls as in Column VII of Table 1. (b) The event in Columns I and II is the announcement of national emergency on March 13th, 2020. Events in Columns III and IV are state-specific announcements of shelter-in-place (stay-at-home) orders. Thus all weeks there are in relative terms. (c) In Columns III and IV we exclude 11 states (Arkansas, Connecticut, Iowa, Kentucky, Nebraska, North Dakota, Oklahoma, South Dakota, Texas, Utah, and Wyoming) that had never issued shelter-in-place orders. All shelter-in-place order dates are from Raifman et al. (2020). (d) In parentheses we report standard errors clustered on state level. *** p<0.01, ** p<0.05, * p<0.1

Figure Appendix Figure 4: Event Study Analysis with County Fixed Effects

Panel A: Equation (2) with no controls



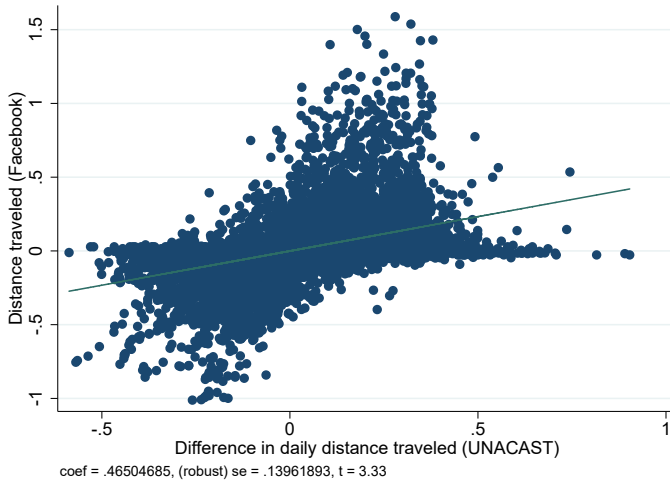
Panel B: Equation (2) with full set of controls



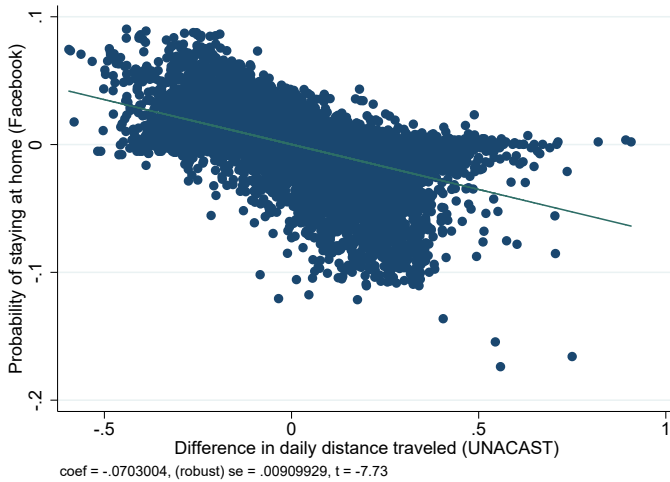
Note: This Figure graphs the results of estimating equation (2) for specification (in Panel D of Table 1) without controls and with the full set of controls. The former is corresponding to the specification in Column I of Table 1. The latter is corresponding to the specification in Column VII of Table 1. Week $t = -1$ is omitted as collinear to county fixed effects. P-values for the joint significance of the pre-trend's coefficients are equal to 0.523 for Panel A and 0.599 for Panel B. This figure reports 90th-percent confidence bands.

Figure Appendix Figure 5: Correlation of UNACAST’s and Facebook’s Data

Panel A: Residual Plot of Facebook’s Distance Traveled and UNACAST’s Differences in Distance Traveled



Panel B: Residual Plot of Facebook’s Probability of Staying at Home and UNACAST’s Differences in Distance Traveled



Note: (a) Panel A depicts residual plots of from the county-level regression of UNACAST’s differences in distance traveled and Facebook’s distance traveled (conditional on Facebook’s pre-COVID baseline and state and date fixed effects). $R^2 = 0.899$. (b) Panel B depicts residual plots of from the county-level regression of UNACAST’s differences in distance traveled and Facebook’s probability of staying home (conditional on Facebook’s pre-COVID baseline and state and date fixed effects). $R^2 = 0.883$.

Table Appendix Table 5: Effect of Fox News Channel Position on Policy Compliance: Core Results using Facebook (County-Level) Data

	I	II	III	IV	V	VI	VII
<i>Panel A:</i>							
	Dependent variable: Probability staying at home						
Fox News channel position	0.001**	0.001**	0.001**	0.001***	0.001***	0.001***	0.001***
x After National Emergency	(0.0005)	(0.0004)	(0.0004)	(0.0003)	(0.0003)	(0.0003)	(0.0003)
R-squared	0.924	0.926	0.926	0.927	0.927	0.927	0.928
Observations	14,827	14,827	14,827	14,827	14,827	14,827	14,827
<i>Panel B:</i>							
	Dependent variable: Distance traveled						
Fox News channel position	-0.012*	-0.013*	-0.015**	-0.015**	-0.016**	-0.016**	-0.016**
x After National Emergency	(0.0067)	(0.0067)	(0.0067)	(0.0067)	(0.0067)	(0.0067)	(0.0063)
R-squared	0.952	0.952	0.954	0.954	0.954	0.954	0.954
Observations	12,765	12,765	12,765	12,765	12,765	12,765	12,765
FEs: State	✓	✓	✓	✓	✓	✓	✓
FEs: Date	✓	✓	✓	✓	✓	✓	✓
# tiles & Facebook pop.	✓	✓	✓	✓	✓	✓	✓
Economic controls		✓	✓	✓	✓	✓	✓
Urban			✓	✓	✓	✓	✓
Population controls				✓	✓	✓	✓
Share nonwhite & migrant					✓	✓	✓
Workable-from-home emp.						✓	✓
Repub. vote share controls							✓

Note: (a) The explanatory variable in all Panels is normalized to mean zero and standard deviation of one. (b) The dependent variable in Panel A is the probability that a person stays home at day t . The dependent variable in Panel B is the daily distance traveled. (c) All regressions include state and date fixed effects, the number of tiles used to construct the dependent variable at date t , number of counties' Facebook users, and the baseline (pre-COVID) dependent variable constructed using corresponding tiles for date t . Economic controls include unemployment rate, economic-dependence county indicator, poverty rate, and median income. Urban controls include eight dummies for urban-rural continuum. Population controls include population, share of population with high-school education, and county's land area. Share nonwhite and migration controls include share of nonwhite population and net domestic migration rate. Workable-from-home employment control includes employment share in workable-from-home industries (according to [Dingel and Neiman 2020](#)). Republican vote share controls include Republican vote share in 2012 and 2016 presidential elections, and 2016 turnout rate. (d) In parentheses we report standard errors clustered on state level. *** $p < 0.01$, ** $p < 0.05$, * $p < 0.1$

Covid Economics 49, 18 September 2020: 85-122

Table Appendix Table 6: Effect of FOX News Channel Position on the COVID-19 Deaths

	I	II	III	IV
<i>Panel A:</i>	Dependent variable: Log # of COVID-19 deaths			
	March 6	March 13	March 20	March 27
Fox News channel position	-0.001 (0.0006)	-0.002 (0.0018)	-0.010* (0.0054)	-0.022* (0.0113)
R-squared	0.058	0.129	0.284	0.456
Observations	2,605	2,605	2,605	2,605
<i>Panel B:</i>	Dependent variable: Fatality rate			
	March 6	March 13	March 20	March 27
Fox News channel position	- -	0.002 (0.0123)	-0.000 (0.0021)	-0.004* (0.0021)
R-squared	-	0.186	0.096	0.060
Observations	-	270	832	1,562
<i>Panel C:</i>	Dependent variable: Log # of COVID-19 cases			
	March 6	March 13	March 20	March 27
Fox News channel position	-0.004 (0.0039)	-0.023 (0.0163)	-0.016 (0.0251)	-0.014 (0.0328)
R-squared	0.346	0.463	0.636	0.682
Observations	2,605	2,605	2,605	2,605

Note: (a) The dependent variable in Panel A is the inverse hyperbolic sin of the cumulative number of COVID-19-related deaths by a specific date. The dependent variable in Panel B is the fatality rate = $\frac{\# \text{ of COVID-19 deaths}}{\# \text{ of COVID-19 cases}}$. The dependent variable in Panel C is the inverse hyperbolic sin of the cumulative number of COVID-19 cases. (b) All regressions include the full set of controls from the most conservative specification in Column VII of Table 1 but without date fixed effects. In Panel B, the (c) COVID-related deaths and number of cases data is from (d) Here we use $\log(\cdot)$ as shorthand for the inverse hyperbolic sin which can be interpreted in the same way as the log function but allows us to keep zero values in number of COVID-19 deaths and cases (see [Burbidge, Magee and Robb 1988](#); [Card and DellaVigna 2017](#)). (e) Number of observations in Panel B changes because the denominator has many zeroes in earlier dates. Hence, there are not enough observations to estimate regression in Column I of Panel B. (f) In parentheses we report standard errors clustered on state

Productivity of working from home during the COVID-19 pandemic: Evidence from an employee survey¹

Masayuki Morikawa²

Date submitted: 12 September 2020; Date accepted: 13 September 2020

Using data from an original survey conducted in June 2020, this study examines the prevalence, frequency, and productivity of working from home (WFH) practices during the COVID-19 pandemic in Japan. The results reveal that the percentage of employees who practiced WFH was approximately 32%. Labor input attributed to WFH arrangements accounted for approximately 19% of total working hours. Highly educated, high-wage, white-collar employees who work in large firms in metropolitan areas tended to practice WFH. The mean WFH productivity relative to working at the usual workplace was about 60% to 70%, and it was lower for employees who started WFH practices only after the spread of the COVID-19 pandemic. Meanwhile, highly educated, and high-wage employees, as well as long-distance commuters, tended to exhibit a relatively small reduction in WFH productivity.

1 I would like to thank Kyoji Fukao, Takeo Hoshi, Naomi Kodama, Daisuke Miyakawa, and Toshihiro Okubo for their helpful comments and suggestions. This research is supported by the JSPS Grants-in-Aid for Scientific Research (16H06322, 18H00858).

2 Professor, Hitotsubashi University; President, Research Institute of Economy, Trade and Industry (RIETI).

Copyright: Masayuki Morikawa

1 Introduction

Following the spread of the COVID-19 pandemic, the practice of working from home (WFH) has been increasing rapidly. During normal times, the percentage of workers participating in WFH arrangements was approximately 10% or less in major advanced countries, but the number of workers who frequently or occasionally conduct their jobs at home has increased suddenly beginning in March 2020 (e.g., Adams *et al.*, 2020; Bartik *et al.*, 2020; Bick *et al.*, 2020; Brynjolfsson *et al.*, 2020; Buchheim *et al.*, 2020; Okubo, 2020). In Japan, although teleworking, including WFH, has been promoted by the government as part of the “Work-Style Reform” in recent years, the share of WFH workers was only about 5% in 2017 (Morikawa, 2018). However, a large number of firms introduced WFH practices to prevent COVID-19 infection. Thus, the number of WFH workers increased further following the declaration of a state of emergency by the Japanese government in April.

Epidemiology models extended by augmenting economic behavior have been developed, and simulation analyses on the effects of social distancing measures, such as a shelter-in-place order, mandatory shutdown of service industries, and school closing to suppress COVID-19 infections have been conducted in many countries (e.g., Atkeson, 2020; Eichenbaum *et al.*, 2020; Jones *et al.*, 2020).³ These studies generally indicate that stringent social distancing policies are effective in mitigating the spread (i.e., “flattening the curve”) of the pandemic, but they have large negative impacts on economic activity, meaning that there is a trade-off, at least in the short-run, between the public’s health and the severity of the recession. Some of the simulation models explicitly take into account WFH practices (e.g., Akbarpour *et al.*, 2020; Aum *et al.*, 2020; Bodenstein *et al.*, 2020; Brotherhood *et al.*, 2020; Jones *et al.*, 2020) because the feasibility of WFH practices can mitigate the trade-off between health and economic activity arising from social distancing policies.

Along with the accumulation of actual data on the number of COVID-19 infections and deaths, empirical evaluations on the effect of WFH have been conducted (e.g., Adams–Prassl *et al.*, 2020; Alipour *et al.*, 2020; Béland *et al.*, 2020a, 2020b; Fadinger and Schymik, 2020; Lin and Meissner, 2020; Mongey *et al.*, 2020). These *ex post* analyses generally confirm that WFH arrangements suppress the spread of the pandemic and/or lessen the negative impact of the pandemic on production and employment.

However, not only the feasibility of WFH, but also its impact on productivity relative to working at the usual workplace, affects the efficacy of WFH in mitigating the negative impact of

³ See Avery *et al.* (2020) and Stock (2020) for the surveys regarding the epidemic models on the spread of COVID-19 such as the SIR (Susceptible, Infected, and Recovered) models.

social distancing policies on the economy. In the simulation studies, the percentage of jobs that can be performed at home is often taken from task-based estimates such as Dingel and Neiman (2020). By contrast, because estimates of WFH productivity have been scarce, simulation studies have assumed arbitrary figures of WFH productivity (e.g., 50% or 70% relative to working at the workplace). To supplement the paucity of studies on the practice of WFH brought about by COVID-19, this study presents quantitative evidence on the prevalence, frequency, and productivity of WFH based on an original survey of employees in Japan during the COVID-19 pandemic.

Our analysis of the survey results revealed that for a large majority of employees in Japan, productivity at home was lower than that at the workplace. The mean WFH productivity relative to working at the usual workplace was about 60% to 70%, and it was lower for employees who started WFH practices only after the spread of the COVID-19 pandemic. Highly educated, high-wage employees, as well as long-distance commuters, tended to exhibit a relatively small reduction in productivity when participating in WFH arrangements. Based on the survey respondents' opinions, the major reasons for the reduced productivity were the loss of quick communication possible only through face-to-face interactions at the workplace, poor telecommunication environment at home relative to that in the office, and the rules (in some cases, for security reasons) and regulations that require some tasks to be conducted in the office.

The remainder of this paper is organized as follows. Section 2 presents a brief review of the related literature and describes the contributions of this study. Section 3 explains the survey data used in this study. Section 4 reports the prevalence and frequency of WFH practices during the COVID-19 pandemic, with focus on the differences in individual characteristics, followed by the results on WFH productivity and how it relates to individual characteristics. Section 5 provides the conclusions and discusses some policy implications.

2 Literature review

Following the spread of the COVID-19 pandemic, several estimations have been presented on how many jobs can potentially be performed at home (e.g., Adams *et al.*, 2020; Dingel and Neiman, 2020; Boeri *et al.*, 2020; Brussevich *et al.*, 2020). Using data on task contents of occupations taken from the Occupational Information Network (O*NET), Dingel and Neiman (2020), an early representative study, estimate that 34% of U.S. jobs can plausibly be performed at home. Boeri *et al.* (2020) indicate that between 23% and 32% of jobs can potentially be carried out at home in major European countries. Adams *et al.* (2020), using unique surveys from the United States and the United Kingdom, document the percentage of *tasks* (on a scale of 0% to

100%) that workers can do from home, which differs from estimates on the percentage of *jobs* achievable at home. Although the share of tasks that can be done from home varies considerably across, as well as within, occupations and industries, the mean figures are around 40% in both countries. The result suggests that some tasks must be performed at the workplace, even for workers whose jobs can mostly be conducted at home.

More recently, using individual-level survey data, several studies have reported results on the percentages of workers who engage in WFH practices during the COVID-19 pandemic (e.g., Bick *et al.*, 2020; Brynjolfsson *et al.*, 2020; Buchheim *et al.*, 2020). These studies show that between 35% and 50% of workers actually engage in WFH arrangements in the United States and some major European countries.⁴ Certain studies report results from firm surveys that about half of firms introduced WFH practices in April 2020 (e.g., Bartik *et al.*, 2020; Buchheim *et al.*, 2020).

Overall, quantitative evidence on the potential and actual percentages of WFH arrangements has been accumulating rapidly. By contrast, evidence on the productivity of employees who practice WFH during the COVID-19 pandemic has been limited. In this respect, Dingel and Neiman (2020) caution that it is not straightforward to use the percentage of jobs plausibly performed at home to estimate the share of output that would be produced under stringent social distancing policies because an individual worker's productivity may differ considerably when working at home versus working at the usual workplace. A rare example of a study on WFH productivity is Bartik *et al.* (2020), which indicates that the productivity of remote workers is about 20% lower than that of non-remote workers, based on a survey of small firms in the United States. However, as the authors have stated, the result reflects the self-selection of workers into WFH.⁵

Bloom *et al.* (2015), for example, present evidence from a field experiment with call center employees in China that during normal times WFH practices enhanced the total factor productivity (TFP) of organizations. The positive effect on productivity arises from both improvements in individual workers' performance and from reductions in office space. By contrast, Battiston *et al.* (2017), exploiting a natural experiment with a public sector organization in the United Kingdom, find that productivity is higher when teammates are in the same room, and that the effect is stronger for urgent and complex tasks. They suggest that teleworking is unsuitable for tasks requiring face-to-face communication. Dutcher (2012), based on a laboratory

⁴ Okubo (2020), using survey data in Japan, reports that participation in telework increased from 6% in January to 17% in June 2020. In his study, telework is defined as working at a specific place (at home or in a public facility) for a specific number of hours using information and communications technologies.

⁵ Morikawa (2018) and Kazekami (2020) indicate that in Japan, there is a positive association between WFH and wages. However, these studies cannot be interpreted as causality running from WFH to wages, because productive workers may self-select into WFH.

experimental approach, indicates that telecommuting may have a positive impact on employee productivity for creative tasks but a negative impact for dull tasks.

These studies indicate that employee productivity under WFH arrangements depends on the characteristics of occupations and specific tasks undertaken. The recent increase in WFH practices has been widespread, involving a variety of white-collar workers, but causal evidence of the productivity of ordinary office workers under WFH arrangements has been scant. Because the recent surge in WFH practices brought about by the COVID-19 pandemic can be considered as a natural experiment, we can observe causal evidence of employee productivity under WFH arrangements through an appropriately designed survey.

Under these circumstances, based on an originally designed survey for individuals conducted in June 2020, this study presents novel observations about the prevalence, frequency, and productivity of employees engaged in WFH practices in Japan. As the quantitative evidence on WFH productivity has been limited, this study contributes to the literature and policymaking for tackling the negative effects of the COVID-19 pandemic. However, it is challenging to measure the productivity of individual workers, particularly of white-collar workers. For instance, the productivity measure obtained from our survey is subjective in nature, and its accuracy can be debated. However, since productivity in our survey is expressed as a percentage of an employee's productivity under WFH conditions relative to the same employee's productivity at the usual workplace, and not a comparison of his/her productivity against other workers, reporting bias arising from overconfidence, for example, can be avoided.

3 Data and methodology

The data used in this study were retrieved from the “Follow-up Survey of Life and Consumption under the Changing Economic Structure” designed by the author of this paper, conducted by the Rakuten Insight, Inc., and contracted out by the Research Institute of Economy, Trade, and Industry (RIETI) in late June 2020.⁶ The online survey questionnaire was sent via e-mail to 10,041 individuals who responded to the previous survey conducted in 2017. In the 2017 survey, the sample individuals were randomly chosen from the 2.3 million registered monitors of Rakuten Insight, Inc., stratified by gender, age (from 20 to 79 years), and region (prefecture), in proportion to the population composition of the 2015 Population Census (Statistics Bureau, Ministry of Internal Affairs and Communications).⁷

⁶ Rakuten Insight, Inc. is a subsidiary of Rakuten, Inc., which is a large online retailer in Japan.

⁷ To be more specific, using a software developed by the Rakuten Research, Inc., the target number of responses was set at the level (i.e., the gender*age*prefecture cell) that was

There were 5,105 respondents (50.8% response rate) to the 2020 survey. The distribution of these respondents by gender and age is presented in **Appendix Table A1**. Compared with the whole population, the survey respondents aged 50 and 60 years were overrepresented, and those aged 20 years was underrepresented. Because this survey was sent to those who responded to the 2017 survey, the aging of respondents in the subsequent three years affected the age distribution.

This study mainly used a sample of 3,324 individuals who were working at the time of the survey. The analyses in this study were based on cross-sectional information obtained from the 2020 survey, but data from the 2017 survey were also used when necessary. For example, the educational attainment of individuals was taken from the 2017 survey.

The major questions regarding WFH arrangements included (1) whether an employee participated in WFH practices and the time the WFH practice started, (2) frequency of WFH, (3) subjective productivity under WFH conditions, and (4) factors that affect WFH productivity. In addition, the survey collected information about various individual characteristics, such as gender, age, and prefecture of residence. Those who were working also provided information on the type of employment (nine categories), occupation (13 categories), industry (14 categories), firm size (13 categories), weekly working hours (eight categories), annual earnings (tax inclusive; 18 categories), prefecture of usual workplace, and commuting hours (round trip; 10 categories). These items were in the form of multiple-choice questions and were generally consistent with those in the Employment Status Survey (Statistics Bureau, Ministry of Internal Affairs and Communications).⁸

The specific question regarding WFH practice was “Did you practice WFH after the onset of the COVID-19 pandemic and the stay-at-home request from the government?” The choices were: (1) “I have been practicing WFH before the COVID-19 pandemic,” (2) “I have started practicing WFH after the onset of the COVID-19 pandemic,” and (3) “I have not practiced WFH.” Next, for those who chose (1) or (2), the survey asked the frequency of WFH: “How many work days did you spend WFH when the frequency of your WFH days was the highest?” This question required a specific figure. For example, for a worker who spent three days in a week WFH (assuming a five-day-work week), the response is 0.6.

Regarding WFH productivity, which is the focus of this study, the question was “Suppose your productivity in the workplace is 100, how do you evaluate your work productivity at home? Please answer this question considering all your tasks.” For this question, it was noted that “If your

proportional to the Population Census. Then, an invitation e-mail was sent randomly by taking into account the predicted response rate. When the number of responses fell short of the target at the cell level, additional invitation e-mails were sent until the target number was met.

⁸ In the analysis presented in Section 4, some categories were integrated into a smaller number of classifications. For example, the type of employment was integrated into standard and non-standard employees.

productivity at home is higher than that in the workplace, please answer with a figure higher than 100.”⁹ In fact, some respondents reported figures higher than 100. Because this productivity measure is subjective, some measurement error of the true productivity was unavoidable. However, it should be stressed that an employee’s productivity under WFH conditions was asked as a relative measurement against his/her own productivity at the usual workplace, not as a comparison with his/her colleagues; thus the figure is unaffected by reporting biases such as the degree of overconfidence or underconfidence.

The question regarding the factors affecting WFH productivity was “What factors negatively affect WFH productivity? Please select the choices relevant to you.” The choices were (1) “Poor telecommunication environment at home relative to the workplace,” (2) “Rules and regulations that require some tasks to be conducted in the office,” (3) “Some tasks cannot be conducted at home even though these are not required by the rules and regulations,” (4) “It is difficult to concentrate on the job because of the presence of family members,” (5) “Lack of a private room specifically designed for work,” (6) “Loss of immediate communication that is only possible through face-to-face interactions with colleagues at the workplace,” (7) “Lack of pressure from boss, colleagues, and subordinates,” and (8) “Other reasons.”

In the following section, we present the cross-tabulation and simple regression results of the answers to the questions explained above.

4 Results and discussion

4.1 Prevalence and frequency of working from home

Among the survey respondents (5,105 in total), there were 3,324 people who were working at the time of the survey.¹⁰ This subsection describes the prevalence and frequency of WFH practices for this sample. **Table 1** shows the tabulated results on the prevalence of WFH practices during the COVID-19 pandemic. About 35.9% (column (1)) of all workers participated in WFH arrangements, of which 10.6% had been under such an arrangement before the COVID-19 pandemic (hereinafter “early WFH adopters”), and 25.3% started the practice after COVID-19 started (hereinafter “new WFH adopters”). However, these figures include self-employed and family workers who usually conduct business at home. When limiting the sample to employees

⁹ The survey system set the minimum (0) and the maximum (200) values for this question.

¹⁰ The number of those who lost their jobs due to the COVID-19 pandemic is 103 (2.0%), and the number of employees who moved to other firms is 48 (0.9%). Most workers in our sample continued working with the same firms after the COVID-19 pandemic started.

(2,718 people), the corresponding percentages are 32.2%, 4.3%, and 27.9%, respectively (column (2)). It is obvious that the large majority of employees started WFH after the onset of the COVID-19 pandemic. The percentage of WFH adopters is somewhat smaller than the comparable figures for the United States and some European countries, as referred to in Section 2.

Table 2 presents cross-tabulated results on the prevalence of WFH practices by employee characteristics. The percentages of males, those aged 20 and 30 years, and those who are highly-educated are higher than the mean. Difference by education is particularly clear: 41.4% and 64.2% of workers with university and postgraduate education, respectively, participate in WFH arrangements. By employment type, the share of WFH adopters is 39.9% for standard employees, which is more than two times higher than the share of non-standard employees (19.7%).¹¹ By industry, information and communication (75.2%) and finance and insurance (58.3%) show higher shares of WFH adopters. By contrast, the shares of WFH adopters are very low in the healthcare and welfare (7.2%), accommodations and restaurants (9.4%), and transport (10.4%) industries. By occupation, trade-related (59.3%), administrative and managerial (55.5%), and professional and engineering jobs have high proportions of WFH adopters. By contrast, production-related (16.0%) and service (16.9%) occupations show very low shares of WFH adopters. In short, the prevalence of WFH adoption is quite heterogeneous across industries and different types of occupation.

Differences by firm size are evident from the results. The share of WFH adopters is 46.8% in firms with 1,000 or more employees, but the share is less than 30% in firms with less than 500 employees. Annual earnings are also strongly associated with the adoption of WFH: about two-thirds of workers earning 9 million yen or higher participate in WFH arrangements. By region, 61.6% of those who live in the Tokyo prefecture adopt WFH, which is far higher than those who live in other prefectures. Similarly, the adoption of WFH is associated with the commuting distance: approximately two-thirds of workers who spend two and a half hours or longer for round trips between home and the workplace participate in WFH arrangements.

Overall, highly educated, high-wage, white-collar employees who work in large firms located in the metropolitan areas tend to participate in WFH practices during the COVID-19 crisis. However, because these individual characteristics correlate with each other, we conducted a simple probit estimation to investigate the true determinants of WFH adoption. The dependent variable is whether WFH is adopted, and the explanatory variables are gender (female dummy), age category dummies, education dummies, annual earnings (expressed in logarithm), commuting hours (expressed in logarithm), employment type (non-standard dummy), industry dummies,

¹¹ Non-standard employees include part-time, hourly-paid, dispatched, contract, and fixed-term employees.

occupation dummies, and firm size dummies.¹² The reference categories for the dummy variables are male, age 40 to 49 years, high school education, standard employee, manufacturing, clerical job, and firm size of 100 to 299 employees.

The results are presented in **Table 3**, where the marginal effects and robust standard errors are reported. The coefficients for the age categories of 20–29 and 30–39 years, university and postgraduate education, annual earnings, commuting hours, information and communications industry, trade-related occupation, and firm size of 1,000 or more are positive and statistically significant, meaning that these characteristics are associated with a higher probability of participating in WFH practice after controlling for other observable characteristics. Meanwhile, the coefficients for transport industry, healthcare and welfare industry, sales occupation, and production-related occupation are negative and significant. Interestingly, the coefficients for female and non-standard employees are insignificant, which differ from the observations through cross-tabulation. The results suggest that female and non-standard employees tend to work in industries and occupations where WFH arrangements are difficult.

Table 4 shows the tabulated results of the frequency of WFH among employees who participated in WFH practice (N = 876). The figures in the first column are the ratio of WFH days to total work days when the WFH frequency was the highest. About 20.4% of these employees did their jobs completely at home (1.0). The mean and the median frequency of WFH are 0.557 and 0.5, respectively. In other words, in the case of a five-day workweek, typical WFH workers spend two to three days a week at home, but as evident from the table, the frequency of WFH is highly dispersed.

Differences in the timing of WFH initiation are small. The mean frequency of WFH for those who engaged in WFH practices before the COVID-19 pandemic (i.e., early WFH adopters) is 0.592, and that for those who started WFH after the onset of the COVID-19 (new WFH adopters) is 0.551 (median figures are 0.55 and 0.5, respectively). According to a survey conducted in 2017, the majority of teleworkers spend only 1 day or less a week (Morikawa, 2018), meaning that the frequency of WFH increased after the COVID-19 pandemic, even for early WFH adopters.¹³

Table 5 presents the mean of the frequency of WFH by individual characteristics. The differences by gender, age, education, and employment type are small, but the difference by industry is large. The frequency of WFH is high for the information and communication industry, and the prevalence of WFH in this industry is also high. By contrast, the transport,

¹² The central values of the earnings categories were applied as a logarithmic transformation to construct the variable of annual earnings. In this calculation, “less than 500 thousand yen” and “20 million yen or more” were treated as 250 thousand yen and 21.25 million yen, respectively. A similar logarithmic transformation was applied to the variable of commuting hours. In this calculation, “four hours or longer” was treated as 4.25 hours.

¹³ In the 2017 survey, the question was about the use of telework, including WFH.

accommodations and restaurants, and healthcare and welfare industries are characterized by both low prevalence and low frequency of WFH. Systematic differences by firm size and annual earnings are not observed, but employees living in Tokyo tend to practice WFH frequently.

Based on the results presented above, we can calculate the individual-level WFH hours by multiplying the usual weekly working hours and the frequency of WFH. The aggregated share of WFH hours can be calculated as the sum of the WFH hours divided by the sum of the weekly working hours of all employees. The resulting aggregate share of WFH is 19.4%: slightly less than one-fifth of work is conducted at home by the employees in our sample. The remaining 80.6% of work is conducted at the usual workplace. Although the number of workers engaged in WFH dramatically increased after the COVID-19 pandemic started, the macroeconomic contribution of WFH labor input was not large because many jobs cannot be done at home and the number of full-time WFH workers is limited.¹⁴

It is expected that WFH contributes to mitigating congestion of public transport. Using data on commuting hours, we can also calculate the reduction of aggregate commuting hours attributable to WFH, which is estimated to be 24.5%. Since both the probability and frequency of WFH is higher among long commuters, the contribution of WFH to the saving of commuting hours is larger than its share of total working hours. This calculation suggests that WFH had a positive impact on reducing the risk of infection arising from physical contact among commuters.

4.2 Productivity of working from home

The distribution of the WFH adopters' subjective productivity at home relative to their usual workplace (= 100) is summarized in **Table 6**. The mean and median of this measure of WFH productivity are 60.6% and 70%, respectively. However, this WFH productivity measure is very heterogeneous: the standard deviation is 35.1% and the gap between the 75th and 25th percentiles is 56.5%. The percentages of WFH adopters whose productivity at home is higher than, equal to, or lower than the productivity at the workplace are 3.9%, 14.2%, and 82.0%, respectively. For a large majority of employees, their productivity at home is lower than their productivity in the office.

Figure 1 depicts the distributions of WFH productivity for the subsamples of early and new adopters. It is clear from the figure that the WFH productivity distribution is very different between these subgroups. The mean of early adopters is 76.8%, which is 18.7% higher than that

¹⁴ As stated before, the earnings of WFH workers are relatively high. The aggregate contribution of WFH to total earnings is 24.5%, which is higher than the figure for simple working hours.

of new adopters (58.1%), and the difference is statistically significant at the 1% level. The lower rows of **Table 6** show a comparison of the figures for those who engaged in teleworking in the 2017 survey and those who did not. The result is essentially the same as that obtained only from the 2020 survey, confirming that the relative WFH productivity is significantly higher for early adopters.

The higher WFH productivity of early adopters reflects both the selection mechanism and learning effect. It is conceivable that early adopters who practice WFH before the pandemic voluntarily self-selected into a WFH arrangement because their jobs are easy to do at home and their working environment at home is not inferior to the workplace. In addition, the accumulation of WFH experience may have improved their productivity at home. However, it should be noted that even for early adopters, their subjective productivity at home is, on average, lower than their productivity at the workplace. The percentage of those exhibiting higher WFH productivity relative to the workplace is only about a third, even for the subsample of early adopters. The results suggest that the WFH productivity of new adopters improves through the effect of learning-by-experience, but we conjecture that their long-run WFH productivity will be about 70% to 80% of their productivity at the workplace.

As stated before, the share of WFH hours to total labor input is about 19.4%, and the contribution of WFH to total earnings is 24.5%. It is possible to make a rough estimate of the loss of aggregate labor productivity arising from WFH as follows:

$$\text{Loss from WFH (\%)} = [\Sigma(\text{earnings}_i) * (\text{WFH frequency}_i) * (1 - \text{WFH productivity}_i)] / \Sigma(\text{earnings}_i).$$

According to this mechanical calculation, the productivity loss is 7.6%. If we assume that the WFH productivity of new adopters converges with those of early adopters through the learning effect, the loss will be reduced by 1.2% to 6.4%.

As the dispersion of WFH productivity is very large, the natural question that comes to mind concerns the differences by individual characteristics. The mean WFH productivity by individual characteristics is reported in **Table 7**. Although the differences by gender, age, and employment type are small, the differences by education, industry, occupation, firm size, and annual earnings are remarkable. The mean WFH productivity stands out in the information and communication industry (73.5%). By occupation, professional and engineering (69.2%) and administrative and managerial (67.5%) occupations show relatively high WFH productivity. As seen in the previous subsection, these industries and occupations are characterized by a high WFH practice rate. These results suggest that efficiency under WFH conditions depends heavily on the nature of the jobs. In addition, the relative WFH productivity is higher for those who have postgraduate education (72.0%), those with annual earnings of 10 million or higher (73.7%), and workers who commute

more than three hours a day between home and the workplace (69.9%).

Table 8 reports simple ordinary least square (OLS) regression results regarding WFH productivity. The basic explanatory variables are the same as those in the probit estimation (whose results are reported in **Table 3**): gender, age, education, annual earnings (expressed in logarithm), commuting hours (expressed in logarithm), employment type, industry, occupation, and firm size. The reference categories for the dummy variables are male, age 40 to 49 years, high school education, standard employee, and firm size of 100 to 299 employees.

The coefficients for high education, annual earnings, and commuting hours are positive and significant, confirming the observation from the simple tabulation. Unexpectedly, the coefficient for non-standard employees is positive and significant at the 5% level. The size of the estimated coefficient (8.489) means that among those who practice WFH, the productivity relative to the workplace of non-standard employees is about 8% higher than that of standard employees. Our interpretation is that the job description of non-standard employees, such as part-time workers, dispatched employees, and contract employees, is clear, and they are less likely to bear the burden of sudden unexpected tasks and coordinating roles in the workplace. The coefficients for the firm size classes are insignificant. Although employees of large firms are likely to practice WFH during the pandemic (see **Table 3**), their relative productivity at home is not different from that of employees working with small firms.

Column (2) of **Table 8** shows the result of using the new WFH adopter dummy as an additional explanatory variable. As expected, the coefficient for this dummy is negative, large, and highly significant. After controlling for the other observable individual characteristics, the WFH productivity of new adopters is 13.7% lower than that of early adopters, although the gap is smaller than the raw comparison (18.7%). Column (3) of the table shows the estimation result when the frequency of WFH as an explanatory variable is added. The estimated coefficient for this variable is positive and highly significant. Quantitatively, the relative WFH productivity of employees with one more day of WFH a week is about 3.5% points higher. This result implies that employees with relatively high WFH productivity tend to practice WFH frequently.

The survey asked for the factors that affect WFH productivity. There are eight choices, as described in Section 3. The results are summarized in **Table 9**. The major reasons for reduced productivity at home are, in descending order, (1) loss of quick communication that is only possible through face-to-face interactions with their colleagues at the workplace (38.5%), (2) poor telecommunication environment at home relative to the workplace (34.9%), (3) rules and regulations that require some tasks to be conducted in the office (33.1%), and (4) some tasks cannot be conducted at home even though these are not required by rules and regulations (32.4%).

Among these obstacles, the telecommunication environment at home can be improved through investments in hardware and software, while inappropriate rules and regulations can be amended

to some extent. Considering the possibility of a prolonged impact of the COVID-19, making investments and effort to reform work practices that are unsuitable for WFH practices are important to improve WFH productivity. However, the loss of face-to-face interactions is an inherent constraint on WFH productivity. Although the development of innovative telecommunication technologies and efficient use of such technologies may mitigate this constraint, it will persist in the foreseeable future as a factor that reduces WFH productivity relative to the workplace.

5 Conclusion

This study, using unique data from an original survey conducted in June 2020, presents evidence on the prevalence, frequency, and productivity of WFH during the COVID-19 pandemic in Japan. For the period covered in the survey, the main results are summarized as follows.

First, the percentage of employees who practiced WFH was about 32%, of which 28% started WFH after the onset of the COVID-19 pandemic. The labor input from WFH were about 19% of the weekly working hours.

Second, highly educated, high-wage, white-collar employees who work in large firms in metropolitan areas tended to practice WFH, which suggests that infection risk and social distancing policies may exacerbate economic disparity among employees.

Third, for a large majority of employees (about 82%) their productivity at home was lower than that in their usual workplace. The mean WFH productivity was about 60% to 70% of the productivity at the workplace and lower for employees that started WFH after the onset of the COVID-19 pandemic. The WFH productivity gap between early adopters and new adopters reflects both the selection mechanism and the learning effect.

Fourth, the aggregate loss arising from inferior productivity at home was estimated to be approximately 7%. If new adopters' WFH productivity converges with the productivity of early adopters, the loss will be reduced by about one percentage point.

Fifth, highly educated, high-wage employees, as well as long-distance commuters, tended to exhibit a relatively small reduction in WFH productivity. Those who productively work at home tended to practice WFH frequently, suggesting a natural selection of work location based on productivity.

Sixth, the lack of face-to-face interactions, poor telecommunication environment at home, and the existence of tasks that must be conducted in the office due to rules and regulations and other reasons were the major impediments to improving productivity at home. This result suggests that investments in hardware and software related to WFH and modifications of inappropriate rules

and regulations may help improve WFH productivity. However, since some important information that is difficult to digitalize will continue to be exchanged through face-to-face interaction, it is difficult to expect WFH productivity to reach the same level as that at the workplace, at least on average. Even after incorporating the positive effect through learning, the maximum average productivity at home is expected to be about 70% to 80% of productivity at the workplace. To achieve further improvements in WFH productivity, innovation in telecommunication infrastructure and software that enables human interactions in a way that is similar to face-to-face communication is necessary.

It is extremely difficult to measure the productivity of individual workers accurately, particularly that of white-collar workers. Since the productivity measure used in this study depends on subjective reporting, measurement errors are possible. However, WFH productivity is expressed as a relative figure to an employee's own productivity at the usual workplace, not as a comparison with other workers. This way, we can avoid reporting bias, for example, those arising from the overconfidence of the respondents.

Although the COVID-19 pandemic is a natural experiment that exogenously increased the adoption of WFH practices among a wide range of white-collar workers, we cannot completely eliminate the selection effect. In addition, it should be noted that as an extreme case, for many service jobs that require physical contact with customers, such as doctors, nurses, hairdressers, and restaurants, the productivity of teleworking is prohibitively low.

References

- Adams, Abigail, Teodora Boneva, Christopher Rauh, and Marta Golin (2020). “Work Tasks That Can Be Done from Home: Evidence on Variation within and across Occupations and Industries.” CEPR Discussion Paper, No. 14901.
- Adams–Prassl, Abi, Teodora Boneva, Marta Golin, and Christopher Rauh (2020). “Inequality in the Impact of the Coronavirus Shock: Evidence from Real Time Surveys.” IZA Discussion Paper, No. 13183.
- Akbarpour, Mohammad, Cody Cook, Aude Marzuoli, Simon Mongey, Abhishek Nagaraj, Matteo Saccarola, Pietro Tebaldi, Shoshana Vasserman, and Hanbin Yang (2020). “Socioeconomic Network Heterogeneity and Pandemic Policy Response.” NBER Working Paper, No. 27374.
- Alipour, Jean–Victor, Harald Fadinger, and Jan Schymik (2020). “My Home Is My Castle: The Benefits of Working from Home During a Pandemic Crisis: Evidence from Germany.” CEPR Discussion Paper, No. 14871.
- Atkeson, Andrew (2020). “What Will Be the Economic Impact of COVID-19 in the US? Rough Estimates of Disease Scenarios.” NBER Working Paper, No. 26867.
- Aum, Sangmin, Sang Yoon (Tim) Lee, and Yongseok Shin (2020). “Inequality of Fear and Self-Quarantine: Is There a Trade-off between GDP and Public Health?” *Covid Economics* 13, 143-174.
- Avery, Christopher, William Bossert, Adam Clark, Glenn Ellison, and Sara Fisher Ellison (2020). “Policy Implications of Models of the Spread of Coronavirus: Perspectives and Opportunities for Economists.” *Covid Economics* 12, 21-68.
- Bartik, Alexander W., Zoe B. Cullen, Edward L. Glaeser, Michael Luca, and Christopher T. Stanton (2020). “What Jobs are Being Done at Home During the Covid-19 Crisis? Evidence from Firm-Level Surveys.” NBER Working Paper, No. 27422.
- Battiston, Diego, Jordi Blanes I. Vidal, and Tom Kirchmaier (2017). “Is Distance Dead? Face-to-Face Communication and Productivity in Teams.” CEPR Discussion Paper, No. 11924.
- Béland, Louis–Philippe, Abel Brodeur, and Taylor Wright (2020a). “The Short-Term Economic Consequences of COVID-19: Exposure to Disease, Remote Work and Government Response.” IZA Discussion Paper, No. 13159.
- Béland, Louis–Philippe, Abel Brodeur, Derek Mikola, and Taylor Wright (2020b). “The Short-Term Economic Consequences of COVID-19: Occupation Tasks and Mental Health in Canada.” IZA Discussion Paper, No. 13254.
- Bick, Alexander, Adam Blandin, and Karel Mertens (2020). “Work from Home after the Covid-19 Outbreak.” CEPR Discussion Paper, No. 15000.
- Bloom, Nicholas, James Liang, John Roberts, and Zhichun Jenny Ying (2015). “Does Working

from Home Work? Evidence from a Chinese Experiment.” *Quarterly Journal of Economics*, 130(1), 165–218.

Bodenstein, Martin, Giancarlo Corsetti, and Luca Guerrieri (2020). “Social Distancing and Supply Disruptions in a Pandemic.” *Covid Economics* 19, 1-52.

Boeri, Tito, Alessandro Caiumi, and Marco Paccagnella (2020). “Mitigating the Work–Safety Trade-Off.” *Covid Economics*, 2, 60–66.

Brotherhood, Luiz, Philipp Kircher, Cezar Santos, and Michèle Tertilt (2020). “An Economic Model of the Covid-19 Epidemic: The Importance of Testing and Age-Specific Policies.” CEPR Discussion Paper, No. 14695.

Brussevich, Mariya, Era Dabla-Norris, Salma Khalid (2020). “Who will Bear the Brunt of Lockdown Policies? Evidence from Tele-workability Measures across Countries.” IMF Working Paper, No. 20-88.

Brynjolfsson, Erik, John J. Horton, Adam Ozimek, Daniel Rock, Garima Sharma, and Hong-Yi TuYe (2020). “COVID-19 and Remote Work: An Early Look at US Data.” NBER Working Paper, No. 27344.

Buchheim, Lukas, Jonas Dovern, Carla Krolage, and Sebastian Link (2020). “Firm-level Expectations and Behavior in Response to the COVID-19 Crisis.” IZA Discussion Paper, No. 13253.

Dingel, Jonathan I. and Brent Neiman (2020). “How Many Jobs Can be Done at Home?” *Covid Economics*, 1, 16-24.

Dutcher, E. Glenn (2012). “The Effects of Telecommuting on Productivity: An Experimental Examination. The Role of Dull and Creative Tasks.” *Journal of Economic Behavior & Organization*, 84(1), 55–363.

Eichenbaum, Martin S., Sergio Rebelo, and Mathias Trabandt (2020). “The Macroeconomics of Epidemics.” NBER Working Paper, No. 26882.

Fadinger, Harald and Jan Schymik (2020). “The Costs and Benefits of Home Office during the Covid-19 Pandemic: Evidence from Infections and an Input-Output Model for Germany.” *Covid Economics*, 9, 107–134.

Jones, Callum J., Thomas Philippon, and Venky Venkateswaran (2020). “Optimal Mitigation Policies in a Pandemic: Social Distancing and Working from Home.” NBER Working Paper, No. 26984.

Kazekami, Sachiko (2020). “Mechanisms to Improve Labor Productivity by Performing Telework.” *Telecommunications Policy*, 44(2), 101868.

Lin, Zhixian and Christopher M. Meissner (2020). “Health vs. Wealth? Public Health Policies and the Economy During Covid-19.” *Covid Economics* 14, 85-106.

Mongey, Simon, Laura Pilossoph, and Alex Weinberg (2020). “Which Workers Bear the Burden

of Social Distancing Policies?” *Covid Economics* 12, 69-86.

Morikawa, Masayuki (2018). “Long Commuting Time and the Benefits of Telecommuting.”
RIETI Discussion Paper, 18-E-025.

Okubo, Toshihiro (2020). “Spread of COVID-19 and Telework: Evidence from Japan.” *Covid Economics*, 32, 1–25.

Stock, James H. (2020). “Data Gaps and the Policy Response to the Novel Coronavirus.” *Covid Economics* 3, 1-11.

Table 1. The prevalence of working from home practice

	(1) All workers	(2) Employees
Doing WFH	35.8%	32.2%
Early WFH adopters	10.6%	4.3%
New WFH adopters	25.3%	27.9%
Not doing WFH	64.2%	67.8%

Note: The percentages in column (2) are calculated after excluding “company executive,” “self-employed,” and “family worker” from all workers.

Table 2. The prevalence of working from home practice by individual characteristics

Categories		WFH	Categories		WFH
Total		32.2%	Administrative & managerial		55.5%
Gender	Male	38.7%	Professional & engineering		43.2%
	Female	22.2%	Clerical		36.7%
Age	20-29	39.9%	Occupation	Sales	11.4%
	30-39	36.0%		Trade	59.3%
	40-49	29.3%		Service	16.9%
	50-59	35.6%		Production & other	16.0%
	60-69	28.0%		1-99	22.7%
	70-79	26.2%		100-299	27.3%
Education	Junior high school	5.7%	Firm size	300-499	29.3%
	Senior high school	17.8%		500-999	40.7%
	Vocational school	21.7%		1,000-	46.8%
	Junior (2-year) college	21.3%		Government	40.9%
	4-year university	41.4%		Less than 2 million yen	13.6%
	Graduate school	64.2%		2-2.99	23.2%
Employment type	Standard	39.9%	Earnings	3-3.99	25.0%
	Non-standard	19.7%		4-4.99	32.9%
Industry	Construction	36.3%		5-5.99	34.6%
	Manufacturing	38.0%		6-6.99	38.8%
	Information & communications	75.2%		7-7.99	43.6%
	Transport	10.4%		8-8.99	55.4%
	Wholesale & retail	24.5%		9-9.99	65.3%
	Finance & insurance	58.3%		10 million yen or more	64.8%
	Real estate	38.8%		Tokyo	61.6%
	Accommodations & restaurants	9.4%		Residence	Aichi & Osaka
	Health care & welfare	7.2%	Other	23.0%	
	Education	42.6%	Less than 0.5 hour	15.0%	
Other services	26.0%	0.5-0.99	27.6%		
Public services	39.3%	Commuting	1.0-1.49	45.6%	
Other industries	33.7%	hours (round trip)	1.5-1.99	48.6%	
			2.0-2.49	48.1%	
			2.5-2.99	67.6%	
			3 hours or longer	66.3%	

Notes: This table indicates the percentage of employees who participate in WFH arrangements. Other industries include agriculture, fisheries, and forestry. Some categories for firm size, earnings, residence, and commuting hours integrate the original choices in the survey questions.

Table 3. The probability of participating in working from home practices: Estimation results

Variables	dF/dx	Std. Err.	Variables (continued)	dF/dx	Std. Err.
Female	-0.014	(0.025)	Real estate	0.051	(0.074)
20-29	0.146	(0.051) ***	Accommodations & restaurants	-0.103	(0.072)
30-39	0.076	(0.030) ***	Health care & welfare	-0.224	(0.021) ***
50-59	0.039	(0.027)	Education	0.093	(0.048) **
60-69	0.045	(0.030)	Other services	-0.009	(0.034)
70-79	0.128	(0.068) **	Public services	0.065	(0.054)
Junior high school	-0.153	(0.081)	Other industries	0.116	(0.043) ***
Vocational school	0.028	(0.039)	Administrative & managerial	0.051	(0.038)
Junior (2-year) college	0.050	(0.040)	Professional & engineering	-0.004	(0.030)
4-year university	0.101	(0.026) ***	Sales	-0.143	(0.039) ***
Graduate school	0.246	(0.052) ***	Trade-related	0.125	(0.046) ***
Ln earnings	0.090	(0.017) ***	Service	-0.067	(0.035) *
Ln commuting hours	0.111	(0.012) ***	Production & other	-0.147	(0.024) ***
Non-standard employee	0.015	(0.029)	99 or smaller	-0.018	(0.029)
Agriculture	-0.065	(0.118)	300-499	-0.016	(0.043)
Construction	0.032	(0.044)	500-999	0.068	(0.043) *
Information & communications	0.298	(0.059) ***	1,000 or larger	0.095	(0.033) ***
Transport	-0.163	(0.035) ***	Government	-0.018	(0.052)
Wholesale & retail	-0.036	(0.038)	Observations	2,656	
Finance & insurance	0.061	(0.051)	Pseudo R ²	0.2599	

Notes: Probit estimations with robust standard errors are in parentheses. ***, **, and * denote significance at the 1%, 5%, and 10% levels, respectively. The categories used as references are male, age 40-49, senior high school, standard employee, manufacturing, clerical, and firm size of 100-299 employees.

Table 4. Distribution of the frequency of working from home

WFH frequency	%
0.1	13.8%
0.2	11.1%
0.3	8.7%
0.4	7.2%
0.5	14.3%
0.6	4.0%
0.7	4.8%
0.8	8.9%
0.9	6.8%
1.0	20.4%

Table 5. The mean frequency of working from home by individual characteristics

Categories		Frequency of WFH (mean)	Categories	Frequency of WFH (mean)
Total		0.557	Administrative & managerial	0.531
Gender	Male	0.536	Professional & engineering	0.583
	Female	0.613	Clerical	0.557
Age	20-29	0.586	Sales	0.647
	30-39	0.538	Trade	0.603
	40-49	0.571	Service	0.513
	50-59	0.533	Production & other	0.500
	60-69	0.581	1-99	0.541
	70-79	0.570	100-299	0.567
Education	Junior high school	0.450	300-499	0.546
	Senior high school	0.502	500-999	0.549
	Vocational school	0.565	1,000-	0.597
	Junior (2-year) college	0.593	Government	0.416
	4-year university	0.555	Less than 2 million yen	0.596
	Graduate school	0.596	2-2.99	0.529
Employment type	Standard	0.545	3-3.99	0.526
	Non-standard	0.596	4-4.99	0.554
Industry	Construction	0.488	5-5.99	0.596
	Manufacturing	0.587	6-6.99	0.548
	Information & communications	0.708	7-7.99	0.481
	Transport	0.282	8-8.99	0.564
	Wholesale & retail	0.587	9-9.99	0.464
	Finance & insurance	0.494	10 million yen or more	0.615
	Real estate	0.421	Tokyo	0.634
	Accommodations & restaurants	0.400	Aichi & Osaka	0.554
	Health care & welfare	0.429	Other	0.496
	Education	0.565	Less than 0.5 hour	0.423
Other industries	Other services	0.605	0.5-0.99	0.539
	Public services	0.368	1.0-1.49	0.549
	Other industries	0.608	1.5-1.99	0.564
		Commuting hours (round trip)	2.0-2.49	0.637
			2.5-2.99	0.565
		3 hours or longer	0.579	

Notes: Other industries include agriculture, fisheries, and forestry. Some of the categories above for firm size, earnings, residence, and commuting hours are integrated version of the original choices in the survey questions.

Table 6. Working from home productivity

	Mean	Std. Dev.	p25	p50	p75	N	Home<Office
All WFH employees	60.6	35.1	30	70	86.5	876	82.0%
Early WFH adopters	76.8	35.5	70	85	100	118	62.7%
New WFH adopters	58.1	34.4	30	60	80	758	85.0%
Telework in 2017	73.8	34.5	50	80	100	81	71.6%
No telework in 2017	59.3	34.9	30	65	85	795	83.0%

Note: The last column indicates the percentage of employees working from home whose productivity at home is less than 100.

Table 7. Working from home productivity by individual characteristics

Categories		Mean WFH productivity	Categories	Mean WFH productivity		
Total		60.6	Administrative & managerial	67.5		
Gender	Male	62.2	Professional & engineering	69.2		
	Female	56.5	Clerical	58.5		
Age	20-29	57.7	Occupation	Sales	40.1	
	30-39	60.1		Trade	57.8	
	40-49	59.6		Service	52.3	
	50-59	62.9		Production & other	49.1	
	60-69	60.3		1-99	57.9	
	70-79	61.0		100-299	64.3	
Education	Junior high school	45.0	Firm size	300-499	65.6	
	Senior high school	48.1		500-999	61.5	
	Vocational school	53.7		1,000-	64.5	
	Junior (2-year) college	61.1		Government	40.5	
	4-year university	61.7		Less than 2 million yen	57.2	
	Graduate school	72.0		2-2.99	44.2	
Employment type	Standard	61.2	Earnings	3-3.99	55.2	
	Non-standard	58.6		4-4.99	51.3	
Industry	Construction	62.2	Residence	5-5.99	58.5	
	Manufacturing	70.1		6-6.99	66.7	
	Information & communications	73.5		7-7.99	61.6	
	Transport	37.5		8-8.99	65.2	
	Wholesale & retail	57.0		9-9.99	62.7	
	Finance & insurance	52.4		10 million yen or more	73.7	
	Real estate	50.3		Tokyo	64.9	
	Accommodations & restaurants	55.0		Aichi & Osaka	62.1	
	Health care & welfare	40.0		Other	56.7	
	Education	54.4		Less than 0.5 hour	53.1	
	Other services	62.8		0.5-0.99	57.4	
	Public services	38.0		Commuting hours (round trip)	1.0-1.49	61.6
	Other industries	67.5			1.5-1.99	61.8
		2.0-2.49	60.9			
		2.5-2.99	61.8			
		3 hours or longer	69.9			

Notes: Other industries include agriculture, fisheries, and forestry. Some categories for firm size, earnings, residence, and commuting hours are integrated versions of the original choices in the survey questions.

Table 8. Working from home productivity: Estimation results

Variables	(1)		(2)		(3)	
	Coef.	Std. Err.	Coef.	Std. Err.	Coef.	Std. Err.
Female	-2.254	(3.461)	-2.566	(3.456)	-4.070	(3.386)
20-29	4.261	(4.889)	4.179	(5.055)	3.768	(4.827)
30-39	3.404	(3.366)	2.854	(3.382)	3.927	(3.323)
50-59	3.894	(3.266)	2.697	(3.289)	4.612	(3.234)
60-69	0.793	(4.293)	0.233	(4.228)	0.829	(4.239)
70-79	11.121	(9.803)	7.987	(9.700)	10.421	(9.454)
Junior high school	48.482	(11.019) ***	36.363	(12.045) ***	44.029	(11.535) ***
Vocational school	6.382	(5.467)	6.243	(5.383)	5.771	(5.265)
Junior (2-year) college	14.022	(5.665) **	14.383	(5.622) **	13.855	(5.551) **
4-year university	13.589	(3.729) ***	13.141	(3.695) ***	12.702	(3.626) ***
Graduate school	19.052	(4.627) ***	18.573	(4.644) ***	17.469	(4.554) ***
Ln earnings	5.485	(2.147) **	5.480	(2.135) **	5.262	(2.061) **
Ln commuting hours	3.002	(1.531) *	2.877	(1.514) *	1.954	(1.511)
Non-standard employee	8.489	(4.289) **	8.087	(4.287) *	7.610	(4.235) *
99 or smaller	-1.120	(3.927)	-1.029	(3.942)	-1.043	(3.811)
300-499	7.466	(5.759)	7.194	(5.795)	7.276	(5.775)
500-999	-2.693	(4.889)	-1.937	(4.921)	-2.411	(4.833)
1,000 or larger	-1.519	(3.833)	-1.467	(3.846)	-2.218	(3.733)
Government	-4.979	(6.779)	-4.992	(6.690)	-5.519	(6.719)
New WFH adopter			-13.660	(4.375) ***		
WFH frequency					0.173	(0.038) ***
Cons.	18.365	(14.942)	32.259	(15.518) **	11.533	(14.520)
Industry dummies	yes		yes		yes	
Occupation dummies	yes		yes		yes	
Observations	828		828		828	
Adjusted R ²	0.1447		0.1577		0.1661	

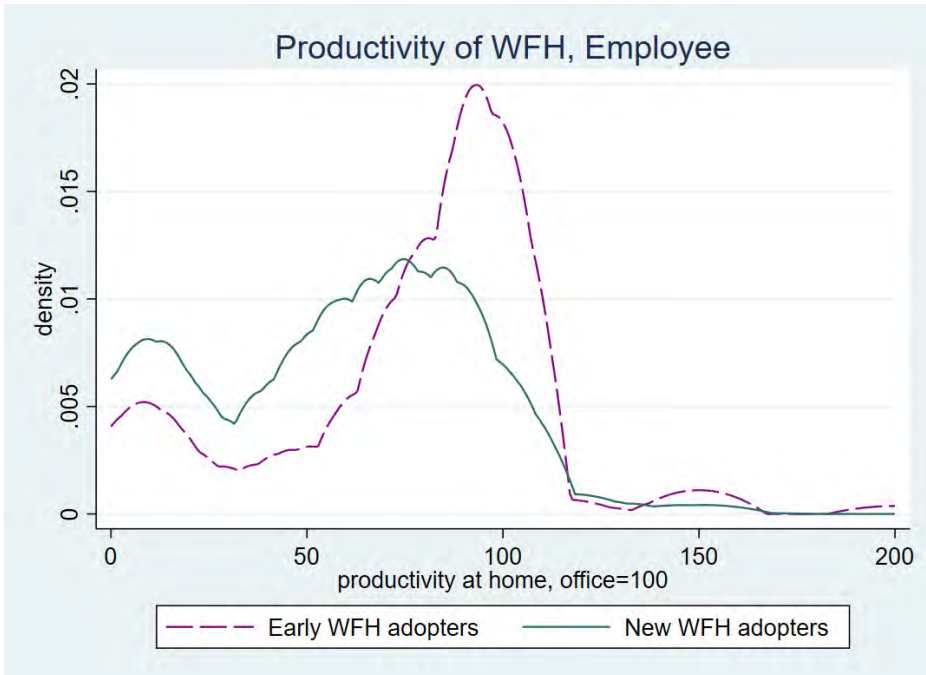
Notes: OLS estimations with robust standard errors are in parentheses. ***, **, and * denote significance at the 1%, 5%, and 10% levels, respectively. The categories used as references are male, age 40–49, senior high school, standard employee, manufacturing, clerical, and firm size of 100–299 employees.

Table 9. The factors affecting working from home productivity

Factors reducing productivity at home		
1	Poor telecommunication environment at home relative to the workplace	34.9%
2	The requirements by rules and regulations that some tasks must be conducted in the office	33.1%
3	Some tasks cannot be conducted at home even though these are not required by rules and regulations	32.5%
4	It is difficult to concentrate on job because of the presence of family members	19.9%
5	Lack of a private room specifically designed for work	15.1%
6	Loss of quick communication that is only possible through face-to-face interactions with their colleagues at the workplace	38.5%
7	Lack of pressure from the boss, colleagues, and subordinates	19.3%
8	Other reasons	10.2%

Notes: Multiple answers were allowed for this question.

Figure 1. Distribution of working from home productivity by the timing of the start of working from home



Note: The label “Early WFH adopters” refers to those who practiced WFH before the COVID-19 pandemic while “New WFH adopters” refers to those who started WFH after the start of the COVID-19 pandemic.

Appendix Table A1. Composition of Survey Respondents

	Respondents	2015 Census
Male	54.3%	49.4%
Female	45.7%	50.6%
20-29	3.8%	13.2%
30-39	12.8%	16.6%
40-49	20.0%	19.6%
50-59	20.2%	16.4%
60-69	29.5%	19.3%
70-79	13.7%	14.9%

Note: The percentages of the 2015 Population Census data were calculated for people aged 20 to 79 years.

The role of global connectedness and market power in crises: Firm-level evidence from the COVID-19 pandemic¹

Jay Hyun,² Daisoon Kim³ and Seung-Ryong Shin⁴

Date submitted: 10 September 2020; Date accepted: 13 September 2020

How do firms' global connectedness and market power affect their performance and resilience during crises? While global production and export networks expose firms to foreign shocks, they potentially make firms less susceptible to domestic shocks through diversification of suppliers and markets. Also, higher market power could provide buffers by allowing bigger margins of adjustments. Using weekly global stock market data, we show that firms with higher global connectedness (via supply chains and exports) and market power (measured by markups) are more resilient to domestic pandemic shocks. These findings contribute to a better understanding of firms' reaction and reallocation during crises.

1 The first three authors are listed alphabetically.

2 Assistant Professor, Department of Applied Economics, HEC Montreal.

3 Assistant Professor, Department of Economics, Poole College of Management, North Carolina State University.

4 Ph.D. Candidate, Department of Economics, University of Pennsylvania.

Copyright: Jay Hyun, Daisoon Kim and Seung-Ryong Shin

1 Introduction

The recent COVID-19 pandemic has influenced our society in various ways. In particular, changes in business environments induced by border closures, lock-down policies, social distancing and preference changes have generated spike in uncertainty, significant disruption in business, and reallocation across firms (see, e.g., [Baker et al. 2020](#), [Barrero et al. 2020](#), [Ding et al. 2020](#), and among many others).¹ During periods of such turmoil, firms with more resilient business models tend to survive and expand more than others, which leads to an important question of what characteristics of firms are vital in managing crises.

We attempt to answer the question with particular emphasis on two characteristics of firms — global connectedness and market power — which play central roles in economics and finance literature and have attracted a great deal of attention in the last decade.² The global economy has so far evolved toward integration through global value chains, trade and migration, and there is now a consensus in media and policy circles that global integration has exacerbated the negative impact of global crises in domestic economies both through the direct spread of the disease and disruption in foreign supply and demand.³ However, more globally connected firms through supply chains and exports could enjoy more diversified portfolio of suppliers and markets, which potentially allows them to buffer negative domestic shocks by making more flexible decision in production and market management.

Another firm characteristic, market power (which we measure through markup), also plays a similar role: firms with higher market power could make them more resilient

¹These papers have documented a pandemic-induced rise in cross-sectional variations in financial market performances across firms. Interestingly, [Giglio et al. \(2020\)](#)'s survey data analysis finds that investors are pessimistic about the short-run aggregate financial and real performance after the pandemic outbreaks, but their expectations about long-run aggregate economic and stock market outcomes are unchanged.

²See [di Giovanni and Levchenko \(2010\)](#); [Acemoglu et al. \(2012\)](#); [Edmond et al. \(2015\)](#); [Barrot and Sauvagnat \(2016\)](#); [Baqae and Farhi \(2019a,b\)](#); [Boehm et al. \(2019\)](#); [Huo et al. \(2019\)](#); [Bigio and La'O \(2020\)](#); [De Loecker et al. \(2020\)](#), and many others in economics, and [Ferreira and Matos \(2008\)](#); [Aguerrevere \(2009\)](#); [Gu \(2016\)](#); [Bustamante and Donangelo \(2017\)](#); [Gofman et al. \(2020\)](#); [Jiang and Richmond \(2019\)](#); [Kojien et al. \(2020\)](#), and many others in finance.

³For example, the United Nations Department of Economic and Social Affairs reported in April 2020 that "... The adverse effects of prolonged restrictions on economic activities in developed economies will soon spill over to developing countries via trade and investment channels. ... In addition, global manufacturing production could contract significantly, amid the possibility of extended disruptions to global supply chains. ..."(*World Economic Situation And Prospects: April 2020 Briefing, No. 136*).

to negative shocks by providing bigger margins of adjustments and flexibility.⁴ A large degree of markup of a firm implies that its products are not easily substituted to others, and that the firm can adjust its price without significant decline of its demand. Therefore, higher market power (or markups) of firms could make them more resilient during crises.⁵

Using panel data of around 8,000 listed firms in 71 countries, we investigate how pre-pandemic firm characteristics, including global connectedness and market power, affect firm performances in response to the COVID-19 pandemic shock. The fundamental challenge we confront is that firms' current and future real performance measures (e.g., sales and profits) are in most cases only available at low-frequency and are not provided to researchers in real-time. To overcome the challenge, we borrow investors' wisdom and use stock market performances, which allows us to avoid data problems as well as forecasting problems.⁶ A firm's market value equates to the present value of the expected future stream of profits (or dividends), which reflects firm's expected real performance. Thus, changes in stock market value (also called market capitalization) reflect investors' information about firms' current and future performances. The intuition behind our empirical approach is also tightly related to [Harvey \(1989\)](#)'s early works on forecasting aggregate economic growth from aggregate financial market data. Recently, [Gormsen and Kojien \(2020\)](#) use the stock market indexes and dividend future market data to forecast economic growth forecasting in reacting to the COVID-19 pandemic.

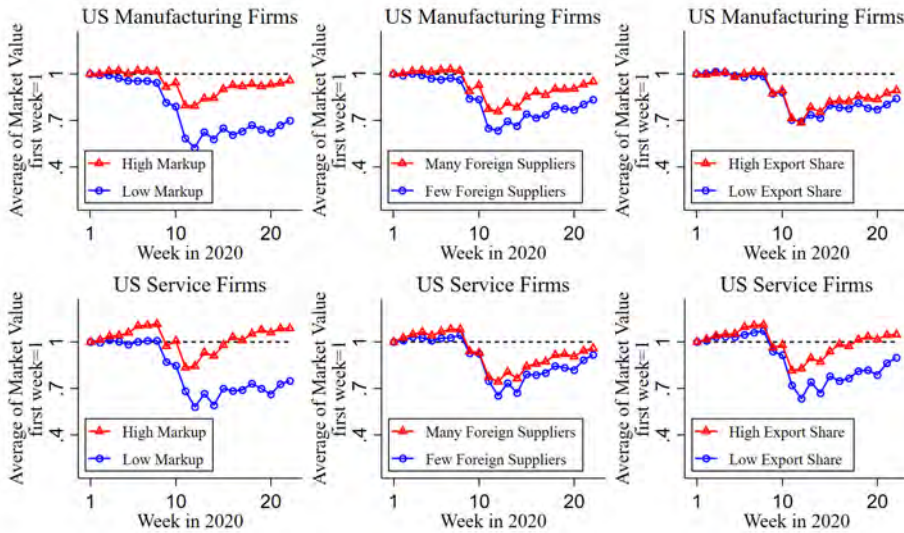
The important role played by global connectedness and market power during the pandemic can be visualized by plotting the evolution of firm market values as a function of their degree of global connectedness (measured by foreign supplier share and export share) and market power (measured by markups). In [Figure 1](#), we plot the evolution of the average market value of firms separately across those in the top and bottom

⁴Our measure of markup is constructed from the firm's cost minimization as in [Hall \(1988\)](#) and [De Loecker et al. \(2020\)](#). We also consider profitability as an alternative measure of market power.

⁵Macroeconomic research has long recognized the importance of markups as propagation mechanisms, e.g., [Hall \(1988\)](#), [Rotemberg and Woodford \(1995\)](#), [Bilbiie et al. \(2012\)](#), [De Loecker et al. \(2020\)](#), and many others. Additionally, [Baqae and Farhi \(2019a,b\)](#) indicate how a degree of markups play a role in macroeconomic through input-output linkages and aggregations. In finance, [Aguerrevere \(2009\)](#), [Gu \(2016\)](#), [Bustamante and Donangelo \(2017\)](#) and many others have investigated asset price implications of market competition, markups and market powers, in which they are different across markets (industries) but not across firms.

⁶See [Gordon \(1959\)](#), [Merton \(1973\)](#), [Lucas \(1978\)](#), [Campbell and Shiller \(1988\)](#) and many others for the discussion on formal link between firms' real activity and financial market performances.

Figure 1: Changes in Market Values of Different Groups of Firms



Notes. The figures plot the average market values of each group of firms over time, which are rebased to one for the first week. The manufacturing and service firms are classified by the Standard Industry Classification (SIC) codes 2000 – 3999 and 7000 – 8999, respectively. In each column, the red squared and blue circled lines are the average market values of top and bottom quantile firms of each measurement of markups, foreign supply, and export networks, respectively. Section 3 describes the details of measurements.

quantiles of markup, foreign supplier share, and export share distributions.⁷ Firms with higher markups and who are more globally integrated through supply chains and exports differentially performed better compared to those with lower markups and who are less globally integrated. This suggests that global production and export networks as well as markups potentially allow firms to be more resilient during the crisis periods.

To do a formal regression analysis, we start by constructing a detailed global firm dataset that combines weekly firm-level stock market information with various firm-level characteristics. Our dataset consists of weekly firm-level market values and stock returns during the first five months of 2020 (January 2nd – May 28th) obtained from Compustat Security Daily database.⁸ We supplement our weekly firm-level data

⁷In the figure, we only consider firms in the US manufacturing and service sectors and plot them separately across sectors to isolate country-specific and sector-traits. In the formal regression analyses, we consider more disaggregated sector definition and consider firms in all countries.

⁸We focus our analysis on the first five months of 2020 to avoid period of political uncertainty

with various pre-pandemic firm characteristics obtained from Compustat Fundamental and Factset Revere database from which we get balance sheet, supply chain, and export information. Our dependent variable is a weekly change in market values by each firm. Our final sample covers 7,879 publicly listed firms in 71 countries.

Our empirical analysis confirms that global connectedness and market power make firms more resilient to the domestic pandemic shock. We regress a firm's weekly market value growth on various explanatory variables including the domestic pandemic shock measured by weekly growth rate in domestic total confirmed cases and its interaction with various pre-pandemic firm characteristics as well as measures of foreign pandemic shocks. These pre-pandemic firm characteristics include measures of global connectedness through global supply chains and exports, markups as a measure of market power, employment, and various financial conditions such as cash, leverage, and RoA. To better isolate the effect of these firm characteristics on market value reactions to the pandemic, we also include firm, industry-time, and/or country-time fixed effects. These fixed effects allow us to control for any time-varying and time-invariant industry and/or country differences that might influence stock market reactions to the pandemic, as well as time-invariant firm characteristics.

We first show that a firm's weekly market value growth decreases if the firm faces increased growth in total confirmed cases in foreign economies (connected through global supply chain and export) as well as its domestic economy. We measure the domestic pandemic shock as weekly growth rate in domestic total confirmed cases, and foreign pandemic shocks through (i) supply chains and (ii) exports as the weighted average of weekly growth rate of foreign total confirmed cases weighted by (i) foreign supplier share in all suppliers and (ii) export share in total sales, respectively. Therefore, global connectedness increases the direct exposure to negative foreign shocks.

Firms' market values, however, decrease less in response to the domestic pandemic shock when they are more globally connected (through global supply chain and export) and have higher market power (measured by markups). Specifically, higher foreign supplier share, export share, and markup measure significantly alleviate the negative impact of the domestic increase in newly confirmed cases (i.e., increase in weekly growth rate of total confirmed cases). Additionally, we consider interaction of the domestic pandemic shock and other firm characteristics such as employment and various financial conditions (cash, leverage, and return on assets) to control the effect of these other

associated with the Black Lives Matter (BLM) movement started at the end of May.

factors on market value reaction to the pandemic. Consistent with [Ding et al. \(2020\)](#), we also find the role played by these pre-pandemic financial conditions, but the global connectedness and market power play independent role beyond the effect of financial conditions.⁹

Our result is in line with recent studies that highlight dual roles played by the global connectedness. [Bonadio et al. \(2020\)](#) show that supply chain renationalisation does not make countries more resilient to pandemic shocks because eliminating reliance on foreign inputs increases reliance on the domestic inputs, making the economy more susceptible to the domestic pandemic shock. While they use a quantitative model to explore the mechanism, our paper empirically investigates the interaction between various firm characteristics—including the global connectedness and market power—and its resilience to the domestic pandemic shock. [Ramelli and Wagner \(2020\)](#) show that the US firms that were more exposed to China initially performed worse during the pandemic while they relatively did better when the crisis spread to the Europe and the US. While they focus on firms in the US, our work complements their study by providing an empirical evidence using global firm data covering nearly 8,000 firms in 71 countries. Also, we explore the role of another important firm characteristic—market power measured by markups—that these papers did not focus on.

This paper is organized as follows. In Section 2, a parsimonious model illustrates the analytical mechanism behind the empirical specification and results. Section 3 describes the main components of the data and measurements. Section 4 presents an empirical specification. Section 5 reports and discusses our main findings. Section 6 checks the robustness of our main results. The last section concludes.

⁹In addition to [Ding et al. \(2020\)](#), [Giglio et al. \(2020\)](#), and [Gormsen and Koijen \(2020\)](#), there exists a growing literature studying the consequences of infectious diseases in asset prices and returns. [Alfaro et al. \(2020\)](#) examine the predictability of expected outbreak changes in aggregate stock returns using the SARS outbreak in Hong Kong and the COVID-19 outbreak in the US. [Caballero and Simsek \(2020\)](#) study the mechanism how asset price spirals and aggregate demand can amplify supply shocks when economic agents have heterogeneous risk tolerance. [Hassan et al. \(2020\)](#) construct text-based measures of the exposure of individual listed firms to epidemic diseases (COVID-19, SARS and H1N1) and discuss asset market implications.

2 A Simple Illustrative Model

This section presents a simplified analytical framework to illustrate firm-level propagation mechanisms derived from global networks and market power.

There are home and foreign countries. We denote home and foreign variables with superscripts H and F , respectively. Each firm produces a different variety. In each period t , a home firm can produce its good by using home and foreign factors, denoted by x_t^H and x_t^F , respectively.

$$y_t = z(Z_t^H x_t^H)^{1-\theta} (Z_t^F x_t^F / \tau)^\theta \tag{2.1}$$

where y_t is the quantity produced, and z is the Hicksian neutral firm-specific productivity level. The aggregate home and foreign productivities, Z_t^H and Z_t^F , are home- and foreign-factor augmenting. The cost share parameter $\theta \in [0, 1]$ represents how much firm production is connected globally. The foreign factor leads to iceberg cost as much as $\tau \geq 1$. For given factor price ($P_{H,t}^x$ and $P_{F,t}^x$) and exchange rate Q_t , cost minimization yields the marginal cost function by $mc_t = [(1 - \theta)^{1-\theta} \theta^\theta z]^{-1} (P_{x,t}^H / Z_t^H)^{1-\theta} (\tau Q_t P_{x,t}^F / Z_t^F)^\theta$.

The firm chooses its prices and quantities of supply in home and foreign markets to maximize its profit:

$$\begin{aligned} \max \quad & p_{y,t}^H y_t^H + Q_t P_{y,t}^F y_t^F - P_{x,t}^H x_t^H - Q_t P_{x,t}^F x_t^F \\ \text{subject to} \quad & y_t^H = (p_{y,t}^H)^{-\sigma} \phi^H D_t^H, \\ & y_t^F = (p_{y,t}^F)^{-\sigma} \phi^F D_t^F, \\ & y_t = y_t^H + \tau y_t^F, \end{aligned}$$

where the total costs, $P_{x,t}^H x_t^H + Q_t P_{x,t}^F x_t^F$, equal to $mc_t \times y_t$. The quantity of supply and price to market $m = H, F$ are denoted by y_t^m and $p_{y,t}^m$, respectively. The firm faces the aggregate demand D_t^m with the consumer's expenditure share $\phi^m \in [0, 1]$ in market $m = H, F$. The price elasticity is denoted by $\sigma > 1$. Then, the optimal prices in terms of destination currency are $p_{y,t}^H = \mu \times mc_t$ and $p_{y,t}^F = (\tau / Q_t) p_{y,t}^H$ in home and foreign markets, respectively, in which the markups in both markets are constant by $\mu = \sigma / (\sigma - 1)$. The profit is given by

$$\text{profit}_t = \left(1 - \frac{1}{\mu}\right) (\mu \times mc_t)^{-\frac{1}{\mu-1}} (ED_t^H + Q_t ED_t^F), \tag{2.2}$$

where $ED_t^H = \phi^H D_t^H$ and $ED_t^F = \phi^F (\tau/Q_t)^{1-\sigma} D_t^F$ are the effective demands in the home and foreign market, respectively, which determine the share of exports in total sales.

To illustrate heterogeneous responses to home and foreign shocks, we log-linearize the above equation (2.2) with percentage deviations from the initial state, denoted by hatted variables.¹⁰

$$\widehat{\text{profit}}_t \approx \frac{1}{\mu - 1} \left[(1 - \theta) \frac{\widehat{Z}_t^H}{\widehat{P}_{x,t}^H} + \theta \frac{\widehat{Z}_t^F}{\widehat{Q}_t \widehat{P}_{x,t}^F} \right] + (1 - \zeta) \widehat{D}_t^H + \zeta \left[\widehat{Q}_t \widehat{D}_t^F + \left(\frac{1}{\mu - 1} \right) \widehat{Q}_t \right], \quad (2.3)$$

where ζ is the export share in total sales at the initial state.¹¹

Differentiation of equation (2.3) with respect to shocks indicate how global networks and markups affect firm’s reaction to crises in home or foreign or both countries. In our model, changes in the aggregate home and foreign demands, denoted by \widehat{D}_t^H and $\widehat{Q}_t \widehat{D}_t^F$, represent home and foreign demand shocks, respectively. Also, we interpret home and foreign aggregate productivity relative to factor prices by supply shocks: $\widehat{Z}_t^H / \widehat{P}_{x,t}^H$ and $\widehat{Z}_t^F / (\widehat{Q}_t \widehat{P}_{x,t}^F)$, respectively.

$$\frac{\partial \widehat{\text{profit}}_t}{\partial \widehat{D}_t^H} = 1 - \zeta, \quad \frac{\partial \widehat{\text{profit}}_t}{\partial (\widehat{Q}_t \widehat{D}_t^F)} = \zeta, \quad \frac{\partial \widehat{\text{profit}}_t}{\partial \left(\frac{\widehat{Z}_t^H}{\widehat{P}_{x,t}^H} \right)} = \frac{1 - \theta}{\mu - 1}, \quad \text{and} \quad \frac{\partial \widehat{\text{profit}}_t}{\partial \left(\frac{\widehat{Z}_t^F}{\widehat{Q}_t \widehat{P}_{x,t}^F} \right)} = \frac{\theta}{\mu - 1}.$$

We put emphasis on two points regarding equation (2.3). First, higher global connectedness in both supply chains and exports, represented by θ and ζ respectively, propagates foreign shocks and alleviates domestic shocks. Higher θ and ζ mean the firm is vulnerable to negative foreign supply and demand shocks, $\widehat{Z}_t^F / (\widehat{Q}_t \widehat{P}_{x,t}^F)$ and $\widehat{Q}_t \widehat{D}_t^F$, but immune to negative domestic supply and demand shocks, $\widehat{Z}_t^H / \widehat{P}_{x,t}^H$ and \widehat{D}_t^H . While high dependence on foreign supply chains and exports could enhance negative foreign shocks during the crisis, it works as a diversified portfolio that buffers any domestic shocks. Second, market power provides more flexibility and margins of adjustments in response to supply shocks.

¹⁰Since $\text{profit}_t = (1 - \mu^{-1}) \times \text{sales}_t$, the percent changes in total sales and profits are identical.

¹¹The initial export share is given by $\zeta = Q_0 ED_0^F / [ED_0^H + Q_0 ED_0^F]$, where $ED_0^H = \phi^H D_0^H$ and $ED_0^F = \phi^F (\tau/Q_0)^{1-\sigma} D_0^F$.

Ultimately we want to investigate how global connectedness and market power of a firm makes it more or less resilient in the time of crisis, but due to shortage of real-time data on firm performances, specifically profits, we use the stock market value data instead. Although profit of a firm is not exactly equal to the current stock market value, our premise is that the expected current and future stream of profits determine the current stock price. The stock loses its value if people expect the long-lasting crisis to lower the current and future profits. We use this fact to make inference on the relationship between a firm's ex-ante factors, such as global networks and markups, and its performance during the crisis. This section has analytically shown that higher global network dependence could act both ways on the profit, that is, propagate foreign shocks while fending off domestic shocks, and that higher markups act positively on the profit by alleviating the supply-side shocks. This paper provides empirical evidence to whether these factors act so on the stock market value as well and draws implications for general performance.

3 Data and Measurements

Our dataset combines firm-level traits, stock market performance, and country-level COVID-19 cases from the FactSet Revere database, Compustat Global and North America: Fundamentals Annual and Security Daily, and Oxford COVID-19 Government Response Tracker. This allows us to construct a firm's weekly market value changes and its characteristics such as the size, markups, supply chain networks, and financial conditions. To measure COVID-19 shocks, we use the country's COVID-19 cases to measure a firm's domestic shocks and construct global COVID-19 shocks through supply chain networks as in [Ding et al. \(2020\)](#). Our weekly frequency sample period is from the first week to the twentieth week in 2020: the first week of January to the last week of May. A detailed discussion of each dataset and the merging procedure can be found in Online Appendix.

3.1 Measurements

Markups Our markup measure follows [Hall \(1988\)](#) and [De Loecker et al. \(2020\)](#), whose approaches use firm's cost minimization. A firm's markup equals the output

elasticity of variable inputs divided by the revenue share of variable costs,

$$\text{Markup}_i = \theta_i^V \times \frac{\text{SALE}_i}{\text{COGS}_i}, \quad (3.1)$$

where SALE_i and COGS_i are the firm i 's sales/turnover (net) and cost of goods sold in Compustat Global and North America: Fundamentals Annual in 2018, respectively. We use De Loecker et al. (2020)'s estimates of output elasticity: θ_i^V . To minimize the impact of outliers, we winsorize the measurement at the 1% and 99% levels.

Global production and export networks FactSet Revere database allows us to measure a firm's global supply chain networks.¹² We measure the production networks of firm i located in country c as follows.

$$\text{ForeignSupplierShare}_i = \sum_{c' \neq c} \frac{\#\text{ofSupplier}_{i,c}^*}{\#\text{ofSupplier}_i}, \quad (3.2)$$

where $\#\text{ofSupplier}_{i,c}^*$ indicates the number of pre-pandemic suppliers from foreign country c' , and $\#\text{ofSupplier}_i$ denotes the firm i 's pre-pandemic total number of suppliers. Also, the share of exports in total sales is

$$\text{ExportShare}_i = \sum_{c' \neq c} \frac{\text{Revenue}_{i,c'}^*}{\text{Revenue}_i}, \quad (3.3)$$

where $\text{Revenue}_{i,c}$ and $\text{Revenue}_{i,c'}^*$ indicate the firm's pre-pandemic revenue in home country c and foreign country c' , respectively. Thus, the pre-pandemic total revenue of firm i located in c is $\text{Revenue}_i = \text{Revenue}_{i,c} + \sum_{c' \neq c} \text{Revenue}_{i,c'}^*$.

Domestic COVID-19 exposure We collect the COVID-19 confirmed case data from the Oxford COVID-19 Government Response Tracker (OxCGRT). For each country, we calculate weekly growth rate of total confirmed cases:

$$\text{Covid}_{c,t} = \ln(1 + \text{ConfirmedCase}_{c,t}) - \ln(1 + \text{ConfirmedCase}_{c,t-1}), \quad (3.4)$$

¹²FactSet Revere database provides information on direct relationships (relationships disclosed by the reporting company) and reverse relationships (relationships not disclosed by the reporting company but by companies doing business with the reporting company).

where total (cumulative) confirmed cases $\text{ConfirmedCase}_{c,t}$ are closing values of each week. Also, we add one to avoid a zero confirmed case in log at the beginning of our sample period.

Global COVID-19 exposure In period t , we measure the global COVID-19 exposures through global production networks of a firm i located in country c as follows.

$$\text{ForeignCovid}_{i,t}^{\text{supplier}} = \sum_{c' \neq c} \frac{\# \text{ofSupplier}_{i,c'}^*}{\# \text{ofSupplier}_i} \times \text{Covid}_{c',t} \quad (3.5)$$

The foreign COVID-19 exposure via suppliers, $\text{ForeignCovid}_{i,t}^{\text{supplier}}$, is equal to the weighted average of foreign country's COVID-19 exposure where the weights are the firm's pre-pandemic number of foreign supplies from a country divided by the number of all suppliers, thus the sum of weights are not always one. Similarly, we construct the global COVID-19 exposures through exports of a firm i located in country c by

$$\text{ForeignCovid}_{i,t}^{\text{export}} = \sum_{c' \neq c} \frac{\text{Revenue}_{i,c'}^*}{\text{Revenue}_i} \times \text{Covid}_{c',t}, \quad (3.6)$$

where the weights are the pre-pandemic revenues in a foreign country over the total revenues in all countries.

Market value We compute a firm's market value (market capitalization) from Compustat Global and North America: Security Daily database. We include global firms that their stocks were actively trading from January to May in 2020. First, we calculate securities' total market value by multiplying the number of common / ordinary shares outstanding by the market price per share. Then, we compute a firm's total market value of all securities in currency of firm's location c and its growth rate (%) as follows.

$$\text{MarketValue}_{i,t} = \sum_{iid \in \text{IID}_i} \text{FX}_{iid,c,t} \times \text{PRCCD}_{iid,t} \times \text{CSHOC}_{iid,t} \quad (3.7)$$

$$\text{MarketValueGrowth}_{i,t} = 100 \times [\ln(\text{MarketValue}_{i,t}) - \ln(\text{MarketValue}_{i,t-1})], \quad (3.8)$$

where iid indexes the equity security, and IID_i is the set of all iid issued by firm i .¹³ $CSHOC_{iid,t}$ and $PRCCD_{iid,t}$ are the number of shares outstanding and the closing price of one share on the last day of each week, respectively. Our database contains a firm's multiple issues with different currencies. We convert prices of securities to the local currency of firm's headquarter: $c = LOC_i$.¹⁴ The exchange rate between firm location's and equity security's currencies, $FX_{iid,c,t}$, is from S&P Global Market Intelligence database. Alternatively, we report the result by converting local currencies into the US dollar in Section 6. Finally, to minimize the impact of outliers, we winsorize weekly market value growth at the 1% and 99% levels.

Financial conditions We collect a firm's financial characteristics from Compustat Global and North America: Fundamentals Annual in 2018. we consider four basic financial characteristics: The cash and short-term investments divided by total assets measures a firm's cash holdings: $Cash_i = CHE_i/AT_i$. Leverage is the debt-to-asset ratio: $Leverage_i = (DLC_i + DLTT_i)/AT_i$ where DLC_i and $DLTT_i$ are the total debts in current liabilities and long term debts, respectively. The return of asset is computed by dividing a firm's net income by total assets: $RoA_i = IB_i/AT_i$ where IB_i is the income before extraordinary items.

3.2 Summary Statistics

Our final sample consists of 165,459 firm-week-level observations covering the first five months of 2020.¹⁵ It includes 7,879 publicly listed firms in 71 countries.¹⁶

During our sample period, an average firm experienced weekly market value growth of -0.935 percent, reflecting the negative impact of the pandemic crisis. Stock return

¹³In the case of cross-listing, the securities have the identical shares outstanding and identifier number (CUSIP / ISIN). In that case, we treat them by the one security iid and use the average of their prices for the market price for iid : $PRCCD_{iid,t}$. Alternatively, we can use the primary listing's price, which gives almost identical to the average price.

¹⁴Alternatively, we instead convert local currencies into the US dollar unit when calculating weekly market value growth rate. This would overstates impacts of local currency appreciation and depreciation on the growth rate of market value. That exchange rate channel will be controlled by country-time fixed effects in our regression. Thus, our results are robust on our choice of basis currency.

¹⁵Our firm-week-level market values and stock returns span from January 2nd to May 28th. Thus, the initial period (1st week) of our weekly firm-level *change* in market values and stock returns indicate the period between January 2nd and January 9th.

¹⁶We exclude utilities firms (SIC 4900 – 4999) and financial firms (SIC 6900 – 6999). We only include countries that have at least 10 firms. Our results are not sensitive to these procedure.

Table 1: Summary Statistics

Firm-Week-level						
Variable	Obs.	Mean	Std. Dev.	P10	P50	P90
MarketValueGrowth (%)	165459	-0.935	9.494	-11.384	-0.217	8.926
StockReturn (%)	165459	-0.926	9.433	-11.297	-0.201	8.883
Covid	165459	0.507	0.653	0.000	0.216	1.494
ForeignCovid ^{supplier}	165459	0.296	0.453	0.000	0.087	0.938
ForeignCovid ^{export}	165459	0.182	0.333	0.000	0.036	0.582
ForeignSupplierShare	165459	0.540	0.387	0.000	0.571	1.000
ExportShare	165459	0.361	0.362	0.000	0.236	0.960
Markup	165459	1.756	1.746	0.940	1.258	2.788
Employment (thousands)	165459	14.465	48.000	0.266	2.976	30.264
Cash	165459	0.159	0.150	0.021	0.114	0.362
Leverage	165459	0.231	0.311	0.000	0.193	0.476
RoA	165459	0.027	0.147	-0.040	0.036	0.117
Firm-level						
Variable	Obs.	Mean	Std. Dev.	P10	P50	P90
ForeignSupplierShare	7879	0.540	0.387	0.000	0.571	1.000
ExportShare	7879	0.361	0.362	0.000	0.236	0.960
Markup	7879	1.756	1.746	0.940	1.258	2.788
Employment (thousands)	7879	14.465	48.003	0.266	2.976	30.264
Cash	7879	0.159	0.150	0.021	0.114	0.362
Leverage	7879	0.231	0.311	0.000	0.193	0.476
RoA	7879	0.027	0.147	-0.040	0.036	0.117
Country-Week-level						
Variable	Obs.	Mean	Std. Dev.	P10	P50	P90
Covid	1491	0.444	0.674	0.000	0.122	1.387

Notes. This table presents the summary statistics of the key variables used in our analyses. The sample includes publicly listed global firms covered in Compustat database (Security Daily and Fundamentals, both North America and Global) and Factset Revere database.

shows similar pattern with average weekly stock return growth of -0.926 percent. During this period, there was a massive increase of COVID-19 confirmed cases. At the firm-week-level, total confirmed cases increased by 50.7 percent on average per week, and the 90 percentile of the distribution experienced 149.4 percent increase per week. Firms are also exposed to foreign COVID-19 cases through global supply chain and export, with average weekly increase of foreign COVID-19 cases given by 29.6 percent (through foreign suppliers) and 18.2 percent (through export).

At the firm-level, we observe that publicly listed firms in our sample are highly integrated to the global economy: on average, 54.0 percent of suppliers located in foreign countries and 36.1 percent of revenues are generated by export. The distribution of markup is quite skewed, with median gross markup 1.258 and mean gross markup 1.756. Finally, consistent with the previous literature, firm size measured by employment is also highly skewed, with mean employment (14,465) significantly exceeding median employment (2,976).

4 Empirical Strategy

Which firms will expand or shrink during the COVID-19 pandemic crisis? Since an individual firm's fundamental performance such as profits and sales is hard to observe in the short run, we use the firm's stock market performance that reflects investors' belief and expectation based on the latest information. In the Gordon growth model and Lucas' asset pricing model, the stock price per share equals the present value of the expected future stream of dividends or profits per share. Thus, we can use changes in a firm's market value, also called market capitalization, to measure its expected fundamental performance growth.

Our main goal is to investigate how a response of firms' market value growth to the pandemic depends on their traits. To achieve this goal, we interact $\text{Covid}_{c,t}$ with firms' pre-2020 characteristics. We estimate the following panel regression equation:

$$\begin{aligned} \text{MarketValueGrowth}_{i,t} &= \alpha \times \text{Covid}_{c,t} + \beta \times \text{ForeignCovid}_{i,t}^{\text{supplier}} + \gamma \times \text{ForeignCovid}_{i,t}^{\text{export}} \\ &\quad + \mathbf{x}'_i \Psi \times \text{Covid}_{c,t} + \boldsymbol{\delta}_{i,t} + \varepsilon_{i,t} \end{aligned} \quad (4.1)$$

where $\text{MarketValueGrowth}_{i,t} \equiv 100 \times [\ln(\text{MarketValue}_{i,t}) - \ln(\text{MarketValue}_{i,t-1})]$ indi-

cates a firm's weekly growth rate of market values, and i , c , t denote firm, country, and time indexes, respectively. The impact of the domestic COVID-19 is a function of firms' traits. The firm's trait vector is denoted by \mathbf{x}_i and includes markup, measures of corporate connection to foreign economies through global supply chain and export (i.e., foreign supplier share and export share), employment, and various financial conditions such as cash, leverage, and return on assets (RoA). Thus, our coefficients of main interest are in the vector Ψ , especially, the coefficients related to markups and global supply chain.

Our regression also includes various fixed effects denoted by $\delta_{i,t}$. This includes firm, industry-time, and/or country-time fixed effects.¹⁷ These fixed effects allow us to control (i) any time-invariant firm characteristics that generate firm-specific trend in market values, (ii) any time-varying and time-invariant industry differences that might affect stock market reactions to the pandemic (e.g., differential intensity of in-person contact with others during work hours, and differential drop in demand across industries), and (iii) time-varying and time-invariant country characteristics that influence stock market performances (e.g., differences in legal and political systems, policy response to the shock, demographic and geographic characteristics).

5 Main Results

In this section we present our main empirical result. We show that firms' global connectedness and market power make firms more resilient to the negative impact of COVID-19 outbreaks.

Table 2 shows the main estimated results of the regression equation (4.1). In all specifications, we include firm fixed effects and sector-by-time fixed effects. In Columns (1) and (2), we regress weekly growth rate of market value on various measures of pandemic shocks. As can be seen from Column (1), a firm's weekly market value growth decreases if the firm faces increased growth in total confirmed cases in domestic economy: a 100 percentage point increase of weekly growth in total confirmed cases (Covid) results in -1.566 percentage point decrease of weekly market value growth. Column (2) further shows that a firm's weekly market value growth also decreases if foreign countries connected through global supply chain and export face larger increase

¹⁷In regression with country-time fixed effects, we do not include $\text{Covid}_{c,t}$ to avoid perfect collinearity.

Table 2: Firm characteristics and response of market values to the pandemic shock

	(1)	(2)	(3)	(4)	(5)
	MarketValueGrowth (%)				
Covid	-1.566*** (0.037)	-1.490*** (0.038)	-2.063*** (0.131)	-2.028*** (0.090)	
ForeignCovid ^{supplier}		-0.066 (0.075)	-0.233*** (0.076)	-0.230*** (0.076)	-0.235*** (0.074)
ForeignCovid ^{export}		-0.778*** (0.101)	-1.006*** (0.111)	-1.031*** (0.111)	-0.776*** (0.120)
Covid×ForeignSupplierShare			0.560*** (0.094)	0.530*** (0.093)	0.305*** (0.094)
Covid×ExportShare			0.215** (0.108)	0.324*** (0.109)	0.392*** (0.116)
Covid×ln(Markup)			0.233*** (0.066)	0.168** (0.066)	0.233*** (0.065)
Covid×ln(Employment)				-0.041** (0.019)	-0.068*** (0.019)
Covid×Cash				0.824*** (0.237)	0.537** (0.241)
Covid×Leverage				-0.107 (0.146)	-0.074 (0.141)
Covid×RoA				0.778*** (0.286)	1.023*** (0.283)
Firm FE	✓	✓	✓	✓	✓
Sector x Time FE	✓	✓	✓	✓	✓
Country x Time FE	-	-	-	-	✓
R ²	0.375	0.375	0.375	0.375	0.473
Observations	165459	165459	165459	165459	165459

Notes. This table shows how global connectedness and market power of firms affect their market values in response to the COVID-19 pandemic during January 2nd to May 28th in 2020. The estimation is based on regression equation (4.1). MarketValueGrowth (%) measures weekly growth rate of market value (in percent) of each firm, Covid is the domestic pandemic shock measured by weekly growth rate of total confirmed cases in domestic country, ForeignCovid^{supplier} and ForeignCovid^{export} measure the foreign pandemic shocks exposed through foreign suppliers and export, respectively, ForeignSupplierShare and ExportShare measure the share of foreign suppliers among total number of suppliers and the share of revenue generated from foreign countries among total revenue, respectively, Markup is measured by equation (3.1). More details on these variables (including Employment and financial variables) can be found in Section 3.1. Sectors are defined at the SIC 2-digit, time fixed effects are at month-by-week-level, and countries are mapped to firms based on headquarter locations. Standard errors (in parentheses) are clustered at the firm-level. *, **, and *** denote significance at the 10%, 5%, and 1% level, respectively.

of total confirmed cases. The effect through export is strong, although the effect through global supply chain is weak and statistically insignificant possibly because of uncontrolled confounding factors that can bias the estimate.

In Column (3), we investigate whether global connectedness and market power make firms more resilient to the pandemic shock. First, we confirm that both domestic and foreign pandemic shocks negatively affect weekly market value growth. But at the same time, we find significant heterogeneous response to the domestic pandemic shock depending on firms' global connectedness and market power: all the coefficients in front of the interaction terms interacting Covid with foreign supplier share, export share, and markup are positive and statistically significant. This implies that firms with larger foreign supplier share, export share, and markup experience *smaller* decrease of weekly market value growth in reacting to the domestic pandemic shock, Covid. This result is consistent with the view that global connectedness and market power make firms more resilient to domestic crises by diversifying the markets and suppliers and by providing more flexibility and margins of adjustments in response to negative shocks.

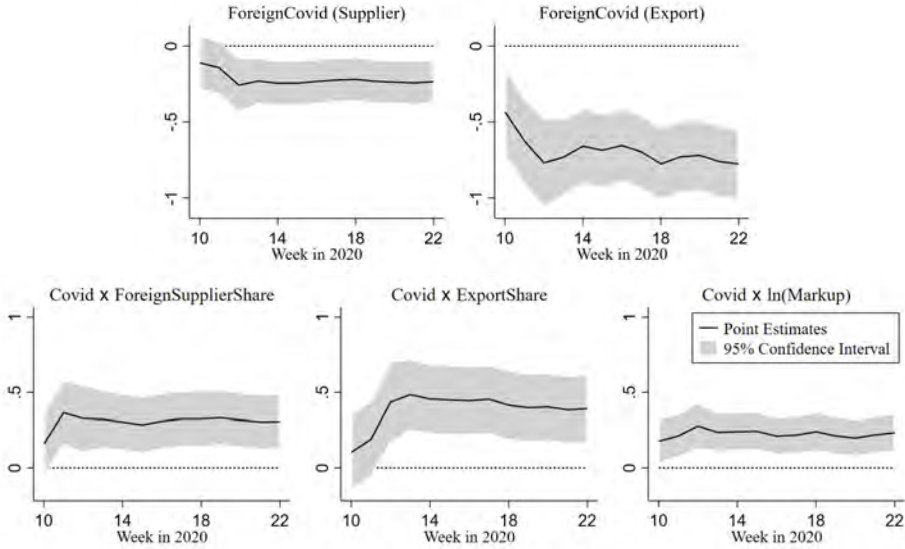
In Columns (4) and (5), we confirm that our results are robust to controlling for additional interaction terms and fixed effects. Column (4) shows that our results are robust to additionally controlling for interactions between Covid and firm size, Cash, Leverage, and RoA.¹⁸ Therefore, our results emphasizing the importance of global connectedness and market power holds even after controlling for the effect of firm size and various financial conditions on market value reaction to the shock. In Column (5), we add country-by-time fixed effects, which absorb any time-varying and time-invariant country characteristics that affect stock market performances. Again, our main results remain robust to adding these fixed effects.

6 Robustness Exercises

In this section, We perform further robustness checks. First, we check sensitivity of our results related to the end of sample period. Second, we show that our results are robust to the alternative measure of market power measured by profitability. Third, our results are robust to various sub-samples such as excluding (i) extremely large or small size of firms and (ii) firms without global connection through supply chains or

¹⁸Our estimation result on the additional interaction terms interacting Covid and various financial conditions are qualitatively consistent with those in [Ding et al. \(2020\)](#).

Figure 2: Visualization of Estimated Coefficients by Changing End-Period



Notes. The figures plot the estimated coefficients and their 95% confidence interval with clustered standard errors at the firm-level, in which the regression includes firm, sector-time, and country-time fixed effects corresponding to Column (5) in Table 2.

exports. Finally, we obtain similar results by using firms’ weekly stock return in place of weekly market value growth.

Terminal point In Figure 2, we investigate whether our results are robust to the choice of terminal points. Specifically, we plot the estimated coefficients and their 95% confidence intervals of our main coefficients of interest by moving the terminal period from the 10th week (March 5th) of 2020 to the 22th week (May 28th).¹⁹ In the exercise, we use Column (5) specification in Table 2. As is clear from the figure, the coefficients of interest remain stable across the terminal periods, implying that our main findings are robust to the choice of the terminal periods and well describe heterogeneous firm

¹⁹Before the 9th week, the COVID-19 outbreaks were limited to specific regions. On 29 February 2020, 99% and 94% of the global total confirmed and daily new COVID-19 cases were in China, Korea, Italy, Japan and Iran. However, the WHO on March 11 officially declared COVID-19 a pandemic when the total confirmed cases were 118,319 (4,620 new) in 114 countries. As Giglio et al. (2020) document, the stock market drastically collapsed on March.

responses during the pandemic.

Alternative measure of market power In the second exercise, we consider a measure of profitability based on what firms generate as a return to their shareholders instead of the markup measure in equation (3.1). That measure is a firm's profitability widely used as a proxy of a degree of markup (see De Loecker et al., 2020, for the details of discussion). The pre-pandemic dividends (share of sales) are collected from Compustat Global and North America: Fundamentals Annual database in 2018: $DVC_i/SALE_i$. As can be seen from Column (1) in Table 3, we confirm that firms with higher profitability are more resilient to the pandemic shock.

Considering sub-samples As a robustness, we also consider the following two sub-samples. First, we drop firms who have employment outside 10 and 90 percentiles of firm size distribution to exclude extreme size of firms (Column (2) in Table 3). Second, we exclude local firms who have zero export revenue and no foreign suppliers (Column (3) in Table 3). In both cases, we get robust results, where higher global connectedness and bigger markup are associated with alleviated negative impact of the domestic pandemic shock.

Stock return Instead of using firms' weekly market value growth, we also consider weekly stock returns. We compute each firm's weekly stock return from Compustat Global and North America: Security Daily database.²⁰ The results are presented in Column (4) in Table 3. Firms' stock returns decrease in response to both domestic and foreign pandemic shocks, but at the same time, those who are more globally connected through supply chains and exports and those who have higher market power are more resilient to the domestic pandemic shock.

²⁰To be more specific, we first calculate securities' dividend adjusted market price per share ($PriceAdjusted_{i,t}$) using the stock price ($PRCCD_{iid,t}$), total return factor ($TRFD_{iid,t}$), and adjustment factor ($AJEXDI_{iid,t}$). Then, we compute a firm's weighted average dividend adjusted market price of all securities in currency of firm's location c with outstanding ($CSHOC_{iid,t}$) weights. Lastly, we calculate the stock return (%) by $StockReturn_{i,t} = 100 \times [\ln(PriceAdjusted_{i,t}) - \ln(PriceAdjusted_{i,t-1})]$.

Table 3: Robustness Exercise

	(1)	(2)	(3)	(4)
	MarketValueGrowth (%)			StockReturn (%)
ForeignCovid ^{supplier}	-0.150*	-0.199**	-0.063	-0.224***
	(0.088)	(0.078)	(0.089)	(0.073)
ForeignCovid ^{export}	-0.895***	-0.845***	-0.790***	-0.847***
	(0.142)	(0.134)	(0.141)	(0.117)
Covid×ForeignSupplierShare	0.249**	0.234**	0.358**	0.301***
	(0.109)	(0.099)	(0.179)	(0.093)
Covid×ExportShare	0.524***	0.431***	0.424***	0.417***
	(0.140)	(0.128)	(0.151)	(0.114)
Covid×ln(Markup)		0.291***	0.261***	0.251***
		(0.079)	(0.083)	(0.065)
Covid×ln(Profitability)	0.154***			
	(0.037)			
Covid×ln(Employment)	-0.029	-0.110***	-0.024	-0.062***
	(0.022)	(0.030)	(0.023)	(0.019)
Covid×Cash	0.378	0.799***	0.505	0.436*
	(0.311)	(0.281)	(0.323)	(0.238)
Covid×Leverage	-0.837***	-0.161	-0.542**	-0.102
	(0.296)	(0.187)	(0.250)	(0.145)
Covid×RoA	0.652	1.271***	1.020**	0.833***
	(0.399)	(0.440)	(0.396)	(0.303)
Specification	Profitability	Drop Extreme	Drop Local	Stock Return
Firm FE	✓	✓	✓	✓
Sector x Time FE	✓	✓	✓	✓
Country x Time FE	✓	✓	✓	✓
R ²	0.539	0.481	0.496	0.477
Observations	108024	132783	103299	165459

Notes. This table repeats Column (5) in Table 2 using alternative specifications to check the robustness of our main result. In Column (1), we use profitability as a measure of market power. In Columns (2) and (3), we consider sub-samples by dropping (i) extreme size of firms—Column (2), and (ii) local firms without global connection—Column (3). In Column (4), we use weekly stock return as dependent variable.

7 Concluding Remarks

Which firms do expand and shrink under the recent pandemic-induced changes in business environments? Recent empirical studies have documented a significant redistribution across firms in stock markets during the COVID-19 pandemic. According to the conventional macro and finance theories, these stock market movements illuminate future as well as current performances of firms in goods markets. Armed with the link between financial and real market outcomes, we investigate the role of firms characteristics in the movements of firms' market value reacting to the COVID-19 outbreaks to illustrate details about firms' rise and fall as a consequence of the pandemic. These are where we attempt to contribute to a growing literature concerning about the consequences of the pandemic in economics and finance.

Our analysis highlights the roles of markups, exports and supply chain networks, which are the core concepts in recent studies in macroeconomics, international economics, industrial organization and finance, in responses to the pandemic-induced structural shocks and uncertainties. The global stock market data show that investors expect that (i) high markup firms respond well to the pandemic-induced domestic shocks, and (ii) global production and export networks improve the firm's performance in reacting to its domestic pandemic shock, although they propagate foreign pandemic shocks, which cause negative impacts on the market value.

Our findings reveal the details of reallocation across firms in the pandemic. The result has important implications for the question of "which traits allow firms to be more resilient than their competitors in responses to crises", highlighting the role of markups and global networks. That gives guidance for policymakers, investors, businesses, and workers to make optimal decisions facing large short- and long-run changes and uncertainties during transition periods of crises.

This paper may shed some light on the post COVID-19 pandemic world. A firm's market value is the present value of the expected future stream of profits. Thus, our findings illuminate stock market investors' information about the post pandemic world. As a result of the pandemic, the cross-sectional distribution would be tilted toward high markup and more globally connected firms.

References

- Acemoglu, Daron, Vasco M. Carvalho, Asuman Ozdaglar, and Alireza Tahbaz-Salehi**, “The Network Origins of Aggregate Fluctuations,” *Econometrica*, 2012, 80 (5), 1977–2016.
- Aguerrevere, Felipe L.**, “Real Options, Product Market Competition, and Asset Returns,” *The Journal of Finance*, 2009, 64 (2), 957–983.
- Alfaro, Laura, Anusha Chari, Andrew N Greenland, and Peter K Schott**, “Aggregate and Firm-Level Stock Returns During Pandemics, in Real Time,” *Covid Economics*, April 2020, 4, 2 – 24.
- Bailey, Michael, Abhinav Gupta, Sebastian Hillenbrand, Theresa Kuchler, Robert J Richmond, and Johannes Stroebel**, “International Trade and Social Connectedness,” Working Paper 26960, National Bureau of Economic Research April 2020.
- Baker, Scott R, Nicholas Bloom, Steven J Davis, and Stephen J Terry**, “COVID-Induced Economic Uncertainty,” Working Paper 26983, National Bureau of Economic Research April 2020.
- Baqae, David Rezza and Emmanuel Farhi**, “The Macroeconomic Impact of Microeconomic Shocks: Beyond Hulten’s Theorem,” *Econometrica*, 2019, 87 (4), 1155–1203.
- and – , “Productivity and Misallocation in General Equilibrium,” *The Quarterly Journal of Economics*, 09 2019, 135 (1), 105–163.
- Barrero, Jose Maria, Nicholas Bloom, and Steven J Davis**, “COVID-19 Is Also a Reallocation Shock,” Working Paper 27137, National Bureau of Economic Research May 2020.
- Barrot, Jean-Noel and Julien Sauvagnat**, “Input Specificity and the Propagation of Idiosyncratic Shocks in Production Networks,” *Quarterly Journal of Economics*, 2016, 131 (3), 1543–1592.
- Bigio, Saki and Jennifer La’O**, “Distortions in Production Networks,” *Quarterly Journal of Economics*, 2020, *Forthcoming*.
- Bilbiie, Florin O., Fabio Ghironi, and Marc J. Melitz**, “Endogenous Entry, Product Variety, and Business Cycles,” *Journal of Political Economy*, 2012, 120 (2), 304–345.
- Boehm, Christoph E., Aaron Flaaen, and Nitya Pandalai-Nayar**, “Input linkages and the transmission of shocks: firm-level evidence from the 2011 Tōhoku earthquake,” *Review of Economics and Statistics*, 2019, 101 (1), 60–75.

- Bonadio, Barthelemy, Zhen Huo, Andrei A Levchenko, and Nitya Pandalai-Nayar**, “Global Supply Chains in the Pandemic,” Working Paper 27224, National Bureau of Economic Research May 2020.
- Bustamante, M. Cecilia and Andres Donangelo**, “Product Market Competition and Industry Returns,” *The Review of Financial Studies*, 04 2017, 30 (12), 4216–4266.
- Caballero, Ricardo J and Alp Simsek**, “A Model of Asset Price Spirals and Aggregate Demand Amplification of a Covid-19 Shock,” Working Paper 27044, National Bureau of Economic Research April 2020.
- Campbell, John Y. and Robert J. Shiller**, “The Dividend-Price Ratio and Expectations of Future Dividends and Discount Factors,” *The Review of Financial Studies*, 1988, 1 (3), 195–228.
- di Giovanni, Julian and Andrei A. Levchenko**, “Putting the Parts Together: Trade, Vertical Linkages, and Business Cycle Comovement,” *American Economic Journal: Macroeconomics*, 2010, 2 (2), 95–124.
- Ding, Wenzhi, Ross Levine, Chen Lin, and Wensi Xie**, “Corporate Immunity to the COVID-19 Pandemic,” Working Paper 27055, National Bureau of Economic Research April 2020.
- Edmond, Chris, Virgiliu Midrigan, and Daniel Yi Xu**, “Competition, Markups, and the Gains from International Trade,” *American Economic Review*, October 2015, 105 (10), 3183–3221.
- Ferreira, Miguel A. and Pedro Matos**, “The colors of investors’ money: The role of institutional investors around the world,” *Journal of Financial Economics*, 2008, 88 (3), 499 – 533. Darden - JFE Conference Volume: Capital Raising in Emerging Economies.
- Giglio, Stefano, Matteo Maggiori, Johannes Stroebel, and Stephen Utkus**, “Inside the Mind of a Stock Market Crash,” Working Paper 27272, National Bureau of Economic Research May 2020.
- Gofman, Michael, Gill Segal, and Youchang Wu**, “Production Networks and Stock Returns: The Role of Vertical Creative Destruction,” *The Review of Financial Studies*, 03 2020. hhaa034.
- Gordon, M. J.**, “Dividends, Earnings, and Stock Prices,” *The Review of Economics and Statistics*, 1959, 41 (2), 99–105.
- Gormsen, Niels Joachim and Ralph S. J. Koijen**, “Coronavirus: Impact on Stock Prices and Growth Expectations,” Working Paper 2020-22, University of Chicago May 2020.
- Gu, Lifeng**, “Product market competition, R&D investment, and stock returns,”

Journal of Financial Economics, 2016, 119 (2), 441 – 455.

Hall, Robert E., “The Relation between Price and Marginal Cost in U.S. Industry,” *Journal of Political Economy*, 1988, 96 (5), 921–947.

Harvey, Campbell R., “Forecasts of Economic Growth from the Bond and Stock Markets,” *Financial Analysts Journal*, 1989, 45 (5), 38–45.

Hassan, Tarek Alexander, Stephan Hollander, Laurence van Lent, and Ahmed Tahoun, “Firm-level Exposure to Epidemic Diseases: Covid-19, SARS, and H1N1,” Working Paper 26971, National Bureau of Economic Research April 2020.

Huo, Zhen, Andrei A Levchenko, and Nitya Pandalai-Nayar, “International Comovement in the Global Production Network,” Working Paper 25978, National Bureau of Economic Research June 2019.

Jiang, Zhengyang and Robert Richmond, “Origins of International Factor Structures,” manuscript, NYU Stern School of Business June 2019.

Koijen, Ralph S. J., Robert Richmond, and Motohiro Yogo, “Which Investors Matter for Equity Valuations and Expected Returns?,” Working Paper 2019-92, University of Chicago June 2020.

Loecker, Jan De, Jan Eeckhout, and Gabriel Unger, “The Rise of Market Power and the Macroeconomic Implications*,” *The Quarterly Journal of Economics*, 01 2020, 135 (2), 561–644.

Lucas, Robert E., “Asset Prices in an Exchange Economy,” *Econometrica*, 1978, 46 (6), 1429–1445.

Ludvigson, Sydney C, Sai Ma, and Serena Ng, “Covid19 and the Macroeconomic Effects of Costly Disasters,” Working Paper 26987, National Bureau of Economic Research April 2020.

Merton, Robert C., “An Intertemporal Capital Asset Pricing Model,” *Econometrica*, 1973, 41 (5), 867–887.

Ramelli, Stefano and Alexander F. Wagner, “Feverish Stock Price Reactions to COVID-19,” *Review of Corporate Finance Studies*, 2020, *Forthcoming*.

Rotemberg, Julio J. and Michael Woodford, “Chapter 9 Dynamic General Equilibrium Models with Imperfectly Competitive Product Markets,” in Thomas F. Cooley, ed., *Frontiers of Business Cycle Research*, Princeton, NJ: Princeton University Press, 1995, pp. 243 – 293.

Unmasking mutual fund derivative use during the COVID-19 crisis

Ron Kaniel¹ and Pingle Wang²

Date submitted: 14 September 2020; Date accepted: 15 September 2020

Utilizing newly available data from the SEC on derivative performance and detailed derivative holdings, this paper studies how derivatives impact mutual fund performance, with an emphasis on the COVID-19 pandemic period. In contrast to previous research concluding derivatives are used for hedging, we find that most active equity funds use derivatives to amplify market exposure. Despite the seemingly small weight, derivatives have a significant impact on funds' leverage and contribute largely to fund returns. In response to the initial outbreak of COVID-19, funds trade more heavily on short derivative positions. This behavior is more prevalent among managers residing in states with early state-level Stay-at-home orders, where the risk of recession is likely more salient. Funds that used derivatives for hedging purposes before the crisis significantly outperform nonusers by over 9% during the initial outbreak, as their distribution of derivative returns shifts to the right. By the end of June, they still outperform by 1.6%. On the contrary, funds that used derivatives to amplify market exposure underperform, and their distribution of derivative returns shifts to the left. While they do shift strategies, they are slow to open short positions and remain mostly amplifying funds. Consequently, by the time they shift, the market has already started to recover, so that they lose on their short positions. The shifts in derivative return distributions during the COVID-19 crisis are mostly driven by swap contracts, which have been ignored by prior studies.

¹ University of Rochester.

² University of Texas at Dallas.

Copyright: Ron Kaniel and Pingle Wang

1 Introduction

Around one-third of mutual funds hold derivatives, and holding them is permitted by most funds. Yet there is little evidence to date of a direct relation between fund performance and derivative use. Making progress in evaluating fundamental hypotheses in this regard, such as whether funds use derivatives to hedge or amplify positions, has been hindered by the lack of appropriate data. A central limitation of data used in the past to tackle this important topic is that it does not enable getting reasonable estimates for the return on a fund's derivative portfolio. The data typically provides only some aggregated balance sheet information at a semi-annual frequency. This is especially limiting in trying to understand dynamics during a concentrated crisis period, such as the crisis in financial markets at the peak of the COVID-19 pandemic.

Using a novel dataset extracted from the SEC's Form N-PORT, we obtain the actual performance of derivative positions at a monthly frequency and provide a detailed examination of derivative use by domestic equity mutual funds in the US. We show that, contrary to the common belief that derivatives are used for hedging and risk management (Koski and Pontiff (1999)), the majority of active equity funds use derivatives to amplify their market exposure, as the median correlation between derivative returns and non-derivative returns is highly positive. Furthermore, despite their seemingly small portfolio weight, derivatives have a significant impact on funds' leverage and a substantial impact on fund returns. In response to the initial outbreak of the COVID-19 pandemic and a market crash of almost 30% in March 2020, fund managers trade more heavily on short derivative positions. Such a trading pattern is more prevalent among managers residing in states with early state-level Stay-at-home order (SAH), where the risk of recession is more salient. Moreover, we find evidence supporting both the hedging channel and amplifying channel. Specifically, the distribution of derivative returns shifts to the right for funds with hedging strategy, and to the left for funds with amplifying strategy. The shift in distributions is mostly driven by swap contracts, which have been ignored by prior studies.

Our paper starts by highlighting that prior research on fund derivative use has overlooked an important derivative class: swaps. Prior work focuses almost exclusively on options and futures, since the data they used did not contain information on other derivatives.¹ The swap contract is one of the largest and most liquid derivative contract classes. Swaps constitute north of 30%.

Our analysis accounts for the variation in the extent of derivative use. We uncover substantial cross-sectional variation in the extent of usage. Taking advantage of the derivative holdings data, we measure the extent of derivative use by the absolute derivative weight and gross leverage and find polarized cross-sectional usage. Within active funds that use derivatives, over 50% are *Token* users with derivative weights of less than 0.2%, while 20% of funds have derivative weights of more than 3%. Even though a 3% derivative weight seems small in absolute terms, we show that it represents 36% gross of leverage and provides funds with abundant exposure to the market.

Token users' performance is, not surprisingly, very similar to nonusers. This explains why exiting papers that try to distinguish performance and risk of users and nonusers by using the option/future usage flag in N-SAR to identify users and then compare the two groups could suffer from limited power. To account for different levels of derivative use, we split derivative users by the extent of usage into three groups, token users, medium users, and heavy users, according to a 50/30/20 cut. Our result shows heavy users underperform nonusers by 1.32% per year using Fama-French five-factor alpha and by 1.92% per year using benchmark-adjusted returns. Moreover, contrary to the similar market beta between users and nonusers documented in Koski and Pontiff (1999), the analysis reveals that heavy users have a considerably lower market beta than nonusers. The difference in beta is driven mostly by their derivative positions, but also by lower exposure to market risk of their equity holdings.

¹Koski and Pontiff (1999), Deli and Varma (2002), Almazan, Brown, Carlson, and Chapman (2004) study options and futures. Frino, Lepone, and Wong (2009) study index futures. Cici and Palacios (2015) and Natter, Rohleder, Schulte, and Wilkens (2016) focus on options alone. An exception is Cao, Ghysels, and Hatheway (2011) that considers total derivative use, but does not consider swaps separately.

An important innovation of our paper is that, in addition to considering fund performance, it is the first paper to directly investigate the performance of derivative positions and how they contribute to fund returns. By obtaining realized and unrealized Profit-and-Loss (PnL) of different derivative classes at a monthly frequency, we are able to estimate the returns of each derivative class separately and together. We define the derivatives' contribution as the ratio between derivative returns and fund returns. Around 20% of the fund-month observations have an absolute derivative contribution of more than 25%. Such a contribution is large, especially considering the relatively small portfolio weight of derivative positions.

Taking advantage of the time-series derivative and non-derivative returns, we study whether fund managers use derivatives for hedging or amplification purposes by calculating their correlation between July 2019 and January 2020. Prior work attempting to answer this question, for example Koski and Pontiff (1999), was forced to tackle it indirectly since the data used in those studies could not facilitate estimating derivative returns. Contrary to the common belief that derivatives are used for hedging, we find that the majority of funds use derivatives to amplify their exposures; the median correlation of 0.34 is large and positive, and 63% of funds have a positive correlation. We further sort funds by the correlation into terciles and define a fund as an amplifying (hedging) fund if its correlation is in the top (bottom) tercile. Over 85% of amplifying funds' derivatives are long positions. Around 50% of hedging funds' derivatives are short positions, which explains the negative correlation between derivative returns and non-derivative returns.

Having demonstrated the importance of derivative positions to both fund holdings and returns, we study how fund managers trade derivatives during the crisis. During the initial outbreak of the COVID-19 pandemic, the S&P 500 index dropped over 30% between 12/31/2019 and 03/23/2020 and fully recovered by the end of July. The sharp market downturn and the unanticipated rebound provide us an ideal laboratory to study managers' trading behavior. Unlike hedge fund managers, most mutual fund managers are restricted from taking short equity positions. Therefore, the flexibility of trading derivatives is crucial

to mutual fund managers if they want to deleverage equity positions and outperform their peers. However, the use of derivatives is a double-edged sword, given the high volatile nature of derivative contracts and the uncertain timing of the market rebound. As the employment risk rose significantly around the peak of the pandemic outbreak, derivative users had incentives to be more conservative and decrease derivative holdings so to pool with the nonusers who are the majority.

Empirically, we find fund managers' derivative use almost doubled from December 2019 to March 2020, the outbreak of the crisis. In September and December 2019, absolute derivative weight in managers' portfolios was around 1.5%. Between January and late March, it significantly increased by 1.41%, 0.72% of which is from long and 0.69% from short positions. The leverage on short derivative positions also increases by 8.3% with a p-value of less than 0.001, whereas there is no change in leverage on long positions. The result suggests that the increase in derivative use on short positions is not simply due to market returns. Fund managers actively put more weight in short positions to hedge against the crisis.

The increased usage is not from the extensive margin but from the intensive margin, as the number of users remains flat. The cumulative distribution function (CDF) of derivative use shifts to the right during the initial COVID-19 outbreak, suggesting that the increased derivative use is not driven by a small number of funds heavily building up their derivative positions. Instead, it is a result of a shift in employing more derivatives by the industry as a whole.²

We further show that the increase in derivative use comes from managers who face a more salient risk of recession. Prior studies find that agents tend to overreact to salient risk situations (Lichtenstein, Slovic, Fischhoff, Layman, and Combs (1978), Dessaint and Matray (2017)). As the number of the COVID-19 cases rose in the US, states gradually implemented Stay-at-home orders (SAH) starting from later March to early April. We utilize the staggered SAH at the state level and conjecture that the COVID-19 risk is more

²The two distributions are significantly different from each other, as the p-value of the Kolmogorov-Smirnov test is less than 1%.

salient for fund managers in states with than without SAH in place. By the end of March 2020, among states with at least one registered mutual fund, 25 states have SAH in place, and 11 states do not. The absolute derivative weights significantly increase for funds with SAH in place, but no significant change occurs for funds without SAH. When we decompose derivative weight by long/short positions and positive/negative weights, we find that most of the variation in managers' reactions comes from the short positions. The dispersion between positive and negative weights widens during the pandemic. The result suggests fund managers who face greater risks from COVID-19 bet more in the short positions but open these positions at different times during the pandemic. When the market rebounded unexpectedly and sharply after March 23, funds that entered late suffer loss from these short derivative positions. In the data, we find that the average time-to-maturity of new short positions significantly decreases during the crisis for funds with SAH, and there is no change in long positions.

How does the increased derivative use contribute to fund returns during the crisis? The effect depends on the types of derivative strategies employed by fund managers before the crisis. Specifically, the distribution of derivative returns shifts to the right for hedging funds in March 2020, but to the left for amplifying funds. Swap contracts, which have been ignored by prior research on fund derivative use, contribute the most to derivative returns during the crisis, followed by future contracts. Options and foreign exchange related contracts contribute little. As a result, hedging funds significantly outperform by an annualized Fama-French five-factor alpha of 14% between February 20, 2020, and March 23, 2020. The benefit of hedging during the crisis does not come for free. When the market rebounded sharply after March 23, hedging funds underperform. The outperformance of hedging funds is not due to their equity holdings, as their hypothetical equity returns do not perform differently than other funds.

To gain more insight into the performance of hedging funds during the crisis, we further incorporate the downside risk into the CAPM model and show that hedging funds perform

exceptionally well out-of-sample. Specifically, we add a down-market dummy, which is equal to one if the market excess return is negative, the squared market excess return, and the interaction terms between the down-market dummy and the (squared) market excess return into the CAPM model. This model takes into account the market crash (jump) and asymmetric sensitivity of fund returns with respect to the market. Using estimated pre-2020 factor loading, we then calculate out-of-sample factor-adjusted returns for funds in 2020. Our result shows that hedging funds have positive factor-adjusted returns in the crisis period, while amplifying funds and nonusers have negative returns. The cumulative gap in factor-adjusted return is 9.2% by March 23, 2020, and the gap remains as large as 6% by the end of June.

The rest of the paper is organized as follows. Section 2 relates our work to the literature. Section 3 describes the data. Section 4 provides an overview of derivative use. Section 5 analyzes the change in managers' trading behavior during the COVID-19 pandemic. Finally, section 6 concludes.

2 Related Literature

Prior data limitations have confounded the ability to analyze the impact of derivative use on mutual fund performance and risk on a couple of fronts.

First, prior literature has focused exclusively on options and futures when referring to derivatives in equity funds. For example, Koski and Pontiff (1999) investigates the use of options and futures by 679 domestic equity mutual funds between 1992 and 1994.³ Deli and Varma (2002), Almazan et al. (2004), and Calluzzo, Moneta, and Topaloglu (2017) study the characteristics of funds and fund families that use options and futures. Cici and Palacios (2015) and Natter et al. (2016) study the performance of option users. The restriction to options and futures was due to the fact that SEC form N-SAR, the main data source used in these papers to identify users, asks whether the fund uses options and futures, but does not

³Throughout the rest of the paper, the term "funds" refers to "domestic equity funds".

ask on other derivatives.⁴ We show that a non-negligible number of funds use swap contracts, which have been overlooked in the existing studies. Our analysis reveals that swaps have an important impact on fund returns, especially during the COVID-19 crisis. Moreover, Even though options are more extensively studied than other derivatives, we show options constitute a small fraction of overall derivatives in equity funds and have little effect on funds' risk exposure.

Early work finds similar performance and risk exposure of derivative users and nonusers (for example Koski and Pontiff (1999)). Cao et al. (2011) show that the seemingly similar performance is a result of pooling token users with other users. Natter et al. (2016) show option users have lower market risk. Our analysis reveals that the lower exposure to market risk of heavy derivative users is driven mostly by funds' derivative portfolios, but also by different equity portfolio risk exposures.

A central contribution of our paper is that we provide the first evidence on how derivative positions contribute to fund returns, including within the pandemic crisis. This is facilitated by the fact that form N-PORT is unique in providing security level information on both unrealized and realized PnL, at a monthly frequency, enabling us to derive an estimate of the returns on over-the-counter and exchange traded derivative positions that the fund utilizes. Derivatives contribute substantially to fund returns, despite their small portfolio weight. Contrary to the common belief that derivatives are used for hedging among mutual funds, we find that more funds use derivatives to amplify than to hedge their exposures to the market, as the median correlation between derivative returns and non-derivative returns is positive.

Our paper also contributes to the literature on mutual funds and the COVID-19 pandemic. The pandemic is an exogenous and unanticipated shock to financial markets that provides good identification of the impact and drivers of funds' performance and strategies.

⁴The identification of usage is derived from item 70 in the N-SAR form, either directly by the authors or from commercial data sets collecting this information. With respect to futures, only the use of index and commodity futures is reported. Item 74 reports basic balance sheet information on options (74G) and options on futures(74H) but not on other derivatives.

Pastor and Vorsatz (2020) study the sustainability and fund performance. Falato, Goldstein, and Hortaçsu (2020) focus on the financial fragility in corporate bond funds. We show that derivatives are used more extensively during the pandemic. The increase stems from the intensive, but not from the extensive margin. Derivative users increase their short derivative positions during the initial outbreak. This is mostly driven by funds in states with SAH in place before the end of March 2020, as the risk is likely to be more salient in states with than without SAH in place.

3 Data

Our study utilizes a newly available dataset from the SEC's Form N-PORT, which contains detailed derivative holdings at the quarterly frequency and derivative performance at the monthly frequency. Following the Investment Company Reporting Modernization reforms adopted in October 2016 and revised in January 2019, mutual funds other than money market funds and small business investment companies are required to file monthly Form N-PORT. The form provides information about their portfolio holdings and performance. Larger entities, funds that together with other investment companies in the same group of related investment companies, have net assets of \$1 billion or more as of the end of the most recent fiscal year of the fund, start to report beginning June 1, 2019. Small entities begin to report beginning on March 1, 2020. Although funds report to the SEC monthly, holding reports are available to the public only at a quarterly frequency, corresponding to the fiscal quarter-ends.

We extract the following information at quarterly and monthly levels from Form N-PORT. The quarterly level data include the fund's total net assets and portfolio holdings. The holding data cover not only equity and debt positions, but also detailed descriptions of over-the-counter and exchange-traded derivative positions, which are not available in the traditional mutual fund data sources, such as the CRSP and Thompson Reuters. We extract

the derivative instrument, portfolio weight, expiration date, and unrealized appreciation or depreciation for each derivative position. The derivative instrument not only includes forwards/futures and options, which are indicated by flags in Form N-SAR, but also covers swaps, swaptions, warrants, and foreign exchange contracts, which have not been documented in prior studies. Due to the small fractions of swaptions and warrants and their similarities to options, we consolidate swaptions and warrants into the options category. For swaps, we identify the securities to be paid and received, the upfront payments, and the notional amount. For futures and forwards, we identify the payoff profile (long/short) and the notional amount. For options, we identify the exercise price, whether it is a call or a put, and whether the fund writes or purchases the option. For foreign exchange contracts, we identify the currency sold/purchased and the notional amount in USD.

The monthly level data include the fund's inflows and outflows that are also available in Form N-SAR, the fund's return, and realized and unrealized PnL of each derivative instrument, which has not been recorded in other data sources.

Our sample covers 10,619 unique funds with Form N-PORT available starting from September 2019. After merging with the CRSP, we have 9950 unique funds, representing 84.83% of the CRSP and 95.04% of total net assets. Our sample contains a wide range of fund styles, including domestic and foreign equity funds, fixed-income funds, mixed funds, and other funds (mortgage-backed funds and currency funds). In this study, we focus on 2909 active domestic equity funds.

In this paper, we use the *pre-crisis period* to denote time before February 20, 2020. We use the *crisis period* or *outbreak period* to denote time period between February 20, 2020, and March 23, 2020, which also follows the definition in Pastor and Vorsatz (2020). We use the **recovery period** to denote time periods between March 24, 2020 and June 30, 2020.⁵ For analyses with only monthly frequency available, we refer to the crisis period as February 2020 and March 2020, and the recovery period as the months between April 2020

⁵We stop on June 30, 2020 because the data only update to June 2020 as the time of writing.

and June 2020.

4 How are Derivatives Used in Mutual Funds?

Previous studies on derivative use in the mutual fund industry have almost exclusively relied on the SEC's Form N-SAR. While the Form N-SAR contains yes-no questions on whether a fund held options or futures, it fails to cover whether other important derivative categories, especially swaps, which turn out to be a major component of derivative positions, have been used by funds, to what extent these derivatives are used, or how much these derivative positions contribute to the fund return or risk. This section provides a comprehensive overview of derivative use by active domestic equity funds and addresses these unanswered questions.

In Section 4.1, we show that there is large cross-sectional variation in the extent of derivative use. Taking into account the variation in derivative use will uncover important differences in performance and risk profiles between derivative users and nonusers. Section 4.2 provides the first evidence on how much derivatives contribute to fund returns.

4.1 The Extent of Derivative Use

Descriptive Statistics of Derivative Use

Our paper uses detailed derivative holdings data and examines the extent of derivative use. We extract the portfolio weight and notional amount of each derivative position from the Form N-PORT. To proxy for the extent of derivative use, we use two measures. The first measure is the sum of *absolute derivative weights* in the portfolio. As fund managers can gain exposure by trading derivatives in both long and short sides, it is necessary to use the absolute derivative weight to capture the extent of derivative use. The second measure is the *gross leverage*, which is the sum of notional amounts of derivative positions scaled by the total net assets.

Panel A of Table 1 shows the number of funds with derivative use in our sample between

September 2019 and June 2020. A fund is classified as a derivative user if it uses derivatives at least once in the sample. The sample contains 2909 active funds, 756 of which (26%) are derivative users. Interestingly, the fraction of derivative users has not changed much in the past two decades, as the fraction of derivative users in Koski and Pontiff (1999) was 21%. Among the derivative users, 432 funds use futures or forwards, 124 funds use swaps, 317 funds use options, and 179 funds use foreign exchange contracts. As a result, by only focusing on options and futures, prior studies have misclassified a nontrivial number of swap users and foreign exchange users as nonusers.

Panel A of Table 1 further breaks down the derivative use by the types of derivatives and highlights the importance of swap contracts in mutual funds. On average, funds have a derivative weight of 2.05%, with the futures contract (0.7%) being the largest derivative type, closely followed by swaps (0.64%). Option contract only represents 0.43% of the portfolio. When measuring derivative use by gross leverage, swap positions provide the largest gross leverage of 22.9%, followed by future positions (20.3%). Option positions merely provide gross leverage of 1.8%.

Derivative Use in Cross-section

There is substantial cross-sectional variation in the extent of derivative use, with half of the funds using a negligible amount of derivatives, and some other funds use derivatives heavily. Such a pattern is also documented in Cao et al. (2011) but has not received enough attention in subsequent studies. Panel B of Table 1 shows that the mean of absolute derivative weight is 2% with a standard deviation of 4.3%. Although the derivative positions' portfolio weight seems small in absolute terms, derivatives provide funds ample exposure to the markets because of the embedded leverage. Specifically, the mean gross leverage is 51.5%, with a standard deviation of 88.1%. Figure 1 visualizes the cross-sectional variations in derivative use. Over 50% of funds have derivative weights (gross leverage) of less than 0.2% (3%), while 20% of funds have derivative weights (gross leverage) of more than 3% (36%).

Table 1
Overview of Derivative Use
 The table shows the summary of derivative use in equity domestic active funds. The sample includes all equity domestic active funds that use derivatives from September 2019 to June 2020. Panel A shows the number of funds with derivative positions, and the breakdown of derivative use by categories. Panel B shows the summary statistics of key variables. Absolute derivative weight is the sum of portfolio weights of derivative positions in absolute value, measured in percentage points. Gross leverage is the sum of notional amount of derivative positions, normalized by the fund size and shown in percentage points. TNA is the total net assets in millions. Derivative return is the sum of monthly realized PnL and change in unrealized PnL from derivative positions, normalized by the fund size from the previous month and shown in basis points. Non-derivative return is the difference between fund return and derivative return, shown in basis points. Derivative contribution is the ratio between derivative return and fund return, shown in percentage points. All variables are winsorized at 1% level.

Panel A: Breakdown of Derivative Usage

	No. of Funds	Absolute Weight	Gross Leverage
Swap	124	0.64	22.89
Future/Forward	432	0.70	20.33
Option	317	0.43	1.78
Foreign Exchange	179	0.28	6.46
All Derivatives	756	2.05	51.46

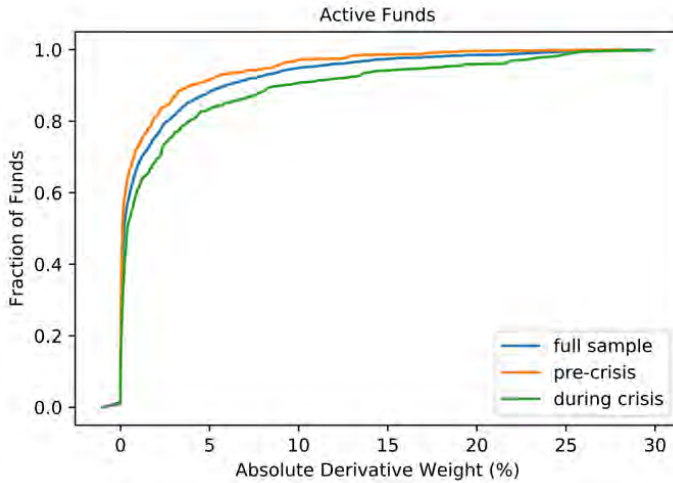
Panel B: Summary Statistics of Key Variables

Variable	Mean	StdDev	Min	10%	20%	30%	40%	50%	60%	70%	80%	90%	Max
Absolute Derivative Weight (%)	2.05	4.32	0	0.01	0.02	0.05	0.1	0.21	0.55	1.29	2.78	5.98	29.86
Gross Leverage (%)	51.46	88.12	0	0	0.28	0.9	1.69	2.7	4.63	14.21	36.38	106.26	512.04
Derivative Contribution (%)	6.06	114.07	-512.49	-30.36	-2.82	-0.31	0.01	0.33	1.13	2.36	6.47	28.83	447.64
Derivative Return (bps)	-8.99	127.13	-923.76	-63.53	-15.16	-4.55	-0.67	0.08	1.57	4.58	18.31	36.58	865.98
Non-derivative Return (bps)	4.11	690.31	-2228.11	-917.88	-428.40	-122.08	15.44	109.59	194.08	276.74	377.56	692.83	1641.42
TNA (\$ mil.)	1761.51	8108.99	1.16	37.41	92.23	177.23	290.11	486.64	732.68	1130.83	1827.38	4655.26	198652.18

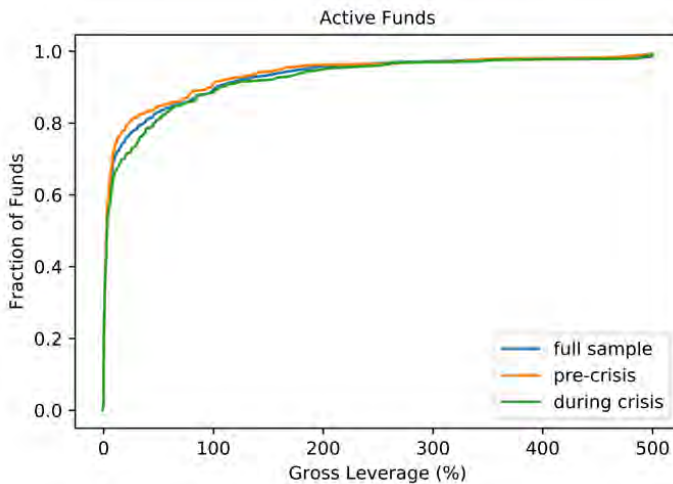
Figure 1
Cumulative Distribution Function of Derivative Use

The figure shows the cumulative distribution functions of the fund-level derivative use. The derivative use is proxied by absolute derivative weight in Panel (a), and by gross leverage in Panel (b). The numbers in x-axis are in percentage. The blue curve represents the full sample between July 2019 and June 2020. The orange curve represents the pre-crisis sample between July 2019 and January 2020. The green curve represents the COVID-19 crisis sample between February 2020 and March 2020.

(a) CDF of Absolute Derivative Weight



(b) CDF of Gross Leverage



Covid Economics 49, 18 September 2020: 172-221

To gain deeper insights into how funds use their derivative positions, we further group derivative users by the extent of usage into the following three categories. For each quarter, funds are sorted by the absolute derivative weight into deciles.⁶ We define *token users* as the funds in the bottom five deciles, *medium users* between the sixth and eighth deciles, and *heavy users* in the top two deciles. We use an uneven 50/30/20 cut instead of an even cut to take into account that a large number of funds only use a negligible amount of derivatives.

Table 2 shows the derivative weights and the corresponding long/short compositions by the types of derivative users. For option positions, a purchased call or a written put is counted as a long position, and a written call or a purchased put is counted as a short position. If a fund receives equity returns and pays a fixed or floating rate to its counterparty in a swap position, it is counted as a long position. In Panel A and B, we can see that futures are the most extensively used derivative class among token and medium users, whereas swaps become the dominant derivative class among heavy users. As a result, prior studies that rely on Form N-SAR to classify derivative users will omit swap users, which are likely to be heavy derivative users.

Furthermore, the extent of derivative use is highly persistent over time. Panel C of Table 2 shows the transition matrix of user types between September 2019 and June 2020. For instance, the probability of a fund staying as a token (heavy) user in the next quarter is 82% (72%). In the subsequent analyses, we backfill the derivative use for periods prior to the availability of Form N-PORT. The persistence in derivative use alleviates the concern that derivative use in 2019 may not be representative in prior years.

Derivative Use and Fund Performance

Koski and Pontiff (1999) find that there is no direct link between fund performance and derivative use. In Table 3, we reexamine this result by taking into account the extent

⁶Our results are robust and quantitatively similar when we sort funds by gross leverage.

Table 2
Derivative Weight and Leverage by the Extent of Use

The table shows fund-level derivative weight (Panel A) and gross leverage (Panel B), grouped by the extent of derivative use. The sample includes equity domestic active funds that use derivatives from September 2019 to June 2020. For each quarter, funds are sorted by the absolute derivative weight into deciles. Token users are the funds in the bottom five deciles, medium users between the sixth and eighth deciles, and Heavy users in the top two deciles. Panel C shows the transition matrix of the user type from the previous quarter to current quarter. The table further shows the composition of long and short positions within each derivative type. For option positions, a purchased call or a written put is counted as a long position, and a written call or a purchased put is counted as a short position. If a fund receives equity returns and pays a fixed or floating rate to its counterparty in a swap position, it is counted as a long position.

Panel A: Absolute Derivative Weight (%)

	All Users	Token Users	Medium Users	Heavy Users
All Derivative	2.05	0.06	1.11	8.36
Future	0.70	0.03	0.64	2.44
% in Long	68.18	88.78	69.51	67.00
Swap	0.64	0.00	0.12	3.02
% in Long	73.03	44.59	65.47	73.52
Option	0.43	0.01	0.23	1.75
% in Long	26.51	69.48	29.87	24.98
Foreign Exchange	0.28	0.02	0.12	1.15
% in Long USD	59.96	89.37	67.54	57.85

Panel B: Gross Leverage (%)

	All Users	Token Users	Medium Users	Heavy Users
All Derivative	51.46	3.04	47.39	177.15
Future	20.33	1.81	27.93	54.80
% in Long	58.11	71.32	48.38	64.39
Swap	22.89	0.28	14.42	91.32
% in Long	51.95	82.09	25.90	57.82
Option	1.78	0.04	2.15	5.56
% in Long	56.25	56.09	20.23	76.86
Foreign Exchange	6.46	0.91	2.90	25.47
% in Long USD	58.16	90.96	73.33	52.69

Panel C: Transition Matrix of User Types

$UserType_{t-1}^t$	Token	Medium	Heavy
Token	0.82	0.17	0.01
Medium	0.21	0.61	0.18
Heavy	0.12	0.16	0.72

of derivative use and regressing equal-weighted portfolio returns of each type of derivative user on various asset pricing models in the past decade, between 2010 and 2019.⁷ Since the derivative use data become available from September 2019, we backfill the derivative use data for periods before September 2019 using the fund's derivative use data in September 2019. Table 3 shows the annualized alphas in percentage points and corresponding factor loading. As shown in Panel A, there is no significant difference in performance between derivative users and nonusers after accounting for common risk factors, which is consistent with findings in Koski and Pontiff (1999). Although derivative users significantly underperform nonusers in benchmark-adjusted returns statistically, the difference of 48 bps per year is economically small.

In Panel B, we further split derivative users by their extent of derivative use into three groups. Nonusers and token users have very similar Fama-French five-factor loading and alphas, consistent with the fact that token users hold a tiny fraction of derivatives, which have a trivial impact on fund returns. However, medium and heavy users' factor loading significantly differs from nonusers and token users by having a lower market beta and size beta. Meanwhile, heavy users significantly underperform nonusers by 1.32% per year under the Fama-French five-factor model and by 1.92% per year in benchmark-adjusted returns.⁸ This result is different from the findings in Koski and Pontiff (1999) that derivative users and nonusers have similar performance and beta.

An alternative explanation for the difference in factor loading between heavy users and nonusers is that they hold stocks with different risk exposure. To test this explanation, we generate hypothetical holding returns for each fund, assuming the reported equity holdings from CRSP and Thompson Reuters are held throughout the quarter.⁹ We then form port-

⁷Our results are robust to alternative time windows.

⁸In untabulated analysis, we find that the underperformance of heavy users is not a result of fund fees. We regress raw returns on factor returns and find a similar gap in alphas. The results are available upon request.

⁹We also construct an alternative version of hypothetical holding returns, which takes into account funds' cash positions, as cash positions can have an impact on the leverage. Our results are robust to this alternative version.

Table 3
Performance of Derivative Users

The table shows the performance of derivative users in the past decade between 2010 and 2019. The sample includes equity domestic active funds. We backfill the derivative use data for periods before September 2019 using the fund's derivative use data in September 2019. Panel A shows the factor loading of users and nonusers. Panel B breaks down derivative users by the extent of derivative use. Panel C shows the factor loading of hypothetical returns, assuming the equity positions are held throughout the quarter. All returns and alphas are annualized and in percentage points.

Panel A: Derivative Users vs Nonusers										
Users	Return	Benchmark	CAPM		FF5			RMW	CMA	
			Alpha	Mktrf	Alpha	Mktrf	SMB			HML
Non-users	11.52*** (2.84)	-2.52*** (-8.4)	-1.80*** (-2.92)	0.988*** (75.94)	-0.96** (-2.48)	0.94*** (100.74)	0.179*** (11.48)	-0.039** (-2.17)	-0.054** (-2.27)	-0.032 (-1.13)
Users	9.72*** (2.68)	-3.00*** (-10.68)	-2.16*** (-3.51)	0.884*** (68.4)	-1.44*** (-2.82)	0.847*** (71.14)	0.117*** (5.88)	-0.018 (-0.79)	-0.078** (-2.57)	0.045 (1.24)
Users - Non	-1.80*** (-3.31)	-0.48*** (-3.6)	-0.36 (-1.04)	-0.105*** (-14.82)	-0.48 (-1.65)	-0.092*** (-14.52)	-0.062*** (-5.83)	0.021* (1.7)	-0.024 (-1.48)	0.077*** (3.99)

Panel B: By Derivative Usage										
Users	Return	Benchmark	CAPM		FF5			RMW	CMA	
			Alpha	Mktrf	Alpha	Mktrf	SMB			HML
Non-users	11.52*** (2.84)	-2.52*** (-8.4)	-1.80*** (-2.92)	0.988*** (75.94)	-0.96** (-2.48)	0.94*** (100.74)	0.179*** (11.48)	-0.039** (-2.17)	-0.054** (-2.27)	-0.032 (-1.13)
Token Users	11.28*** (2.81)	-2.16*** (-8.24)	-1.92*** (-3.26)	0.979*** (79.33)	-0.96** (-2.57)	0.927*** (113.17)	0.177*** (12.35)	0.001 (0.09)	-0.072*** (-3.48)	-0.019 (-0.75)
Medium Users	8.52** (2.51)	-3.72*** (-10.27)	-2.40*** (-3.36)	0.813*** (52.02)	-2.04*** (-2.84)	0.791*** (47.21)	0.069** (2.47)	-0.028 (-0.87)	-0.071* (-1.68)	0.068 (1.34)
Heavy Users	6.96** (2.39)	-4.44*** (-12.39)	-2.28*** (-3.02)	0.687*** (41.59)	-2.28*** (-2.91)	0.678*** (38.03)	0.041 (1.36)	-0.056 (-1.64)	-0.056 (-1.25)	0.155*** (2.86)
Heavy - Non	-4.56*** (-3.31)	-1.92*** (-6.19)	-0.48 (-0.8)	-0.301*** (-20.25)	-1.32** (-2.13)	-0.262*** (-19.35)	-0.139*** (-6.12)	-0.017 (-0.66)	-0.003 (-0.08)	0.187*** (4.56)

Panel C: Hypothetical Returns									
Users	Return	CAPM		FF5			RMW	CMA	
		Alpha	Mktrf	Alpha	Mktrf	SMB			HML
Non-users	13.44*** (3.12)	-0.60 (-0.95)	1.052*** (73.41)	0.24 (0.65)	0.995*** (105.8)	0.212*** (13.43)	-0.039** (-2.17)	-0.051** (-2.14)	-0.037 (-1.3)
Token Users	13.32*** (3.06)	-0.96 (-1.47)	1.06*** (77.87)	0.24 (0.63)	1.0*** (127.39)	0.2*** (15.2)	0.008 (0.54)	-0.079*** (-3.97)	-0.03 (-1.28)
Medium Users	12.48*** (3.11)	-0.48 (-0.67)	0.971*** (57.01)	0.02 (0.06)	0.932*** (56.07)	0.169*** (6.07)	-0.029 (-0.91)	0.004 (0.09)	0.024 (0.48)
Heavy Users	11.88*** (3.01)	-0.96 (-1.29)	0.953*** (60.31)	-0.48 (-0.71)	0.924*** (56.01)	0.1*** (3.62)	-0.042 (-1.34)	-0.065 (-1.54)	0.011 (0.22)
Heavy - Non	-1.56** (-2.25)	-0.36 (-0.5)	-0.098*** (-7.16)	-0.72 (-1.26)	-0.071*** (-4.99)	-0.112*** (-4.7)	-0.003 (-0.12)	-0.013 (-0.37)	0.048 (1.12)

t statistics in parentheses
* p < 0.1, ** p < 0.05, *** p < 0.01

folios based on hypothetical returns and regress them on factor returns. Panel C of Table 3 reports the results. The difference in hypothetical market beta between heavy users and nonusers is -0.07, which explains 27% of the market beta difference between heavy users and nonusers, whereas the remaining difference stems from derivative positions and intra-quarter trading. The difference in size beta, to the contrary, can be almost exclusively explained by the reported equity holdings.

4.2 Derivative Contribution to Fund Returns

How derivative positions contribute to fund returns is an open question. Given the similar hypothetical equity returns but largely different realized returns between heavy users and others, it is crucially important to understand the performance of derivative positions. In this section, we extract monthly realized and unrealized PnL of derivative positions between July 2019 and June 2020, and shed light on how important derivative positions are to fund returns.¹⁰

We calculate derivative returns as the sum of realized PnL and the change in unrealized PnL, scaled by the fund's total net assets in the previous month. We then define the derivative contribution to fund returns as the ratio between the derivative return and the fund return. In our sample period, the average monthly derivative return is -9 bps, with a standard deviation of 127 bps, which is shown in Table 1. As a comparison, the average non-derivative return is 4 bps, and its standard deviation is 690 bps. Derivatives have very volatile returns, especially considering their relatively small portfolio weights. Specifically, the standard deviation of the monthly non-derivative returns is five times larger than that of derivative returns, but non-derivative positions weigh over 40 times larger than derivative

¹⁰The first report is available in September 2019, which contains monthly performance measures starting in July 2019.

positions.

$$Derivative\ Return_t = \frac{PnL_t^{Realized} + PnL_t^{Unrealized} - PnL_{t-1}^{Unrealized}}{TNA_{t-1}}$$

$$Derivative\ Contribution_t = \frac{Derivative\ Return_t}{Fund\ Return_t}$$

The blue curve in Figure 2(a) shows the CDF of derivative contribution in our sample between July 2019 and June 2020. The derivative contribution in the figure is winsorized between -0.5 and 0.5 for the ease of presentation. Derivatives contribute heavily to fund returns. Specifically, about 10% of the fund-month observations have derivative contribution over 30%, and another 10% of observations have derivative contribution less than -22%. Derivatives play a larger role in fund returns among medium and heavy users. Figure 2(b) excludes token users and focuses on medium and heavy users. In this subsample, 40% of the fund-month observations have derivative contribution above 20% or below -20%.

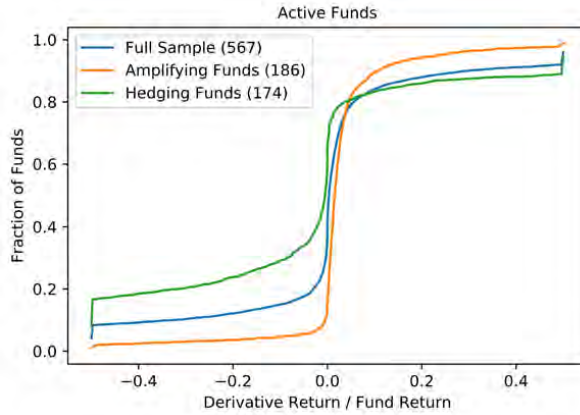
Taking advantage of the time-series derivative returns, we then classify funds into either the *amplifying* category or *hedging* category, depending on the correlation between derivative and non-derivative returns. Specifically, for each fund, we calculate the correlation between the derivative returns and non-derivative returns from July 2019 to February 2020.¹¹ Figure 3 shows the histogram and fitted kernel of the correlation. Contrary to the commonly perceived hedging purposes, the majority of funds use derivatives to amplify their market exposure. The median correlation of 0.34 is large and positive, and 63% of funds have a positive correlation. To take into account the clusters of funds in both tails of the correlation histogram, we group funds by the correlation into terciles. A fund is classified as an amplifying (hedging) fund if its correlation is in the top (bottom) tercile. The correlation of amplifying funds ranges between 0.78 and 1, whereas the correlation of hedging funds ranges between -1 and -0.08. In other words, unlike amplifying funds with highly

¹¹We stop in January 2020 because we will take the pre-crisis fund types and run analysis on how amplifying/hedging funds react during the pandemic.

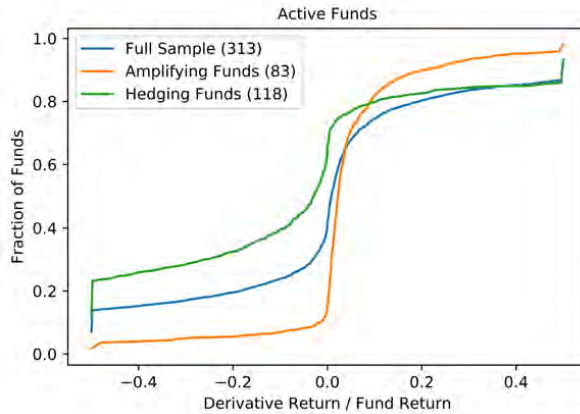
Figure 2
Derivative Contribution to Fund Return

The figure shows the cumulative distribution function of the fund-level derivative contribution to return. Derivative return in month t is calculated as the sum of realized PnL and change of unrealized PnL in month t , normalized by the fund total net assets in month $t - 1$. Derivative contribution to fund return is the ratio between derivative return and fund return. For each fund, we calculate the correlation between the derivative returns and non-derivative returns from July 2019 to February 2020. Funds are sorted by the correlation into terciles. A fund is classified as an amplifying (hedging) fund if its correlation is in the top (bottom) tercile. Funds are also sorted by the absolute derivative weight into deciles. Panels (b) show the CDF for funds in the top five deciles. The blue curve shows the CDF in the full sample. The orange curve shows the CDF for amplifying funds. The green curve shows the CDF for hedging funds. The numbers in parentheses show the average number of funds per month.

(a) Derivative Contribution for All Funds



(b) Derivative Contribution For Medium and Heavy Users

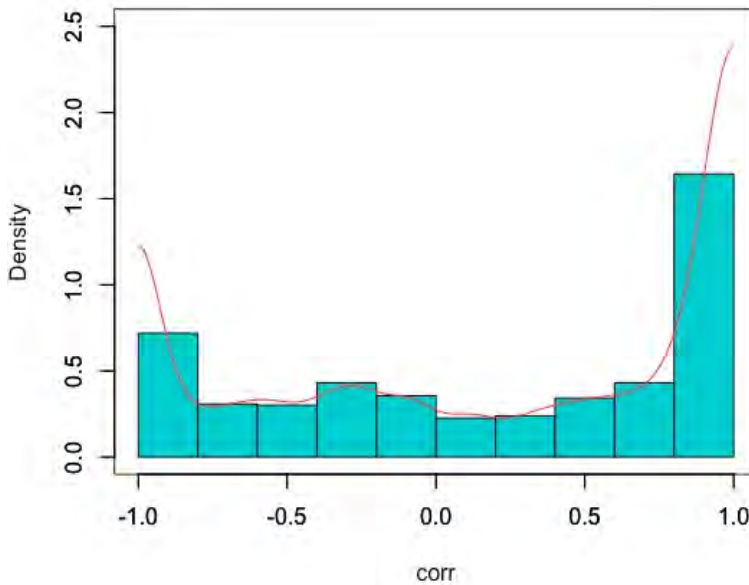


positive correlation, some hedging funds have relatively weak correlation between derivative and non-derivative returns.¹² Amplifying and hedging funds have similar sizes as nonusers. Specifically, hedging funds on average have a size of \$1.65 billion, amplifying funds \$1.69 billion, and nonusers \$1.73 billion. In terms of the market cap, amplifying funds in total have an asset-under-management of \$0.46 trillion, hedging funds \$0.54 trillion, and nonusers \$3.8 trillion.

Figure 3

Distribution of the Correlation between Derivative and Non-derivative Returns

The figure shows the histogram and fitted kernel of the correlation between derivative and non-derivative monthly returns. The sample contains all active derivative users between July 2019 and January 2020.



The orange and the green curves in Figure 2 show the CDF of the derivative contribution for amplifying funds and hedging funds, respectively. The green curve sits higher than the orange curve, especially in the negative contribution region. The p-value of the Kolmogorov-Smirnov test, which examines the difference between two distributions, is less than 1%. The

¹²We have also examined the alternative cutoff of correlations by assigning amplifying funds with a correlation above 0.5 and hedging funds with a correlation below -0.5. The results are robust to such alternative definition.

result is consistent with the classification that the derivative returns of hedging funds are negatively correlated with non-derivative returns.

Tables 4 and 5 show the derivative weight and gross leverage of amplifying and hedging funds. Take heavy users and their derivative weight as an example. Amplifying funds and hedging funds differ mainly by the composition of long and short positions. Amplifying funds tend to invest heavily in long positions, whereas hedging funds put relatively more weight in short positions. Specifically, as shown in Table 4, amplifying funds have 85% futures and 87% swaps in long positions, whereas hedging funds have 43% futures and 50% swaps in long positions. Hedging funds also invest relatively more in options, which have a portfolio weight of 1.03% on average, than amplifying funds, which have a weight of merely 0.04%. Furthermore, hedging funds tend to be more levered than amplifying funds. In Table 5, the gross leverage of hedging funds is 65.4%, almost two times larger than that of amplifying funds. The difference in gross leverage is mainly driven by swaps. For example, within heavy users, the gross leverage of swaps is 33.8% for amplifying funds, and it is 100.9% for hedging funds.

The difference in long/short derivative composition between amplifying and hedging funds also affects their factor loading, as shown in Table 6. In Panel A, hedging funds have a market beta of 0.84, and amplifying funds have a market beta of 0.93. The difference in beta between hedging funds and amplifying funds is -0.09, with a t-stat of 14. In Panel B, hedging funds and amplifying funds have the same hypothetical market beta. The result suggests that the difference in ex-post market beta between hedging and amplifying funds is due to their different strategies of derivative use.

Panel C of Table 6 compares the performance among nonusers, heavy amplifying funds, and heavy hedging funds. There is no difference in performance between heavy hedging funds and nonusers, after controlling for Fama-French five-factors. However, heavy amplifying funds significantly underperform nonusers by 2.05% per year, which explains why heavy users underperform nonusers in Table 3. Surprisingly, even though amplifying funds use

Table 4
Derivative Weight by Amplifying/Hedging Funds

The table shows fund-level derivative weights, grouped by whether the fund uses derivatives for amplifying or hedging. The sample includes equity domestic active funds that use derivatives. For each fund, we calculate the correlation between the derivative returns and non-derivative returns from July 2019 to January 2020. Funds are sorted by the correlation into terciles. A fund is classified as an amplifying (hedging) fund if its correlation is in the top (bottom) tercile. For each quarter, funds are sorted by the absolute derivative weight into deciles. Token users are the funds in the bottom five deciles. Medium users are the funds between the sixth and eighth deciles. Heavy users are the funds in the top two deciles. The table further shows the percentage of long and short positions for each derivative type. For option positions, a purchased call or a written put is counted as a long position, and a written call or a purchased put is counted as a short position. If a fund receives equity returns and pays a fixed or floating rate to its counterparty in a swap position, it is counted as a long position.

Panel A: Amplifying Funds

	All Users	Token Users	Medium Users	Heavy Users
All Derivative	1.31	0.06	1.14	6.69
Future	0.79	0.06	0.99	3.22
% in Long	84.92	91.99	84.30	84.87
Swap	0.33	0.00	0.05	2.31
% in Long	87.13	100.00	87.87	87.08
Option	0.04	0.01	0.09	0.05
% in Long	46.41	77.94	41.28	51.30
Foreign Exchange	0.16	0.00	0.02	1.11
% in Long USD	47.14	84.84	61.59	46.57

Panel B: Hedging Funds

	All Users	Token Users	Medium Users	Heavy Users
All Derivative	2.75	0.08	1.03	8.04
Future	0.56	0.01	0.25	1.58
% in Long	45.68	71.26	55.85	43.65
Swap	0.67	0.01	0.15	2.10
% in Long	49.35	31.48	40.65	50.11
Option	1.03	0.02	0.41	3.00
% in Long	17.82	66.66	14.61	17.99
Foreign Exchange	0.49	0.05	0.22	1.36
% in Long USD	67.28	89.72	66.94	66.23

Table 5
Gross Leverage by Amplifying/Hedging Funds

The table shows fund-level gross leverage, grouped by whether the fund uses derivatives for amplifying or hedging returns. The sample includes equity domestic active funds that use derivatives. For each fund, we calculate the correlation between the derivative returns and non-derivative returns from July 2019 to January 2020. Funds are sorted by the correlation into terciles. A fund is classified as an amplifying (hedging) fund if its correlation is in the top (bottom) tercile. For each quarter, funds are sorted by the absolute derivative weight into deciles. Token users are the funds in the bottom five deciles. Medium users are the funds between the sixth and eighth deciles. Heavy users are the funds in the top two deciles. The table further shows the percentage of long and short positions for each derivative type. For option positions, a purchased call or a written put is counted as a long position, and a written call or a purchased put is counted as a short position. If a fund receives equity returns and pays a fixed or floating rate to its counterparty in a swap position, it is counted as a long position.

Panel A: Amplifying Funds

	All Users	Token Users	Medium Users	Heavy Users
All Derivative	23.37	2.97	23.03	105.53
Future	11.16	2.63	19.19	26.05
% in Long	64.79	85.35	52.02	78.89
Swap	5.72	0.27	3.04	33.79
% in Long	79.29	100.00	83.62	77.70
Option	0.05	0.01	0.14	0.01
% in Long	53.13	51.09	52.73	85.68
Foreign Exchange	6.45	0.05	0.67	45.68
% in Long USD	50.05	88.94	58.79	49.56

Panel B: Hedging Funds

	All Users	Token Users	Medium Users	Heavy Users
All Derivative	65.44	3.98	68.24	139.37
Future	15.86	0.93	26.55	22.40
% in Long	40.58	34.87	40.01	41.65
Swap	39.83	0.22	29.85	100.92
% in Long	24.01	52.82	7.88	29.38
Option	4.54	0.12	5.94	8.50
% in Long	51.37	55.70	15.74	79.71
Foreign Exchange	5.21	2.70	5.91	7.55
% in Long USD	71.68	91.81	72.18	62.18

Table 6
Performance of Amplifying/Hedging Funds

The table shows the performance of amplifying and hedging funds between 2010 and 2019. We backfill the derivative use data for periods before September 2019 using the funds' information in September 2019. Panel A shows the factor loading of real returns. Panel B shows the factor loading of hypothetical returns, assuming the equity positions are held throughout the quarter. In Panel C, funds are double sorted by the extent of derivative use and by whether the fund is an amplifying or a hedging fund into groups. The panel compares the performance among nonusers, heavy amplifying funds, and heavy hedging funds. The monthly five-factor alphas are reported for each portfolio. All returns and alphas are annualized and in percentage points.

Panel A: Amplifying vs Hedging Funds

	ret	alpha	mktrf	smb	hml	rmw	cma
Amplifying	10.80*** (2.71)	-1.44*** (-3.94)	0.928*** (111.97)	0.18*** (12.94)	0.006 (0.35)	-0.026 (-1.22)	-0.005 (-0.19)
Hedging	10.08*** (2.87)	-0.96** (-2.06)	0.837*** (78.45)	0.056*** (3.11)	-0.024 (-1.19)	-0.111*** (-4.12)	0.053 (1.65)
Hedging - Amplifying	-0.72 (-1.17)	0.48 (1.64)	-0.091*** (-13.99)	-0.124*** (-11.35)	-0.03** (-2.39)	-0.086*** (-5.17)	0.058*** (2.93)

Panel B: Hypothetical Returns

	ret	alpha	mktrf	smb	hml	rmw	cma
Amplifying	13.08*** (3.05)	-0.04 (-0.08)	0.99*** (121.73)	0.213*** (15.63)	-0.007 (-0.43)	-0.018 (-0.89)	-0.016 (-0.64)
Hedging	13.44*** (3.16)	0.24 (0.72)	0.999*** (127.92)	0.109*** (8.35)	0.004 (0.26)	-0.088*** (-4.46)	0.001 (0.03)
H-L	0.36 (0.91)	0.20 (0.84)	0.01 (1.31)	-0.104*** (-8.31)	0.011 (0.74)	-0.07*** (-3.71)	0.016 (0.73)

Panel C: Decompose Heavy Users

	ret	alpha	mktrf	smb	hml	rmw	cma
Nonusers	11.52*** (2.84)	-0.96** (-2.48)	0.94*** (100.74)	0.179*** (11.48)	-0.039** (-2.17)	-0.054** (-2.27)	-0.032 (-1.13)
Heavy Amplifying	6.72* (1.9)	-3.01*** (-3.53)	0.775*** (36.41)	0.224*** (6.28)	0.047 (1.14)	-0.038 (-0.7)	0.056 (0.87)
Heavy Hedging	8.76*** (2.87)	-1.32* (-1.66)	0.741*** (41.04)	-0.033 (-1.11)	-0.102*** (-2.94)	-0.112** (-2.45)	0.186*** (3.39)
Hedging - Amplifying	2.04* (1.82)	1.69** (2.02)	-0.034* (-1.69)	-0.257*** (-7.56)	-0.148*** (-3.81)	-0.074 (-1.44)	0.13** (2.1)
Amplifying - Nonusers	-4.68*** (-4.86)	-2.05*** (-2.99)	-0.163*** (-9.48)	0.043 (1.48)	0.081** (2.48)	0.013 (0.31)	0.086 (1.66)
Hedging - Nonusers	-2.64** (-2.04)	-0.36 (-0.42)	-0.197*** (-13.64)	-0.215*** (-8.87)	-0.067** (-2.41)	-0.061 (-1.66)	0.216*** (4.92)

derivatives to gain exposure to the market, their realized market beta is still lower than that of nonusers.

5 Derivative Use During the COVID-19 Pandemic

Unlike the financial crisis, the COVID-19 pandemic started as a healthcare crisis, which provides researchers an exogenous and unanticipated shock to financial markets. The pandemic offers good identification of the impact and drivers of funds' performance and strategies. How do fund managers trade derivatives during the COVID-19 pandemic? On the one hand, derivative users may reduce derivative positions given the extremely volatile market and pool with the majority of nonusers.¹³ As derivative positions are highly leveraged, they will generate extreme returns in either direction. Due to the high employment risk faced by fund managers during the pandemic, derivative users may rather forgo the potential upside and seek job security by reducing derivative positions. Moreover, as the number of COVID-19 cases continued to rise in the US, many states gradually implemented Stay-at-home orders (SAH). Fund managers are restricted to work from home, which may further reduce their trading activity.

On the other hand, derivative positions allow fund managers to trade on the short side of the market, which is especially important because almost all funds' equity positions are long positions. Such flexibility provides hedging against the market downturn. Moreover, agents tend to react to salient risks (Lichtenstein et al. (1978) and Dessaint and Matray (2017)), which makes derivative trading more likely during the pandemic, especially for fund managers residing in states with SAH in place, where the risk of potential recession is likely to be more salient.

Therefore, it remains an empirical question of whether managers trade more derivatives during the pandemic, and for what purposes. In this section, we first study managers' reac-

¹³The S&P 500 index dropped by 34% between 02/20/2020 and 03/23/2020, and the VIX index soared from 15.56 on 02/20/2020 to 82.69 on 03/16/2020, and then fell to 53.54 on 03/31/2020.

tions to the COVID-19 pandemic at the aggregate level. We examine the time-series changes in derivative allocation. Second, we study whether the changes in derivative allocation are greater when fund managers face more salient risk. In particular, we group fund managers by whether a fund resides in states with SAH in place before the end of March 2020, and compare the difference in change of portfolio allocation between the two groups of funds. Lastly, we study how derivative positions contribute to fund returns during the crisis and the implications of derivative performance on fund returns.

5.1 Time-series Change in Derivative Use

Table 7 shows the change in portfolio allocation from the last quarter of 2019 to the first quarter of 2020. The first column shows the unconditional change in allocation. The second to fourth columns split the sample by the derivative use into token users, medium users, and heavy users. The classification of derivative users is based on the absolute derivative weight in the last quarter of 2019 to rule out the look-ahead bias.

Derivatives are used more extensively during the COVID-19 pandemic. From column (1) of Table 7, the absolute derivative weight increases by 1.41%. Note that the absolute derivative weight in December 2019 is 1.47%, so that the derivative use increases by 96.24% on a relative scale during the pandemic. A large part of the increase in derivative use is driven by heavy users, which is shown in column (4).

Moreover, the increase in derivative use is driven by fund managers increasing their bets on short positions. On a relative scale, derivative use in short positions increases by 134%, which almost doubles the increase of 75.7% in long positions. Interestingly, both the positive and negative derivative weights of short positions increase, suggesting that the increased bet on short positions could be a result of funds entering short derivatives at different time. Specifically, short derivative positions with positive weights increase by 193.5%, and short positions with negative weights increase by 91.4%. On the contrary, the increased derivative use in long positions is solely driven by positions with negative weights. How do short

Table 7
Change in Portfolio Allocation During COVID-19
 The table shows the change in portfolio allocation of active funds during the COVID-19 pandemic. The sample includes derivative users that report holdings in February 2020 and March 2020. Funds are sorted by the absolute derivative weight at the last quarter of 2019 into token users, medium users, and heavy users, following a 50/30/20 cut. The percentage numbers in parenthesis show the relative change in weight from the previous quarter.

	Full Sample	Token Users	Medium Users	Heavy Users
Absolute Derivative Weight	1.41*** (96.24%)	0.32*** (974.99%)	1.1*** (172.39%)	4.72*** (73.31%)
- Long	0.72*** (75.7%)	0.1*** (320.33%)	0.45*** (111.88%)	2.73*** (65.5%)
- Long Positive	-0.03 (-3.6%)	0.04*** (200.54%)	0.24*** (71.02%)	-0.62 (-18.42%)
- Long Negative	0.75*** (415.05%)	0.05*** (597.92%)	0.21*** (311.46%)	3.36*** (422.56%)
- Short	0.69*** (134.31%)	0.23*** (7286.57%)	0.64*** (278.84%)	1.99*** (87.69%)
- Short Positive	0.42*** (193.52%)	0.03*** (3336.36%)	0.36*** (326.52%)	1.51*** (161.97%)
- Short Negative	0.27*** (91.44%)	0.2*** (8909.38%)	0.28*** (234.1%)	0.48 (35.94%)
Equity	-2.2*** (-2.66%)	-1.22*** (-1.31%)	-3.91*** (-5.08%)	-2.29*** (-3.59%)
Debt	0.24 (4.34%)	0.13 (8.01%)	0.03 (0.42%)	0.98 (6.33%)
STIV/Repo	1.4*** (20.15%)	0.7*** (16.36%)	2.44*** (31.93%)	1.71 (12.74%)
Cash	0.83*** (47.36%)	0.79*** (111.84%)	1.12*** (29.71%)	0.56 (36.36%)

positions lose money when the market is down by 20% in the first quarter of 2020? The market is down by over 30% between February 20 and March 23, then sharply rebounds to -19% by the end of March. The payoff of short positions largely depends on when managers enter positions, which we will discuss in more details in Section 5.3, where we analyze the cross-sectional derivative trading.

The increase in derivative use does not come from extensive margin, as the number of derivative users slightly changed from 742 in the last quarter of 2019 to 754 in the first quarter of 2020. Moreover, the increase in derivative use is not driven by a small number of funds heavily building up their derivative positions. Instead, it is a shift in employing more derivatives by the entire industry. As shown in Panel A of Figure 1, the CDF of the absolute derivative weight shifts to the right during the crisis. The absolute derivative weight in the pre-crisis period is first-order stochastic dominated by the crisis period with a p-value less than 0.1%, suggesting a shift towards extensively using derivatives by fund managers.

5.2 Managers' Reaction to Stay-at-home Order

The previous section shows the time-series increase in derivative use. In this section, we explore the cross-sectional variation in derivative use during the initial outbreak of the pandemic. As the number of COVID-19 cases rose in the US, many states have imposed state-level Stay-at-home Order (SAH) to reduce COVID-19 spread. The staggering of SAH introduction at the state level allows us to test, cross-sectionally, how the pandemic influence fund managers' trading strategy on derivative positions. By the end of March, 25 states have SAH in place, and 11 states do not.¹⁴ Focusing on a sample of funds reporting in March 2020, we have 377 derivative users in states with SAH before March 31, 2020, and 72 users in states without SAH.

Figure 4 shows the derivative weights before and during the COVID-19 pandemic. The sample includes funds that report holdings in September 2019, December 2019, and March

¹⁴We only study states with at least one mutual fund. Figure 5 shows a map of states with SAH status by March 31, 2020.

2020. The orange (blue) bars show the average derivative weights of funds residing in states with (without) SAH in place before the end of March 2020. The solid black lines represent the corresponding 95% confidence interval. The number in the parenthesis shows the number of funds in each group. The total number of funds in the analysis is less than the number of all derivative users in our sample because not all funds report at the calendar quarter-end.

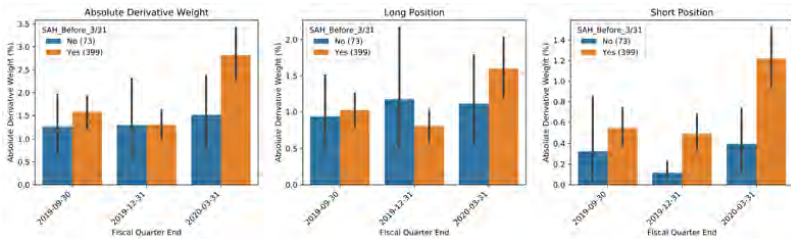
As shown in Panel (a) of Figure 4, derivative use, proxied by the absolute derivative weight, increases significantly from 1.3% in December 2019 to 3% in March 2020 for funds residing in states with SAH in place, whereas there are no significant reactions for funds in states without SAH. Diving into long and short positions reveals a larger jump of the absolute derivative weight from short positions on a relative scale than long positions for funds with early SAH in place. The results suggest that fund managers actively bet on short positions using swaps and futures when entering into the pandemic, and the pattern is more prevalent among managers in states with early SAH in place, as the risk of a potential recession is likely to be more salient in them. Moreover, the change in derivative use between September 2019 and December 2019 is insignificant, which rules out the alternative explanation that there might be a common trend of increased derivative use for funds in states with early SAH.

Panel (b) of Figure 4 further decomposes the derivative weight by whether it is a long or short position and whether the weight is positive or negative. Consider the two graphs on the right-hand side of Panel (b) as an example. The distance between the top bar and the bottom bar widens in March 2020. Even though managers trade more derivatives in short positions when entering the pandemic, they enter at different time so that some funds have positive weights of short derivative positions, while others have negative weights. Note that the market rebounded sharply after March 23. The portfolio weight of short derivative positions will depend largely on when managers opened the positions. In untabulated results, we find that the average time-to-maturity of new short derivative positions significantly decreases from six months in pre-crisis period to four months during the crisis among SAH funds.

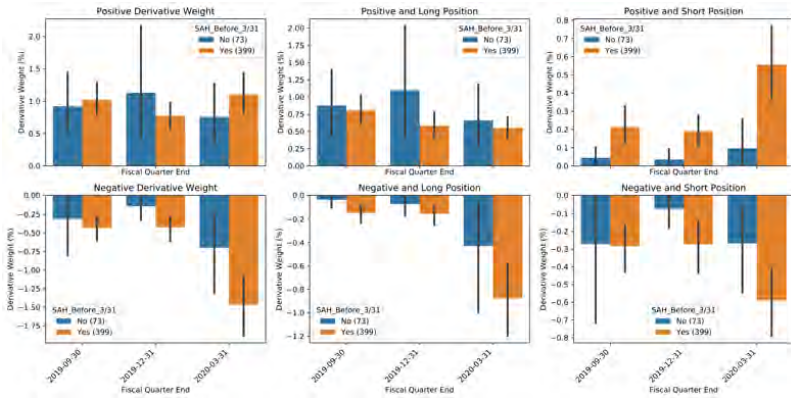
Figure 4
Derivative Weight and Stay-at-home Orders

The figure shows the derivative weights of active funds before and during the COVID-19 pandemic. The sample includes funds that report holdings in September 2019, December 2019, and March 2020. The orange (blue) bars show the average derivative weights of funds residing in states with (without) the Stay-at-home order in place before the end of March 2020. The solid black lines represent the corresponding 95% confidence interval. The number in the parenthesis shows the number of funds in each group. Panel (a) shows the absolute derivative weight for two groups. Panel (b) further decomposes the derivative weight by whether it is long or short positions, and by whether the weight is positive or negative. Panel (c) shows the gross leverage and net leverage for both existing positions and new positions.

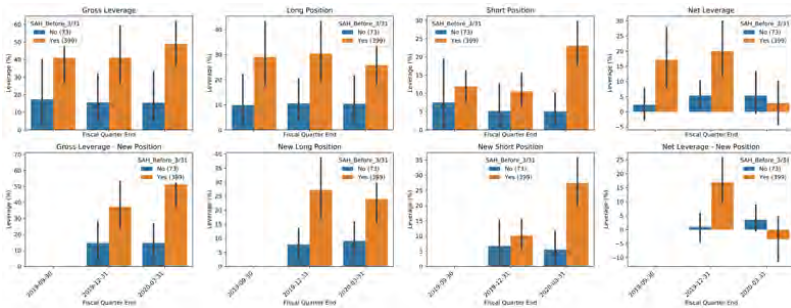
(a) Absolute Derivative Weight and SAH



(b) Derivative Weight Decomposition



(c) Derivative Leverage



Covid Economics 49, 18 September 2020: 172-221

In contrast, there is no change in long positions or among funds without SAH. The results suggest that, even among managers who face salient risk of recession and seek downside protections by shorting derivatives, there is large cross-sectional variation in market timing. Fund managers who opened short positions fairly late during the crisis will incur losses when the market rebounded sharply and unexpectedly after March 23, 2020.

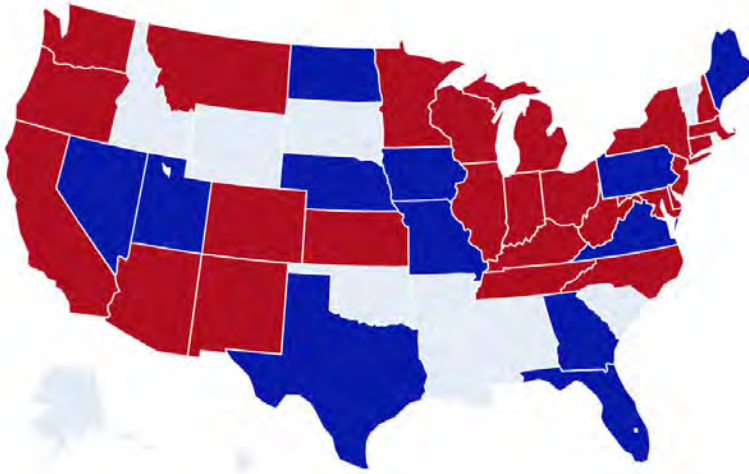
Panel (c) of Figure 4 shows how derivative leverage changes quarter-by-quarter. The top row shows the leverage of all positions, and the bottom row shows the leverage of new positions. We can see that there is a large jump in leverage of short derivative positions for funds with SAH in place, whereas there is no response for funds without SAH by the end of March. Our results suggest, as the risk of economic downturn becomes more salient in states with SAH in place, managers actively seek exposure to hedge against market downturn.

One may concern that funds in states with early SAH are inherently different from funds in states without SAH. For example, New York, Massachusetts, and California have SAH before the end of March, and these states have large financial centers and a large number of registered mutual funds. To rule out this alternative explanation, we conduct analyses on a subsample, where states with and without SAH are geographically adjacent to each other and have a comparable number of funds. Specifically, we include funds in the following states: Colorado, Ohio, Minnesota, Wisconsin, Kansas, Texas, Pennsylvania, Missouri, Iowa, and Nebraska. The first five states have SAH before March 31, 2020, and the remaining five states do not have SAH by the end of March. A map of states with their SAH status is shown in Figure 5.

Figure 6 shows the derivative weight and leverage of funds in these ten states. Note that the number of funds in each group is now balanced, 63 funds in states with early SAH, and 69 funds in states without SAH. Funds in states with early SAH, such as Colorado, Ohio, Minnesota, Wisconsin, and Kansas, increase the derivative use, which is mainly driven by the short positions, whereas funds in the remaining five states have little change in derivative use. Our result shows that managers' response to COVID-19 crisis is more prevalent when

Figure 5
Map of Stay-at-home Order

The figure plots the status of Stay-at-home order by March 31, 2020. The red (blue) states have SAH in place before (after) March 31, 2020. The white states do not have active domestic equity funds registered.



the risk of a potential recession becomes more salient, and it is not simply driven by some unobserved characteristics among managers in large financial centers.

5.3 Derivative Performance During the Crisis

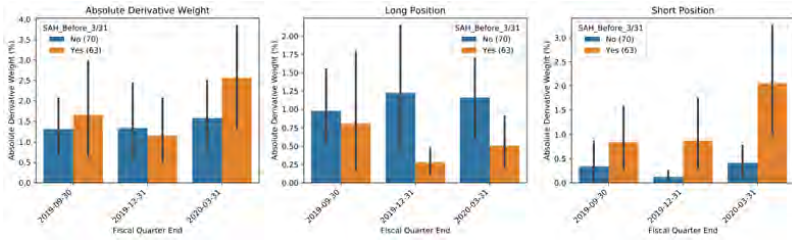
Having documented the increased derivative use during the crisis, it is interesting to see how derivative positions perform and how they contribute to fund returns, with a focus on the COVID-19 crisis period. So far, no studies systematically examine the performance of derivative positions. Using monthly level realized and unrealized PnL from N-PORT, we are the first to shed light on derivative performance and explore its impact on funds' overall returns.

Panels (a) and (b) of Figure 7 show the distribution of derivative and non-derivative returns before and during the crisis. The pre-crisis period is between July 2019 and January 2020. The crisis period includes February 2020 and March 2020. The distribution of non-

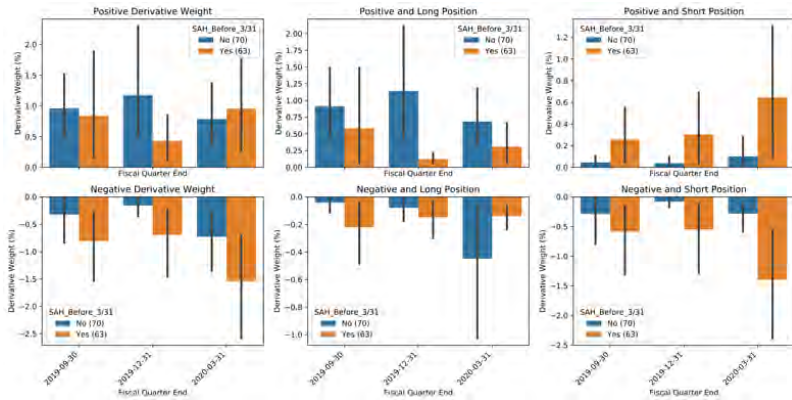
Figure 6
Stay-at-home Around the Border

The figure shows the change in derivative weight in response to Stay-at-home order around borders. Different from Figure 4, the sample only includes funds in the following states: CO, OH, MN, WI, KS, TX, PA, MO, IA, NE. The first five states have SAH before March 31, 2020.

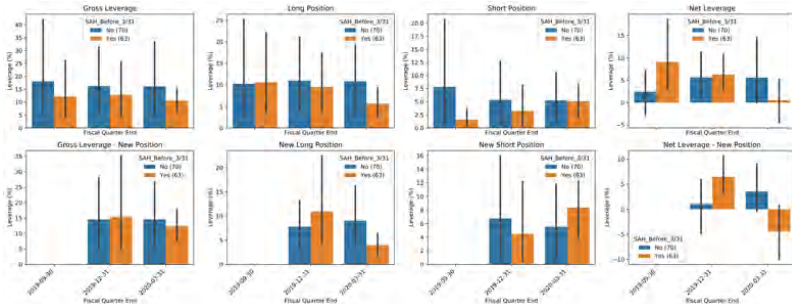
(a) Absolute Derivative Weight and SAH



(b) Derivative Weight Decomposition



(c) Derivative Leverage

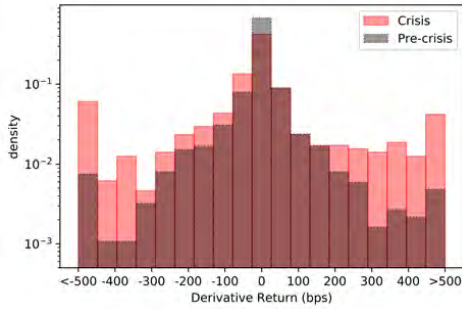


derivative returns follows a bell curve centered slightly positive before the crisis, and it shifts with massive density to the left during the crisis, which is not surprising because of the market crash.

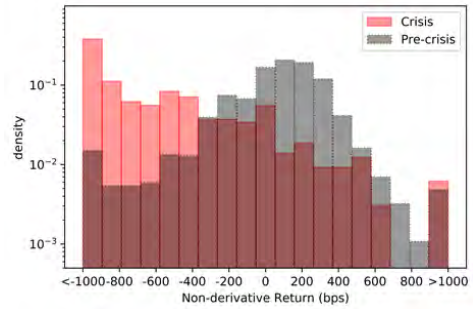
Figure 7
Distribution of Derivative Return in Crisis

The figure shows the distribution of derivative and non-derivative returns. Panel (a) and (b) compare the distributions in pre-crisis and during crisis periods. Panel (c) and Panel (d) compare the distributions of amplifying and hedging funds during the crisis. For panels (a) and (c), derivative returns are plotted between -5% and 5%, with a bandwidth of 50 bps. Densities of returns that are greater (smaller) than 5% (-5%) are stacked at the boundary. For panels (b) and (d), non-derivative returns are plotted between -10% and 10%, with a bandwidth of 100 bps. Densities of returns that are greater (smaller) than 10% (-10%) are stacked at the boundary. Crisis period is defined as February 2020 and March 2020. Pre-crisis period is between July 2019 and January 2020. The y-axis is in log-scale.

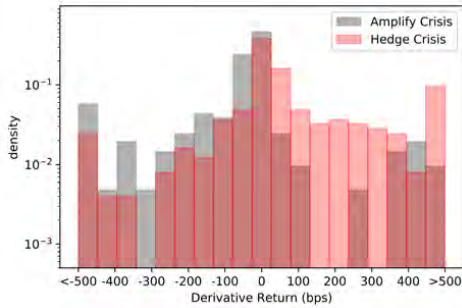
(a) Derivative Return



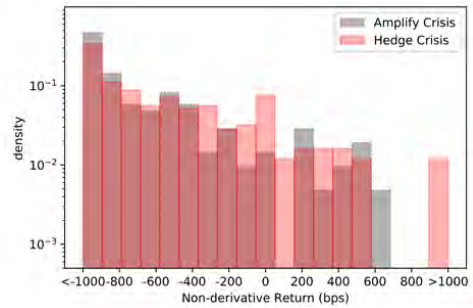
(b) Non-derivative Return



(c) Derivative Return - Amplify vs Hedge



(d) Non-derivative Return - Amplify vs Hedge



Interestingly, the distributions of derivative returns are centered around zero both pre-crisis and during the crisis. What is different in crisis period is that the distribution has fatter tails than pre-crisis period. This is consistent with the increased short derivative positions

and the divided opinions on when to open these positions shown in Figure 4. Managers who built short derivative positions before or during the initial market crash will gain, whereas managers who were slower to react opened short positions around the unanticipated market rebound will lose substantially. The distributions are significantly different from each other, as the p-values of Kolmogorov-Smirnov tests are less than 1%.

Although we do not directly observe the exact date when managers trade derivatives, we show that our pre-crisis classification of amplifying and hedging funds can explain the cross-sectional variation in derivative returns during the crisis. Panels (c) and (d) of Figure 7 compare return distributions for amplifying and hedging funds. Note that the derivative returns of hedging funds are more likely to have large positive returns than amplifying funds during the crisis, whereas the distributions of non-derivative returns are similar between the two groups. Among heavy derivative users, hedging funds have derivative returns of 1.4% per month during the crisis period, whereas amplifying funds have derivative returns of -1.3% per month.

How do amplifying funds lose from derivative positions during the crisis? In untabulated results, we find that amplifying funds significantly increase short derivative composition, from the pre-crisis level of less than 10% to 27% during the crisis. The increase in short positions is not merely due to a decrease in long positions. In fact, amplifying funds actively increase their short leverage from 2.5% to 11.4%. Despite the increase in short positions, amplifying funds still have massive exposure to the market due to their outstanding long positions, which will incur large losses when the market crashes.

Amplifying funds also lose from their new short positions. The average time-to-maturity of new short positions decreases from 6 months in pre-crisis periods to 3 months during the crisis, whereas there is no change in long positions. Unlike amplifying funds, hedging funds open short positions with a time-to-maturity of 6 months, both in pre-crisis periods and during the crisis. As fund managers typically enter a fixed set of derivative contracts, the decreased time-to-maturity of amplifying funds' short positions suggests that they may

enter positions later than they would otherwise in pre-crisis period.¹⁵ When the market unexpectedly rebounds on March 23, amplifying fund managers lose on the newly entered short positions. Moreover, the negative unrealized PnL of amplifying funds' outstanding short positions in the holdings report of March 2020 also supports our conjecture that they are late to trade short derivatives. Specifically, the average unrealized PnL of amplifying (hedging) funds' short positions is about -15 bps (43 bps) in their March 2020 holdings report.

Figure 8 decomposes derivative returns by derivative instruments and show the return distribution of each instrument during the crisis. We can see that most of the cross-sectional variation in derivative returns comes from swap contracts, followed by futures. Options and foreign exchange related contracts provide limited variation in derivative returns. This finding highlights the importance of swap contracts to active equity funds, which have been overlooked in the previous studies.

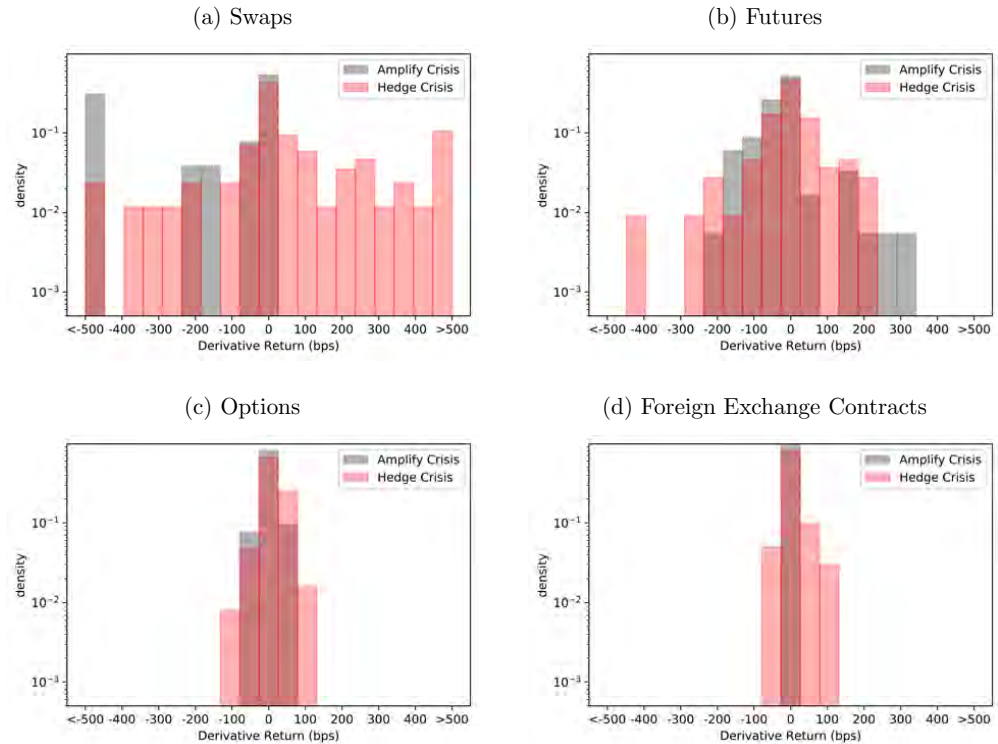
Next, we show how derivative strategies impact fund returns, especially during the crisis. Table 8 shows the performance of derivative users relative to nonusers during the COVID-19 pandemic. Similar to Pastor and Vorsatz (2020), our sample spans from January 1, 2019 to June 30, 2020, and includes all derivative users and nonusers. The crisis period is defined between February 20, 2020, and March 23, 2020. The recovery period is from March 24, 2020. Derivative users are classified by the extent of derivative use and by the pre-crisis correlation between derivative and non-derivative returns into nine (3-by-3) groups, and we only report the coefficient estimates for heavy hedging and heavy amplifying funds due to space limit.¹⁶ All coefficient estimates are in annualized percentage points. The dependent variables from columns (1) to (4) are fund returns, benchmark adjusted returns, CAPM alphas, and Fama-French five-factor alphas. The dependent variables from columns (5) to (8) are hypothetical fund returns based on reported equity positions. All dependent variables

¹⁵We find no changes in the number of unique short derivative positions from pre-crisis period to the crisis period.

¹⁶Token users have very similar performance with nonusers. Medium users behave similarly as heavy users. The full table is available upon request.

Figure 8
Distribution of Derivative Instrument Return in Crisis

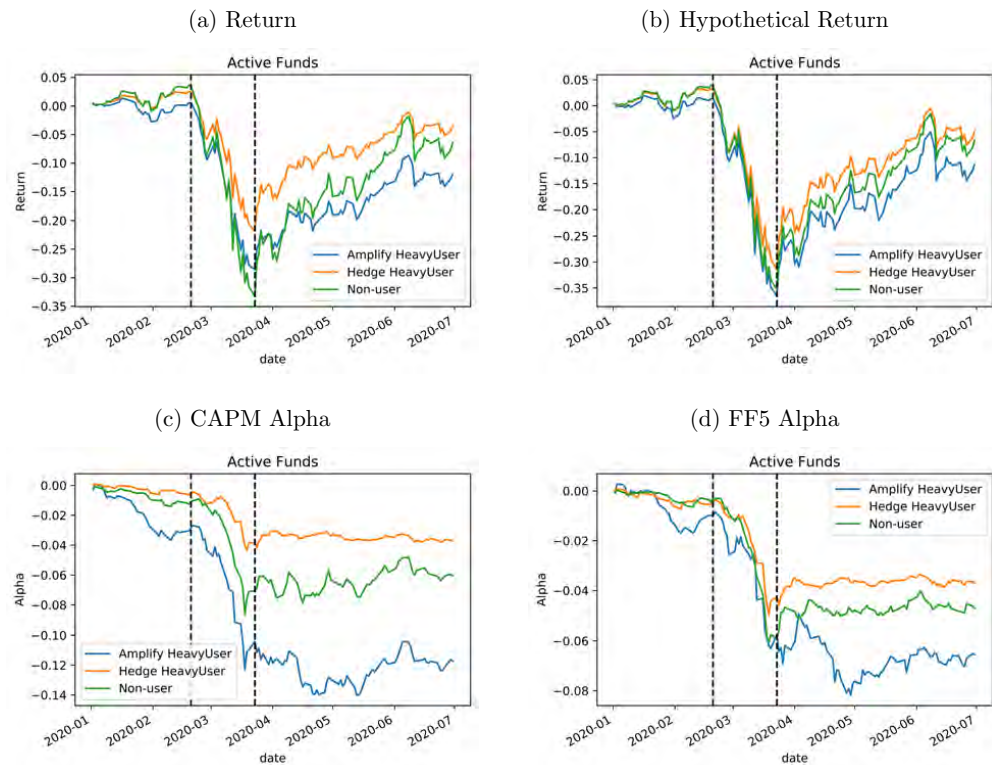
The figure shows the return distribution of derivative instruments. For all instruments, derivative returns are plotted between -5% and 5%, with a bandwidth of 50 bps. Densities of returns that are greater (smaller) than 5% (<-5%) are stacked at the boundary. Crisis period is defined as February 2020 and March 2020. The y-axis is in log-scale.



are in annualized percentage points.

Figure 9
Fund Performance in COVID-19 Pandemic

The figure shows the cumulative returns and alphas for active funds starting in January 2020. Nonusers are the funds without derivative positions. For derivative users, funds are sorted by the absolute derivative weight into deciles. Token users are the funds in the bottom five deciles. Medium users are the funds between the sixth and eighth deciles. Heavy users are the funds in the top two deciles. Derivative users are further partitioned by the correlation between derivative and non-derivative returns prior to February 2020 into three terciles. Amplifying funds are in the top tercile, and hedging funds are in the bottom tercile. The figure shows the performance of nonusers, heavy amplifying users, and heavy hedging users. Token users behave similarly to nonusers. Daily alphas are estimated using a one-year rolling window. The dotted vertical lines indicate the start of crisis period (February 20, 2020) and recovery period (March 24, 2020).



Heavy hedging funds significantly underperform nonusers in returns during normal times, while they significantly outperform nonusers by an annualized 8.9% CAPM alpha and 14% Fama-French five-factor alpha during the crash period. Such outperformance during the crash stems their derivative positions and active trading, as there is an insignificant differ-

Covid Economics 49, 18 September 2020: 172-221

Table 8
Performance During the COVID-19 Pandemic: Amplify vs Hedging

The table shows the performance of derivative users from January 1, 2019, to June 30, 2020. Daily alphas are estimated using fund daily returns with a one-year rolling window. All dependent variables are in annualized percentage points. The dummy variable *crash* is equal to one between February 20, 2020, and March 23, 2020. The dummy variable *recovery* is equal to one between March 24, 2020, and June 30, 2020. The sample includes all derivative users and nonusers. Among derivative users, funds are further classified by the extent of derivative use in the last quarter of 2019 into token, medium, and heavy users. Derivative users are also grouped by the pre-crisis correlation between derivative returns and non-derivative returns into terciles. Funds in the top (bottom) tercile are classified as amplifying (hedging) funds. The performance of nonusers is served as the baseline in all regressions. We only report heavy amplifying funds and heavy hedging funds due to page space. All regression specifications include fund controls, time fixed effect, and style fixed effect. All standard errors are clustered at fund level.

	(1) <i>Ret</i>	(2) $Ret_{heavy}^{BenchAdj}$	(3) α_{CAPM}	(4) α_{FF5}	(5) Ret_{heavy}	(6) $Ret_{heavy}^{BenchAdj}$	(7) α_{CAPM}	(8) α_{FF5}
AmplifyHeavy	0.0361 (0.01)	1.884 (1.57)	1.995 (0.97)	1.284 (0.81)	-5.393** (-1.96)	-3.692** (-2.01)	-3.676 (-1.44)	-3.183 (-1.63)
HedgeHeavy	-3.462** (-2.19)	1.004 (1.32)	0.210 (0.16)	-0.426 (-0.43)	-0.365 (-0.22)	2.860*** (2.59)	-0.290 (-0.19)	-0.502 (-0.43)
AmplifyHeavy × crash	33.54*** (8.78)	-7.393*** (-4.02)	6.673** (2.12)	-0.474 (-0.20)	4.317 (1.15)	-2.20 (-0.82)	-4.804 (-1.38)	-11.30*** (-4.24)
HedgeHeavy × crash	36.45*** (6.81)	-9.573*** (-3.72)	8.889** (2.02)	14.01*** (4.13)	6.984 (1.34)	-2.93 (-1.56)	1.640 (0.34)	6.223* (1.68)
AmplifyHeavy × recovery	-26.07*** (-4.93)	2.659 (1.05)	-2.859 (-0.66)	-1.382 (-0.41)	-7.095 (-1.16)	0.990 (0.24)	-0.489 (-0.09)	-0.935 (-0.22)
HedgeHeavy × recovery	-49.02*** (-14.12)	-9.110*** (-5.45)	-9.539*** (-3.34)	-6.024*** (-2.74)	-12.83*** (-3.50)	16.81*** (6.87)	-5.009 (-1.48)	-2.549 (-0.98)
Controls	Yes	Yes	Yes	Yes	Yes	Yes	Yes	Yes
TimeFE	Yes	Yes	Yes	Yes	Yes	Yes	Yes	Yes
StyleFE	Yes	Yes	Yes	Yes	Yes	Yes	Yes	Yes
Adjusted R^2	0.0833	0.0615	0.123	0.0760	0.0874	0.0465	0.134	0.0770
F	118.7	30.92	9.979	18.02	8.473	96.42	3.448	12.04
N	1024206	1024206	1024206	1024206	944067	944067	943817	943817

t statistics in parentheses

* $p < 0.1$, ** $p < 0.05$, *** $p < 0.01$

ence in hypothetical equity returns between the two groups. Like most insurance products, although heavy hedging users outperform during the crisis, they underperform nonusers during the recovery.

Heavy amplifying funds do not differ in performance from nonusers in pre-crisis periods. They outperform nonusers by an annualized 6.7% CAPM alpha during the crisis, but the performance gap becomes insignificantly different from zero using the Fama-French five-factor model. During the recovery, heavy amplifying funds significantly outperform nonusers only by returns, but not by risk-adjusted alphas. One potential driving force of amplifying funds' mediocre performance is that they opened short derivative positions fairly late in March so that the derivative positions drag down their overall performance.

Figure 9 shows the cumulative performance of funds since 2020.¹⁷ Consistent with Table 8, the performance gap between heavy hedging users and nonusers widens during the crisis period and gradually shrinks in the recovery period. The gap does not completely diminish by the end of June. In fact, the gap in Fama-French five-factor alpha between heavy hedging users and nonusers remains flat since May 2020. Moreover, there is no difference in hypothetical returns among all funds, suggesting that the gap in performance at least partially comes from the derivative positions.

To cleanly identify whether the outperformance of heavy hedging funds comes from derivative positions or active trading of stocks, we study the monthly fund return and decompose it into derivative and non-derivative returns. Table 9 shows the return decomposition for the crisis period and recovery period. In panel A, heavy hedging funds have an average return of -5.24% during the crisis. Their derivative return is 1.4%, which plays a crucial role in helping funds minimize their losses from non-derivative positions (-6.63%). The difference between hypothetical return and non-derivative return is 2.44%, which can be viewed as the upper bound of the gain from active trading. Heavy amplifying funds, to the contrary, suffer losses both from their derivative positions (-1.3%) and from their active trading (-1.82%).

¹⁷The graph only shows the cumulative performance for heavy hedging funds and heavy amplifying funds. The full performance comparison among all derivative user groups is available upon request.

Table 9
Fund Return Decomposition

The table shows the monthly fund return decomposition for the crisis period and recovery period. Similar to Table 8, the table presents heavy amplifying funds, heavy hedging funds, and nonusers. For each fund-month observation, fund return is decomposed into two parts: derivative return and non-derivative return. We also calculate the monthly hypothetical equity return based on the most recent equity holdings. Columns 1-4 show monthly averages of derivative return, non-derivative return, fund return, and hypothetical return, respectively. All numbers are at monthly frequency and are in percentage points. The crisis period is between February 2020 and March 2020. The recovery period is between April 2020 and June 2020.

Panel A: Crisis Period

	Derivative Return	Non-derivative Return	Fund Return	Hypothetical Return
Nonusers			-11.78	-11.54
Heavy Amplify	-1.31	-10.02	-11.33	-8.20
Heavy Hedging	1.40	-6.63	-5.24	-9.07

Panel B: Recovery Period

	Derivative Return	Non-derivative Return	Fund Return	Hypothetical Return
Nonusers			6.88	6.82
Heavy Amplify	0.89	4.87	5.76	6.49
Heavy Hedging	-1.68	5.17	3.49	5.92

Active trading by nonusers has a tiny impact on fund performance, as the difference between hypothetical return and fund return is only 0.24%. Panel B shows the decomposition for the recovery period. During the recovery period, heavy hedging funds take losses from their derivative positions (-1.68%) and active trading (-0.75%), which is consistent with their hedging strategy. Heavy amplifying funds gain from derivative returns by 0.89% per month, but the magnitude is much smaller than what they have lost during the crisis. Similar to the crisis period, they lose from active trading by 1.62%.

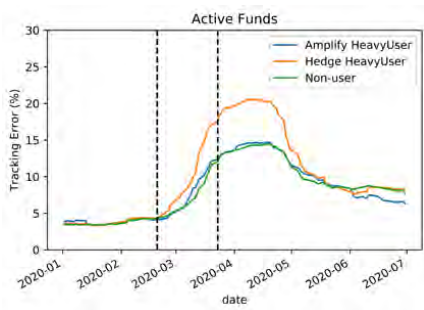
Figure 10 shows various risk measures of funds starting from 2020. Panel (a) and (b) show the tracking error of fund realized returns and hypothetical returns, respectively. Tracking error is calculated as the annualized 30-day rolling standard deviation of the difference between fund returns and benchmark returns.¹⁸ Funds all started at a similar tracking error of 5% before the crisis. The tracking error of heavy hedging funds spikes up to almost 20% during the crisis period, suggesting that their performance significantly differs from their

¹⁸The peak of tracking error after March 23 is due to the 30-day rolling estimation.

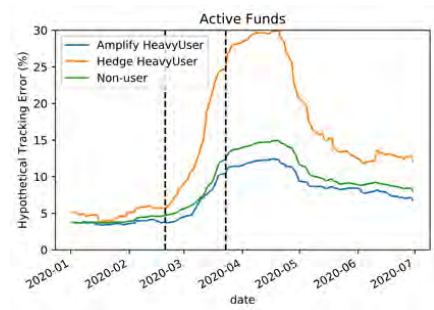
Figure 10
Fund Risk in COVID-19 Pandemic

The figure shows the tracking error and volatility of active funds starting in January 2020. Nonusers, heavy amplifying users, and heavy hedging users are defined as in Figure 9. Panel (a) shows the annualized tracking error, which is the 30-day rolling standard deviation of the difference between fund returns and benchmark returns. Panel (b) shows the annualized hypothetical tracking error, which is the 30-day rolling standard deviation of the difference between fund hypothetical returns and benchmark returns. Panels (c) and (d) shows the 30-day rolling return volatility and hypothetical return volatility, scaled by the 30-day rolling average of VIX. Panel (e) shows the 30-day rolling volatility of the difference between fund return and hypothetical return, scaled by the 30-day rolling average of VIX. The dotted vertical lines indicate the start of crisis period (February 20, 2020) and recovery period (March 24, 2020).

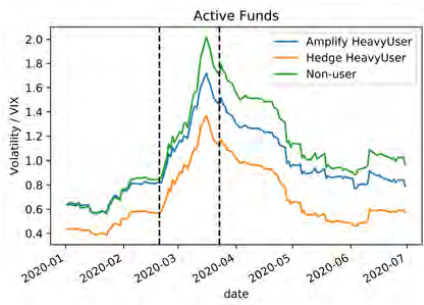
(a) Tracking Error



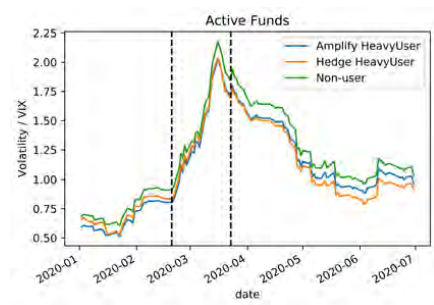
(b) Hypothetical Tracking Error



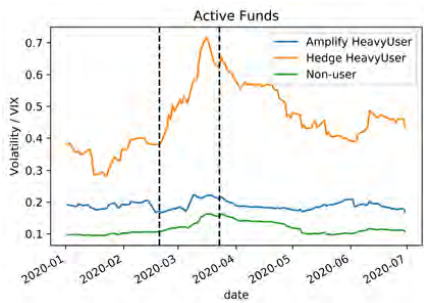
(c) Volatility / VIX



(d) Hypo Volatility / VIX



(e) Volatility of (ret - ret^{hypo}) / VIX



Covid Economics 49, 18 September 2020: 172-221

benchmark. At first glance, it seems that the derivative positions and active trading of heavy hedging funds make fund returns riskier and further deviating from the benchmark. However, heavy hedging funds' hypothetical tracking error jumps up to around 30%, even more than the realized tracking error. Taking the two pieces of evidence together, we show that heavy hedging funds hold equities that perform very differently from their benchmark in the crisis, and derivative positions and active trading reduce the tracking error.

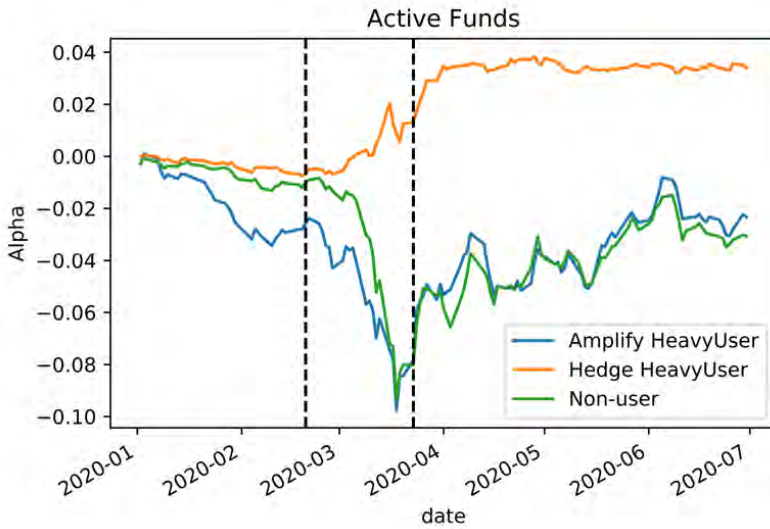
Panel (c) of Figure 10 plots the 30-day rolling volatility scaled by the 30-day rolling average of the VIX index. Heavy hedging users have lower volatility than other funds, and the gap widens during the crisis period. On the contrary, the hypothetical volatility is similar between hedging users and others, as is shown in panel (d). The result suggests that, during the crash, while equity returns have similar volatility, derivative positions of hedging funds yield positive returns. Overall, fund returns are not as volatile as other funds. Panel (e) plots the volatility of the performance gap between realized and hypothetical fund returns, scaled by the 30-day rolling average of the VIX index. A large measure suggests either active trading on equity positions, large returns from derivative positions, or both. The measure spikes for hedging users during the crisis period, but remains relatively flat for nonusers and amplifying users. This result further supports the evidence that hedging users' outperformance during the crisis is mainly from their derivatives trading, rather than equity holdings.

To formally test whether hedging users are better equipped than others when there is a market crash, we incorporate market-downturn factors into the CAPM model. The factor model includes a down-market dummy that is equal to one if the market return is negative, the excess return of the market and its squared term, and their interaction terms with the down-market dummy. We then use 5-year daily returns before 2020 to estimate the factor loading and calculate the out-of-sample daily alpha in 2020. Specifically, for each fund, we

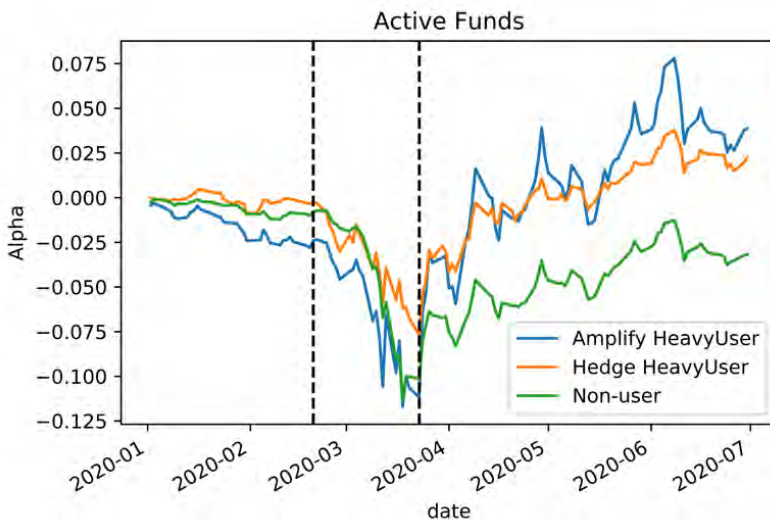
Figure 11
Derivatives and Crash Risk

The figure shows the cumulative down-market alphas starting in January 2020. Nonusers, heavy amplifying users, and heavy hedging users are defined as in Figure 9. The factor model includes a down-market dummy, the excess return of the market and its squared term, and their interaction terms with the down-market dummy. For each fund, we estimated the factor loading use 5-year daily fund returns before 2020. We then calculate the daily down-market alpha using the estimated factor loading and plot the average cumulative alpha for each fund group.

(a) Down-market Alpha



(b) Hypothetical Down-market Alpha



Covid Economics 49, 18 September 2020: 172-221

run the following regression:

$$r_t - rf_t = \beta_0 + \beta_1 \mathbb{1}_{mktf_t < 0} + \beta_2 mktf_t + \beta_3 mktf_t^2 + \beta_4 mktf_t \mathbb{1}_{mktf_t < 0} + \beta_5 mktf_t^2 \mathbb{1}_{mktf_t < 0} + \epsilon_t,$$

where $mktf$ is the market excess return, r is the fund return, and rf is the risk-free rate.

Figure 11 shows the cumulative alpha starting from 2020. Surprisingly, after controlling for the market downturn risk, hedging users have even positive alphas in the crisis period. Meanwhile, the gap in alphas with other funds does not diminish during the recovery period. Specifically, the performance gap is as large as 9.2% on March 23, and it remains around 6% afterward. Moreover, the gap is not driven by different equity holdings, as the hypothetical alphas are very similar across all funds. Our result has important implications for investors with strong hedging motives, who value performance the most when the market crashes.

6 Conclusion

Research on derivative use by mutual funds and the impact of derivative trades on funds' performance has been hampered by the lack of sufficiently granular data. Taking advantage of data that has become available only recently, we are able to shed new light on questions that were hard to evaluate earlier, overturning some prior conclusions.

Our data have two key advantages over the ones used in prior studies. First and foremost, our data include information not only on derivative positions, but also on realized and unrealized capital gains. This enables us to compute returns on the funds' derivative portfolios and compute derivatives' contribution to fund performance in differing market conditions. Second, capital gains of derivative positions are at a monthly frequency, allowing us to analyze behavior over fairly short time intervals, such as the crisis in financial markets during the outbreak of the Covid-19 pandemic. In addition, the data provide information not only on the extent of options and futures usage, but also on other derivative classes. Specifically, the data cover swaps, which account for a significant component of derivative portfolios of

active equity mutual funds and play a significant role in generating cross-sectional differences in performance during the Covid-19 period. Swaps have been ignored by prior research on mutual funds.

Early research identified the usage but not the extent of options and futures. To a large extent, that research failed to find differences in performance and risk between derivative users and nonusers. Our analysis shows that this non-result stems from the fact that over 50% of derivative users are token users with a derivative weight of less than 0.1%. Once we focus on funds that use derivatives extensively, we find significant differences both in performance and risk. Particularly, derivative users typically underperform nonusers and have lower market risk exposure. The lower exposure to market risk stems mostly from derivative positions, but not exclusively from them. The equity portfolio of funds that extensively use derivatives has a lower market beta than that of nonusers. Furthermore, in contrast to the commonly perceived view in the literature, we show derivatives are used by the majority of funds (63%) to amplify market exposure, rather than for hedging and risk management.

We utilize the Covid-19 pandemic as an exogenous shock that significantly impacts financial markets to evaluate the impact of derivative use on fund performance during periods of uncertainty. We are able to analyze not only what is the impact of existing positions on fund performance, but also to evaluate funds' trading in response to the crisis.

We show the extent of derivative use has a substantial impact on fund performance during both the breakout and recovery phases in financial markets. Fund managers increase short derivative positions to hedge against the possible recession. However, this pattern is mostly concentrated among funds registered in states with early Stay-at-home orders, making the risk of recession highly salient. Funds that use derivatives to amplify returns prior to the pandemic also increase short positions. However, even after their shift in strategy, they remain mostly amplifiers and sustain significant losses during the outbreak phase. Furthermore, relative to hedgers, their increase of short positions is delayed. Consequently, since the

recovery started unexpectedly on March 23, they enter too late into these short positions, leading to significant losses during the recovery phase as well. Hedgers, to the contrary, gain substantially from their derivative positions and outperform others during the crisis. Although hedgers underperform nonusers during the recovery phase, the performance gap they established during the crisis does not completely diminish by the end of our sample.

Our paper has potential policy implications on risk-taking by the mutual fund industry. Access to derivatives not only allow fund managers to hedge and risk management, but may also encourage managers to take on unnecessary risk to the detriment of fund investors. Retrospectively, amplifying funds, which constitute the majority of funds that use derivatives, do not deliver outperformance during the non-crisis period, and incurred substantial losses during the crisis period. Therefore, it is debatable whether allowing funds to have full access to derivative markets adds value to investors.

There are a few natural extensions one could consider. First, consider fixed income funds, something we are starting to work on. Second, while we conducted analyses at the derivative class level, one could envision analyzing at the individual security level as well. Third, consider how derivative strategies vary throughout the calendar year and how they are related to interim past performance. These are left for future research. Specifically, since N-PORT reports become a requirement only recently, it will probably be a couple of years until one can carefully consider the third.

References

- Almazan, Andres, Keith C. Brown, Murray Carlson, and David A. Chapman, 2004, Why constrain your mutual fund manager?, *Journal of Financial Economics* 73, 289–321.
- Calluzzo, Paul, Fabio Moneta, and Selim Topaloglu, 2017, Use of Leverage, Short Sales, and Options by Mutual Funds, *SSRN Electronic Journal* .

- Cao, Charles, Eric Ghysels, and Frank Hatheway, 2011, Derivatives do affect mutual fund returns: Evidence from the financial crisis of 1998, *Journal of Futures Markets* 31, 629–658.
- Cici, Gjergji, and Luis-Felipe Palacios, 2015, On the use of options by mutual funds: Do they know what they are doing?, *Journal of Banking & Finance* 50, 157–168.
- Deli, Daniel N., and Raj Varma, 2002, Contracting in the investment management industry: Evidence from mutual funds, *Journal of Financial Economics* 63, 79–98.
- Dessaint, Olivier, and Adrien Matray, 2017, Do managers overreact to salient risks? Evidence from hurricane strikes, *Journal of Financial Economics* 126, 97–121.
- Falato, Antonio, Itay Goldstein, and Ali Hortaçsu, 2020, Financial Fragility in the COVID-19 Crisis: The Case of Investment Funds in Corporate Bond Markets, Working Paper 27559, National Bureau of Economic Research.
- Frino, Alex, Andrew Lepone, and Brad Wong, 2009, Derivative use, fund flows and investment manager performance, *Journal of Banking & Finance* 33, 925–933.
- Koski, Jennifer Lynch, and Jeffrey Pontiff, 1999, How Are Derivatives Used? Evidence from the Mutual Fund Industry, *The Journal of Finance* 54, 791–816.
- Lichtenstein, Sarah, Paul Slovic, Baruch Fischhoff, Mark Layman, and Barbara Combs, 1978, Judged frequency of lethal events, *Journal of Experimental Psychology: Human Learning and Memory* 4, 551–578.
- Natter, Markus, Martin Rohleder, Dominik Schulte, and Marco Wilkens, 2016, The benefits of option use by mutual funds, *Journal of Financial Intermediation* 26, 142–168.
- Pastor, Lubos, and M. Blair Vorsatz, 2020, Mutual Fund Performance and Flows During the COVID-19 Crisis, *Covid Economics* 38, 1–36.

Assessing the ethnic employment gap during the early stages of COVID-19

Maria Mavlikeeva¹

Date submitted: 7 September 2020; Date accepted: 8 September 2020

The outbreak of COVID-19 led to a spike in the unemployment rate and a decrease in the number of job openings. It is unknown whether this shock in the labor market affects different groups of job seekers equally. With the help of a correspondence study I describe the relationship between labor market conditions and ethnic labor inequality. The results provide evidence of the changes in the ethnic employment gap during the early stage of the COVID-19 outbreak. Moreover, these changes are accompanied by fluctuations in the labor market competition.

¹ University of Kassel.

Copyright: Maria Mavlikeeva

1. Introduction

One of the adverse effects of the spreading COVID-19 virus is the dramatic shock to the labor market. According to an official report of the International Labour Organization (ILO), there is a loss in working hours worldwide in 2020. In comparison with the last quarter of 2019, there is a strong decline in working hours of 5.4 percent during the first quarter of 2020 and 14 percent during the second quarter of 2020.¹ This raises the question whether the observed labor shock has an equally severe effect for different ethnic groups.

A number of studies focusing on ethnic hiring inequality provide evidence of unfavourable treatment toward minority job applicants (Bertrand and Mullainathan, 2004; Baert, 2018). If the prospective employers have a choice between the candidates, they more often show the preference towards the candidates with native sounding names. However, little is known whether this ethnic employment gap changes during the time of COVID-19 pandemic.

Previous studies investigating whether the ethnic imbalance depends on the tightness of the labor market provide contradicting findings (Baert et al., 2015; Carlsson et al., 2018; Boulware and Kuttner, 2019). The present study exploits the unique situation in the labor market characterized by dynamic changes caused by the COVID-19 outbreak. In order to assess the ethnic employment gap during the first months of the pandemic I conduct a correspondence study in the Moscow labor market². The fictitious resumes with randomly varied names of applicants are sent to the real job openings. The aim is to investigate whether the recruiters are equally interested in the applicants with native or ethnic minority sounding names.

Ethnic minorities can be subject to marginalization especially during economic crises and the resulted fluctuations in the labor market, such as the current one caused by COVID-19. Presently only a few studies provide evidence regarding this issue (Baert et al., 2015; Carlsson et al., 2018; Boulware and Kuttner, 2019). Baert et al. (2015) use correspondence experimental framework to assess the fluctuations in ethnic hiring inequality. As a measurement of the labor market tightness, the researchers use data reported by the Public Employment Service (PES). Combining the results of the experiment with the data provided by the PES, the authors find no ethnic employment gap among occupations which have a low number of candidates and the longer mean duration of filling the vacancy. Whereas there is a significant ethnic imbalance for

¹ ILO Monitor: COVID-19 and the World of Work. Fifth edition (June 30 2020):

https://www.ilo.org/global/topics/coronavirus/impacts-and-responses/WCMS_749399/lang--en/index.htm

² A series of studies attempt to uncover labor market issues during the pandemic (Brodeur et al., 2020; Guven et al., 2020; Fairlie et al., 2020). Various observational studies are currently registered (see EEA COVID Registry: <https://www.eeassoc.org/index.php?site=JEEA&page=298&trs=299>). However, to the best of my knowledge, there is no other registered correspondence study that aims to assess the hiring discrimination during the COVID-19 outbreak.

occupations with a high number of applicants. These findings speak in favour of a positive relationship between an ethnic employment gap and labor market tightness.

Applying different measurements of ethnic discrimination in the US labor market, Boulware and Kuttner (2019) come to the same conclusion. The authors use administrative data of the US Equal Employment Opportunity Commission (EEOC), which provides the number of reported discrimination charges for different groups including ethnic minorities. As the level of discrimination varies among states, the researchers further analyse the unemployment rate in every state using the data from the Local Area Unemployment Statistics provided by the Bureau of Labor Statistics (BLS). These findings indicate growing ethnic discrimination under slack labor market conditions, when a large number of job seekers face a lack of posted vacancies.

Carlsson et al. (2018) reach a different conclusion evaluating the link between ethnic inequality and the condition of the Swedish labor market. As estimates for ethnic discrimination, the authors use the data from three correspondence studies conducted earlier. However, the researchers use two different approaches for measuring labor market tightness. One method is the same used in the aforementioned studies, where the condition of the labor market is estimated from the unemployment ratio provided by the Swedish Employment Agency. As an alternative measurement of labor market tightness the authors use the callback rate for native female applicants (based on the results of previous field experiments). They take the callback rate for this group of applicants as a basis and according to variations in this rate, they evaluate the changes in labor market conditions. Applying both these methods, the authors find that the ethnic employment gap decreases in a slack labor market.

One of the limitations of the aforementioned studies is that it is hard to find perfect measurements of labor market tightness as well as of the ethnic discrimination level. In the present paper the experimental method of correspondence study is applied to assess the ethnic employment gap, an approach widely adopted by researchers for assessing hiring discrimination (Bertrand and Mullainathan, 2004; Rich, 2014; Zschirnt and Ruedin, 2016; Baert, 2018). However, the distinctive feature of this research is that the level of ethnic discrimination is measured under the condition of rapidly changing labor market competition during the COVID-19 outbreak. I expect that the ethnic employment gap increases during the early stages of the COVID-19 pandemic because of the growing slackness of the labor market.

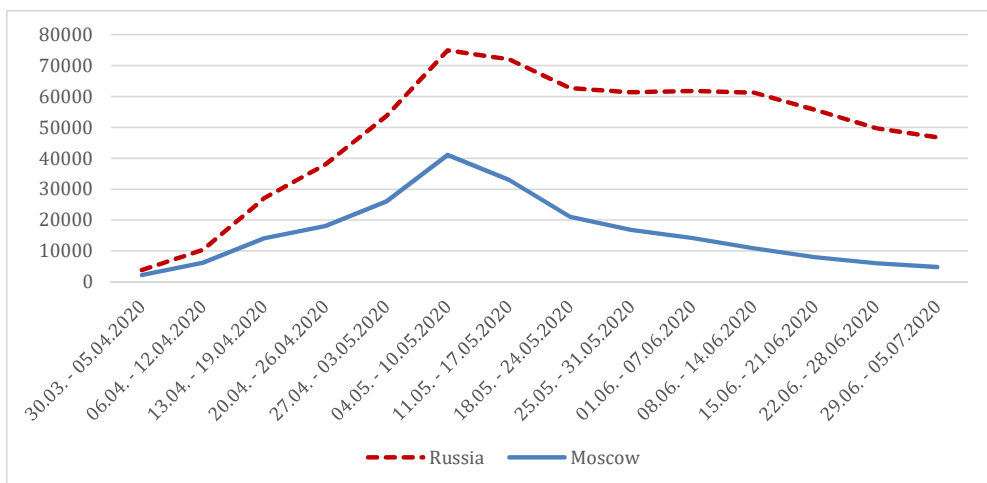
2. The spread of COVID-19 and labor market conditions in Moscow during the early stages of the pandemic

The COVID-19 virus, which originated from China, affected many other countries. Among the countries that suffer the most from Covid-19 such as the USA, Italy, Spain, Iran, Brazil and India, is also Russia. March 2 2020 was the beginning of the COVID-19 outbreak in Russia. Since then, the government has reported a growing number of new daily cases.

Being the city with the highest population in Russia (12.5 mln), Moscow has been particularly affected by the virus. On June 30 221,598 COVID-19 cases were registered in Moscow, which is more than one third of the overall number of registered cases in the whole country at this time (647,849).³

Figure 1 presents the reported new COVID-19 cases in Russia and separately in Moscow for the lockdown period between April 1 and June 30. As the situation began to develop so rapidly, the government decided to react with the imposition of some restrictive measures. On March 5 2020, the Mayor of Moscow, Sergej Sobyenin, issued a decree imposing the high alert regimen in the city⁴. A further series of decrees with additions and amendments were issued until the end of June. Table 1 presents the timeline of the key measures taken according to these decrees in Moscow.

Figure 1: New registered COVID-19 cases in Moscow and in Russia overall



Source: www.coronavirus-monitor.info , www.coronavirus.jhu.edu

³ <https://coronavirus-monitor.info/country/russia/moskva/>

⁴ <https://cdn.sobyenin.ru/static/pdf/ukaz-12-um-22-06.pdf>

At the end of March the Russian government announced non-working days for the citizens until April 30 2020 with the preservation of the full normal wage⁶. However, the first decrees regulating supportive measures for small and midsize businesses were issued later in April. On April 14 a Commission for the Support of Small and Midsize Businesses was created. On April 27 the Russian government introduced subsidies for businesses in the sectors most affected by the spread of coronavirus.⁷ These regulations came into force only in May 2020, which caused feelings of insecurity and uncertainty for the businesses in April.

Table 1: The timeline of COVID-19 measures in Moscow

Date	Measures
02.03.2020	First COVID-19 case is registered in Russia
05.03.2020	The high alert regimen is imposed
16.03.2020	State of emergency is imposed Mayor of Moscow, S. Sobyenin, recommends switching to working from home if possible
21.03.2020	Schools and kindergartens are closed
30.03.2020	Imposition of lockdown
28.04.2020	Lockdown is extended
12.05.2020	1st step of lockdown easing
27.05.2020	Lockdown is extended
01.06.2020	2nd step of lockdown easing
09.06.2020	Requirement of electronic authorisation for necessary travel is cancelled
22.06.2020	3rd step of lockdown easing

Source: www.sobyenin.ru

⁶ The Presidential Decree of 2 April 2020 <http://kremlin.ru/events/president/news/63134>

⁷ The Decree of April 14 2020 <https://sozd.duma.gov.ru/bill/942517-7>

The Decree of April 27 2020 <http://government.ru/docs/39582/>

Table 2: The rate of unemployment in Russia in February-June 2020

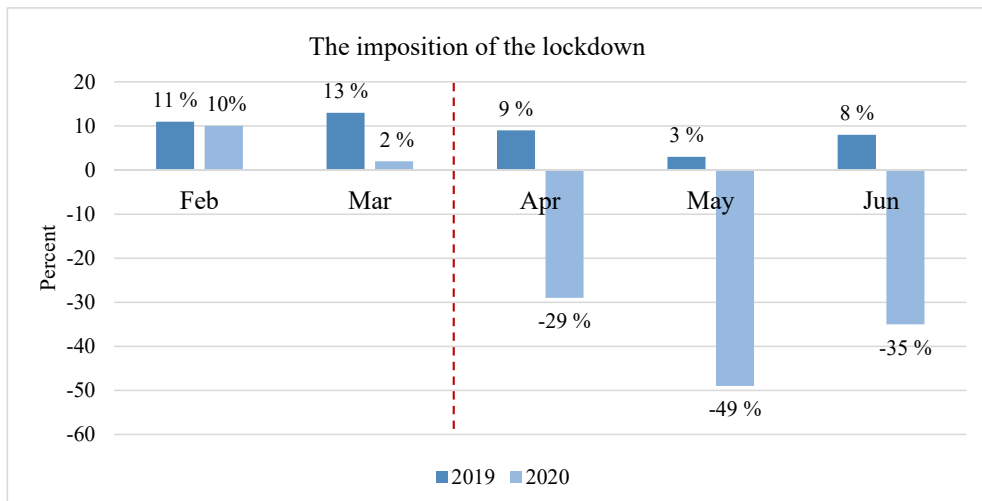
	Before Lockdown		After Lockdown		
	February	March	April	May	June
Number of unemployed persons according to ILO* (thousands)	3425	3485	4286	4513	4606
Number of officially registered unemployed persons (thousands)	730	727	1311	2143	2787

Note: *Persons, who are not hired or self-employed, have no income and are available for work (not only officially registered in the Employment Office).

Source: https://rosstat.gov.ru/bgd/free/B20_00/Main.htm

On April 7 2020, the Russian Agency of International Information (RIA Novosti) reported that almost 30 % of the workers were sent on unpaid leave or switched to a contract payment system⁸. As a lockdown was imposed, it became hard for the companies to fulfil their obligations to pay salaries, as most of them had little or no revenue. Moreover, a certain percentage of companies had to dismiss their employees. This fact is reflected in the official unemployment statistics (Table 2), which shows a spike in the unemployment rate after March 2020.

Figure 2: Changes in posted vacancy rate in Moscow



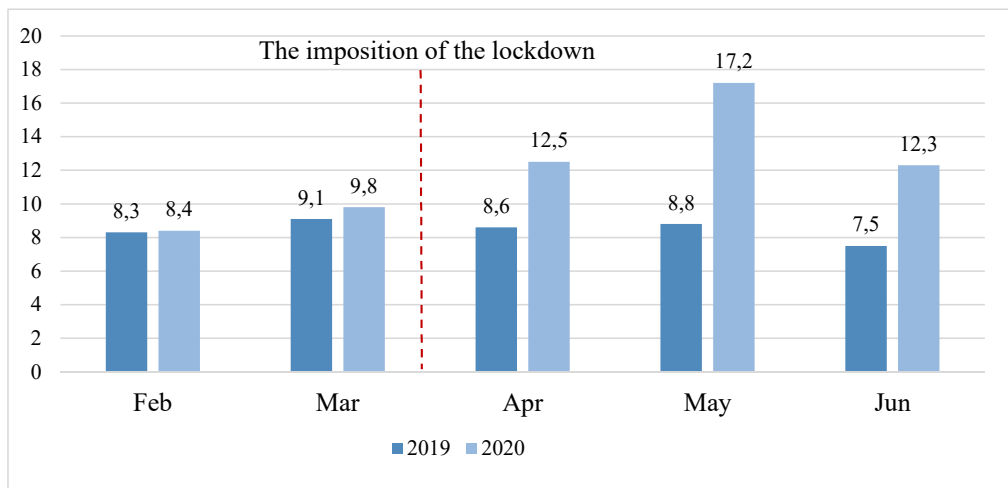
Source: <https://stats.hh.ru/>

⁸ The Centre of Strategic Research Survey, ria news <https://ria.ru/20200407/1569685001.html>

The situation in the labor market was further exacerbated by the lack of new posted vacancies for job seekers, as a lot of companies cannot afford to hire new employees or even have to completely pause their activity. The Figure 2 shows the number of active vacancies, posted monthly on one of the main recruitment platforms in Russia, Head Hunter.⁹

The increase in the unemployment rate together with the reduction in job openings increased the slackness of the labor market. Figure 3 shows the monthly changes in labor market competition in Moscow between 2019 and 2020. Starting in April 2020, there is a drastic increase in the number of applicants per vacancy: In May the ratio almost doubles in comparison with the same period in 2019, with more than 17 posted resumes for each active job opening.

Figure 3: Labor market competition in Moscow



Note: The ratio between the number of posted resumes and the number of active vacancy postings

Source: <https://stats.hh.ru/>

This situation in the labor market has especially affected ethnic minorities. One of the main ethnic minority groups in Russia is formed by the people originally from different regions of Central Asia, such as Uzbekistan, Tajikistan and Kyrgyzstan. This ethnic group partly consists of immigrants, who stayed in Russia after the collapse of the Soviet Union. Another part of this group are those who have come to Russia due to the relative attractiveness of the Russian labor market. The immigrants from Central Asia continue to live transnationally (Varshaver et al.,

⁹ Since there is usually a delay between the period of interest and the issue of the official statistical reports, this study relies upon the data from one of the main recruitment platform in Russia (www.hh.ru), published on their statistic page <https://stats.hh.ru/> and also provided at my request by the Statistical Department.

2020). Members of this ethnic group are treated as ethnic minorities in Russia (Bessundov, 2016).

A survey conducted in Russia in July 2020 gives an overview of the situation in the labor market that native workers and members of ethnic minority groups from Central Asia faced during the first months of the COVID-19 pandemic (Varshaver et al., 2020). More than 2000 respondents took part in online questionnaire. The results of this survey indicate that 38 percent of ethnic minority respondents in Moscow lost their job, in comparison with 21 percent of native respondents (overall in Russia: 40 and 23 percent respectively). Another 38 percent of ethnic employees taking part in the survey have had to stay on unpaid leave. Members of ethnic minority groups further report that 54 percent of them lost all sources of income (native employees: 30 percent). What is also interesting to mention is that 3 percent of native respondents have already found a new job, whereas the proportion of ethnic respondents managed to be hired is lower: 2 percent.

The present study aims to examine whether there is adverse treatment towards representatives of the ethnic minority groups on the application stage and whether the level of the ethnic employment gap varies depending on the tightness of the labor market.

3. Experimental Design

To evaluate the ethnic employment gap under changing labor market conditions I conduct a correspondence study in the Moscow labor market. The experimental design is a replication of a study conducted in 2017 (for a more detailed description please see Asanov and Mavlikeeva, 2020)¹¹. Right after the imposition of the lockdown, in the time period from the beginning of April until the end of June 2020, I sent 1440 resumes in response to 360 posted job openings.

The experiment has a 2 x 2 factorial design, where in response to every real job opening four fictitious resumes are sent. The applicants differ in their ethnicity and previous work experience. All candidates reveal their ethnicity status by their names: Two of four candidates have native sounding names, the other two have ethnic sounding names. Additionally, the employment history of applicants is varied in resumes for generalization of the results in line with the previous experiment (Asanov and Mavlikeeva, 2020). One group of applicants have recently graduated from university and are looking for their first job, whereas the other group have between 1.5 and 3 years of previous work experience.

¹¹ AEA RCT Registry. July 14. <https://doi.org/10.1257/rct.1308-22.200000000000003>

The following types of applications are sent to every vacancy:

- (1) Applicant with native sounding name and work experience,
- (2) Applicant with ethnic sounding name and work experience,
- (3) Applicant with native sounding name who is recently graduated,
- (4) Applicant with ethnic sounding name who is recently graduated.

All resumes contain the same sections and there is a database with the descriptions for every section. For the purposes of this experiment a specially developed computer program is used. This program randomly takes a description for every section from the database and creates a resume with a unique ID number according to the type of application. Gender is assigned randomly according to the generated name. Four created applications are sent in random order with a time lag of more than ten hours.

All the sections in the resumes are randomized. Thus the resumes are of equal quality on average and all of them contain the same sections for professional experience, qualifications, soft and language skills. It is important to note that all candidates have the language skills section in their resumes, where they report Russian as their mother language and additionally one foreign language (English, German, French or Spanish).

The applications are sent to posted job openings in different occupational fields that vary in the extend of face to face interaction with customers. The following occupations are chosen for this study: Advertising and Marketing Professionals (2431, skill level 4)¹², Real Estate Agents and Property Managers (3334, skill level 3), General Office Clerks (4110, skill level 2), Answering Service Operators (4223, skill level 2), Receptionists (4226, skill level 2), Messengers, Package Deliverers and Luggage Porters (9621, skill level 1).

In order to track and match callbacks with the corresponding resumes a unique domain and a telephone number are attached to every type of resume. I classify invitations for an interview or requests for any additional information from the candidate as a *callback*. All calls, emails and SMSes received from prospective employers are answered in order to reject the invitation and inform the recruiters that the applicant is no longer interested in the position.

¹² Occupation code and skill level according to ISCO 2008: International Standard Classification of Occupations (2008), 'International Standard Classification of Occupations', ISCO-08 I, 1-420.

4. Results

The main results of the experiment are reported in Table 3. As can be seen there is a difference both in the callback rate and the ethnic employment gap between the three first months of the COVID-19 outbreak.

The overall callback rate is 8.82, which is lower than in the previous experiment conducted in 2017, where the observed overall callback rate was 9.6 (Asanov and Mavlikeeva, 2020). The difference between the results provided by both studies is marginal. This relatively small difference can be explained by the specificity of the job vacancies during the COVID-19 outbreak and smaller sample size of the present experiment. Due to the decrease in the number of posted vacancies during the lockdown, I had to send fewer applications in comparison with the previous study. The specific nature of companies that post vacancies during the lockdown period might play an even more important role in this pattern. These companies differ from those that posted job openings in 2017, in pre-COVID times. However, as the present study is focused on analysing the changes in callback rates between the first months of the COVID-19 pandemic, the results should be viewed on the monthly basis. The lowest callback rate (5.42) is observed during the first month of the lockdown in Moscow, April. In the next month, May, the callback rate almost doubles, growing to 10.21. The increasing trend continues in June, where the callback rate reaches 10.84.

Table 3: The callback rate and the ethnic employment gap during the early stage of COVID-19

	April	May	June	Overall
Overall callback rate	5.42 [480]	10.21 [480]	10.84 [480]	8.82 [1440]
Ethnic majority callback rate	5.84 [240]	13.34 [240]	13.75 [240]	10.97 [720]
Ethnic minority callback rate	5.00 [240]	7.08 [240]	7.92 [240]	6.67 [720]
Ethnic gap ratio	1.17	1.88	1.74	1.65
Number of sent resumes	480	480	480	1440

Note: the numbers of sent resumes are given in brackets

The difference in callback rates among the occupational fields under study reflects the demand for these occupations during the first months of the COVID-19 outbreak. Such professions as Receptionists and Office Clerks are not highly demanded during this period, having the callback rate 5.42 and 4.17 respectively. Advertising and Marketing Professionals have the lowest callback rate among the occupations represented in the experiment (2.50). Whereas applications sent to the posted vacancies for Answering Service Operators (11.25) and Messengers, Package Deliverers and Luggage Porters (10.42) receive much more responses from prospective employers. This difference in callback rates can be explained by the fact that many companies have to switch to the remote work during the lockdown. The highest callback rate is observed for Real Estate Agents and Property Managers (19.17). The high demand for this occupation can be due to the fact that the activity in the real estate market was not suspended as in other occupational fields. Anecdotal evidence shows that a certain part of the population decided to invest their savings into real estate because of economic uncertainty caused by the pandemic and falling ruble exchange rate. Additionally, those people who lost their sources of income and were not able to pay back their credit loans, had to sell their properties.

The nature of the recruiters' responses also varies during this period. In April and May some candidates received emails where the prospective employers told them that they cannot make any decision regarding applications because of the current situation caused by the pandemic. Due to the uncertainty caused by the imposition of the lockdown, the recruiters informed the candidates that the recruitment process has been suspended until they have a clearer picture of how the company will operate. Here are the selected extracts from some of these emails:

[...] At the moment the office is closed due to the current situation in the city. I will definitely contact you as soon as we return to a full-fledged work schedule. Unfortunately, there is not even an opportunity to conduct an interview. Thank you for your understanding and interest in our company.

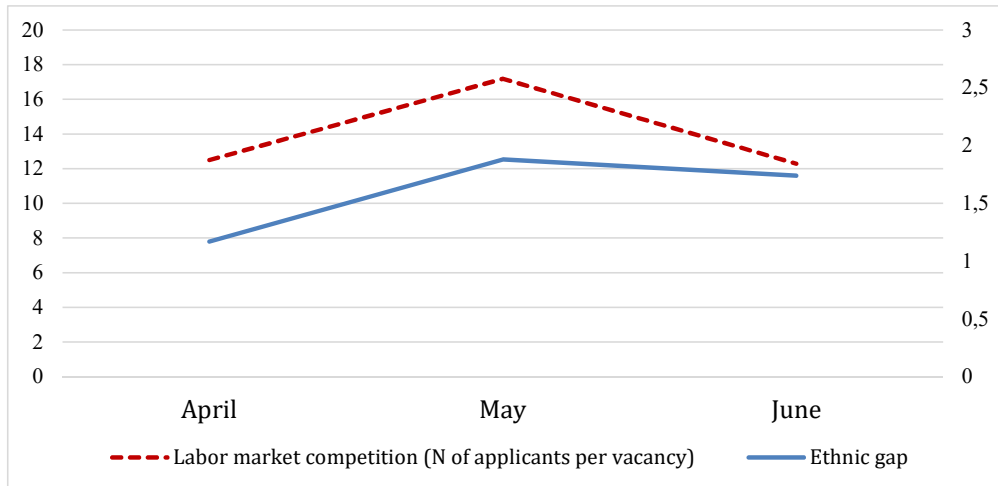
[...] Please note that due to the pandemic the search for candidates for this vacancy has been temporarily suspended. Immediately after returning to normal work, we will review your resume. If the vacancy is still relevant, we will contact you. We hope for your understanding.

[...] The company has temporarily "frozen" the vacancy (budget optimization is being determined). If you do not mind, when it resumes and it is still relevant for you, I will contact you.

However, the prospective employers began to invite applicants for face to face interviews in May. In June no emails regarding the difficulties in the recruitment process caused by the COVID-19 situation were received.

Further findings show that the overall ratio of ethnic employment gap is 1.65 , which is comparable with the ratio observed in the previous experiment (1.64) (Asanov and Mavlikeeva, 2020). However, there are fluctuations in the level of the ethnic employment gap during the first three months of the COVID-19 outbreak. The lowest rate can be observed in April (1.17). In May ethnic inequality grows, reaching the rate of 1.88 . During the third month of the lockdown, the ethnic gap decreases slightly to 1.74 . Figure 4 shows the variations in the ethnic employment gap during the first three months of the pandemic as well as the fluctuations in the slackness of the labor market. As can be seen from the graph, slackness reaches its peak in May, when there are about 17 job seekers per posted vacancy. The level of ethnic inequality is also the highest in this month.

Figure 4: Labor market condition and the ethnic employment gap during the three first months of the COVID-19 outbreak



5. Discussion and conclusion

Having started in Russia in the beginning of March the COVID-19 pandemic spread rapidly throughout the whole country during the following months. Moscow became the epicenter of the virus. The compulsory measures the government had to take in order to slow down the further spreading of the infection severely affected the life of the citizens. One of the main adverse effects of these measures is labor market disruption. Starting from the first month of the lockdown, April, the unemployment rate increased drastically. At the same time, there was a decrease in the number of posted job openings during the first months of the lockdown. These factors in combination caused the slackness of the labor market. People faced uncertainty during the early stages of the COVID-19 outbreak. As employees were officially sent on paid leave until the end of April, companies did not know when they would be able to operate as usual, which can also be seen in the responses of recruiters.

The rapidly changing situation in the labor market affected strongly members of ethnic minority groups. The results of the experiment indicate that the fluctuations in the labor market tightness are accompanied by variations in the ethnic employment gap. The overall level of ethnic inequality is comparable with previous findings (Asanov and Mavlikeeva, 2020). However, the overall ethnic gap ratio is a result of the lowest rate during the first month of the lockdown. Facing economic uncertainty during April, businesses were in a state of suspense, which might also explain the lowest callback rate in April compared with the two following months. The ethnic employment gap reaches its peak in May, when the highest rate of labor market competition is observed. In June, both the slackness of the labor market and the ethnic inequality ratio decrease.

This paper contributes to the existing literature by assessing the level of ethnic discrimination under the condition of changing labor market competition. The descriptive results indicate that the ethnic employment gap fluctuates according to labor market tightness. These findings support the theory that there is a link between labor market conditions and ethnic imbalance. Further research is needed to analyze if those results hold outside Russia.

References

- Asanov, I and Mavlikeeva, M. (2020), “Is Self-employment a Career Trap? Large-Scale Field Experiment in the Labor market.”, Working paper
- Baert, S., Cockx, B., Gheyle, N. and Vandamme, C. (2015), “Is there Less Discrimination in Occupations where Recruitment is Difficult?”, *Industrial and Labor Relations Review*, 68(3): 467-500. DOI: 10.1177/0019793915570873
- Baert, S. (2018), “Hiring Discrimination: An Overview of (Almost) All Correspondence Experiments Since 2005”, In *Audit Studies: Behind the Scenes with Theory, Method, and Nuance*, Springer International Publishing, 63–77. DOI: 10.1007/978-3-319-71153-9_3
- Bertrand, M. and Mullainathan, S. (2004), “Are Emily and Greg More Employable Than Lakisha and Jamal? A Field Experiment on Labor Market Discrimination”, *American Economic Review* 94(4): 991-1013. DOI: 10.1257/0002828042002561
- Bessudnov, A. (2016), “Ethnic Hierarchy and Public Attitudes towards Immigrants in Russia”, *European Sociological Review* 32(5), 567-580.
- Brodeur, A., Gray, D. M., Islam, A. and Bhuiyan, S., “A Literature Review of the Economics of Covid-19.” IZA Discussion Paper No. 13411, Available at SSRN: <https://ssrn.com/abstract=3636640>
- Boulware, K.D. and Kuttner, K.N. (2019), “Labor Market Conditions and Discrimination: Is There a Link?”, *AEA Papers and Proceedings*, 109: 166-70. DOI: 10.1257/pandp.20191086
- Carlsson, M., Fumarco, L. and Rooth, D.O. (2018), “Does Labor Market Tightness Affect Ethnic Discrimination in Hiring?” IZA Discussion Papers 11285, Institute of Labor Economics (IZA), <http://hdl.handle.net/10419/177089>
- Fairlie, R. W., Couch, K. and Xu, H. (2020), “The Impacts of COVID-19 on Minority Unemployment: First Evidence from April 2020 CPS Microdata” (Working Paper No. 27246; Working Paper Series), National Bureau of Economic Research, <https://doi.org/10.3386/w27246>
- Güven, C., Sotirakopoulos, P. and Ulker, A. (2020), “Short-term Labour Market Effects of COVID-19 and the Associated National Lockdown in Australia: Evidence from Longitudinal Labour Force Survey”, *COVID Economics*, (44): 186-224. Available at: <https://cepr.org/content/covid-19>

- Rich, J. (2014), “What Do Field Experiments of Discrimination in Markets Tell Us? A Meta Analysis of Studies Conducted Since 2000”, IZA Discussion Paper No. 8584, Available at SSRN: <https://ssrn.com/abstract=2517887>
- Varshaver, E., Ivanova, N. and Rocheva, A. (2020), “Положение мигрантов в России во время пандемии коронавируса (COVID-19): результаты опроса (Migrants in Russia during the COVID-19 Pandemic: Survey Results)”, DOI: 10.13140/RG.2.2.12985.60005
- Zschirnt, E. and Ruedin, D. (2016), “Ethnic discrimination in hiring decisions: a meta-analysis of correspondence tests 1990-2015”, *Journal of Ethnic and Migration Studies* 42(7), 1115-1134. DOI:10.1080/1369183X.2015.1133279